Downhole Gasification (DHG) For Improved Oil Recovery

Sanchez Monsalve, Diego

Award date:
2014

Awarding institution:
University of Bath

DOWNHOLE GASIFICATION (DHG) FOR IMPROVED OIL RECOVERY

DIEGO ALEJANDRO SÁNCHEZ MONSALVE

A thesis submitted for the degree of Doctor of Philosophy

University of Bath

Department of Chemical Engineering

June 2014

ABSTRACT

Gas injection, the fastest growing tertiary oil recovery technique, holds the promise of significant recoveries from those depleted oil reservoirs around the world which fall into a pressure range of (50-200) bar mainly. However, its application with the usual techniques is restricted by the need for various surface facilities such as enormous gas supply and storage. The only surface facility that downhole gasification of hydrocarbons (DHG) requires, on the other hand, is a portable electricity generator.

DHG consists in producing inert gases, H_2, CO, CO_2 and CH_4 through the steam reforming reaction of a part of the produced oil in a gasifier-reformer reactor positioned alongside the producer well in the reservoir. The gases, mainly H_2 -the most effective displacing gas among produced gases- are injected into a gas cap above the oil formation, to increase oil recovery through a gas displacement drive mechanism. So far, DHG has only been tested under laboratory conditions using methane, pentane/reservoir gas and naphtha/reservoir gas as feedstock at conditions of reservoir pressure up to 130 bar. The studies varied reaction temperature, steam to carbon (S/C) ratio, catalyst types and catalyst loading in the gasifier-reformer reactor of a small pilot scale rig. These experimental studies demonstrated that pressure is one of the main factors influencing the effectiveness of the DHG process.

From this starting point, the present investigation was directed at extending the pressure range up to 160 bar in the gasifier-reformer reactor using a naphtha fraction as feedstock in order to investigate whether the conversion and H_2 concentration in produced dry gas can be maintained at acceptable levels under conditions of high pressure. To this end, experimental studies were carried out within the laboratory using the existing DHG rig on the small pilot scale, which was successfully commissioned and revamped for the purposes of this study.

Initially, the investigation focused on exploring operating conditions, namely, steam to carbon (S/C) ratio, length of the gasifier-reformer reactor tube/ catalyst loading and the relative performance of two different catalysts. Subsequently, experiments on shutdown/start up cycles followed by variation of temperature were performed to simulate the effect of sudden electrical disruptions that usually occur in field operations.

Experimental results using naphtha at pressure from 80 to 160 bar at 650 ºC, S/C= 6 achieved total feedstock conversion, no coke deposits and, most importantly, high H_2 concentration in the produced dry gas (56-63 vol. % plus other gases). The best result was obtained with a crushed HiFUEL R110 catalyst (40-60 wt. % of $NiO/CaO.Al_2O_3$) and a reactor tube length of 72 cm, but the results with a C11-PR catalyst (40 wt. % of $NiO/MgO.Al_2O_3$) and a reactor tube length of 30 cm were similarly favourable. These results were supported by results of a

numerical DHG model which indicated total feedstock conversion and values of H_2 around 67 vol. % (using n-heptane as model surrogate).

The results suggest that the DHG process is technically feasible at the pressure values studied, perhaps up to 200 bar where there are many hundreds of depleted, light oil reservoirs, especially in North America and other parts of the world below that pressure value.

ACKNOWLEDGEMENTS

Writing up this doctoral thesis has definitely been a challenge and it has been product of assistance and support of many individuals.

I would like to thank PDVSA Intevep S.A., Scotoil Services LTD and University of Bath for the support to this research. I would like to express my greatest appreciation to my major advisors Emeritus Professor Malcolm Greaves and Dr. Pawel Plucinski for their guidance, patience and encouragement.

I also thank to Mrs. Marta Carrillo, MSc. Magaly Quintero, MSc. Yefrenck Castro and Mrs. Mileydi Rodriguez for indispensable help through fruitful discussions and positive environment at all times.

I am very grateful to all technical staff in Chemical Engineering Department for support and assistance, especially Mr. Fernando Acosta, Mr. John Bishop and Mr. Robert Brain who provided orientation and made the environment very friendly.

On similar lines, I take this opportunity to thank friends, family and my parents that have taught me values and wishes to improve myself as a better person every single day.

This doctoral thesis is dedicated to God, my grandparents: Dina, Eloisa, Antonio and Alejo who are always in my heart, my parents and siblings who always believed in my dreams! Thank you.

"God grants victory to perseverance"

Simón Bolivar

The Liberator of five nations from Spanish rule: Venezuela, Colombia, Ecuador, Panamá, Peru and Bolivia

TABLE OF CONTENTS

LIST OF FIGURES

CHAPTER 2: LITERATURE SURVEY

CHAPTER 3: MATERIALS AND EXPERIMENTAL DOWNHOLE GASIFICATION (DHG) RIG

CHAPTER 4: EXPERIMENTAL PROCEDURE, DATA ANALYSIS AND CHARACTERISATION OF SAMPLES

CHAPTER 5: DHG PRODUCED DRY GAS COMPOSITION USING METHANE FEEDSTOCK

CHAPTER 6: DHG PRODUCED DRY GAS COMPOSITION USING NAPHTHA FEEDSTOCK

CHAPTER 7: THEORETICAL MAXIMUM OF DHG PRODUCED DRY GAS COMPOSITION USING METHANE AND NAPHTHA FEEDSTOCK

APPENDICES

LIST OF TABLES

CHAPTER 2: LITERATURE SURVEY

CHAPTER 3: MATERIALS AND EXPERIMENTAL DOWNHOLE GASIFICATION (DHG) RIG

CHAPTER 4: EXPERIMENTAL PROCEDURE, DATA ANALYSIS AND CHARACTERISATION OF SAMPLES

CHAPTER 5: DHG PRODUCED DRY GAS COMPOSITION USING METHANE FEEDSTOCK

CHAPTER 6: DHG PRODUCED DRY GAS COMPOSITION USING NAPHTHA FEEDSTOCK

CHAPTER 7: THEORETICAL MAXIMUM OF DHG PRODUCED DRY GAS COMPOSITION USING METHANE AND NAPHTHA FEEDSTOCK

APPENDICES

NOMENCLATURE

A	Tube Cross Sectional Area
A/D	Analog/Digital
°API	Degrees American Petroleum Institute
bbl	Barrels
°C	Degrees Celsius
C_1~C_{10}	Carbon Atoms from 1 to 10
Cp_i	Calorific Capacity of Fluid *i*
1-D	One Dimension
2-D	Two Dimensions
3-D	Three Dimensions
$D_{particle}$	Diameter of Spherical Particles
°F	Degrees Fahrenheit
ΔG_R°	Gibbs Free Energy
ΔH_{298}^o	Enthalpy at Standard Conditions, 298.15 K and 1 bar
$\Delta H_{R,\,T}^o$	Enthalpy of a Chemical Reaction at Different Temperatures
HK 40	High Alloy Nickel Chromium
i	Fluid
K	Degrees Kelvin
K_T	Equilibrium Constant at Temperature T
K_{298}	Equilibrium Constant at 298.15 K
M_i	Molecular Weight
$M_{mixture}$	Molecular Weight of Mixture
Mid-IR	Middle Infrared
m_{CH4}	Mass of CH_4
$m_{naphtha}$	Mass of Naphtha
m_{H2O}	Mass of Water
m_{CO}	Mass of CO
m_{CO2}	Mass of CO_2
m_{H2}	Mass of H_2
n_{CH4}	Mole of CH_4 in the Equilibrium
$n_{0,CH4}$	Initial Mole of CH_4 in the Equilibrium
n_{H2O}	Mole of H_2O in the Equilibrium
$n_{0,H20}$	Initial Mole of H_2O in the Equilibrium
n_{CO}	Mole of CO in the Equilibrium
$n_{0,CO}$	Initial Mole of CO in the Equilibrium
n_{CO2}	Mole of CO_2 in the Equilibrium
$n_{0,CO2}$	Initial Mole of CO_2 in the Equilibrium
n_{H2}	Mole of H_2 in the Equilibrium
$n_{0,H2}$	Initial Mole of H_2 in the Equilibrium
T	Temperature
t	Time

P	Pressure
$Q_{mixture}$	Volumetric Total Inlet Flow Rate
R	Ideal Gas Constant
Re	Reynolds Number
S/C	Steam to Carbon Ratio
S/HC	Steam to Hydrocarbon Ratio
ΔT	Temperature Difference
$(T,P)_o$	Temperature and Pressure at Lab Room Condition, 293.15 K and 1.01 bar
$(T,P)_{DHG}$	Temperature and Pressure at DHG operation condition
U_{total}	Total Uncertainty
U_{cal}	Calibration Uncertainty
U_{stab}	Stability Uncertainty
$U_{Measured\ reading}$	Measured Reading Uncertainty
$V_{effective}$	Effective Volume
$V_{reactor}$	Volume of Reactor (Gasifier-reformer)
x_i	Mole Fraction of Fluid *i*
$	Dollars
$.MMSCF^{-1}	Dollars per Million Standard Cubic Feet

Greek symbols

α_i	Stoichiometric Coefficient of Fluid *i*
α_k	Stoichiometric Coefficient of Reaction *k*
$\varepsilon_{catalyst\ bed}$	Voidage of Catalyst Bed
$\partial\varepsilon$	Differential of Conversion in the Equilibrium
$\Delta\varepsilon_i$	Difference of Conversion in the Equilibrium of Fluid *i*
∂K	Differential of Equilibrium Constant
μ_i	Viscosity of Fluid *i*
$\mu_{mixture}$	Viscosity of Mixture, cP
ρ	Specific density
ρ_i	Density of Fluid *i*
$\rho_{mixture}$	Density of Mixture
τ	Residence Time
Φ	Tube External Diameter

ABBREVIATIONS

API	American Petroleum Institute
ASTM	American Standard Test Technique
BEC	Backscattered Electron Composition
BSED	Back Scattered Electron Diffraction
DAC	Data Acquisition
DHG	Downhole Gasification
EDX	Energy Dispersive X-ray
EOR	Enhanced Oil Recovery
FCM	First-Contact Miscible
FIA	Hydrocarbon Type Analysis
GSA	Geometric Surface Area
GSCI	Gravity Stabilised Gas Injection
HAZOP	Hazard And Operability Study
HC	Hydrocarbon
HTC	Heat Transfer Coefficient
ID	Internal Diameter
IOR	Improved Oil Recovery
IR	Infrared
KV	KiloVolts
LEL	Lower Explosive Limit
MCM	Multiple Contacts Miscible
MMP	Minimum Miscibility Pressure
MSDS	Material Safety Data Sheet
OOIP	Original Oil In Place
PC	Personal Computer
PD	Pressure Drop
PDVSA	Petróleos de Venezuela S.A.
PONA	Hydrocarbon Type Analysis
RS	Rapid-Share
RSS	Root Sum Squared
SCBA	Self-Contained Breathing Apparatus
SDS	Safety Data Sheet
SEI	Secondary Electron Imaging
SEM	Scanning Electronic Microscopy
SI	System International
SIMDIS	Simulated Distillation
SS	Stainless Steel
STP	Standard Conditions, 273.15 K and 1 bar
SV	Space Velocity
TWT	Tube Wall Temperature
UEL	Upper Explosive Limit
UK	United Kingdom
USA	United States of America
USB	Universal Serial Bus
WAG	Water Alternating Gas

WGS	Water Gas Shift
XDS	X-Ray Diffuse Scattering

CHAPTER 1: INTRODUCTION

1.1 Thesis context

The world is finite. The known major oil fields contain 94 % of the world's known oil and are accordingly the most critical for future global oil supplies. The peak global oil finding year was 1962. Since then, the global discovery rate has dropped sharply in all regions, especially those associated with light oils (Greaves et al., 2006, Babadagli, 2007, Ivanhoe, 1997 and Secen, 2005). About thirty giant fields comprise half of the world's oil reserves and most of them are categorised as mature fields. Their future development requires new and economically viable techniques as well as proper reservoir management strategies (United energy group PLC, 2008).

Techniques of enhanced oil recovery are therefore of the highest importance. The emphasis is mainly on their applicability in terms of effectiveness (incremental recovery) and efficiency (cost and recovery time). Gas injection, the fastest growing enhanced oil recovery/improved oil recovery (EOR/IOR) technique, holds the promise of significant recoveries from depleted and abandoned oil reservoirs. Studies of the status of gas injection oil recovery show that N_2 and flue gas have declined or become extinct and only two injectants, CO_2 (miscible) and hydrocarbon (miscible and immiscible) gas have continued in use. However, their application at field scale is restricted to within the gas processing plant and other surface facilities (Ivanhoe, 1997, Schutle, 2005, Tzimas et al., 2005, Balbinski et al., 2003 and Lubas).

Downhole gasification of hydrocarbons (DHG), first proposed by Davidson and Yule (Davidson, 2001), differs from the usual gas injection techniques for oil recovery in one major respect: it does not require any of these surface facilities for its application at field scale. Additionally, a portable electricity generator is sufficient to provide the energy required for the process.

DHG consists in introducing gases into reservoirs through steam reforming reactions of a part of the produced oil through a gasifier-reformer reactor positioned alongside the producer well. The gases are injected into a gas-cap above the oil formation to maintain or increase the reservoir pressure, hence increasing the oil recovery (Greaves et al., 2005). DHG is mainly designed for improving oil recovery from light oil reservoirs with an ^{o}API gravity higher than 30 ^{o}API. However, its use may extend to the recovery of some medium and heavy oils which can be displaced at economical rates whether significant light naphtha are contained (Greaves et. al., 2006).

A gasifier-reformer reactor is normally operated at pressures below 35 bar, in a temperature range of 750 ^{o}C to 1000 ^{o}C for hydrogen production in

surface operations. However, the DHG process needs to operate at a much higher pressure: from 50 to 200 bar. Many thousands of depleted light oil reservoirs throughout the world fall into this higher pressure range.

So far, Greaves et al. (2004), Greaves et al. (2005), Greaves et al. (2006) and Greaves et al. (2008) have carried out studies on DHG using methane, pentane with reservoir gas and naphtha with reservoir gas in the laboratory using an experimental rig on a small pilot scale. They demonstrated that pressure is one of the main factors influencing the effectiveness of the DHG process. The total conversion to hydrogen decreased from around 60 vol. % in the produced dry gas to 35 vol. %, when pressure was increased up to 130 bar in a gasifier-reformer reactor of dimensions (½-inch x 30 cm) and operated at (710-760) ^{o}C. The levels of H_2 could be maintained more or less constant (within a range) because of the interplay of other factors such as steam to carbon (S/C) ratio, temperature and (potentially suboptimal) catalyst loading (Greaves at al., 2008).

1.2 Research scope

The DHG process has never been considered for operation using naphtha feedstock at pressures higher than 130 bar. Hence, our research was to extend the pressure range up to 160 bar in the gasifier-reformer operation with a naphtha fraction to investigate whether conversion and H_2 concentration in produced dry gas can be maintained at acceptable levels. To this end, experimental studies in the laboratory were carried out using an existing DHG rig on a small pilot scale.

Initially, the investigation focused on exploring steam to carbon (S/C) ratio values that would avoid any serious effect of carbon deposition on the catalyst. Next, the length of the gasifier-reformer reactor was increased by 100 % (from 30 cm to 72 cm) to be the same length as the catalyst loading. Two different catalysts were also tested: C11-PR, which was used in previous DHG investigations (Greaves et al. 2004, Greaves et al. 2005, Greaves et al. 2006 and Greaves et al. 2008), and a new one, crushed HiFUEL R110.

Finally, experiments with shutdown/start up cycles followed by variation of temperature (from 600 ºC to 750 ºC) were performed to simulate sudden electrical disruptions usually occurring in field operations. All of these studies are directed at exploring the technical feasibility of DHG implementation on a more developed scale, i.e. pilot test.

This involved the following areas of work:

(1) The commissioning and revamping carried out on the existing experimental small pilot scale DHG rig included some modifications and optimisations, which were all directed at increasing the feedstock

conversion and achieving a higher hydrogen (H_2) concentration in the produced dry gas. This is crucial since it is this gas which mainly drives gas displacement where the DHG process is implemented for the purpose of oil recovery.

(2) A series of basic DHG experiments using methane feedstock were performed to verify the benchmark of previous experiments and to understand procedures for operating the experimental rig prior to using the naphtha feedstock. Failures to optimize these procedures could lead to the rapid deterioration of the catalyst activity, the conversion and H_2 concentration as our main gas of interest, and the possible cessation of operation due to coke blocking the catalyst.

To support the DHG experimental results, calculations of the H_2 concentration in the dry gas composition in the equilibrium were carried out by means of a numerical model using ASPEN PLUS at DHG operating conditions at the experimental phase. The numerical results allowed us to analyse discrepancies and evaluate the performance of the DHG operation within the laboratory. Moreover, they helped us to understand which operating conditions or parameters should be optimised and at what measure, in order to obtain optimal H_2 concentration in produced dry gas for the DHG process in depleted oil reservoirs.

1.3 Thesis structure

This thesis consists of eight (8) chapters which can be briefly described as follows:

Chapter 1 is an introduction which brings the research into context and highlights the surrounding issues. It describes the scope, purpose and structure of the thesis.

Chapter 2 is a literature survey that provides a brief summary of Downhole gasification (DHG) fundamentals to define the terms used in this study, followed by a review of recent developments associated with the process and its feasibility of application in oil reservoirs. For a proper understanding of the process, a discussion of the fundamentals of enhanced oil recovery/improved oil recovery (EOR/IOR) techniques by gas Injection, mechanisms of oil recovery by gas injection and steam reforming process of hydrocarbons will also be provided.

Chapter 3 describes the materials and the experimental small pilot scale rig utilised for the DHG studies within the laboratory. The assembly, commissioning, further optimisations and the final assembly of the rig (carried out before the experimental phase) are examined.

Chapter 4 indicates the procedures, data processing and characterisation of samples used in the DHG studies via laboratory. The technical reliability

of our experimental results was vital; therefore, special attention was paid to the facts of: how to run a DHG experiment in a safe manner, how to take samples for analysis; how to process data once the experiment has been completed; and how technically reliable our results are. All those details are described.

Chapter 5 covers the series of basic DHG experiments performed with methane feedstock to verify the benchmark of previous investigations realised by Greaves et al. (2004), Greaves et al. (2005) in the rig and, at the same time, to establish a clear baseline of results. Likewise, this precautionary approach prior to using the naphtha feedstock was necessary in order to understand the procedures for operating the DHG rig. The produced dry gas composition, in particular the conversion and H_2 concentration, from the experiments are analysed and discussed throughout. Finally, major findings are summarized and concluding remarks made.

Chapter 6 covers the main DHG experiments performed with naphtha feedstock used to represent the naphtha fraction to be extracted and vaporised from oil into reservoirs in the event of DHG implementation at field scale. It details the experiments conducted at a range of pressure from 80 bar up to 160 bar and shows the results obtained.

An overall analysis of the produced dry gas composition in terms of conversion and H_2 concentration summed with space velocity, residence time and Reynolds number from experimentation provides an insight into the technical feasibility of DHG implementation on a more developed scale, i.e. pilot testing and enables us to envisage briefly how the DHG concept might be applied. This is described in this chapter followed by the major findings and concluding remarks.

Chapter 7 demonstrates the numerical model developed for the DHG process where the theoretical maximum of produced dry gas composition in the equilibrium was calculated at operating conditions from the experimental phase using methane (chapter 5) and naphtha (chapter 6) feedstock. Those values were compared with our experimental results and analysis of discrepancies and the performance of the DHG operation via laboratory are examined. Additionally, sensitivity studies are presented in a very wide range of pressure (2-180) bar and temperature (500-900) ºC using methane and naphtha (n-heptane as model surrogate). Finally, the major findings and concluding remarks are summarized.

Chapter 8 presents the conclusions of the work in this thesis and some recommendations for future work are proposed.

References

BABADAGLI, T., 2007. Development of mature oil fields — A review. *Journal of petroleum science and engineering,* 57, pp. 221–246.

BALBINSKI, E., GOODFIELD, M., JAYASEKERA, T., WOODS, C., 2003. *Potential for geological storage and EOR from CO injection into UKCS oilfields.* United Kingdom: UK Department of trade and industry's sustainable hydrocarbon additional recovery programme (SHARP).

DAVIDSON, I.D., 2001. *Enhanced oil recovery by In situ gasification.* International patent application WO 01/81723. November 01, 2001.

GREAVES, M., RATHBONE, R., XIA, T., BENTHAHER, A., DUGGAN, S., 2004. *Downhole gasification for improved oil recovery and gas production (phase 1) experimental studies (1 Nov 2002 – 31 Oct 2004).* United Kingdom: University of Bath, (Confidential internal report).

GREAVES, M., XIA, T., RATHBONE, R. AND BENTAHER, A., 2005. Underground gasification for improved oil recovery. *Canadian international petroleum conference,* 7-9 June 2005 Calgary. Calgary: Petroleum Society Canadian Institute of Mining, Metallurgy & Petroleum, pp. 38-48.

GREAVES, M., RATHBONE, R., XIA, T., BENTHAHER, A., 2006. Experimental study of a novel In situ gasification technique for improved oil recovery from light oil reservoirs. *JCPT,* 45(8), pp. 41-47.

GREAVES, M. AND XIA, T.X., 2008. Producing hydrogen and incremental oil from light oil reservoirs using downhole gasification. *Canadian international petroleum conference,* 17-19 June 2008 Calgary. Calgary: Petroleum Society Canadian Institute of Mining, Metallurgy & Petroleum, pp. 14-24.

IVANHOE, L.F., 1997. Get Ready For Another Oil Shock!. *The futurist,* January/February.

LUBAŚ, J. *Selection of the best technique of increasing the recovery factor for BMB – the largest polish oil reservoir.* Germany: Oil and Gas Institute: Krosno Branch, (2WP0-5).

SCHUTLE, W.M., 2005. Challenges and strategy for increased oil recovery. Proceedings of the *International Petroleum Technology Conference,* 21-23 November 2005 Doha. Qatar: pp. 02-09.

SEČEN, J., 2005. IOR and EOR – chances for increase of oil production and recoveries in existing, mature reservoirs. Proceedings of the 13th *European Symposium on Improved Oil Recovery,* 25-27 April 2005 Budapest Hungary. Hungary: Rudarsko-geološko-naftni zbornik, pp. 27-30.

TZIMAS, E., GEORGAKAKI, A., GARCIA, C., PETEVES, S.D., 2005. *Enhanced oil recovery using carbon dioxide in the European energy system.* Netherlands: DG JRC, INSTITUTE FOR ENERGY, (Report EUR 21895 EN).

UNITED ENERGY GROUP PLC, 2008. *All about oil and gas: from the beginning to present day.* United Kingdom: U.S. Energy Department.

CHAPTER 2: LITERATURE SURVEY

2.1 Introduction

This section provides a brief summary of Downhole gasification (DHG) fundamentals to define the terms used in this study followed by a review of recent developments associated with the process and its feasibility of application in light oil reservoirs. For a proper understanding of the process, a discussion of the fundamentals of tertiary recovery by gas injection, the mechanisms of oil recovery by gas injection and the steam reforming process of hydrocarbons will also be provided.

Downhole gasification (DHG) in light oil reservoirs is a relatively new area of investigation. The original idea was first proposed by Davidson and Yule (2001). In some measure, this original idea was influenced by simple understanding of the in situ combustion process, but it was then realised that the gasification-reforming process needed to be self-contained, or isolated, from the actual reservoir in a separate 'reactor' assembly (gasifier-reformer). The process carried out by means of this underground equipment has subsequently been assigned the designation DHG process module or process.

The main idea of the process, then, is to generate displacement gases in the reservoir, using a DHG unit(s)/module(s). The in situ generation of gases by gasification-reforming (on the basis of steam reforming reactions) of a fraction of mobilised light crude oil, has a number of benefits: principally, the DHG process is not dependent on having a supply or reservoir of gas available, and there is no requirement to transport/pipeline the gas to the reservoir. This is a first requirement for operating any oil recovery (EOR/IOR) process: that there is a large volume of an 'expensive' fluid (gas) to inject into the reservoir to effect gas displacement of the immobile or residual oil. Hence, the DHG process is not limited to any particular location, onshore or offshore. Secondly, part of the in situ produced gas is hydrogen (H_2), which is a valuable component that can be produced, or stored in the reservoir for later use.

In reviewing the literature, the main attention is directed to gas injection reservoir processes, since it is this that underlies the DHG process. Whether the gas comes from the surface. i.e. transported from a gas reservoir, or is generated in situ by the DHG process, is material to the particular oil displacement process.

2.2 Oil recovery in reservoirs

Recovery of hydrocarbons from an oil reservoir occurs in several recovery stages. These are:

- Primary recovery

- Secondary recovery
- Tertiary recovery

In each one of these stages, the energy from the reservoir (normally called the reservoir drive) enables the displacement of crude oil and natural gas from the subsurface rock to the production well. **Primary recovery**, uses the natural energy of the reservoir as a drive, **secondary recovery**, uses the injection of water or gas from the surface whilst in **tertiary recovery**, the recovery includes by a wide range of techniques widely called **Enhanced oil recovery (EOR)** that are applied to reservoirs in order to increase production rate and recovery efficiency. Primary and secondary recovery usually extract roughly 35 % of the original oil in place (OOIP) in the case of light oils. Secondary and tertiary recovery extract 12-20 % approximately and both together are commonly called **Improved oil recovery (IOR)** and also includes all possible techniques (horizontal wells, downhole pumps, reservoir profiling, etc.) for improving oil recovery where an EOR technique is restricted to reservoir processes (Frank et al., 1998, Ahmed, 2001).

Nowadays, there are enhanced oil recovery/improved oil recovery (EOR/IOR) techniques specially designed to increase recovery efficiency which may be classified under three categories or brands:

- Thermal
- Chemical
- Gas Injection
- Microbial EOR also called MEOR

All of these techniques are very expensive hence the choice of technique to be implemented will depend on which is deemed to be the most economical, once extensive economical studies based on reservoir rock characteristics have been carried out. EOR/IOR techniques are applied just after the point at which the oil rate history curve has reached its top maximum value by using primary and secondary techniques after which the oil recovery rate starts declining progressively.

Figure 2.1 shows a schematic oil rate history curve from the end of a waterflood and the application of an EOR technique: solvent injection in this case. The solid black curve shows the rate history; the shaded blue and green portions the waterflood as secondary recovery and the EOR technique, respectively. Time t_1 is the date of the start of the solvent injection (Lake and Walsh, 2008).

Since this study is focused on gas Injection, the next section will discuss only this process.

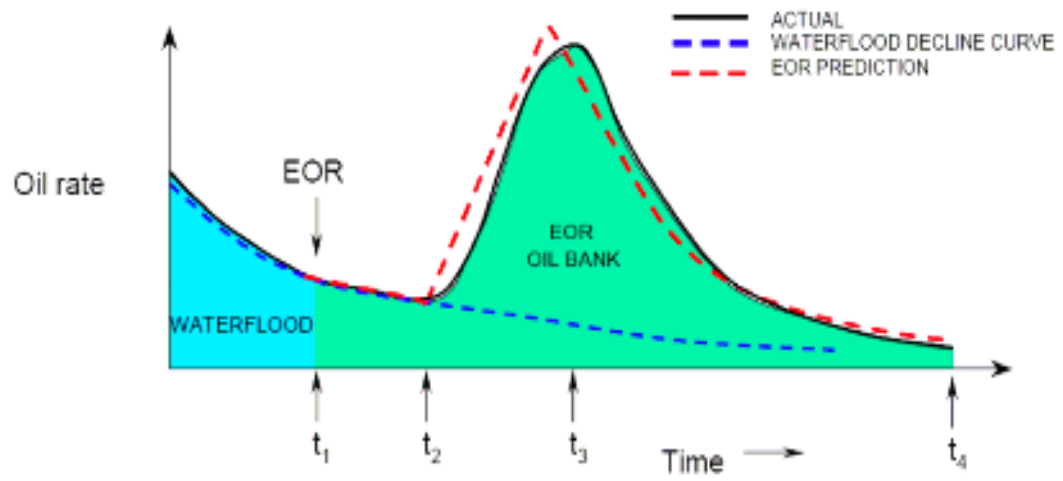

Figure 2.1 An example of an oil rate history curve (Lake and Walsh, 2008).

2.2.1 Oil recovery (EOR/IOR) by gas injection

Miscible gas injection and immiscible gas injection are the two major types of gas injection. In miscible gas injection, the gas is injected at or above minimum miscibility pressure* (MMP) which causes miscibility of the gas injected in the oil. Conversely, immiscible gas injection is conducted at pressures below MMP. This low pressure of gas injected is used to maintain reservoir pressure or to form a gas cap as in the DHG process; in this way, production cut-off is prevented, thereby increasing the rate of production.

Tzimas et al. (2005) mention two main techniques for gas injection, **GSGI** (Gravity stabilised gas injection), applicable where gravity forces dominate and **WAG** (Water alternating gas), applicable where viscous forces dominate. It is important to distinguish between these two techniques which have quite different characteristics in terms of sequestrable gas, timescales and economics.

Gravity stabilised gas injection (GSGI): this technique is illustrated in Figure 2.2 which shows gas being injected at the crest of an anticlinal reservoir and water and oil being produced from a downward moving oil bank.

* Minimum miscibility pressure (MMP) is the lowest pressure required to achieve multiple contact miscibility between injected fluid and oil.

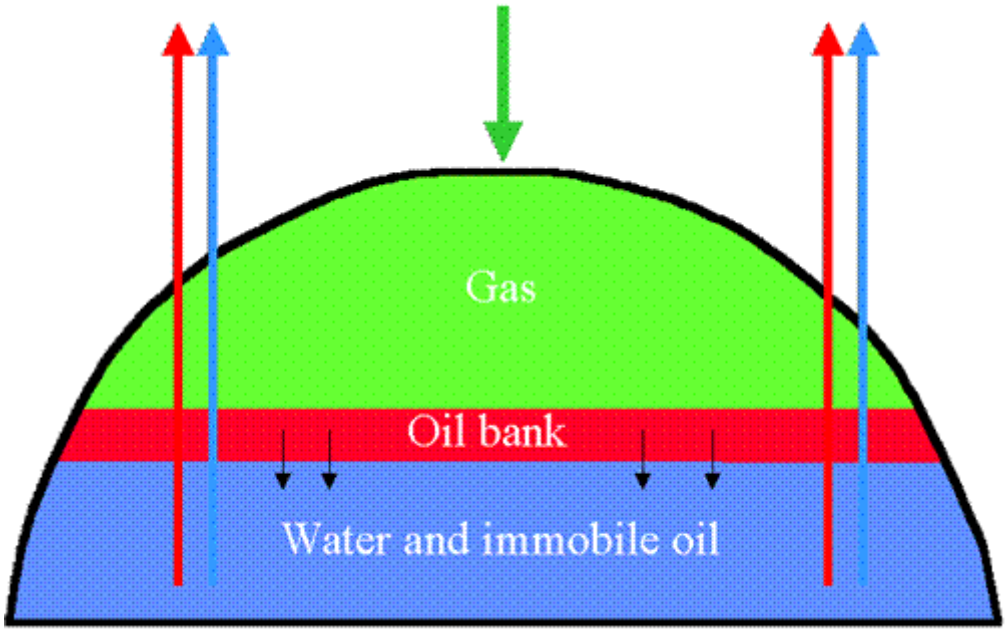

Figure 2.2 Schematic of GSGI technique (Tzimas et al., 2005).

This technique is applied near the end of a reservoir's normal producing life. It is a natural technique for gas sequestration (for instance CO_2 or methane) in that the volume of gas that can be injected depends mainly on the hydrocarbon pore volume[†]. This means, however, that in its classical application, large volumes of gas may have to be injected relatively slowly to fill up the reservoir, while maintaining a stable flood front before oil recovery can be obtained (Tzimas et al., 2005). Projects may need to last for 10-15 years in order to pay for the initial high investment and produce a profit.

Additional wells will also be required and recompletions will also be necessary as the flood front moves downwards. Although the technically achievable oil recovery from this technique may be large, these last two factors significantly reduce the economic value of the oil produced. However, if substantial credit is available from sequestrating gas, the production of incremental oil can be deferred. This would allow for gas injection at a high rate and for a delay in the subsequent oil production: oil would be then produced once equilibration has occurred and the oil has had time to drain downwards under gravity.

Water alternating gas (WAG): this technique is illustrated in Figure 2.3 which shows gas being injected alternately with water downdip and oil being produced updip (Tzimas et al., 2005).

Water is injected alternately with gas in order to help stabilise the displacement. For this technique, applicable to viscous dominated

[†] A pore volume is the volume of water required to replace (flush out) water in a certain volume of saturated porous media.

reservoirs, the ideal is for the flood front to proceed along the reservoir layers and for the gas to be miscible with the oil. Two main mechanisms may operate. Oil displaced primarily by gas rather than water may be more mobile, facilitating production. Gas may also sweep different pathways to water, for example, local highs, recovering oil uncontactable by water injection. These alternative mechanisms give the technique some robustness, particularly with respect to reservoir heterogeneities (Tzimas et al., 2005).

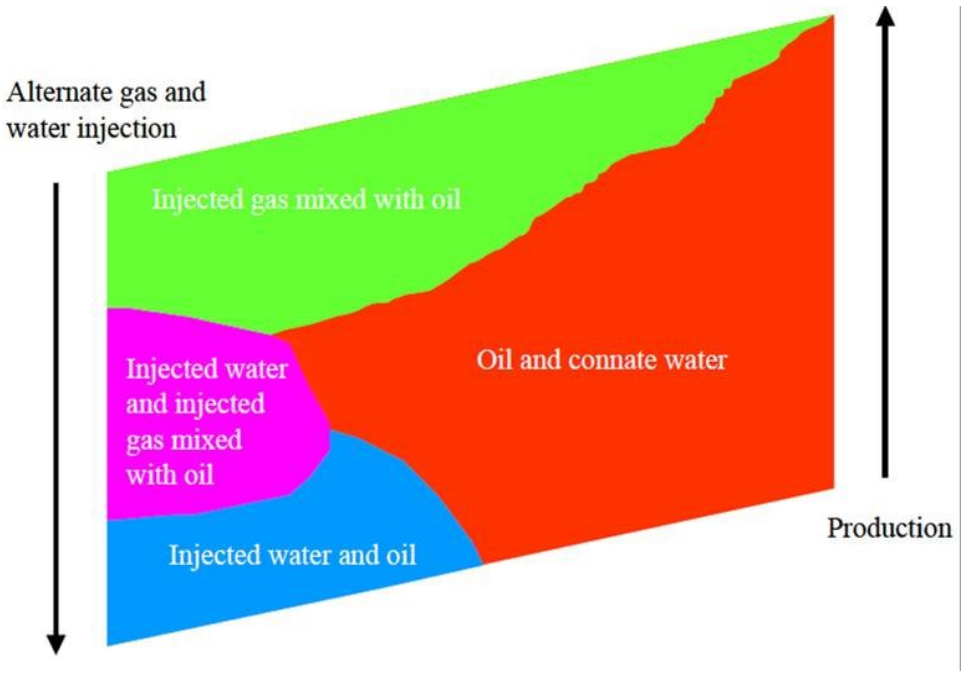

Figure 2.3 Schematic of WAG technique (Tzimas et al., 2005).

WAG can be applied a few years before the normal end of field life and does not necessarily require the drilling of additional wells. However, it has a lower gas sequestration potential as gas may travel through complex pathways, rather than uniformly, so a gas cap may not be formed. Gas may therefore arrive earlier at production wells and so a greater degree of gas re-cycling can occur.

The volume of gas sequestrated therefore depends more on the reservoir heterogeneity and rock-fluid properties, and less on the hydrocarbon volume. On the other hand, incremental oil may be recovered relatively early compared to GSGI, since less of the reservoir needs to be contacted to produce it, so projects can be shorter, say 3 to 5 years. Lower implementation costs also tend to make this technique more economic for IOR than GSGI.

The applicability of these two techniques is summarized in the following table (2.1).

Table 2.1 A comparison of WAG and GSGI techniques (Tzimas et al., 2005)

WAG	GSGI
Short	Long
Early oil	Late Oil
Smaller	Larger
Robust	Only one oil recovery mechanism
Gas re-cycling inevitable	Gas re-cycling avoidable

2.3 Mechanisms of oil recovery by gas injection

The displacement pressure, temperature and oil composition in the reservoir and injected gas determine the mechanism of displacement of oil using gas injection by some of the techniques above described. The selection of what technique is adequate to use is mainly based on the mechanisms of oil recovery that are implemented.

The mechanisms can be broadly characterized by three processes, namely first-contact miscible (FCM); multiple contacts miscible (MCM) and immiscible process (Ahmed, 2001, Khan and Islam, 2007, Kulkarni, 2005, Stalkup Jr, 1985). This section discusses briefly the immiscible process as the topic of interest in this research.

2.3.1 Immiscible process

If a solvent is injected to displace oil at a pressure below the MMP of that oil and solvent, the displacement process will be an immiscible process. The displacement pressure required for an immiscible process is lower than that required for a multiple contact miscible process. Thus, recovery of oil is not very high in an immiscible process because the gas front and the oil do not form a single-phase mixture. Thus, the sweep efficiency of the invading gas front is low and as a result the amount of oil left in the porous medium is slightly larger than that for the multiple contact miscible (MCM) or the first contact miscible (FCM) processes (Nouar and Flock, 1983).

The mechanism of an immiscible process is described with the help of a triangular diagram shown in Figure 2.4. In Figure 2.4, the injected solvent composition is represented by point G and the in-situ oil composition is represented by point 0. The phase envelope for this fluid system at pressure Pi and at temperature T is represented by BCD where point C is the critical point of the fluid mixture. As the injected gas moves forward, it strips off intermediate components from the oil, and the composition of the gas mixture follows the dew-point line (BC) until the composition reaches the limiting point G_1. The limiting point is determined by the tie-line passing through the original oil and the equilibrium oil composition 0e.

In Figure 2.4, it can be seen that the limiting composition (G_1) of the gas phase cannot form a single-phase mixture with the in-situ oil (0). The composition of the oil will follow the bubble point line as the oil is becoming stripped of its intermediate components. The limiting composition of the residue oil will be 0_1. The limiting composition is determined by the tie-line passing through the point of original gas composition (G) and the point of equilibrium gas composition (Ge).

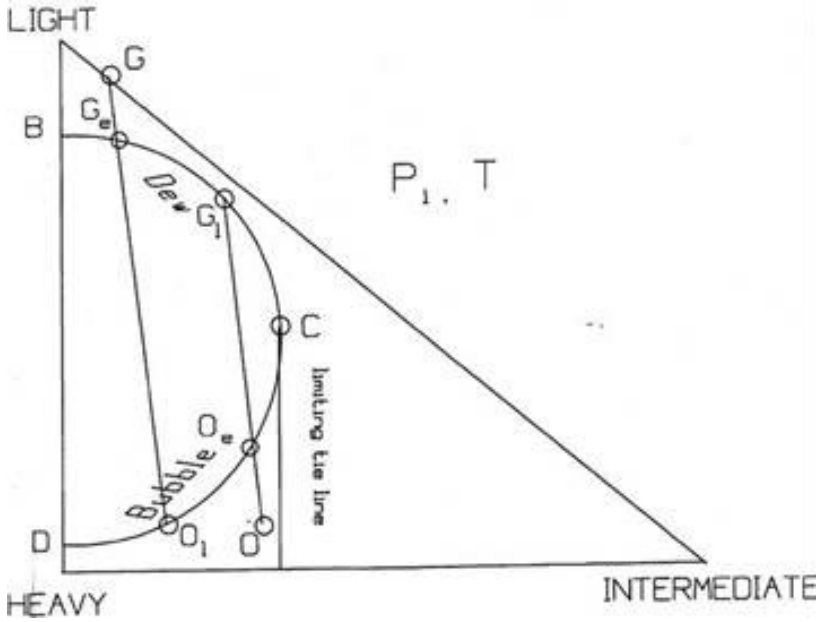

Figure 2.4 Triangular diagram for an immiscible process (Saha, 1993).

When a light gas such as pure methane or nitrogen is used to displace an oil depleted of light hydrocarbons, then the displacement process may possibly be an immiscible process at a displacement pressure within the practical range (138-276) bar (Stalkup Jr, 1985). As a rule of thumb, it can be said that if the compositions of both the injected solvent and the reservoir oil lie to the left side of the limiting tie line in a triangular diagram, the displacement process will be an immiscible one (Stalkup Jr, 1985). To use an immiscible process to recover oil is not a desirable choice because the recovery of oil will be lower than that obtained from MCM or FCM processes. Sometimes, however, due to economic constraints such as the high cost of rich solvent, and technical constraints, such as the problem of boosting the low reservoir pressure, the immiscible process is the only choice for gas flooding operations.

2.4 Steam reforming of hydrocarbons

2.4.1 Definition and reactions

Hydrocarbon steam reforming is an important process in hydrogen

production and it is the basis of gasification-reforming reactions in the DHG process. Hydrogen (H_2) is a valuable material for the chemical and petrochemical industry and it is also used as a clean combustible. The steam reforming process transforms a liquid hydrocarbon feedstock with water in gas phase into a gaseous mixture constituted by CO_2, CO, CH_4, and H_2. The main reactions are the following (Mathiassen, 2003, Melo and Morlanes, 2005):

$$CH_4 + H_2O \Leftrightarrow CO + 3H_2 \quad \Delta H^o_{298} = 206\ kJ.mol^{-1} \tag{2.1}$$

$$CO + H_2O \Leftrightarrow CO_2 + H_2 \quad \Delta H^o_{298} = -41.2\ kJ.mol^{-1} \tag{2.2}$$

$$C_nH_m + nH_2O \Rightarrow nCO + \left(n + \frac{1}{2}m\right)H_2 \quad \Delta H^o_{298} < 0 \text{ where } n > 1 \tag{2.3}$$

$$CH_4 + CO_2 \Leftrightarrow 2CO + 2H_2 \qquad \Delta H^o_{298} = 247\ kJ.mol^{-1} \tag{2.4}$$

$$CH_4 + 2H_2O \Leftrightarrow CO_2 + 4H_2 \quad \Delta H^o_{298} = 165\ kJ.mol^{-1} \tag{2.5}$$

A catalyst, commonly containing nickel as the active component, is used, and the process has come to be known as steam reforming. The process is typically operated with excess steam (S/C > 4) at temperatures above 800 °C. The composition of the product gas generally approaches that expected at equilibrium very closely.

In the case of methane feedstock, the steam reforming reaction (2.1) and the water gas shift reaction (2.2) are reversible. Reaction (2.4) is the difference between reaction (2.1) and reaction (2.2). It is evident from the principle of Le Chatelier that at higher temperatures less methane and more carbon monoxide are present in the produced dry gas composition and that methane content increases with pressure and decreases with increasing S/C ratio (Beyer et al., 2005, Zeinalipour-yazdi and Efstathiou, 2009). This is illustrated in Figure 2.5.

A high hydrocarbon‡ feedstock can instead be fully converted thanks to the irreversibility of the reaction (2.3). However, the produced dry gas composition is also determined by the thermodynamic equilibrium between gaseous species, reactions (2.1, 2.2, 2.4, 2.5) and relies on the operating conditions at which the process takes place: pressure, temperature and steam to carbon (S/C) ratio.

The produced gas composition can be estimated from thermodynamic calculations because it will in most cases be close to that of the equilibrated gas. A list of equilibrium constants may be found in Kemin et

‡ A hydrocarbon with a number of carbon atoms higher than 1 – methane.

al. (2004), Ancheyta-jurez et al. (2001), Jones et al. (2008) and Jim (2006). The overall heat of reactions (2.1)-(2.3) may be positive, zero, or negative, depending on the operating conditions.

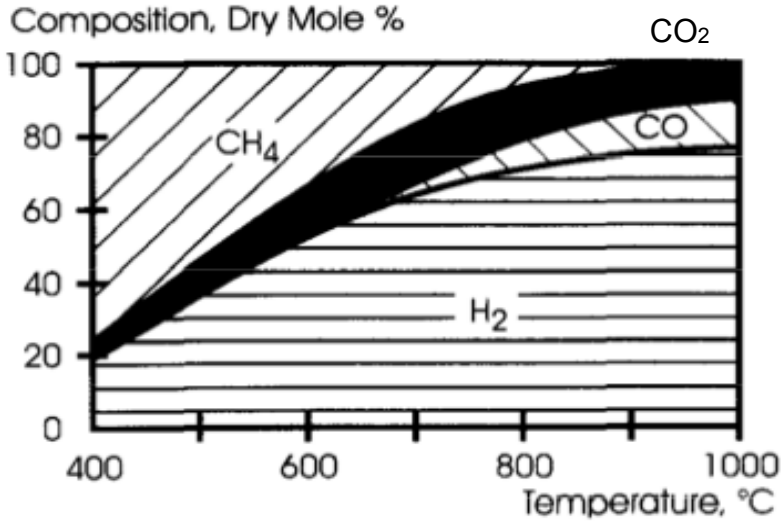

Figure 2.5 Produced dry gas composition in steam reforming using methane feedstock. Pressure= 30 bar, S/C= 4 (Dybkjaer, 1995).

Reactions (2.1) and (2.3) may be accompanied by the following reactions of carbon formation (Beurden, 2004):

$$2\mathrm{CO} \Leftrightarrow C + CO_2 \quad \Delta H^{o}_{298} = -171.66\ kJ.mol^{-1} \tag{2.6}$$

$$CH_4 \Leftrightarrow C + 2\mathrm{H}_2 \quad \Delta H^{o}_{298} = 75.36\ kJ.mol^{-1} \tag{2.7}$$

$$C_nH_m \Rightarrow nC + \frac{m}{2}H_2 \tag{2.8}$$

Reaction (2.6) is normally referred to as the 'Boudouard reaction'. At high temperatures (above 650 ^{o}C), higher hydrocarbons may react in parallel to reaction (2.3) by thermal cracking (pyrolysis or "steam cracking") into olefins which may easily form coke (Beyer at al., 2005, Reyes et al., 2003, Xu et al., 2008, Froment, 2008) via reaction (9) :

$$C_nH_m \Rightarrow Olefins \Rightarrow Polymers \Rightarrow Coke \tag{2.9}$$

Reactions (2.6) and (2.7) are reversible, whereas (2.8) and (2.9) are irreversible for n > 1.

2.4.2 Influence of reaction parameters on produced dry gas composition

In order to obtain the desired produced dry gas composition it is essential to consider the following variables:

- Hydrocarbon feedstock characteristics
- Steam to carbon (S/C) ratio
- Temperature
- Pressure

The feedstock for the reformer can be any hydrocarbon ranging from a hydrogen-rich off-gas or natural gas to heavy naphtha. At a low S/C ratio and at low exit temperatures, the overall reaction is only slightly endothermic or may even be exothermic if the feedstock contains high concentrations of higher hydrocarbons. This is caused by methanation of carbon monoxide formed by the reaction (2.3) reflected in a high content of methane in the product gas. In such cases, it is possible to carry out the process without external heating, i.e. in an 'adiabatic pre-reformer' (Reyes et al., 2003).

However, for the production of gases with lower methane content such as synthesis gas and hydrogen-rich gas, a high outlet temperature is required along with an additional reformer and, the overall reaction becomes strongly endothermic (Beyer at al., 2005). In such cases, Melo and Morlanes (2005) stated that operating conditions of low pressure, high temperature and high S/C ratio are ideal.

Maximum conversion to hydrogen by the reverse shift reaction (2.2) is favoured by a high steam to carbon (S/C) ratio. However, a high steam to carbon (S/C) ratio results in low process efficiency due to the low volume of hydrogen generated per time unit (Melo and Morlanes, 2005). In order to compensate for this, the reformer outlet temperature can be increased. A high temperature with lower S/C ratio also changes the equilibrium of the shift reaction towards hydrogen (Beyer et al., 2005).

In Figures 2.6 and 2.7 the produced dry gas composition at the reformer outlet is shown as a function of the steam to carbon (S/C) ratio and the outlet temperature for a case where the feedstock is naphtha (Beyer et al., 2005).

Traditionally, the steam to carbon (S/C) ratio in reformers has been relatively high due to the risk of carbon formation to the detriment of economic efficiency. The development of new highly active steam reforming catalysts including noble metal based catalysts (Chemiczny, 2007, Benitex et al., 2009, Santos et al., 2003, Kumar et al., 2008), the use of sulphur passivated reforming (Santos et al., 2003, Andrew, 1969), and the installation of adiabatic pre-reformers (Sperle et al., 2005, Pasel et

al., 2004) have made it possible to reduce the (S/C) ratio to below 4-6 using naphtha as feedstock.

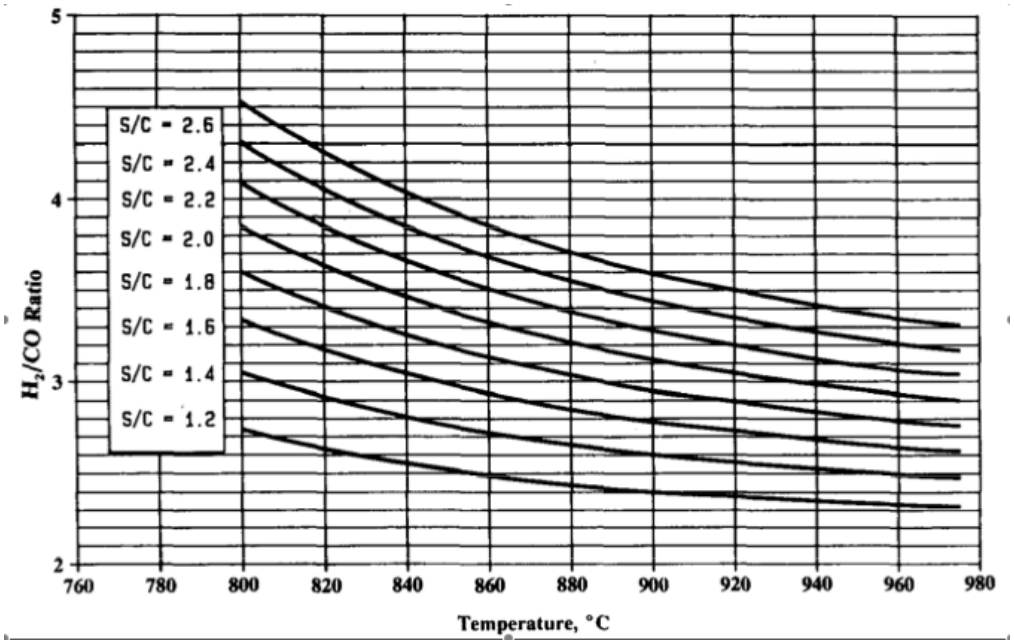

Figure 2.6 Hydrogen to carbon monoxide ratio in produced dry gas versus temperature. Naphtha feedstock, pressure 21.6 bar (Dybkjaer, 1995).

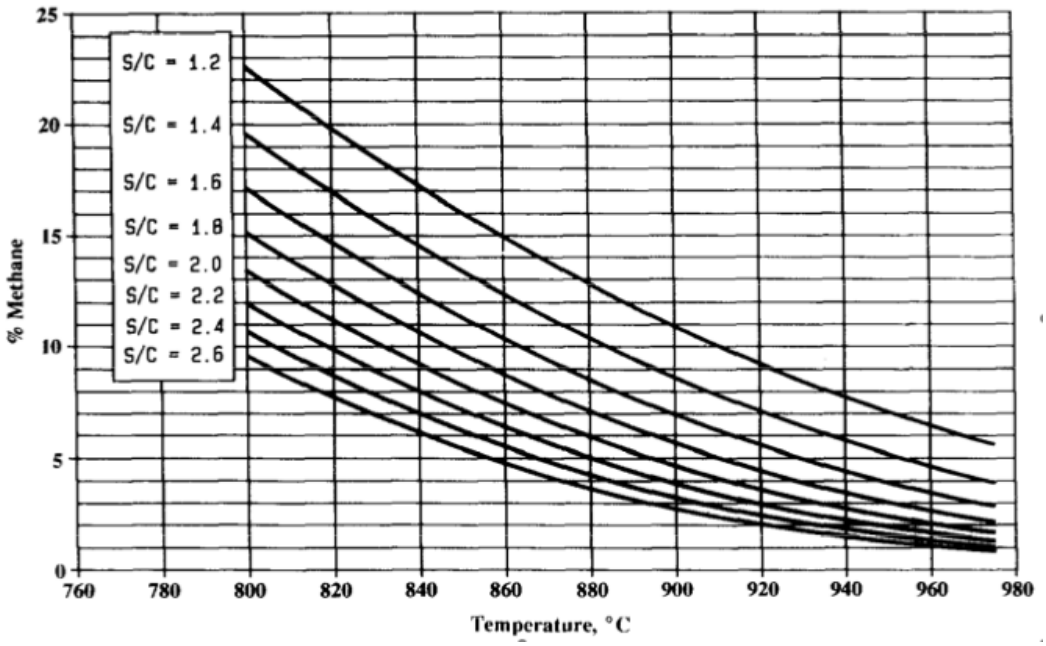

Figure 2.7 Methane content in produced dry gas versus temperature. Naphtha feedstock, pressure 21.6 bar (Dybkjaer, 1995).

Pressure strongly affects reaction (2.1) while reactions (2.2, 2.3) are not affected. Irreversibility of higher hydrocarbon first reaction is the main cause. However, as was mentioned previously, the produced dry gas

composition is a complex consequence of thermodynamic equilibriums from reactions involved in the steam reforming process. Every reaction, including those to form carbon deposits, has specific reaction conditions in which particular product or reactant formation are favoured.

For instance, an increase in pressure results in high methane content using higher hydrocarbons (naphtha) feedstock and results in low hydrogen content when methane is used as feedstock instead. In such cases, the rest of the reaction parameters are adjusted to obtain the desired produced dry gas.

Normally, the highest acceptable pressure is chosen on the basis of the desired produced dry gas. In other cases, the pressure is dictated by the requirements of the downstream separation or purification processes or simply by the initial conditions of the reactor, i.e. a DHG process where pressure is dictated by an oil reservoir which is relatively high, (80-180) bar approximately.

2.4.3 Catalysts used

The steam reforming reaction takes place on the surface of a solid catalyst which should have the following characteristics (Melo and Morlanes, 2005):

- High mechanical resistance
- High thermal stability
- High resistance to carbon formation
- High catalytic activity
- High selectivity towards hydrocarbon gasification-reforming

Type: Commercially, nickel based catalysts are used widely since they provide a good activity/cost ratio. Nickel is supported by a material that confers sufficient mechanical and thermal resistance for the process, aluminium oxide with additives that prevent carbon formation are normally used (Rostrup-Nielsen, 1975, Melo and Morlanes, 2005, Beurden, 2004, Xu et al., 2008, Seo et al., 2008, Andrew, 1969, Sperle et al., 2005, Mathure et al., 2007, Melo and Morlanes, 2008). Alkali addition (KO_2) (Melo and Morlanes, 2005, Melo and Morlanes, 2008) and basic supports (MgO) are commonly used for this purpose (Pan et al., 2005, Golebiowski et al., 2004).

Commercial nickel-based catalysts usually provide enough activity to reach a full conversion within the limits given by the mechanical design. The approach to equilibrium for steam reforming is closely related to the effective catalyst activity above 700 ºC (Christensen, 2005, Melo and Morlanes, 2005, Melo and Morlanes, 2008, Kemin et al., 2004, Mathure et al., 2007, Yanhui and Diyong, 2001, Dreyer et al., 2006, Goud et al., 2007, Sharma et al., 2007).

In particular, Ni/Al_2O_3 catalysts have been recognized as typical catalysts for steam reforming due to their low cost and high catalytic activity (Melo and Morlanes, 2008). The Ni/Al_2O_3 catalysts, however, require high reaction temperatures and excess amounts of steam to prevent carbon deposits on the catalyst surface.

The catalytic activity of Ni/Al_2O_3 is closely related to both nickel content and nickel dispersion, but these two factors have opposite effects on the catalytic activity. With increasing nickel content, for example, the catalytic activity of Ni/Al_2O_3 increases due to the increased number of active nickel sites, but the dispersion of nickel particles decreases due to the sintering of nickel species. Hence, the nickel content of conventional Ni/Al_2O_3 catalysts used in the steam reforming reactions does not exceed 12 wt. % to avoid severe sintering of nickel particles during the reactions. However, they may show an inferior catalytic activity due to the insufficient number of active nickel sites.

Many attempts have been made to increase the catalytic activity of Ni/Al_2O_3 in steam reforming (Seo et al., 2008, Takenaka et al., 2008, Santos et al., 2003, Andrew, 1969, Sperle et al., 2005). The performance of Ni/Al_2O_3 catalysts in the steam reforming reactions depends not only on the nature and structure of active nickel, but also on the chemical and physical properties of Al_2O_3 (Seo et al., 2008).

Apart from nickel catalysts, catalysts based on precious metals (noble Group VIII metals) such as platinum or rhodium are also used, taking advantage of the coke reduction generated and their high catalytic activity (Seo et al., 2008, Takenaka et al., 2008, Sharma et al., 2007, Stefanescu et al., 2007).

However, the high cost associated with these precious metal catalysts is driving some researchers to develop alternative catalysts such as Co-based catalysts (Chemiczny, 2007, Andrew, 1969, Kumar et al., 2008, Stefanidis et al., 2008, Chen et al., 2008).

Size: The particle size seems to be an important factor for steam reforming catalyst activity. Recent studies have been aimed at developing catalysts of a smaller size in order to increase (Rostrup-Nielsen, 1975):

- Activity, by increasing geometric surface area per unit volume (GSA)
- Heat transfer coefficient (HTC), by improving the catalyst packing and contact with the tube wall
- Decreased catalyst bed pressure drop (PD), by increasing the pellet voidage and/or size

In 1941 the first true shaped catalyst was introduced, which was a ring that showed a significant improvement over the ordinary solid cylinders used previously. Since then, multiple holes or adding flutes to the outside

structure have been considered to order to increase the geometric surface area. An example of these variations is shown in the Figure 2.8 with KATALCO catalysts.

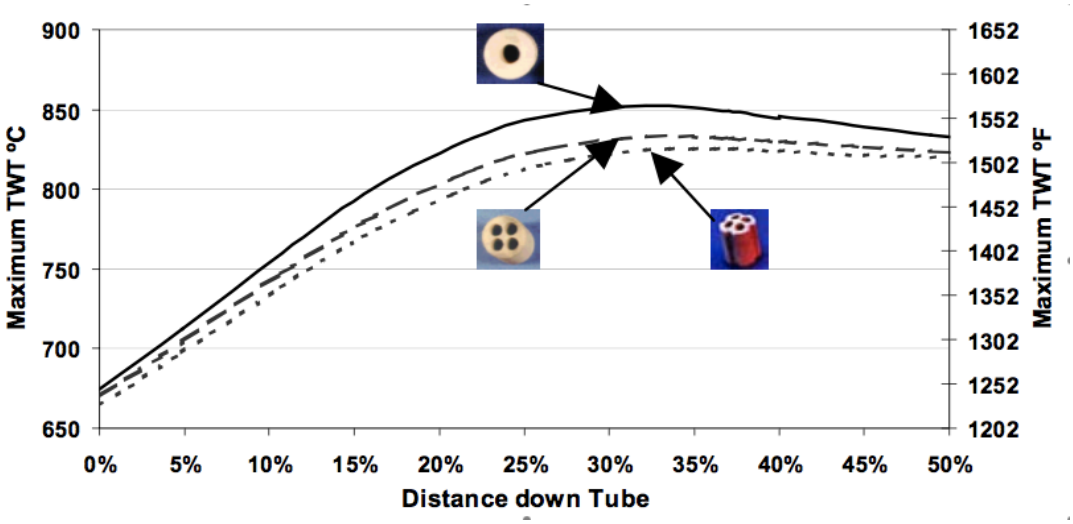

Figure 2.8 Tube wall temperature (TWT) with different KATALCO catalyst generations (Rostrup-Nielsen, 1975).

The catalysts can be also updated in order to be more carbon resistant: smaller sizes have been reported to be better (Christensen, 2005). Borowiecki (1987) reported a higher carbon deposition rate on larger Ni particles during steam reforming of butane. Chen et al. (2008), found that the size of the nickel crystal had an influence on the coking rate. They indicated that a lower coking rate occurred on the smaller sized Ni particles.

However, small nickel crystals will sinter quickly at high temperatures during reaction. This may be partly prevented by a stable micropore system because the nickel particles may hardly grow larger than the pore diameter of the support.

In summary, effective catalyst activity is a complicated function of the particle size and shape and the operating conditions.

2.4.4 Deactivation of catalysts used

According to Christensen (2005) there are three primary causes for catalyst deactivation in steam reforming:

- Carbon formation
- Sintering
- Poisoning

In this research, carbon formation and sintering will be discussed as the main topics of interest in this research.

Carbon formation: Whisker carbon is the principal product of carbon formation in steam reforming (Christensen, 2005 and Helveg et al., 2011), and it is the most destructive form of carbon over nickel catalysts. It may be formed from higher hydrocarbons or from methane if the S/C ratio is too low (Helveg et al., 2011).

The carbon whiskers have high mechanical strength and destroy catalyst particles when they hit the pore walls. This process may result in increasing pressure drop and hot tubes, which complicates the operation (Christensen, 2005). The mechanism for carbon whiskers has been described as being carbon transport through the bulk of the nickel (Helveg et al., 2011).

The carbon formation in whisker form can be minimized by ensemble size control and by preventing carbide formation. It is suggested that carbide is the essential intermediate route to coke in whisker form and it is assumed that prevention of carbide formation on the surface slows down the carbon formation process (Rostrup-Nielsen, 1975).

Minimizing carbon formation is also a function of the support. Promoting the catalyst with alkali has been known to enhance the carbon resistance. A spillover of steam (or OH^- species) from the catalyst support to the nickel surface is assumed to occur during steam reforming. Alkali promoted catalysts have ten times larger surface coverage of H_2O and OH^- than non-promoted catalysts. It has been reported [53] that equilibrium coverages and heats of adsorption were lower on magnesia, with a high spillover effect, than on non-promoted catalysts (Shinku et al., 2008).

Sintering: This is an important cause of the deactivation of nickel particles in steam reforming catalysts. There are many parameters that influence the sintering process: reaction temperature, pressure, catalyst composition, structure and support morphology (Christensen, 2005). Rostrup-Nielsen (1975) and Twigg (1989) have studied those parameters more deeply and have indicated that elevated temperatures and the presence of water are the most important. Results showed that they may rapidly accelerate sintering.

Sintering is the loss of surface area of the active species of the catalyst. Two different sintering mechanisms have been proposed: the atom migration mechanism and the particle migration and coalescence mechanism. Atom migration refers to the process where metal atoms are emitted from one metal particle and captured by another metal particle. In the particle migration process, the particles themselves move over the support and collide to form larger particles. The driving force for both processes is the difference in surface energy, which varies inversely with the particle size (Bartholomew, 2001). The shape of the particle size distribution is characteristic for the different sintering mechanisms.

2.4.5 The process in industrial plants using naphtha feedstock

Steam reforming for hydrogen production was first applied commercially by the Standard Oil Company of New Jersey (now ExxonMobil) in 1930 at Baton Rouge, USA. However, a lower temperature version of steam reforming that allowed the production of methane for residential use attracted attention around the world in the 1960s (Reyes et al., 2003).

This process developed the use of very light cut from crude oil (naphtha/higher hydrocarbons) as feedstock and began in regions of the world where natural gas was not readily available. Later on it was extended by the Exxon Company. Highly paraffinic naphtha was destined to steam reforming while highly aromatic naphtha, less desirable here, was destined for another type of process known as catalytic reforming (Reyes et al., 2003).

The use of the same name, reforming, for both processes has been a source of confusion, but it should be clearly understood that they have no connection to one another. The catalytic reforming process is not operated with steam as a reactant and is utilised for producing high-octane-number aromatic hydrocarbons in gasoline with the aid of so-called ´bifunctional´ precious metal catalysts (Reyes et al., 2003).

Highly active and stable nickel catalysts for application in ´residential gas´ or methane production were also developed in the 1960s and their use for hydrogen production directly from naphtha was applied some years later. Thanks to that, today we can think of overall steam reforming using naphtha feedstock as a process that involves two major parts: production of methane followed by conversion of that methane into H_2 and CO/CO_2 as primary products (Holladay et al., 2008, Damle et al., 2008, Pan et al., 2005, Udengaard et al., 2004, Seo et al., 2008, Önsan, 2007, Seo et al., 2008).

Nowadays, industrial steam reforming plants using naphtha feedstock commonly involve two sections although it is also possible to find a single fired tubular reformer only. Those sections are:

- An adiabatic prereformer
- Tubular reformers

Adiabatic prereformer: The adiabatic prereformer converts naphtha into a mixture of methane (CH_4), steam (H_2O), carbon monoxide (CO), carbon dioxide (CO_2) and hydrogen (H_2). Operating conditions are: elevated pressures (30-40) bar, reaction temperatures of (400-450) °C and S/C ratios in the range of 8-12 to limit the formation of carbon deposits (coke) on the catalyst (Froment, 2008, Takenaka et al., 2008).

The initial action in the prereformer is the decomposition of the reactant

hydrocarbon and then the formation of CO and H_2 as primary products as a first step. Reaction (2.10) is an example taking n-hexane as a model and it represents this step by the overall reaction (Reyes et al., 2003):

$$C_6H_{14} + 6\mathrm{H_2}O \Rightarrow 6\mathrm{CO} + 13\mathrm{H_2} \quad \Delta H^{o}_{298} = 954.59\ kJ.mol^{-1} \tag{2.10}$$

This reaction is highly endothermic. The second step of the process consists of reaction (2.3) and the reverse of reaction (2.6) which are both exothermic and which are close to being equilibrated at operating conditions. Increasing the pressure and decreasing the temperature drives the reaction (2.6) to the left, as desired for prereformers (Reyes et al., 2003).

The low temperature requires a catalyst with a high surface area to obtain sufficient activity and resistance to poisoning especially by sulphur. The optimal shape of the catalyst particle depends on the specific application and on the plant capacity. In many cases catalyst particles of a cylindrical shape in a size of 3-5 mm are used (Reyes et al., 2003). This particle provides a large surface area for access of the gas into the pore system.

The pressure drop over the prereformer is often low (< 0.4 bar) for small or medium-scale plants even with such particles giving low void. For large-scale plants, a shape-optimised catalyst will be an advantage and particles in the form of rings or large cylinders with axial holes are usually the preferred choice for minimum pressure drop and high activity (Reyes et al., 2003).

Deactivation of the prereformer catalyst may take place during operation. The cause is typically sulphur but sintering and other poisons may also play a role. The approach to equilibrium and the content of higher hydrocarbons in the prereformer exit are generally close to zero and constant throughout the operation period of the prereformer (Reyes et al., 2003).

Carbon formation here is an irreversible reaction that can only take place in the first part of the reactor with the highest concentration of higher hydrocarbons. Carbon may form even if thermodynamics predict no affinity at equilibrium. The criterion for carbon formation can be described as a kinetic competition between the carbon forming and steam reforming reactions.

Tubular reformers: In industrial practice, tubular reformers are catalyst-filled tubes placed in the radiant part of the heater. Typical inlet temperatures are 550-750 ºC, and the produced gas leaves the reformer at 750-950 ºC (Christensen 2005). Here, methane generated previously in adiabatic prereforming using naphtha feedstock is converted to hydrogen, carbon monoxide and carbon dioxide by steam reforming.

In a typical reformer furnace 50 % of the heat produced by combustion in the burners is transferred through the reformer tube walls and absorbed by the process. The other half of the fired duty is available in the hot flue gas and is recovered in the waste heat section of the reformer for preheating duties and for steam production. This makes the overall thermal efficiency of the reformer approaching 95 % (Christensen 2005).

A typical reformer reactor contains 40-300 tubes normally made of centrifugally cast high alloy nickel chromium steel (HK 40), a material that contains 25 wt. % chromium and 20 wt. % nickel. Recently, micro alloy has been used and it contains 25 wt. % chromium, 35 wt. % nickel, niobium and traces of other elements like zirconium and titanium (Williams et al., 1993). The internal tube diameter varies from 9 to 16 cm, and the heated length of the tube is normally within the range of 6-12 m. Figure 2.9 shows a Topsoe reformer furnace (Mathiassen, 2003, Beyer et al., 2005).

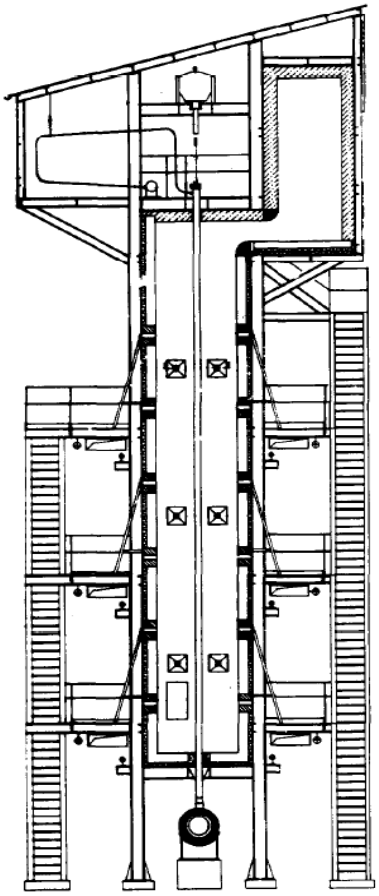

Figure 2.9 Reformer furnace designed by Topsoe for high outlet temperature (Dybkjaer, 1995).

Although the basic reformer design on the market has not changed much over the last decades, there have been considerable developments in the field of reformer tube materials, process calculations and catalysts. Optimisation of the tube pitch, the tube-to-tube distance, tube row

distance, higher number of tubes, lower heat exchange area and new materials used for tubes are the main topics for research and industrial applications (Rostrup-Nielsen, 1975, Dybkjaer, 1995, Reyes et al., 2003, Lomax, 2001).

Chemical engineering advances have also enabled the use of sophisticated computer models to simulate the reformer performance on the basis of the individual burner duties, the feed stream characteristics, the properties of the catalyst and the reformer geometry (Kemin et al., 2004, Ancheyta-jurez et al., 2001, Jones et al., 2008, Nummedal et al., 2005, Schwaab, 2009, Froment, 2008, Xu and Froment, 1989, Wei and Iglesia, 2004, Abreu et al., 2008).

Figure 2.10 shows the materials used for reformer tubes during recent decades. The high alloy reformer tubes are expensive and account for a large part of the reformer costs. The reliability of the tubes is also important, because tube failure could result in long down-periods for retubing and hence expensive loss of production (Yong and Qiang, 2005, Myer, 2006).

The maximum allowable stress value in the tube is strongly influenced by the maximum tube wall temperature (Mathiassen, 2003). This phenomenon can be shown in Figure 2.11 where micro-alloys offer significant benefits over older materials in the areas of inlet pressure, inside diameter of the tubes, peak tube wall temperature and tube design temperature (Rostrup-Nielsen, 1975).

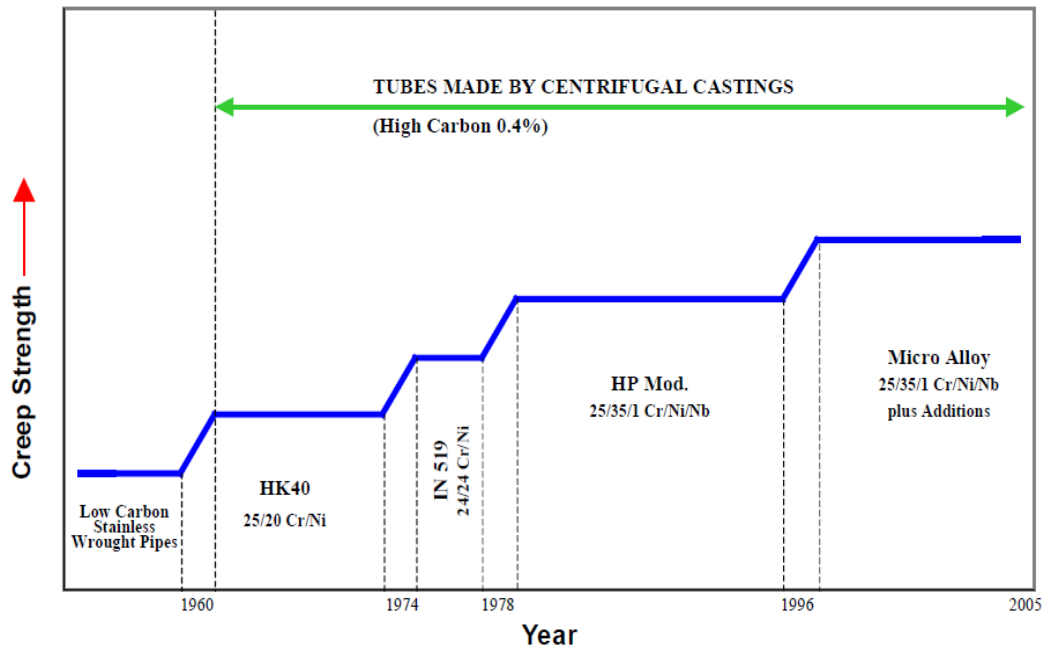

Figure 2.10 Reformer tube materials (Christensen, 2005).

Tube inlet pressures have increased from around 20 bar up to more than 40 bar and the inner diameter of the reformer tubes has increased in stages from 3.8 inch (97.2 mm) to 5 inch (127 mm) over the last decades (Rostrup-Nielsen, 1975).

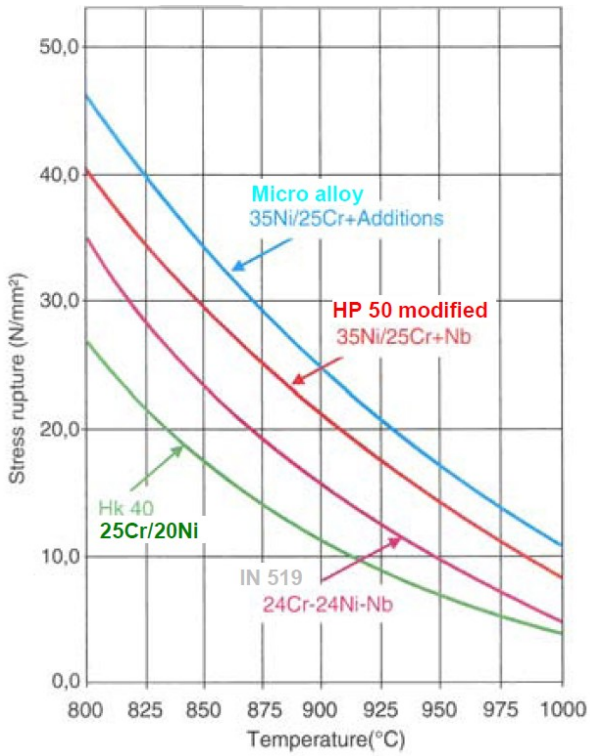

Figure 2.11 Stress-to-rupture values of reformer tube materials (Christensen, 2005).

2.4.6 Numerical models to calculate produced dry gas composition

The use of numerical models is an invaluable tool in the design and optimisation of the steam reforming process. The chemical conversion versus time ratio can be determined by combining reaction kinetics, pore diffusion, pressure drop, and the effects of catalyst deactivation and poisoning.

Several numerical models have been developed based on thermodynamic or kinetic principles at industrial and lab scale using different hydrocarbons as feedstock. Some of them are even currently employed in plants around the world to maximise operation efficiencies despite their limitations or the necessity for more computation. To compensate for this, investigations still continue to simulate more closely industrial runs and new reformer designs (Hayes and Mmbaga, 2013).

Reformer modelling can be classified into four groups (Padban and

Becher, 2005, Johnson Matthey Catalysts, 2010):

- Furnace side modelling flame impingement and radiant and convective heat transfer.
- Gas feed systems modelling the flow in fuel and process gas feed headers.
- Tube side modelling detailed kinetics, heat transfer and pressure drop of the process.
- Process models as an entire system.

Nowadays, the literature review shows several examples of numerical models related to all of these. Our interest is focused on the tube side modelling group since predictions of dry gas composition in steam reforming can be obtained here.

There are two ways to run tube side numerical models. One way considers reformer dimensions (1-D, 2-D and 3-D) and another considers process state: steady or unsteady (Papageorgiou and Froment, 1995, Shayegan et al., 2008, Kvamsdal, et al., 1999, Pedenera et al., 2003, Quinta-ferreira et al., 1995, Sreejith et al., 2013, Padban and Becher, 2005, Galluci et al., 2004, Shayegan et al., 2008).

Numerical models by reformer dimensions: In the one dimensional axial model (1-D) temperature and concentration profile are simulated while the mass/energy balance is solved by empirical equations (Papageorgiou and Froment, 1995). Two-dimensional (2-D) models add radial concentration (Kvamsdal, et al., 1999, Pedenera et al., 2003, Quinta-ferreira et al., 1995, Shayegan et al., 2008, Marin et al., 2012a, Marin et al., 2012b) while three-dimensional (3-D) models are able to show species distribution in three directions.

Although the latter require more computation, they can help to further understanding of heat/mass transfer in the reformer. This is crucial in steam reforming since it is well known that steam reforming operates mainly in a diffusion-controlled regime where the heat/mass transfer drives the conversion. A few 3-D models have been developed. Quiceno et al. (2006) demonstrate a 3-D model for methane steam reforming with catalytic partial oxidation over platinum gauze where they coupled flow and detailed surface reaction chemistry in the study.

Numerical models by process state: Produced dry gas composition in steam reforming is strongly determined by equilibrium reactions; hence, thermodynamic models are ideal for use here. They enable the calculation of equilibrium constants and they predict equilibrium dry gas composition (Karamarkovic and Karamarkovic, 2010) enabling evaluation of the influence of given parameters on the process at steady state. However, such models provide no information about transient state (unsteady). Moreover, thermodynamics by itself is not enough to determine reactor

sizing and design. In this case, a kinetics model might be very helpful.

ASPEN PLUS is becoming the preferred simulation tool for steam reforming at steady state (Castello 2013, Wahyudiono et al., 2012) while CFD (Computational Fluid Dynamics) is used for models at unsteady state (Johnson Matthey catalysts, 2010).

Both allow the development of powerful numerical models for design, performance monitoring, optimization and business planning since any design on an industrial scale for steam reforming must take into consideration thermodynamic calculations or theoretical maximum in the equilibrium as their starting point followed by fluid mechanics (Shayegan et al., 2008, Kavsmdal et al., 1999, Galucci et al., 2004, Pedenera et. al. 2003, Padban and Becher, 2005, Nahar and Madhani, 2010).

The first numerical model trial for thermodynamic calculations, which is commonly named theoretical maximum in steam reforming, was carried out by Rostrup-Nielsen (1984) and was based on computer techniques developed previously by Kjaer (1972). Rostrup-Nielsen listed some equilibrium constants and, therefore, compositions in the equilibrium. Currently, they are considered to be the basis of any numerical model developed so far (Turpeinen et al., 2008).

Years later, other techniques for the estimation of compositions in the equilibrium were published. Twigg (1989) using his knowledge of the thermodynamic data, reports graphs from which concentrations of reactants in the equilibrium after reactions can be determined for specified feedstocks and usual operating conditions, temperatures of (650-950) ºC and pressures lower than 30 bar.

So far, no numerical studies at downhole gasification (DHG) conditions, that is, the higher pressure of (80-180) bar, have been reported. Numerical studies have showed maximum pressure of 30 bar (Bhatta and Dixon, 1967, Abashar, 2013, Wang and Wang, 2010) and one exceptional study showed a numerical model at 70 bar approximately using ethanol feedstock with application in fuel cell vehicles (Papadias et al., 2010).

Thus, it was very challenging to carry out calculations of theoretical maximum or composition in the equilibrium for the DHG process using its typical operating conditions of pressure (up to 160 bar) and temperature (600-650) ºC with methane and naphtha (n-heptane as model surrogate). It was equally challenging to carry out sensitivity studies of pressure and temperature to predict DHG behaviour in terms of conversion and H_2 in produced dry gas (vol. %) in a very wide range of pressure (2-180) bar and temperature (500-900) ºC using methane and naphtha.

Our first trials were carried out using the commercial chemical simulator ASPEN PLUS by Gibbs free energy minimisation whose numerical results

are described and analysed in chapter 7.

Turpeinen et al. (2008) carried out a thermodynamic analysis of an alternative hydrocarbon-based feedstock conversion to hydrogen using ASPEN PLUS. The alternative feedstocks were coke oven gas, refinery gas and biogas. Specific energy consumption and specific CO_2 were used as the indicators for the production performance. A steam reforming process using natural gas feedstock was used as reference. Results demonstrated that hydrogen can be produced efficiently from an energetic point of view and in an environmental-friendly way.

Another numerical study of theoretical maximum or composition in the equilibrium using ASPEN PLUS was carried out by Alexander Shirley (2005) in his doctoral thesis, *A transient steam reforming process to produce hydrogen from methane for use in fuel cells,* who carried out manual calculations as a first step to validate the use of ASPEN PLUS as a simulation tool for steam reforming. Additionally, he showed that steam reforming reactions are favoured by low pressure and high temperature with conversions approaching 100 % at 900 ºC using methane feedstock. High steam to carbon (S/C) ratios improved conversion but they decreased hydrogen yield and process economic efficiency.

2.5 Downhole gasification (DHG) for improved oil recovery

2.5.1 Downhole gasification (DHG) process

Downhole gasification (DHG) is a new light oil recovery technique, which has potential application in depleted, or partially depleted, light oil reservoirs. The DHG process patented by Ian Davidson, who was the Managing Director of Scotoil Group, UK in 2001, is based on the principle of inert gas generation by gasification-reforming (steam reforming reactions) of hydrocarbons from the reservoir (Davidson, 2001).

Gasification-reforming is the term used in this research for the chemical reactions involved in DHG. ´Gasification´ is so named since the aim is to convert hydrocarbon feedstock into a gaseous mixture of H_2, CO, CO_2, CH_4 and ´reforming´ is so named, since the process is carried out through steam reforming reactions.

The produced gas is driven into the gas cap in order to enable an incremental oil recovery via GSGI (Gravity stabilised gas injection) or another suitable immiscible process for gas displacement such as WAG (Water alternating gas), where H_2 is the main gas on account of its lower solubility in oil and water in comparison to CO, CO_2 and CH_4. The new technique of oil recovery considered as IOR has a high potential application in depleted light oil reservoirs where the pressure is around 200 bar or less.

The economics of the DHG process look attractive according to studies done by Greaves et al., (2006), Greaves et al., (2008), where the cost of oil production per barrel is relatively low, especially if heat is recovered from the hot gas stream. The hydrogen generated can be stored in the reservoir and is also a valuable resource which may be commercialised after maximum oil recovery is reached.

The gas can be produced by using a specially designed gasification unit shown in Figure 2.12 which mainly consists of a vaporiser and a gasifier (called ´gasifier-reformer´ in this research to distinguish it from the typical industrial steam reformer). The vaporiser is used to produce near-stoichiometric amounts of hydrocarbons and water as a gas feed stream to the gasifier. The composition of the vaporised gas comprises hydrocarbon (HC) gases (mainly methane), certain oil/light naphtha fractions and water (steam).

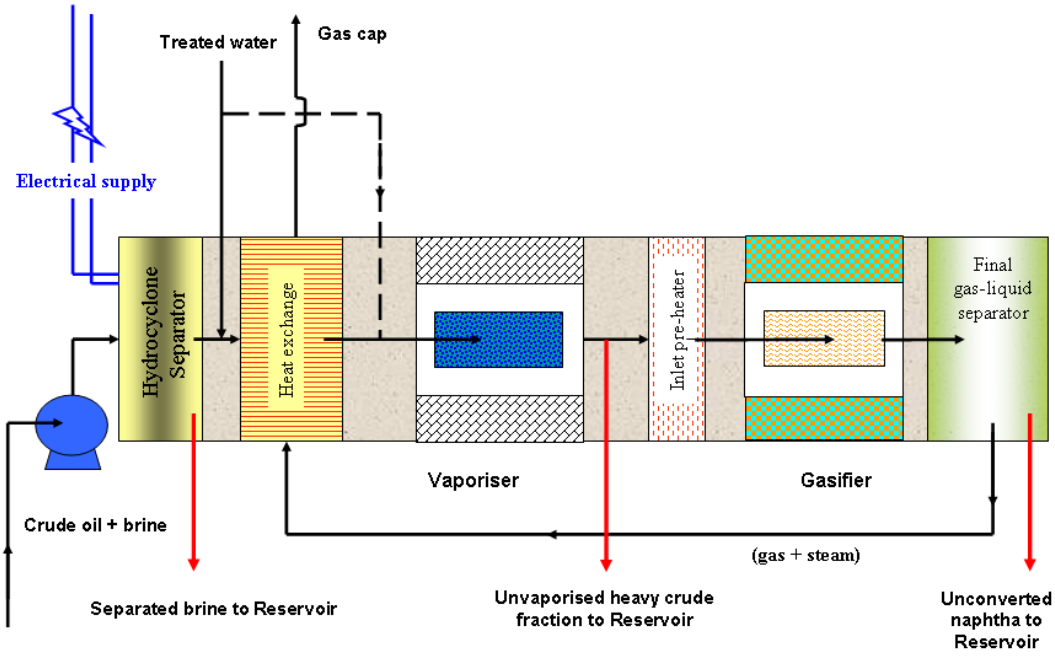

Figure 2.12 Concept of downhole gasification unit (Greaves et al., 2004).

The vaporisation process of part of the crude oil is implemented to separate the light ends (C_1~C_{10}) from the heavy ends which contain most of the catalyst poison elements such as sulphur and chlorides, in order to maximize catalyst life and, therefore, life of the gasifier-reformer. The light ends from the vaporisation are fed into the gasifier-reformer, while the heavy ends are discharged into the oil production stream. A light oil typically contains up to about 1.00 % total sulphur, mainly mercaptanes (Greaves et al., 2008), although the light end fraction will usually contain much less, tens or a few hundred ppm.

The DHG process of this vaporised feed occurs within the gasifier-

reformer and is based fundamentally on steam reforming reactions at the high pressures proper to oil reservoirs. The reactions were described in the section 2.4.1 (Equations 2.1-2.8), which convert hydrocarbons into hydrogen (H_2), carbon monoxide (CO), carbon dioxide (CO_2) and methane (CH_4).

The produced gas may also contain water and unconverted hydrocarbons. The process may also involve the use of a suitable catalyst (Greaves et al., 2008). At reservoir scale, DHG involves four sub-systems:

- Downhole pump
- Vaporiser
- Gasifier-reformer
- Gas charge line (riser)

The DHG assembly can be attached to horizontal or vertical wells. Figure 2.13 and 2.14 show the DHG unit attached to producer wells in the reservoir. The produced gas is directed into a gas cap formation in the reservoir and any gas production is therefore limited to those gases which are released from crude oil during its production process. In the figure, the section comprised of the vaporiser and gasifier-reformer units is referred to as the downhole gasifier. Some potential advantages of DHG can be enumerated according to Greaves et al. (2008):

- No surface compression system required.
- Package gasifier-reformer unit(s) can be installed in a wide range of light oil reservoirs, if equipped with horizontal or extended reach well(s).
- Gasifier-reformer units can be sold ‘off-the-shelf’ and supplied to small field operators to boost recovery from depleted/mature reservoirs.
- Applicable to large and small reservoirs.
- Can be installed in remote reservoirs, using portable electricity generators.
- Potentially large market, especially for small operators.
- Can operate at periods when electricity is cheap.
- Gas generated downhole is stored in the gas cap, to be produced later.
- If a water-gas shift reaction is predominant, hydrogen may be a major product gas.
- The number of gasifier-reformer units can be tailored to particular reservoir conditions.
- The gasifier-reformer unit cost ($\$.MMSCF^{-1}$) is comparable to other gas injection techniques, but without the large infrastructure installation cost.

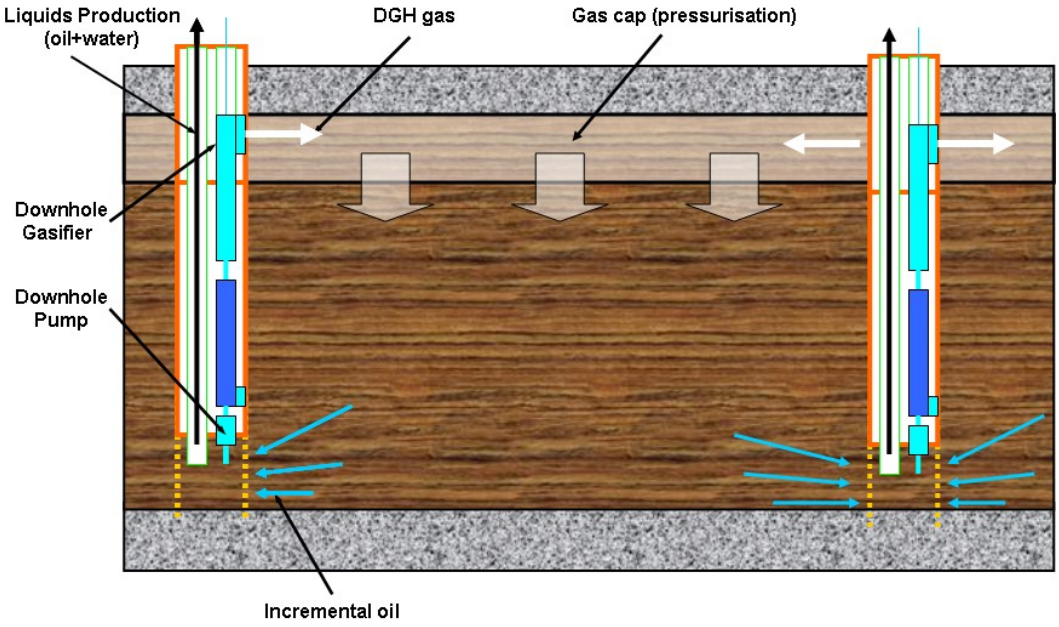

Figure 2.13 Concept of downhole gasification unit into light oil reservoir with vertical producer well (Greaves et al., 2008).

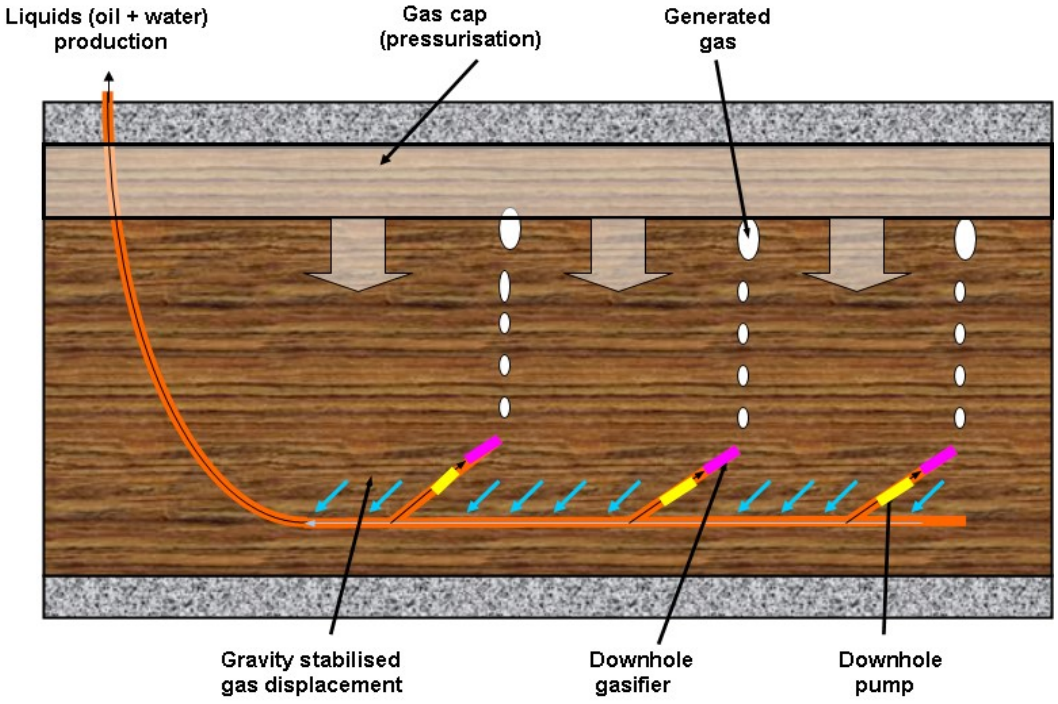

Figure 2.14 Concept of downhole gasification unit into light oil reservoir with horizontal producer well (Greaves et al., 2008).

2.5.2 State of the art

The DHG process is designed mainly as an improved oil recovery technique for light oil reservoirs with ºAPI gravity greater than 30 ºAPI, and with additional possible application to heavier crudes in the ºAPI gravity

range (20-30) ºAPI. Preliminary simulation studies (Greaves et al., 2004) indicate that DHG can be applied in reservoirs that have been previously water flooded, or depleted to a low residual oil level. Not too low however: economic factors probably favour residual oil levels of not less than 30 %. Those reservoirs not worked for reasons of marginality, size or location might also be able to be exploited by using DHG (Greaves et al., 2005, Greaves et al., 2006).

One of the main concerns of this process is the operating pressure required for the success of the DHG process in a reservoir. Pressure in light oil reservoirs is usually much higher than that used on the surface for steam reforming plants. For steam reforming plants, pressure is low because chemical reactions are thermodynamically favoured by high temperature and low pressure. This apparently would limit DHG implementation. However, biomass gasification technologies demonstrate the contrary.

Biomass gasification technologies produce hydrogen and energy at operating conditions very similar to those used by DHG and they are currently in the implementation stage (Dermibas, 2010, Knezevic et al., 2010, Susanti et al., 2010) which is an indication of their technical and economic feasibility.

Biomass gasification performs with hot pressurised water using organic wastes feedstock around the critical point, T>374.15 °C; P>221 bar. The process is based on steam reforming reactions among other chemical reactions (partial oxidation and autothermal reforming) to obtain considerable conversions. Depending on the feedstock used, the total produced dry gas H_2, CO, CO_2 and CH_4 may be used for different purposes.

Some examples are represented by Azadi (2012), Azadi and Farnood (2011), Azadi et al. (2009) where model compounds of biomass and real samples were reacted in water at (350-900) ºC at pressures from 200 bar to 450 bar. Results demonstrated technical-economic feasibility. At subcritical conditions (<221 bar, 374 ºC) the process is usually improved by adding a heterogeneous catalyst, while at supercritical conditions (>221 bar, 374 ºC), the process is improved by using supercritical water as the gasifying-reforming agent, taking advantage of its unique properties (Castello and Fiori, 2011, Castello, 2013, Susanti et al., 2011).

Extrapolating from these trials, DHG implementation looks very promising, since DHG could be applied in oil reservoirs with pressures lower than 200 bar using hydrocarbon feedstocks which are less corrosive than oxygenates and other organic material of which biomass is mainly composed (Osada et al., 2007, Wahyudiono et al., 2012).

However, the DHG process has never been considered previously for

operation in oil reservoirs. Neither has it been operated at such high pressures nor have any numerical models to predict behaviour and dry gas composition been developed yet.

So far, Greaves and his research group (Greaves et. al. 2004, Greaves, et al., 2005, Greaves et al., 2006, Greaves, et al., 2008) have carried out the only feasibility experimental studies to demonstrate that pressure is one of the main factors influencing the effectiveness of the DHG process. Other variables were also studied, such as temperature, S/C ratio and types and the loading of the catalyst into the gasifier-reformer.

Pressure: This research group showed that the total conversion to hydrogen decreased from around 60 % hydrogen in the produced gas to nearly 40 % when the pressure was increased from 60 to 90 bar and they expected a reduction below 30 % at pressures around 130 bar. Results reported in Greaves et al., 2008 indicated that the hydrogen value was between 35 to 60 % all the way to 130 bar using naphtha with reservoir gas feedstock. Conversion could be maintained more or less constant (within a range) by the appropriate choice of operating conditions.

Temperature: Reaction conversion is strongly affected by the temperature of the gasifier-reformer. Over the range 682 °C to 760 °C, an increment on gas production was observed of 10 % considering 38 % as the base level. Under suitable operating conditions, therefore, a hydrogen concentration of around 50 % can be achieved, with a total conversion to inert gas approaching 70 %.

Higher temperatures than 730 ºC were required to convert a light naphtha with reservoir gas feedstock compared to previous studies using pentane with reservoir gas feedstock (Greaves et al., 2008).

S/C: The gasifier-reformer conversion efficiency was improved as the S/C ratio increased from 3 to 6 using pentane or naphtha with reservoir gas feedstock. However, conversion did not appear to be greatly affected by the S/C ratio in the pressure up to 130 bar (Greaves et al., 2008).

Carbon deposition can be satisfactorily controlled by using a sufficiently high value of the S/C ratio, so that any deposited carbon is effectively removed (gasified).

Catalyst type and loading: Greaves and co researchers (2004) carried out studies on two types of steam reforming catalysts, C11-NK and C11-PR. The C11-PR catalyst proved to be superior, compared to the C11-NK, in terms of conversion efficiency and also mechanical strength, or robustness.

The amount of catalyst which was loaded into the reactor strongly affected conversion. For instance, with 14.8 grams of catalyst (C11-PR), the

hydrogen concentration in the produced gas was 48 %, and the total conversion was 70 %, at (95-135) bar, while the hydrogen concentration only reached 40 % when the catalyst loading was reduced to 10 grams. Using just 5 grams of catalyst, the hydrogen concentration was trending below 40 % (Greaves et al., 2008).

Hydrocarbon feedstock: Greaves et al., 2006, Greaves at al., 2008 continued studies using pentane/naphtha with reservoir gas feedstock at pressures up to 130 bar observing no total feed conversion to gases, H_2, CO and CO_2. Presence of coke deposits and liquid residue in the accumulator were detected after experimental tests and hydrogen in produced gas achieved between 35 % and 60 % at pressures up to 130 bar.

References

ABUADALA, A. AND DINCER, I., 2010. Efficiency evaluation of dry hydrogen production from biomass gasification. *Thermochimica acta,* 507, pp. 127–134.

ABREU, C.M., SANTOS, D.A., PACIFICO, J.A., LIMA, M.N., 2008. Kinetic evaluation of methane – carbon dioxide reforming process based on the reaction steps. *Ind. Eng. Chem. Res.,* 47, pp. 4617-4622.

AHMED, T., 2001. *Reservoir engineering handbook.* 2nd ed. U.S.: Elsevier.

AL-ANAZI, B.D., 2007. Enhanced oil recovery techniques and nitrogen injection. *CSEG RECORDER,* pp. 28-33.

ANCHEYTA-JUREZ, J., VILLAFUERTE-MACAS, E., DAZ-GARCA, L., GONZALEZ-ARREDONDO, E., 2001. Modelling and simulation of four catalytic reactors in series for naphtha reforming. *Energy fuels,* 15(4), pp. 887-893.

ANDREW, S.P., 1969. Catalysts and catalytic processes in the steam reforming of naphtha. *I & EC Product research and development,* 8(3), pp. 321-324.

AZADI, P., 2012. *Hydrogen production using catalytic supercritical water gasification of lignocellulosic biomass.* Thesis (PhD). University of Toronto, Toronto.

AZADI, P. AND FARNOOD, R., 2011. Review of heterogeneous catalysts for sub- and supercritical water gasification of biomass and wastes. *International journal of hydrogen energy,* 36, pp. 9529-9541.

AZADI, P., SYED, K.M. AND FARNOOD, R., 2009. Catalytic gasification of biomass model compound in near-critical water. *Applied catalysis A,* 358, pp. 65-72.

BABADAGLI, T., 2007. Development of mature oil fields — A review. *Journal of petroleum science and engineering,* 57, pp. 221–246.

BALBINSKI, E., GOODFIELD, M., JAYASEKERA, T., WOODS, C., 2003. *Potential for geological storage and EOR from CO injection into UKCS oilfields.* United Kingdom: UK Department of trade and industry's sustainable hydrocarbon additional recovery programme (SHARP).

BARTHOLOMEW, C.H., 2001. Mechanisms of catalyst deactivation. *Applied catalysis A,* 212, pp. 17–60.

BENITEX, V.M., VERA, C.R., RANGEL, M.C., YORI, J.C., GRAU, J.M., PIECK, C.L., 2009. Modification of multimetallic naphtha-reforming catalysts by Indium addition. *Ind. Eng. Chem. Res.,* 48(2), pp. 671-676.

BEURDEN, P.V., 2004. *On the catalytic aspects of steam-methane reforming*. ECN, (ECN-I--04-003).

BEYER, F., BRIGHTLING, J., FARNELL, P., FOSTER, C., 2005. Steam reforming – 50 years of development and the challenges for the next 50 years. Proceedings of the *AIChe 50th Annual Safety in Ammonia Plants and Related Facilities Symposium,* 26-29 September 2005 Toronto. Canada, pp. 01-12.

BOROWIECKI, T., 1987. Nickel catalysts for steam reforming of hydrocarbons: direct and indirect factors affecting the coking rate. *Applied catalysis,* 31, pp. 207–220.
CALLAHAN, F.J., 1993. *Tube fitter's manual.* U.S.: Swagelok Co.
CASTELLO, D., 2013. *Supercritical water gasification of biomass.* Thesis (PhD). University of Trento, Trento.
CASTELLO, D. AND FIORI, L., 2011. Supercritical water gasification of biomass: Thermodynamic constraints. *Bioresource technology,* 102, pp. 7574-7582.
CHEMICZNY, P., 2007. New catalysts for steam reforming. *Polish journal of chemistry,* 86(7), pp. 617-620.
CHEN, Y., WANG, Y., XU, H., XIONG, G., 2008. Efficient production of hydrogen from natural gas steam reforming in palladium membrane reactor. *Applied catalyst B: Environmental,* 80, pp. 283-294.
CHRISTENSEN, K.O., 2005. Steam Reforming of Methane on Different Nickel Catalysts. Thesis (PhD). Norwegian University of Science and Technology, Trondheim.
COLPAN, C.O., HAMDULLAHPURM, F., DINCER, I. AND YOO, Y., 2010. Effect of gasification agent on the performance of solid oxide fuel cell and biomass gasification systems. *International journal of hydrogen energy,* 35, pp. 5001–5009.
DAMIANI, L. AND TRUCCO, A., 2010. An experimental data based correction technique of biomass gasification equilibrium modelling. *Journal of solar engineering,* 132, pp. 0310-0311.
DAMLE, A.S., 2008. Hydrogen production by reforming of liquid hydrocarbons in a membrane reactor for portable power generation - experimental studies. *Journal of power sources,* 186, pp. 167–177.
DAVIDSON, I.D., 2001. *Enhanced oil recovery by In situ gasification.* International patent application WO 01/81723. November 01, 2001.
DEMIRBAS, A., 2010. Hydrogen production from biomass via supercritical water gasification. *Energy sources, part A: Recovery, utilization and environmental effects,* 32(14), pp. 1342-1354.
DREYER, B.J., LEE, I.C., KRUMMENACHER, J.J., SCHMIDT, L.D., 2006. Autothermal steam reforming of higher hydrocarbons: n-decane, n-hexadecane, and JP-8. *Applied Catalysis A: General,* 307, pp.184–194.
DYBKJAER, I., 1995. Tubular reforming and autothermal reforming of natural gas – an overview of available processes. *Fuel processing technology,* 42, pp. 85 – 107.
FRANK, J., MARK, C., MARK, G., 1998. *Hydrocarbon exploration and production.* U.S.: Elsevier.
FROMENT, G.F., 2008. Kinetic modelling of hydrocarbon processing and the effect of catalyst deactivation by coke formation. *Catalysis reviews,* 50, pp. 01-18.
GALLUCI, F., PATURZO, L. AND BASILE, A., 2004. A simulation study of the steam reforming of methane in a dense tubular membrane reactor. *International journal of hydrogen energy,* 29, pp. 611-617.

GOLDSTEIN, R.J., ECKERT, E.R.G., IBELE, W.E., PATANKAR, S.V., SIMON, T.W., KUEHN, T.H., STRYKOWSKI, P.J., TAMMA, K.K., BAR-COHEN, A., HEBERLEIN, J.V.R., DAVIDSON, J. H., BISCHOF, J., KULACKI, F.A., KORTSHAGEN, U., GARRICK, S., SRINIVASAN, V., 2002. Heat transfer – a review of 2002 literature. *International journal of heat and mass transfer,* 48, pp. 819-927.

GOLEBIOWSKI, A., STOLECKI, K., PROKOP, U., KUSMIEROWSKA, A., BOROWIECKI, T., DENIS, A., SIKORSKA, C., 2004. Influence of potassium on the properties of steam reforming catalysts. *React. Kinet. Catal. Let.,* 82(1), pp. 179-189.

GOULD, B.D., CHEN, X., SCHWANK, J.W., 2007. Dodecane reforming over nickel-based monolith catalysts. *Journal of catalysis,* 250, pp. 209-221.

GREAVES, M., RATHBONE, R., XIA, T., BENTHAHER, A., DUGGAN, S., 2004. *Downhole gasification for improved oil recovery and gas production (phase 1) experimental studies (1 Nov 2002 – 31 Oct 2004).* United Kingdom: University of Bath, (Confidential internal report).

GREAVES, M., XIA, T., RATHBONE, R. AND BENTAHER, A., 2005. Underground gasification for improved oil recovery. *Canadian international petroleum conference,* 7-9 June 2005 Calgary. Calgary: Petroleum Society Canadian Institute of Mining, Metallurgy & Petroleum, pp. 38-48.

GREAVES, M., RATHBONE, R., XIA, T., BENTHAHER, A., 2006. Experimental study of a novel In situ gasification technique for improved oil recovery from light oil reservoirs. *JCPT,* 45(8), pp. 41-47.

GREAVES, M. AND XIA, T.X., 2008. Producing hydrogen and incremental oil from light oil reservoirs using downhole gasification. *Canadian international petroleum conference,* 17-19 June 2008 Calgary. Calgary: Petroleum Society Canadian Institute of Mining, Metallurgy & Petroleum, pp. 14-24.

GREEN, D.W., WILLHITE G.P., 1998. Enhanced Oil Recovery. *Society of Petroleum Engineers*, Texas.

HAWKINS, G.B., 2010. *Steam reforming practical operation.* GBH Enterprises, LTD. Available from: http://www.gbhenterprises.com/

HAYES, R.E. AND MMBAGA, J.P., 2013. *Introduction to chemical reactor analysis.* 2nd edition. New York: CRC Press.

HELVEG, S., SEHESTED, J. AND ROSTRUP-NIELSEN, J.R., 2011. Whisker carbon in perspective. *Catalysis today,* 178, pp. 42– 46.

HOLLADAY, J.D., HU, J., KING, D.L., WANG, Y., 2008. An overview of hydrogen production technologies. *Catalysis today,* 139, pp. 244–260.

HUTCHINSON, C. A., BRAUN, P.H., 1961. Phase Relations of Miscible Displacement in oil Recovery. *AIChE J.*, 7, pp. 64-72.

IVANHOE, L.F., 1997. Get Ready For Another Oil Shock!. *The futurist,* January/February.

JIM, S., 2006. *ISA Handbook of measurement equations and tables.* 2nd edition. U.S.: ISA.

JOHNS, R.T., 1996. Miscible gas displacement of multicomponent oils. *Society petroleum engineers journal,* SPE 30798.

JOHNSON MATTHEY CATALYSTS, 2010. *Industrial catalytic processes course.* Bath: Johnson Matthey Press.
JONES, G., JAKOBSEN, J.G., SHIM, S.S., KLEIS, J., ANDERSSON, M.P., ROSSMEISL, J., PEDERSEN, F.A., BLIGAARD, T., HELVEG, S., 2008. First principles calculations and experimental insight into methane steam reforming over transition metal catalysts. *Journal of catalysis,* 259, pp. 147-160.
KAMINSKY, R.D., 1999. Estimation of two phase flow heat transfer in pipes. *Transactions of the ASME,* 121, pp. 74-80.
KARMAKAR, M.K. AND DATTA, A.B., 2011. Generation of hydrogen rich gas through fluidized bed gasification of biomass. *Bioresource technology,* 102, pp. 1907–1913.
KARAMARKOVIC, R. AND KARAMARKOVIC, V., 2010. Energy and exergy analysis of biomass gasification at different temperatures. *Energy*, 35, pp. 537–549.
KEMIN, L., HAI-YAN, G., SHI-WEI, P., 2004. A study on naphtha catalytic reforming reactor simulation and analysis. *Journal of zhejiang university SCIENCE,* 6B(6), pp. 590-596.
KHAN, M.I., ISLAM, M.R., 2007. *Petroleum engineering handbook - sustainable operations.* U.S.: Elsevier.
KLINS, M.A., 1984. Carbon dioxide flooding. *International human resources development corporation,* Boston.
KNEZEVIC, D., VAN SWAAIJ, W. AND KERSTEN, S., 2010. Hydrothermal conversion of biomass II: Conversion of wood, pyrolysis oil and glucose in hot compressed water. *Industrial & engineering chemistry research,* 49, pp. 104-112.
KUMAR, S., AGRAWAL, M., KUMAR, S., JILANI, S., 2008. The production of Syngas by dry reforming in membrane reactor using alumina-supported Rh catalyst: a simulation study. *International journal of chemical reactor engineering*, 6(A109), pp. 01-37.
KVAMSDAL, H. M., SVENDSEN H. F. AND OLSVIK O., 1999. Dynamic simulation and optimization of a catalytic steam reformer. *Chemical engineering science,* 54, pp. 2697–2706.
QUICENO, R., PEREZ-RAMIREZ, J., WARNATZ, J. AND DEUTSCHMANN, O., 2006. Modelling the high-temperature catalytic partial oxidation of methane over platinum gauze: detailed gas-phase and surface chemistries coupled with 3D flow field simulations. *Applied catalysis A,* 303, pp.166–176.
QUINTA-FERREIRA, R.M., SIMOES, P.M. AND RODRIGUES, A.E., 1995. Simulation of tubular reactors packed with large-pore catalysts with spherical geometry. *Computers & chemical engineering,* 19, pp. 351–356.
LAKE, L.W., WALSH, M.P., 2008. *Enhanced oil recovery (EOR) field data: literature search.* U.S.: University of Texas.
LANG, P., AURACHER, H., 1996. Heat transfer to nonmiscible liquid-liquid mixtures flowing in a vertical tube. *Experimental thermal and fluid science,* 12, 364-372.

LOMAX, F.D., 2001. *Application of concurrent development practices to petrochemical equipment design.* Thesis (PhD). Virginia Polytechnic Institute and State University, U.S.
LUBAŚ, J. *Selection of the best technique of increasing the recovery factor for BMB – the largest polish oil reservoir.* Germany: Oil and Gas Institute / Krosno Branch, (2WP0-5).
LYONS, W.C., PLISGA, G.J., 2005. *Standard handbook of petroleum and natural gas engineering.* 2nd ed. U.S.: Elsevier.
MARIN, P., PATIN, Y., DIEZ, F. AND ORDONEZ, S., 2012. Fixed bed membrane reactors for WGSR-based hydrogen production: Optimisation of modelling approaches and reactor performance. *International journal of hydrogen energy,* 37, pp. 4997-5010.
MARIN, P., PATIN, Y., DIEZ, F. AND ORDONEZ, S., 2012. Modelling of hydrogen perm-selective membrane reactors for catalytic methane steam reforming. *International journal of hydrogen energy,* 37, pp. 18433-18445.
MATHIASSEN, O.M., 2003. *CO_2 as injection gas for enhanced oil recovery and estimation of the potential on the Norwegian continental shelf.* Stavanger: NTNU – Norwegian University of Science and Technology, (Part I - CO_2 injection for enhanced oil recovery).
MATHURE, P.V., GANGULY, S., PATWARDHAN, A.V., SAHA, R.K., 2007. Steam reforming of ethanol using a commercial nickel-based catalyst. *Ind. Eng. Chem. Res.*, 46, pp. 8471-8479.
MELO, F., MORLANES, N., 2005. Naphtha steam reforming for hydrogen production. *Catalysis today*, 107–108, pp. 458–466.
MELO, F., MORLANES, N., 2008. Naphtha steam reforming for hydrogen production. *Catalysis today,* 107–108, pp. 458–466.
MELO, F., MORLANES, N., 2008. Synthesis, characterization and catalytic behaviour of NiMgAl mixed oxides as catalysts for hydrogen production by naphtha steam reforming. *Catalysis today,* 133–135, pp. 383–393.
MIKHAILOV, G.M., MIKHAILOV, V.G., KONDAKOVA, L.A., REVA, L.S., 2004. Prediction of the convective heat transfer coefficient for the transient and turbulent flows in a tube. *Theoretical foundations of chemical engineering,* 39(6), pp. 658-662.
MYER, K., 2006. *Mechanical engineer's handbook – energy and power.* U.S.: John Wiley & Sons.
NAHAR, G.A. AND MADHANI, S.S., 2010. Thermodynamics of hydrogen production by steam reforming of butanol: analysis of inorganic gases and light hydrocarbons. *International journal of hydrogen energy,* 35(1), pp. 98–109.
NOUAR, A., FLOCK, D. L., 1983. Parametric analysis on the determination of the minimum miscibility pressure in slim tube displacements. Proceedings of the *34th Annual Technical Meeting of the Petroleum Society of CIM,* 10 - 13 May 1983.
NUMMEDAL, L., RØSJORDE, A., JOHANNESSEN E., KJELSTRUP, S., 2005. Second law optimization of a tubular steam reformer. *Chemical engineering and processing,* 44, pp. 429–440.

ÖNSAN, Z.I., 2007. Catalytic processes for clean hydrogen production from hydrocarbons. *Turk J. chem.,* 31, pp. 531-550.

OSADA, M., SATO, T., WATANABE, M., SHIRAI, M. AND ARAI, K., 2007. Catalytic gasification of wood biomass in subcritical and supercritical water. *Combustion science and technology,* 178(1-3), pp. 537-552.

PADBAN, N. AND BECHER, V., 2005. *Literature and state-of-the-art review (Re: Methane Steam Reforming).* CHRISGAS, (October 2005_WP11_D89).

PAN, Y., WANG, Z.Y., KAN, T., ZHU, X.F., LI, Q.X., 2005. Hydrogen production by catalytic steam reforming of bio-oil, naphtha and CH_4 over $C_{12}A_7$-Mg catalyst. *Chinese journal of chemical physics,* 19(3), pp. 190-192.

PAPAGEORGIOU, J. N. AND FROMENT, F., 1995. Simulation models accounting for radial voidage profiles in fixed-bed reactors. *Chemical engineering science,* 50(19), pp. 3043-3056.

PASEL, J., CREMER, P., WEGNER, R., PETERS, R., STOLTEN, D., 2004. Combination of autothermal reforming with water-gas-shift reaction – small-scale testing of different water-gas-shift catalysts. *Journal of power sources,* 126, pp. 112-118.

PEDENERA, M. N., PINA J., BORIO D. O. AND BUCALA, V., 2003. Use of a heterogeneous two-dimensional model to improve the primary steam reformer performance. *Chemical engineering journal,* 94, pp. 29–40.

RIBATSKI, G., THOME, J.R., 2007. Two phase flow and heat transfer across horizontal tube bundles – A review. *Heat transfer engineering,* 28(6), pp. 508-524.

REYES, S.C., SINFELT, J.H., FEELEY, J.S., 2003. Evolution of processes for synthesis gas production: recent developments in an old technology. *Ind. Eng. Chem. Res.,* 42, pp.1588-1597.

RHUMA, A.N., 1992. *Minimum Miscibility Pressures of CO_2/ Hydrocarbon Systems; Evaluation of Existing Prediction Techniques and Development of a New Correlation.* Dissertation (MSc). University of Saskatchewan, Saskatchewan.

ROSTROUP – NIELSEN, J.R., 1975. *An investigation of catalysts for tubular steam reforming of hydrocarbons.* Copenhagen: Danish Technical Press Inc.

SADOOGHI, P. AND RAUCH, R., 2012. Sulphur deactivation effects on catalytic steam reforming of methane produced by biomass gasification. Proceedings of the *2012 COMSOL conference*. 2012 Milan.

SAHA, S., 1993. *Numerical and physical simulations of the displacement of synthetic oil mixtures.* Thesis (PhD). University of Saskatchewan, Saskatchewan.

SANTOS, D.C., LISBOA, J.S., PASSOS, F.B., NORONHA, F.B., 2003. Characterisation of steam-reforming catalysts. *Brazilian journal of chemical engineering,* 21(02), pp. 203-209.

SCHUTLE, W.M., 2005. Challenges and strategy for increased oil recovery. Proceedings of the *International Petroleum Technology Conference,* 21-23 November 2005 Doha. Qatar: pp. 02-09.

SCHWAAB, M., ALBERTON, A.L., FONTES, C.E., BITTENCOURT, R.C., PINTO, J.C., 2009. Hybrid modelling of methane reformers. 2. Modelling of the industrial reactors. *Ind. Eng. Chem. Res.,* pp. A-G.

SEČEN, J., 2005. IOR and EOR – chances for increase of oil production and recoveries in existing, mature reservoirs. Proceedings of the 13th *European Symposium on Improved Oil Recovery,* 25-27 April 2005 Budapest Hungary. Hungary: Rudarsko-geološko-naftni zbornik, pp. 27-30.

SHAYEGAN, J., YOUSEF MOTAMED HASHEMI, M. M. AND VAKHSHOURI, K., 2008. Operation of an industrial steam reformer under severe condition: A simulation study. *The Canadian journal of chemical engineering,* 86, pp. 747–755.

SHARMA, P.O., ABRAHAM, M.A., CHATTOPADHYAY, S., 2007. Development of a novel metal monolith catalyst for natural gas steam reforming. *Ind. Eng. Chem. Res.,* 46(26), pp. 9053-9060.

SHINKU, L., JOONGMYEON B., SUNGKWANG L. AND JOONGUEN, P., 2008. Improved configuration of supported nickel catalysts in a steam reformer for effective hydrogen production from methane. *Journal of power sources,* 180, pp. 506–515.

SHIRLEY, A., 2005. *A transient steam reforming process to produce hydrogen from methane for use in fuel cells.* Thesis (PhD). University of Bath, Bath.

SEO, J.G., YOUN, M.H., LEE, H.I., KIM, J.J., YANG, E., CHUNG, J.S., KIM, P., SONG, I.K., 2008. Hydrogen production by steam reforming of liquefied natural gas (LNG) over mesoporous nickel-alumina xerogel catalysts: Effect of nickel content. *Chemical engineering journal,* 141, pp. 298-304.

STALKUP Jr., F.I., 1985. *Miscible Displacement, Monograph Volume 8.* Society of Petroleum Engineers, Henry L Doherty Series.

STEFANESCU, A., VAN VEEN, A.C., DUVAL-BRUNEL, E., MIRODATOS, C., 2007. Investigation of a Ni-based steam reforming catalyst developed for the coating of microstructures. *Chemical engineering science,* 62, pp. 5092-5096.

STEFANIDIS, G.D., DIONISIOS, S.D., VLACHOS, G., 2008. Millisecond methane steam reforming via process and catalyst intensification. *Chem. Eng. Technol.,* 31(8), pp.1201–1209.

SPERLE, T., CHEN, D., LODENG, R., HOLMEN, A., 2005. Pre-reforming of natural gas on a Ni catalyst Criteria for carbon free operation. *Applied Catalysis A: General*, 282, pp. 195–204.

SUSANTI, R., NUGROHO, A., LEE, J., KIM, Y. AND KIM, J., 2011. Noncatalytic gasification of isooctane in supercritical water: A strategy for high-yield hydrogen production. *International journal of hydrogen energy,* 36, pp. 3895-3906.

SUSANTI, R., VERIANSYAH, B., KIM, J. AND LEE, Y., 2010. Continuous supercritical water gasification of isooctane: A promising reactor design. *International journal of hydrogen energy,* 35(5), pp. 1957-1970.

TAKENAKA, S., ORITA, Y., UMEBAYASHI, H., MATSUNE, H., MASAHIRO, K., 2008. High resistance to carbon deposition of silica-coated Ni catalysts in propane stream reforming. *Applied catalysis A: General,* 351, pp. 189-194.

THOMAS, F.B., OKAZAWA, T., ERIAN, A., ZHOU, X.L., BENNION, D.B. AND BENNION, D.W., 1995. Does miscibility matter in gas injection?. *Petroleum society of CIM and CANMET,* 90-95, pp. 01-12.

THOME, J.R., 2003. On recent advances in modelling of two phase flow and heat transfer. *Heat transfer engineering,* 24(6), pp. 46-59.

TURPEINEN, E., RAUDASKOSKI, R., PONGRA, E. AND KEISKI, R.L., 2008. Thermodynamic analysis of conversion of alternative hydrocarbon-based feedstocks to hydrogen. *International journal of hydrogen energy,* 33, pp. 6635-6643.

TWIGG, M.V., 1989. *Catalyst Handbook*. 2nd edition. England: Wolfe Press.

TZIMAS, E., GEORGAKAKI, A., GARCIA, C., PETEVES, S.D., 2005. *Enhanced oil recovery using carbon dioxide in the European energy system.* Netherlands: DG JRC, INSTITUTE FOR ENERGY, (Report EUR 21895 EN).

UDENGAARD, N.R., 2004. Hydrogen production by steam reforming of hydrocarbons. *American chemical society, division fuel chemistry,* 49(2), pp. 906-907.

UNITED ENERGY GROUP PLC, 2008. *All about oil and gas: from the beginning to present day.* United Kingdom: U.S. Energy Department.

WAHYUDIONO, MACHMUDAH, S. AND GOTO, M., 2012. Utilization of sub and supercritical water reactions in resource recovery of biomass wastes. *Engineering journal,* 10, pp. 4186-4198.

WEI, J., IGLESIA, E., 2004. Isotopic and kinetic assessment of the mechanism of reactions of CH_4 with CO_2 or H_2O to form synthesis gas and carbon on nickel catalysts. *Journal of catalysis,* 224, pp. 370-383.

WILLIAMS, J.J., ROSENBERG, R.A., MCDONOUGH, L.J., 1993. *Lined reformer tubes for high pressure reformer reactors.* United States patent office 5,254,318. October 19, 1993.

XIN, R.C., AWWAD, A., DONG, Z.F., EBADIAN, M.A., 1996. Heat transfer of air/water two phase flow in helicoidal pipes. *ASME,* 118, pp. 442-448.

XU, J., FROMENT, G.F., 1989. Methane steam reforming, methanation and water-gas shift: 1. Intrinsic kinetics. *AIChE journal,* 35(1), pp. 88-103.

XU, J., YEUNG, C.M., NI, J., MEUNIER, F., ACERBI, N., FOWLES, M., TSANG, S., 2008. Methane steam reforming for hydrogen production using low water-ratios without carbon formation over Ceria coated Ni catalysts. *Applied Catalysis A: General,* 345, pp. 119–127.

YANHUI, W., DIYONG, W., 2001. The experimental research for production of hydrogen from n-octane through partially oxidizing and steam reforming technique. *International Journal of Hydrogen Energy*, 26, pp. 795–800.
YAWS, C.L., 2007. *Yaw's handbook of thermodynamic properties for hydrocarbons and chemicals compounds.* U.S.: Elsevier.
YEH, G.J. *Steam reforming computer program.* Saudi Arabia: Saudi Aramco.
YONG, B., QIANG, B., 2005. *Subsea pipelines and risers.* U.S.: Elsevier.
ZEINALIPOUR-YAZDI, C.D., EFSTATHIOU, A.M., 2009. Preadsorbed water-promoted mechanism of the water-gas shift reaction. *The journal of physical chemistry,* 112(48), pp. 19030-19039.

CHAPTER 3: MATERIALS AND EXPERIMENTAL DOWNHOLE GASIFICATION (DHG) RIG

3.1 Introduction

This section presents the materials and rig used for the downhole gasification (DHG) experiments of this research. The laboratory experiments carried out represent the main body of the research; therefore, an extensive work programme via laboratory was necessary to carry out. Assembly, commissioning, further optimisations and final assembly of the downhole gasification (DHG) rig utilised in previous works (Greaves et al., 2004, Greaves et al., 2005, Greaves et al., 2006, Greaves et al., 2008). These preparatory procedures are summarized here.

The primary goal was to revamp and update an existing small pilot scale DHG rig to accommodate the new operating conditions of pressure higher than 130 bar (up to 160 bar) and to incorporate a new automatic data acquisition system. When the commissioning test stage was completed, a series of further optimisations and modifications of the rig were carried out, all directed at increasing conversions and achieving higher hydrogen (H_2) concentration in the produced dry gas (section 3.3) since this gas is the main driver for gas displacement where the DHG process is implemented as oil recovery technique in reservoirs.

Those new improvements included a more efficient injection system of water and naphtha to feed the rig, the minimisation of heat loss from the connecting tube between the vaporisation and gasification-reforming sections of the rig and a longer gasifier-reformer reactor tube to increase catalyst loading (section 3.4). A final DHG rig design with a list of the equipment, instruments and lab tubing used will be presented in this chapter.

3.2 Materials used for DHG experiments

3.2.1 Feedstock

Methane and naphtha feedstock were selected for the complex nature of the DHG experiments. Methane/water to perform basic experiments (Chapter 5) while naphtha/water to develop this research where variables such as the extension of pressure range (> 130 bar), reactor length (from 30 cm to 72 cm), catalyst loading (from 15.2 g to 36.1 g) and types of catalysts, C11-PR and HiFUEL R110, were studied (Chapter 6).

Methane permitted the establishment of a firm baseline and a better understanding of steam reforming reactions at DHG operating conditions since it is the simplest (only one carbon-contained) and major component of gas caps in oil reservoirs.

The DHG experiments using naphtha provided an insight into the technical feasibility of the DHG process concept which envisages the usage of a light oil-cut, vaporised from the crude oil. Typically, the crude oil flowing into the production well might contain of the order of 10 per cent naphtha depending on the API grade.

Water: The water used (H_2O) was deionised (Electrical conductivity at 25 ºC = 0.5 $\mu S.cm^{-1}$). Minerals and salts were removed to avoid catalyst poisoning in the gasifier-reformer reactor. Specific density, ρ= 1000 $Kg.m^{-3}$ at Standard temperature and pressure (Reid et al., 1987).

Methane: The methane used (CH_4) was at high purity (99.9999 %) and high pressure (200 bar). Standard 9 kg. methane cylinders (Ultrahigh purity N5.5) were supplied by BOC Gases Company. Specific density, ρ= 0.6556 $Kg.m^{-3}$ at Standard temperature and pressure (Reid et al., 1987). For details see Appendices, section A.1.

Naphtha: A light oil fraction of naphtha from the Pembroke Refinery in the United Kingdom (UK) was used. The naphtha fraction corresponded to reformate fraction which is commonly used as feedstock for iso-pentane reformer. It was very light with a high content of saturates and no sulphur or nitrogen presence (see Appendices, section A.2). Table 3.1 shows its physicochemical properties:

Table 3.1 Physicochemical properties of the naphtha.

Properties	**Range**
Boiling point, ºC	108
Density ρ, $Kg.m^{-3}$	691
Gravity, ºAPI	79.0
Corrosion @122 ºF, rating	1A
Benzene, Volume %	< 0.2
Mercaptan	Negative
Hydrocarbon Type (FIA), volume %	
Aromatics Olefins Saturates	<0.3 <0.3 99+
Sulfur, ppm wt.	<0.1
Nitrogen, ppm wt.	<0.1

Twigg (1989) reported what type of naphtha fractions might be suitable for steam reforming reactions. Making use of this research, our naphtha and its compositional specifications were compared to the tables presented by Twigg (1989) prior to experiments and fortunately, they confirmed its technical suitability for DHG since our process of gasification-reforming occurs through steam reforming reactions.

n-heptane has a boiling point temperature of 100 ºC and a density of 689

$Kg.m^{-3}$ at Standard temperature and pressure (Perry and Green, 1984) which is very similar to the values reported for our naphtha. For that reason, this molecule was chosen as the model surrogate for calculations in the experimental phase (Chapter 6) and the numerical DHG model (Chapter 7).

Nitrogen (N_2) of high purity (99.9999 %) and high pressure (200 bar) was used in the rig for gas leaking detection and to purge the system prior to every DHG experiment. Standard 9 kg nitrogen cylinders (Ultrahigh purity N6.0) were also supplied by BOC Gases Company (see Appendices, section A.3).

3.2.2 Catalyst

The DHG process requires the presence of a catalyst in the gasifier-reformer reactor as was mentioned in literature survey (chapter 2). In this research, two types of catalysts were used: C11-PR from Sud-Chemie and crushed HiFUEL R110 from Alfa Aesar, a Johnson Matthey Company (Figure 3.1).

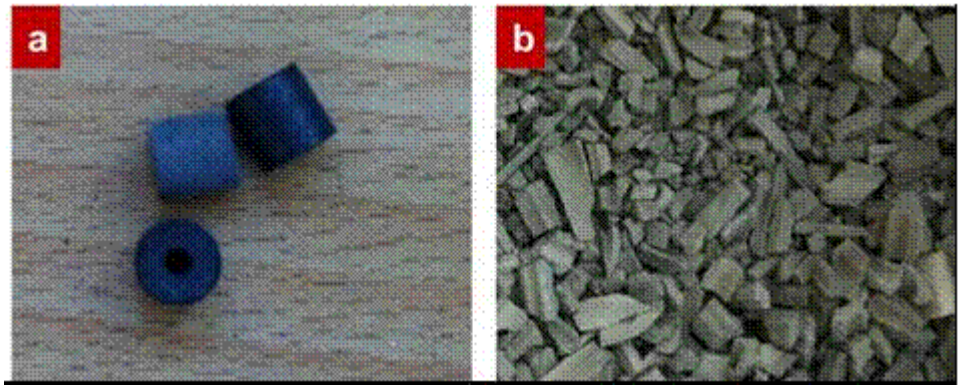

Figure 3.1 (a) C11-PR catalyst from Sud Chemie (b) crushed HiFUEL R110 catalyst from Alfa Aesar.

Experiments commenced using C11-PR rings, dimension 6x6x2 mm, as the catalyst due to their effectiveness in previous DHG investigations realised by Greaves et al. (2004), Greaves et al. (2005), Greaves et al. (2006), Greaves et al. (2008). Considerable hydrocarbon conversion to H_2, CO, CO_2 and CH_4 (produced dry gas composition) at studied conditions of pressure (50-130 bar) and temperature (550-760 ºC) were observed with a good balance of its catalytic activity and its structural strength (hardness).

C11-PR is a pre-reforming catalyst of Nickel oxide (40 wt. %) on alumina support developed for conversion of feedstock from natural gas to heavy naphtha (having a final boiling point as high as 200 ºC) on an industrial scale and C11-PR typical operating temperature oscillates between 380-520 ºC (see Appendices, section A.4). Once the DHG experiments with C11-PR catalyst were completed using methane and naphtha feedstock, a

new catalyst was considered based on the experimental results, the crushed HiFUEL R110 from Alfa Aesar, a Johnson Matthey Company (Chapter 6).

HiFUEL R110 is also made of Nickel oxide (40-60 wt. %) on a ceramic support. Every cylinder has 4 holes and 4 domed flutes and it is adequate to treat naphtha feedstock in steam reforming. Typical operating temperatures are between 450-750 ºC (see Appendices, section A.5). Unfortunately, the HiFUEL R110 catalyst size was higher than that permitted for the internal diameter of the DHG reactor. Hence, it was decided to crush it into smaller pieces prior to experiments (Details are in chapter 6, section 6.4).

3.3 Downhole gasification (DHG) rig

The experimental work in this research inherited an existing rig that was originally used for a first series of DHG experiments during 2002-2004 thanks to a collaborative effort between the Institute of Petroleum Engineering, Heriot-Watt University and the IOR Research Group, University of Bath and the latter was fully in charge of the experimental work.

The rig was commissioned on the basis of its original design and flowsheet. However, some minor revamping was carried out in order to update the rig to the new operating conditions of pressure (>130 bar), a faster and more reliable data acquisition system (MATLAB) and further safety considerations. Details are discussed here in section 3.3. A second stage of modifications and optimisations was carried out as a consequence of performed commissioning tests on the rig with the original design. The revised design and assembly used in this research is shown in section 3.4.

3.3.1 Original unit

The original unit is shown in Figure 3.2.

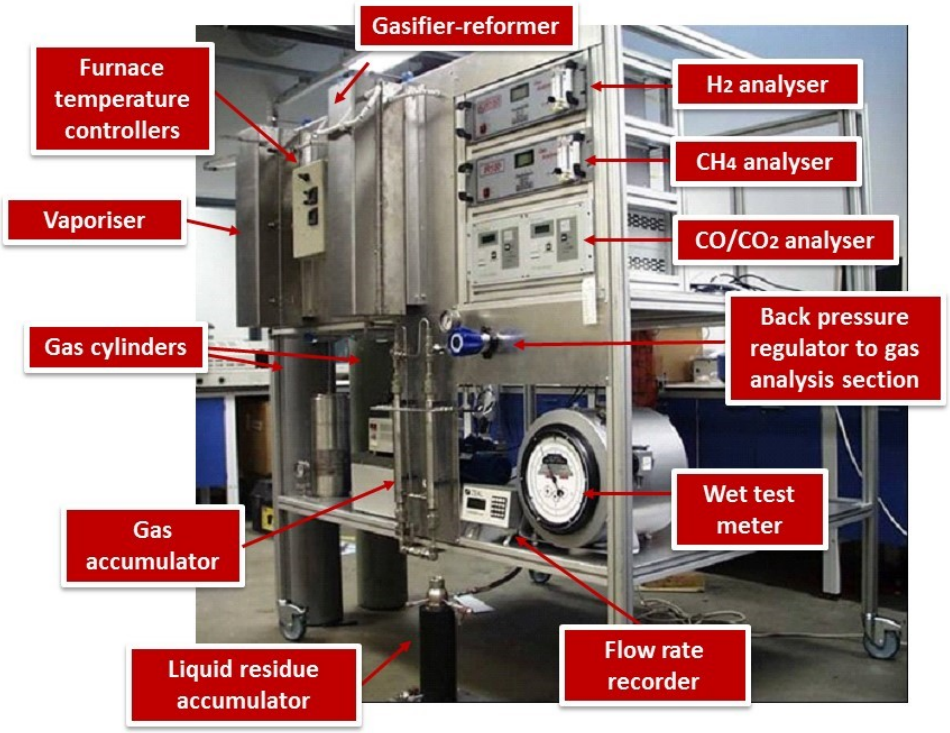

Figure 3.2 Original DHG rig (Greaves et al., 2008)

The rig was initially designed to operate at the following maximum operating conditions:

- Pressure 180 bar
- Vaporisation temperature 600 °C (internal temperature in the vaporiser)
- Gasification-reforming temperature 800 °C (internal temperature in the reactor)

On account of safety considerations, operating conditions usually were:

- Pressure 50-130 bar
- Vaporisation temperature 200-450 ^{o}C (internal temperature in the vaporiser)
- Gasification-reforming temperature 500-750 ^{o}C (internal temperature in the reactor)

The internal temperature in the vaporiser or reactor refers to the temperature reached and measured inside the tube acting as vaporiser or gasifier-reformer reactor. The respective furnace temperatures are dependent on the calibration or commissioning tests of both furnaces. In this investigation both processes were carried out and details are discussed in this chapter, section 3.3.4.

3.3.2 Rig sections

The rig is comprised by seven sections whose functions are:

- Water (H_2O) and naphtha injection
- Vaporisation
- Methane (CH_4) and nitrogen (N_2) injection
- Gasification-reforming
- Liquid-gas separation
- Produced dry gas analysis
- Data acquisition and monitoring

Water (H_2O) and naphtha injection: This section included equipment, instruments, valves, connections and lab tubing designed for the injection of liquids, water (H_2O) and naphtha into the vaporiser. In addition, a vacuum pump was also included to clean the system of any liquid residue after tests. The original design comprised:

- Two liquid injection pumps
- Two mass flow meters to measure liquid injected to the system
- Two glass containers or cylinders
- Four needle valves
- Two Non-return valves as safety and protection for the liquid injection pumps

- Two gate valves for residue discharge before and after DHG experiments
- One mixing entry point prior to the vaporiser
- One vacuum pump for residue discharge before and after the DHG experiments
- ¼ -inch Stainless steel (SS) lab tubing 316L

The Figure 3.3 shows the glass containers used for the water and naphtha and liquid injection pumps from the existing DHG rig.

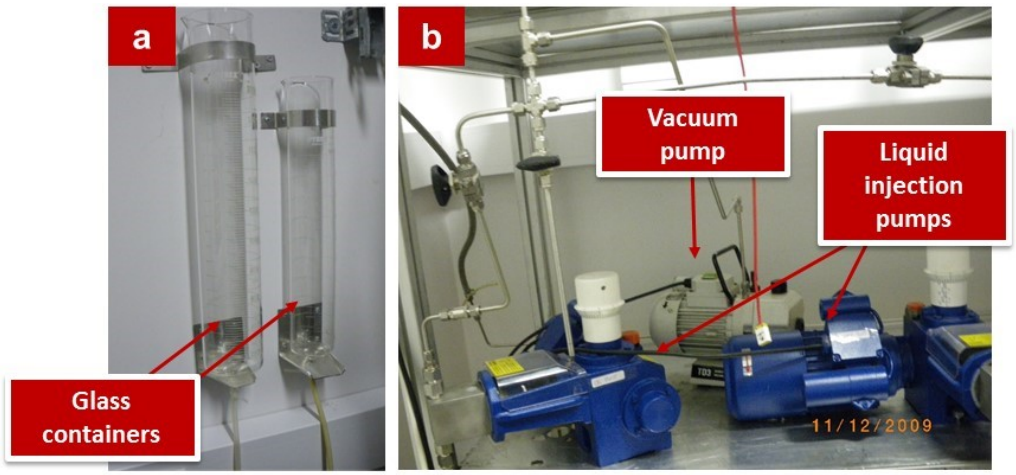

Figure 3.3 (a) glass containers for water and naphtha (b) injection and vacuum pumps.

Vaporisation: This section was used to vaporise the water and naphtha to feed the gasifier-reformer reactor since chemical reactions of steam reforming occur in gas phase only. The section included:

- One furnace to heat up the vaporiser reactor
- One ⅛ -inch x 30 cm stainless steel (SS) coiled tube connected to a 1 –inch x 30 cm stainless steel (SS) tube 316L. This represented the vaporiser reactor
- One thermocouple to measure the outlet vaporiser temperature

Methane (CH_4) and nitrogen (N_2) injection: The injection of gases was carried out after the vaporisation section, as the methane did not require an additional process of gasification. Nitrogen as purge gas was injected in the middle of the rig to facilitate the removal process of any residue in the exits, gate valves and vent ports.

The original design included:

- Gas cylinders for delivery
- One filter to remove any solid particles
- Two mass flow controllers
- Two pressure gauges

- One non-return valve to protect rig equipment
- One relief valve
- ¼ -inch stainless steel (SS) lab tubing 316L

Gasification-reforming: This is the main section of the rig since the steam reforming reactions (gasification-reforming process) occur in the gasifier-reformer reactor tube. The original section included:

- One furnace to heat up the gasifier-reformer reactor
- ⅛ -inch x 30 cm stainless steel (SS) coiled tube 316L as pre-heating prior to the gasifier-reformer reactor. The pre-heating unit is used to heat up the feed prior to the reactor avoiding any mechanical damage or disintegration of the catalyst from thermal shock
- ½ -inch x 30 cm stainless steel (SS) tube 316L as the gasifier-reformer reactor
- Two thermocouples to measure inlet and outlet gasifier-reformer temperature
- One pressure gauge
- ¼ -inch Stainless steel (SS) lab tubing 316L

Liquid-gas separation: Basically this consisted of a series of units which separated the gas at the exit of the gasifier-reformer reactor from unconverted water and hydrocarbon feedstock which was condensable (in our case, unconverted naphtha). In this investigation, the produced gas once separated is named dry gas or produced dry gas. The liquid-gas separation section comprised:

- One condenser which has a jacket where a cooling liquid may circulate to keep the outlet produced gas from the gasifier-reformer at a low temperature to facilitate the water condensation process
- One liquid residue accumulator of high pressure. Capacity 2 L
- One gas accumulator comprised of one (1) or two (2) tubes, depending on DHG experimentation, connected together, one behind the other (1 –inch x 45 cm stainless steel SS316L). This allowed the complete separation of the gas from the liquid
- One needle valve
- One relief valve
- One gate valve for residue discharge connected to the high pressure accumulator
- One non-return valve
- ¼ -inch stainless steel (SS) lab tubing 316L

Produced dry gas analysis: Once the dry gas was generated and separated from any liquid residue, values of outlet flow rate and composition by volume percentage were analysed. For the analysis, the system pressure was reduced to values near to atmospheric pressure, 1.01 bar thereby avoiding any damage to the analysers. This section included:

- One filter to remove any solid particles
- One back pressure regulator connected to the wet test meter and gas analysers
- One wet test meter coupled to the flow rate recorder
- Three gas analysers for H_2, CO, CO_2 and CH_4
- Two vents, open system port for gas discharge. One connected directly to the rig and another vent connected to the gas analysers
- ¼ -inch stainless steel (SS) lab tubing 316L

Data acquisition and monitoring: the original design involved a computer (PC), an acquisition date interface, thermocouples, pressure transducers and data acquisition software programmed to monitor and log pressure, temperature and flow rates from the rig. All of those units were controlled from the PC. However, details of the original components used in 2004 were not specified and therefore, an update and automatisation was required as our first task for rig revamping.

3.3.3 Assembly requirements

Prior to a preliminary DHG rig assembly and to conduct commissioning tests in a safe manner, it was vital to keep in mind the new maximum operating conditions in which our DHG experiments would be performed. Maximum operating conditions were:

- Pressure 230 bar
- Vaporisation temperature 600 ºC (internal temperature in the vaporiser)
- Gasification-reforming temperature 800 ºC (internal temperature in the reactor)

For safety reasons, real operating conditions were:

- Pressure 50-160 bar
- Vaporisation temperature 350-550 ºC (internal temperature in the vaporiser)
- Gasification-reforming temperature 600-750 ºC (internal temperature in the reactor)

To achieve these operational requirements safely a good selection was required of material that would be able to withstand the higher pressure range at high temperature. Secondly, an updated data acquisition and monitoring section enabled us to log and save all data online and, thirdly, a lab room provided us with all the facilities. The three requirements are examined here.

Material selection: The selection of appropriate materials was more crucial for the vaporiser and gasifier-reformer reactor tubes than for the rest of the DHG sections which involved mainly lab tubing for connections.

The vaporiser and gasifier-reformer reactors' material fundamentally required resistance to high pressure combined with high temperature (ASME, 2008, Viswanathan, 1989). Because of that, the nature of the material and wall thickness were critical.

The entire DHG rig was constructed from high quality steel alloys, stainless steel SS-316L as the original design, since references such as Callahan (1993) have indicated its technical reliability at the desired pressure range. However, wall thickness varied depending on temperature range. In the case of the vaporiser the wall thickness was thinner in comparison to that of the gasifier-reformer. For the rest, i.e. the lab tubing connections the wall thickness was same as that used by Greaves´ group.

Callahan (1993) shows graphs on maximum allowable working pressure versus temperature for different lab tubing materials at different diameters and wall thicknesses. Figure 3.4 shows one of the graphs given for ¼ -inch stainless steel (SS) lab tubing 316L.

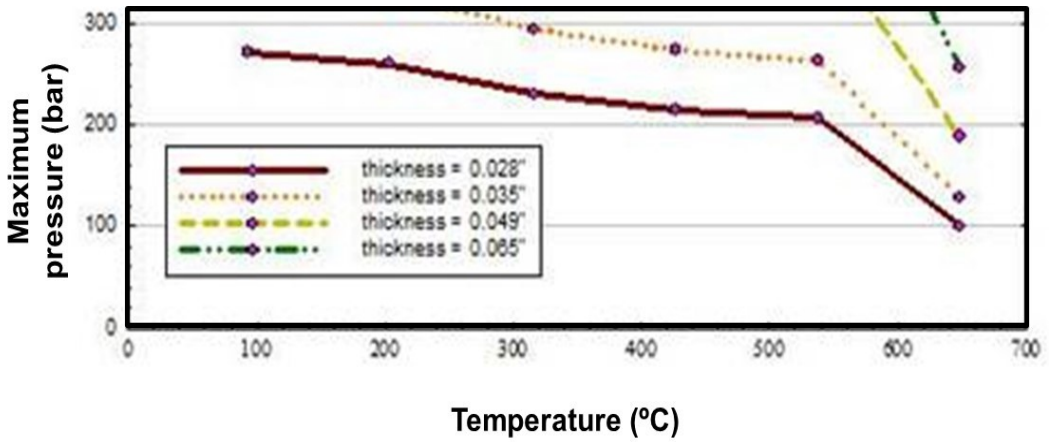

Figure 3.4 Allowable working pressure versus temperature for stainless steel 316L (Adapted from Callahan, 1993).

The graph indicates that the influence of pressure and temperature on material resistance is strongest above 550 ºC since a drastic decline of material life is present. However, this declination is fairly compensated for by higher wall thickness (higher resistance). Based on this, a particular wall thickness was selected for every DHG section: the highest wall thickness was for the gasifier-reformer reactor (0.083 inch), almost three times that of the original used by Greaves et al., (2004), followed by that for the vaporiser and connecting tubes (see details in 3.4.2 for final rig design).

It is important to note that despite the considerable wall thickness for the gasifier-reformer reactor in stainless steel SS-316L, special care was always given to the fact that the material is still not sufficiently strong to withstand the range of pressure and temperature used in DHG over the

very long operating time period (over 24 hours). Under these conditions, the material approached the allowable maximum values (Callahan, 1993). Therefore, as an extra safety precaution, a new gasifier-reformer reactor tube was always utilised for each DHG experiment following which it was immediately replaced by a new unit.

For the purpose of our investigation this material was satisfactory. In the case of future work where the aim will be to extend even more the range of pressure and temperature at an even longer reaction time, the selection of new materials for the gasifier-reformer is recommendable. In chapter 2, the literature survey, some good options were mentioned, such as different types of Hastelloys which are currently utilised in industrial plants. This requirement, therefore, should not present a problem (see section 2.4.4).

On the other hand, optimisations and developments in new materials or additives have been carried out at lab scale (Pinkwart et al., 2004, Susanti et al., 2011) which is a positive development since some of them could also be used. Moreover, these researchers have produced a bibliographic review of reactor materials for supercritical water gasification using hydrocarbon resources/ model compounds for biomass gasification. This process of gasification produces hydrogen as the main produced dry gas via steam reforming and other reactions and, most importantly, its operating conditions are similar to ours in DHG: a reaction temperature of (500–800) ºC, P= (221–280) bar.

Automatisation and update of data acquisition and monitoring section: The flow path of data from the sensors and gas analysers in the rig to the workstation (computer) is illustrated in Figure 3.5.

The section was constructed in the Department of Chemical Engineering by an electrical technician. Data were collected using two digital USB interfaces and two analog/digital (A/D) acquisition modules connected to a Windows PC running a LABVIEW 8.5. The LABVIEW virtual instrument was a homemade development which was used for the concatenation, display and storing of all data.

The time of each temperature, pressure, inlet/outlet flow rates and produced dry gas composition data was recorded as part of the data post processing. The outlet dry gas flow rate generated from the wet test meter was also saved with LABVIEW, unfortunately the corresponding flow recorder did not have specialised software installed for it.

The flow recorder was rather old and it was a bit difficult to make it work alongside the research. A big effort was made to record and save the dry gas outlet flow rate online during the DHG experiments. In some cases, it was impossible and flow rates were taken manually.

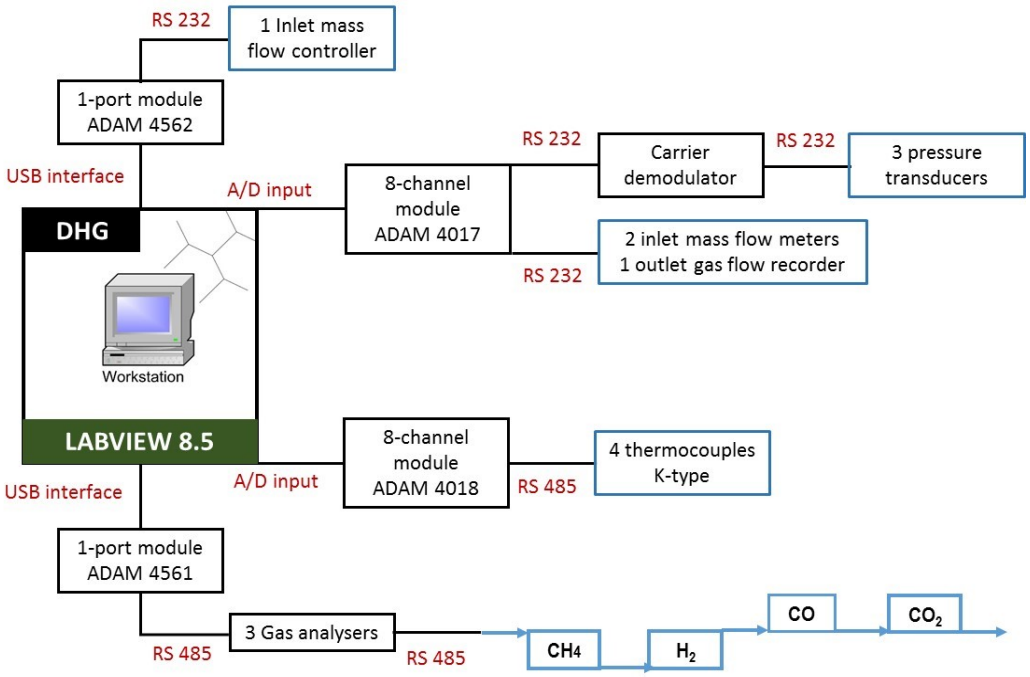

Figure 3.5 Data acquisition and monitoring section from DHG rig.

Safety and preparedness: Safety was of main concern during the DHG experimental phase since the combination of high pressures and temperatures represented a high risk requiring a high standard of precaution and operability. The greatest foreseeable hazard was a rupture/explosion of the rig during a DHG experiment at high pressure and temperature using methane or naphtha feedstock (flammable).

Because of that, the system had a remote technique to stop all hydrocarbon feedstock flow to the rig, stop the flow of energy to the furnaces and turn on alarm system if necessary. The remote stop switch was located near the lab room exit, approximately 2 m from the experiment. Experiments were only conducted when two or more people trained in the safety and experimental procedures were present.

The gas cylinders store was located outside the lab room as was the solvent store for naphtha. Every new relief valve to be connected to the rig was previously calibrated at the required pressure conditions in which the DHG experiments were performed and their safety seals located into the device were checked and replaced for new units prior to utilisation. A back pressure regulator was installed as the vent valve in the vent port at the end of the rig for gas discharge (Figure 3.6). This permitted control of the flow at high pressures (>130 bar).

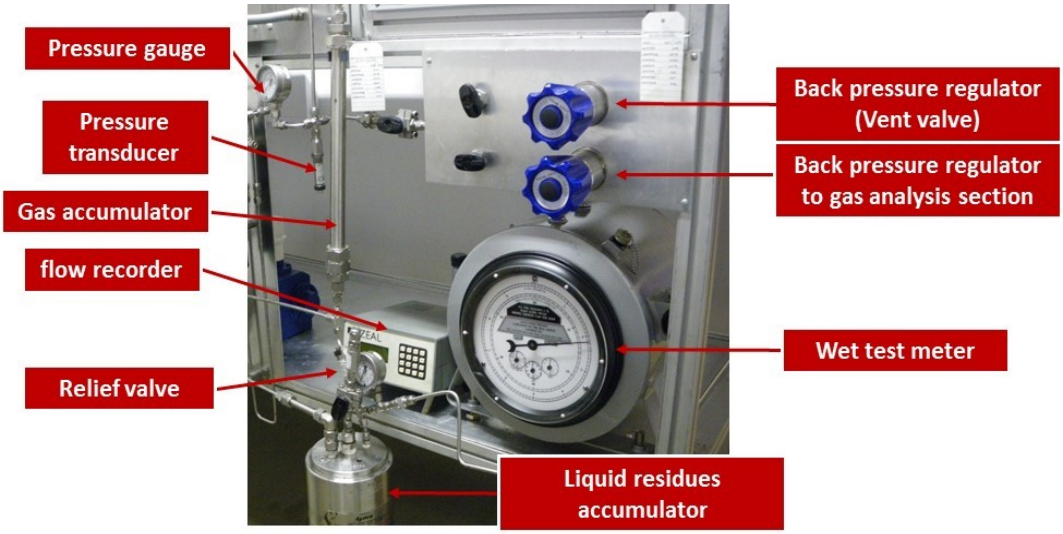

Figure 3.6 Back pressure regulator installed as vent valve.

Due to the liquid residue accumulator being a handmade design for high pressure, the installation of an extra relief valve on its top was mandatory (Figure 3.7).

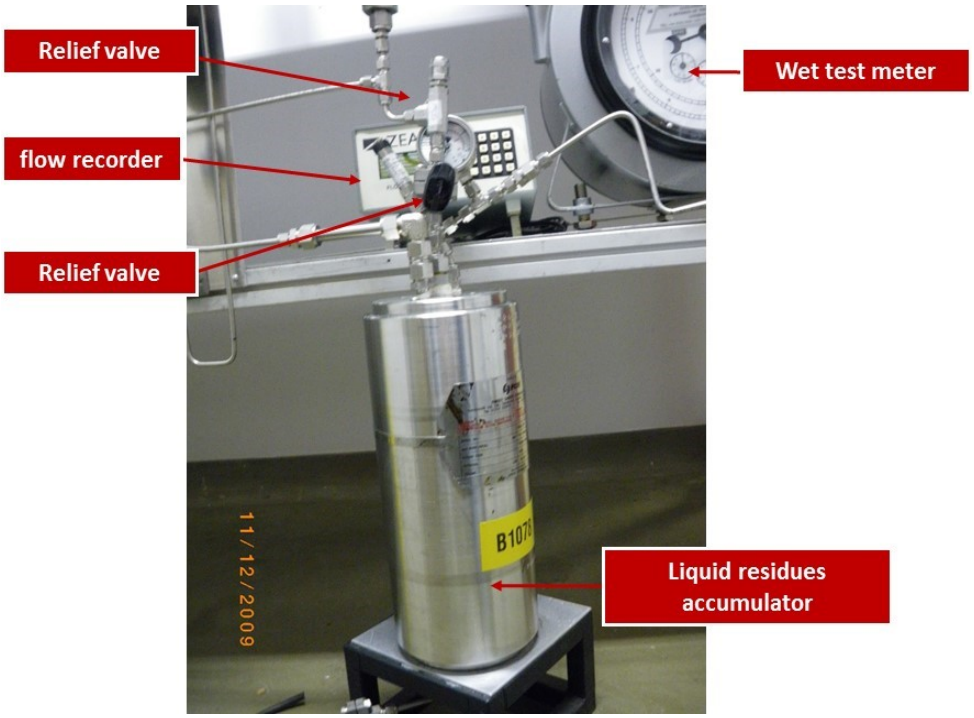

Figure 3.7 Liquid residues accumulator.

Lab room facilities: The lab room contained a ventilation system and gas disposal vent out of the lab room which was used during every DHG experiment. Methane (CH_4), carbon monoxide (CO), hydrogen (H_2) and oxygen (O_2) detection alarms were provided as was a smoke detector/alarm.

3.3.4 Commissioning tests

Once the DHG assembly was completed, the next step was the commissioning stage to test the rig capability and functionality at the pressure and temperature conditions under study in this research (P>130 bar) and T= (600-750) ºC for the gasifier-reformer reactor). Moreover, it was also important to check the correct reading and logging of data in the new data acquisition and monitoring section. Table 3.2 shows the operating conditions used during the commissioning tests.

Table 3.2 Commissioning tests.

	Test	Operating conditions *	Variable *
No catalyst in the Gasifier-reformer [Dimensions: Φ ½ -inch x 30 cm]	A1	20 ºC N_2	**Pressure (bar)**
			220
	A2	20 ºC N_2 180 bar	**Water flow rate ($L.min^{-1}$)**
			0.0022
			0.0050
			0.0100
	A3	20 ºC N_2 180 bar	**Naphtha flow rate ($L.min^{-1}$)**
			0.0002
			0.0010
			0.0020
	A4	20 ºC N_2 180 bar	**Methane flow rate ($L.min^{-1}$)**
			0.2000
			1.0000
			2.0000
	A5	N_2 180 bar	**Furnace temperature**
			Vapouriser (500-600) ºC
			Gasifier-reformer 800 ºC
	A6	20 ºC N_2 180 bar	**N_2 flow rate ($L.min^{-1}$)**
			1.0000
	B1	N_2 180 bar	**Furnace temperature**
			Vapouriser 500 ºC
			Gasifier-reformer 800 ºC
			Heating tape 360 ºC
(*) Average values			

Based on these results, a series of further modifications and improvements of the rig was carried out and will be shown in the next section 3.3.5.

Pressure test: A pressure test was the first performance requirement carried out. This was done using high pressure nitrogen (N_2). Figure 3.8 shows a pressure test as example mode. The pressure was increased gradually up to 180 bar and once no leaks were detected for (12-24) hours, the pressurisation continued up to 220 bar for another 12 hours. This procedure was realised prior to every DHG experiment.

During the pressure test, pressure readings were monitored on the pressure inlet and outlet of the gasifier-reformer with the new data acquisition system to confirm its functionality.

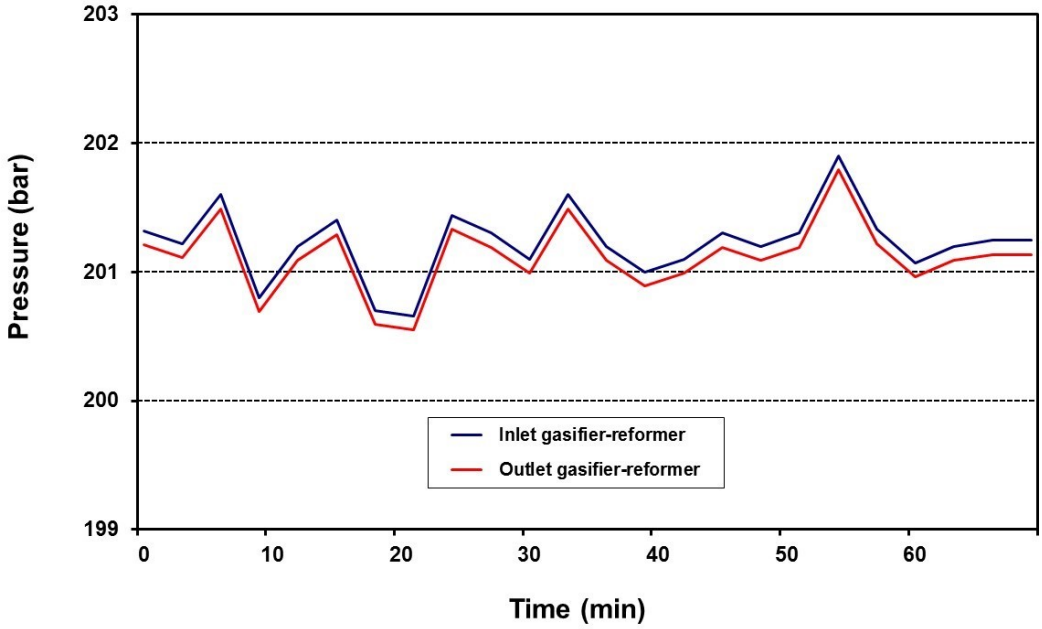

Figure 3.8 Test A1: Commissioning pressure test using nitrogen (N_2).

Tests of injection system, inlet flow rates: The naphtha and water injections were individually tested at atmospheric conditions (1.01 bar, 20 ºC) and at high pressure (180 bar) with the system already pressurised with nitrogen. Likewise, methane was injected using the mass flow controller to the rig already pressurised with nitrogen (180 bar) and, in both cases, the operability of the rig was validated.

The data acquisition and monitoring section was also completely operative to log the inlet flow rates. Three regions of inlet flow rates at which water, naphtha and methane would be injected in the DHG experiments, were tested to evaluate the operability of the injection system. Figures 3.9, 3.10 and 3.11 show the results as example mode.

The mass flow meters and controller were previously calibrated by the manufacturer at high pressure (Maximum pressure = 200 bar) using their corresponding feedstock, naphtha, water or methane.

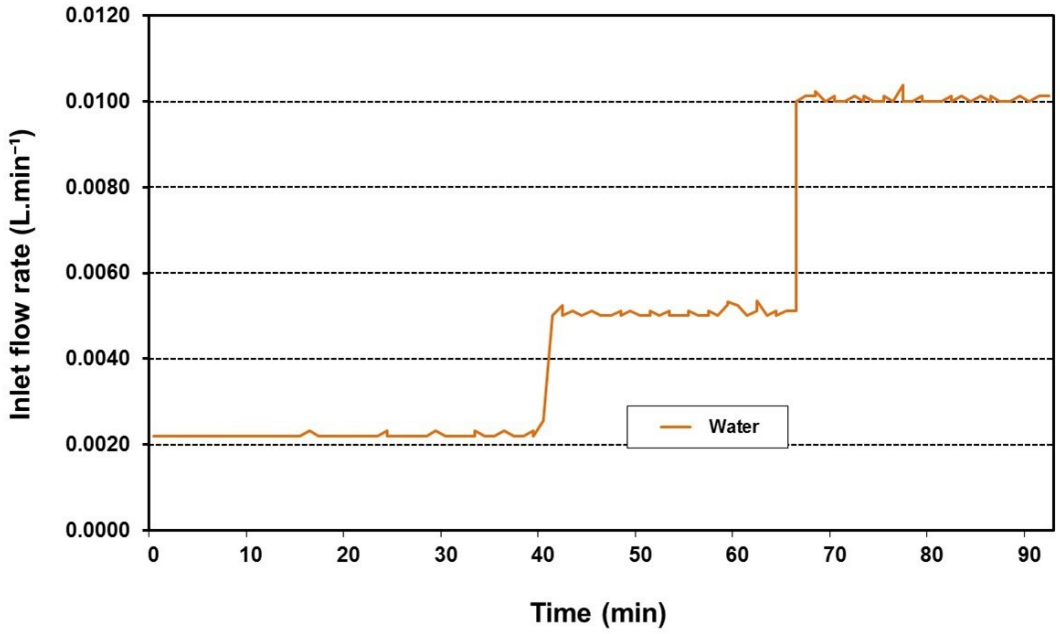

Figure 3.9 Test A2: Water injection into the rig already pressurised with nitrogen (N_2) at 180 bar.

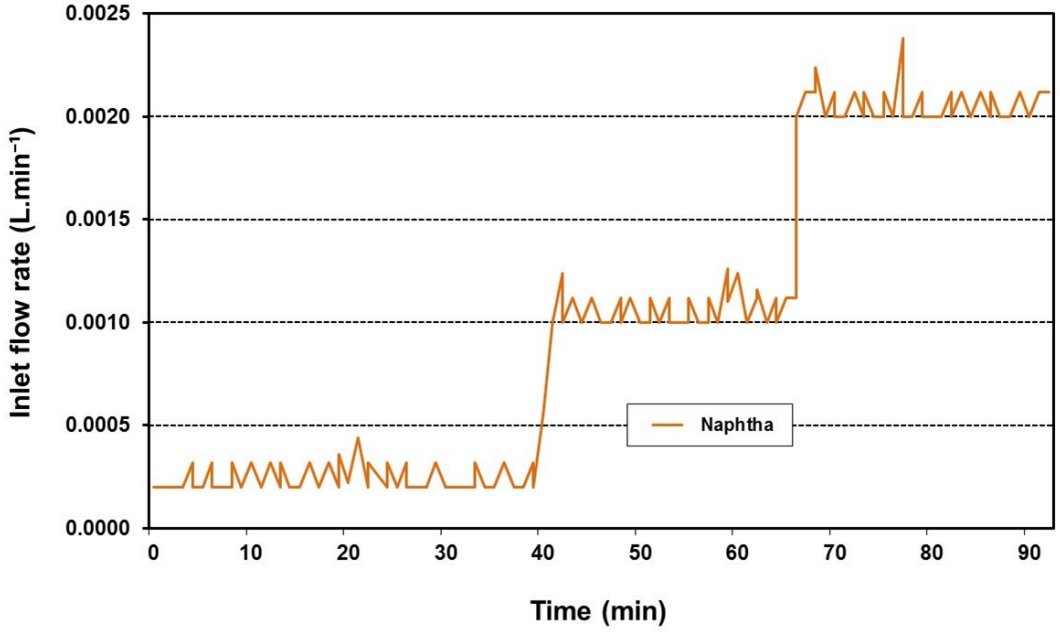

Figure 3.10 Test A3: Naphtha injection into the rig already pressurised with nitrogen (N_2) at 180 bar.

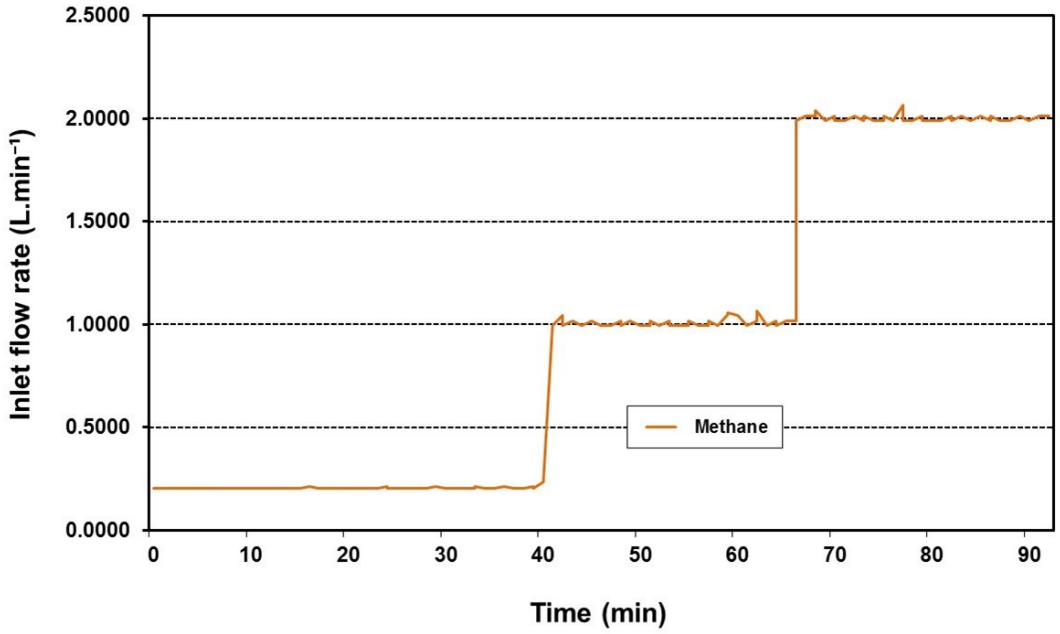

Figure 3.11 Test A4: Methane injection into the rig already pressurised with nitrogen (N_2) at 180 bar.

These types of tests were done periodically (every 3 weeks) to guarantee the operability of the injection system, mass flow meters and controller (inlet flow rates).

Temperature test: the rig having been pressurised previously with nitrogen at 180 bar, a temperature test was carried out for two reasons: (1) to see if injected water could be vaporised to steam and (2) to check the operability of a new program to adjust furnace temperature through their controllers. In the temperature test, water was injected into the vaporiser, passing onto the gasification-reforming section. The gasifier-reformer reactor, the original design, was connected to the rig with no catalyst bed inside.

The new program in the controllers adjusted the furnace temperature by regulating its energy consumption in order to keep the fluid temperature relatively constant within the exits of the vaporiser and the gasifier-reformer. To achieve that, the controllers monitored the internal temperature of fluids in both sections through thermocouples.

For the vaporisation section, the program guaranteed complete water vaporisation keeping the outlet vaporiser temperature higher than the corresponding saturated steam temperature. In the case of the gasification-reforming section, the program ensured that the internal reactor temperature remained relatively constant to the temperature under study.

As example mode Figure 3.12 shows the results obtained in test 5 where

furnace temperature from the vaporisation section was varied in the range of 500-600 ºC to get an outlet vaporiser temperature of 380 ºC, while the furnace from gasification-reforming section was at 800 ºC to get an outlet gasifier-reformer temperature of 700 ºC.

Figure 3.12 shows that, effectively, the outlet vaporiser temperature was 382 ºC approximately, which is higher than the saturated steam temperature at 180 bar (357 ºC) guaranteeing complete water vaporisation in the test throughout. The furnace temperature required was 600 ºC for vaporiser.

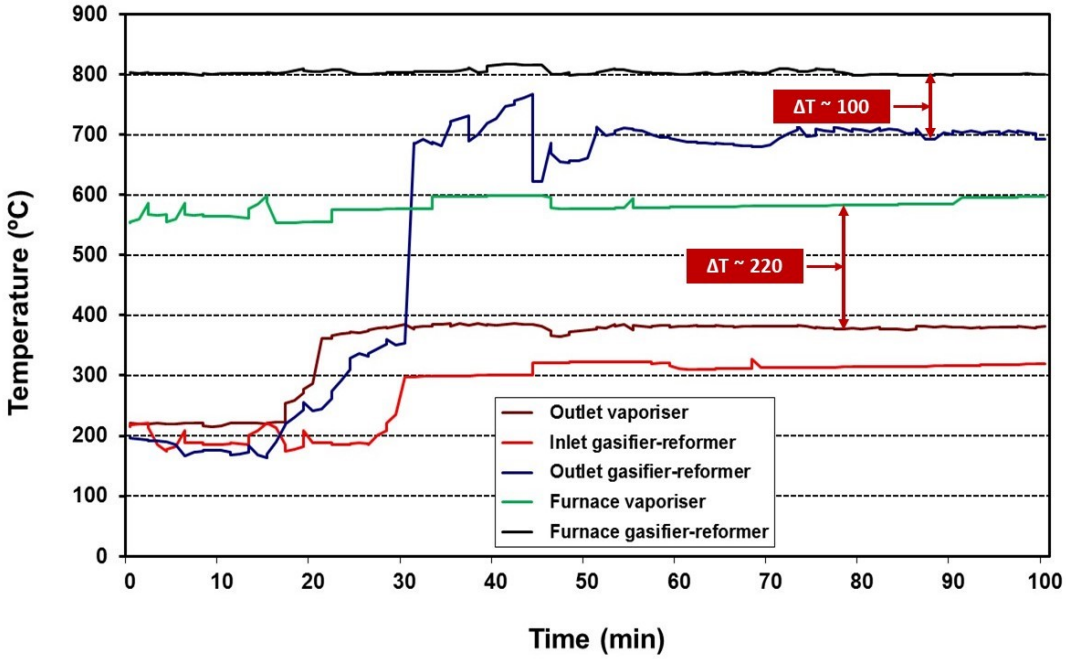

Figure 3.12 Test A5: Temperature during water injection into the rig already pressurised with nitrogen (N_2) at 180 bar.

This undoubtedly represents a temperature gradient between the furnace temperature and the outlet fluid temperature of 220 ºC, which is important. Hence, improving the original vaporiser design to reduce this gradient was a task to carry out. For details, see next section 3.3.5 related to further modifications and optimisations.

In relation to the gradient between the furnace temperature and the outlet fluid temperature in the gasification-reforming section, this was not significant, (ΔT=100 ºC) being an acceptable value. Thus, the original design of the reactor was not modified. In practice during the experimental phase, the furnace temperature was always approximately 100 ºC above that needed to achieve the desired outlet temperature from the gasifier-reformer.

It is important to note that Figure 3.12 shows the significant temperature

drop suffered by the steam in the connecting tube between the vaporisation and gasification-reforming sections: in fact the outlet vaporiser temperature passed from 382 ºC to 320 ºC as the inlet gasifier-reformer temperature. This unwanted drop in temperature also needed to be modified as the second task (see next section 3.3.5).

Overall, the furnace temperature controllers program was operative and fully functional based on our results as showed from Test A5. For that reason, the temperature controllers program was always used in DHG experiments.

Outlet flow rate record: It was found a little difficult to graph the values of the outlet flow rates monitored during the DHG experiments. The wet test meter with the flow recorder model was bit old, which made it complicated to find the correct software from a manufacturer to log, save and graph the data online. However, an effort was made to construct homemade software to compensate for this.

Figure 3.13 shows as example mode a preliminary test to validate the homemade software (Test A6). To validate the software the inlet flow rates of nitrogen flowing through the system were compared with the outlet flow rates once the rig reached 180 bar. Measurements at the exit of the system were carried out once the back pressure regulator reduced the pressure to values near to atmospheric pressure, 1.01 bar according to the instructions for the wet test meter specifications (Appendices, section A.6).

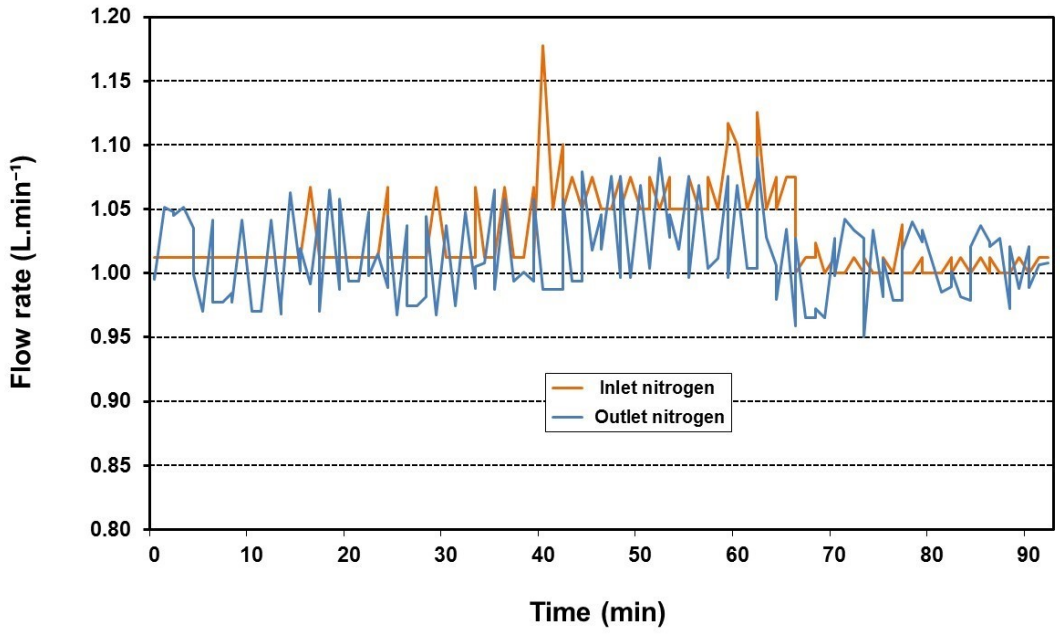

Figure 3.13 Test A6: Outlet flow rates.

The software was validated in terms of values and signal stability. The flow

rates measured by the mass flow and wet test meter showed similar values, despite fluctuations in the measurement signals. Note that the signal stability proper to the equipment itself has an acceptable error margin (< 5 %).

Unfortunately, the difficulty of recording online during the tests continued in the DHG experimental phase. Sometimes, graphs of outlet dry gas flow rates were not obtained and only average values were able to be reported since readings were taken manually during the important periods of interest during the experiments.

The recommissioning of the flow meter recorder and software took a long time and therefore, it was decided to continue the experimental phase meanwhile, and make a special effort to record online the outlet flow rates in the main DHG experiments.

For future work, an updated flow recorder enabling the logging and saving of data online during DHG experiments is recommended.

3.3.5 Further modifications and optimisations

Commissioning tests performed on the original design of the DHG rig, showed the necessity of modifications to the new reactor section and the connecting tube between the vaporisation and gasification-reforming sections. Once the changes were completed, the rig was again tested and evaluated. Details will be discussed here as well as any difficulties found throughout.

Additionally, other optimisations on the gasification-reforming section were performed as a consequence of: (1) the use of naphtha feedstock in the DHG rig and, (2) our interest in increasing the gasifier-reformer reactor length and catalyst loading. A new series of tests were carried out to validate the new changes before the DHG experiments started to run.

New vaporiser reactor: The vaporiser reactor was modified to improve the original design and maximise heat transfer efficiency from furnace to reactor and from the reactor to the feed: water and water/naphtha. This reduced the energy consumption from the furnace needed to vaporise the fluids in the vaporiser reactor. As mentioned in the previous section in test A5, the original design showed a temperature gradient of 220 ºC between the furnace and outlet vaporiser temperatures using just water fluid.

The original design used by Greaves et al. (2004), Greaves et al. (2005), Greaves et al. (2006) and Greaves et al. (2008) was constructed with a stainless steel tube 316L, 1 inch in diameter, 0.083 inch tube wall thickness and 30 cm in length. This tube was connected to a 316L stainless steel coil tube, ⅛-inch diameter, 0.028 inch tube wall thickness and 30 cm coiled tube length (1.5 m straight tube length approximately).

The design was changed in our investigation to two coiled tubes connected together, both made of stainless steel (SS) 316L, ⅛ -inch diameter, 0.028 inch tube wall thickness and 30 cm coiled tube length (6 m straight tube length each). Figure 3.14 shows the vaporiser reactor used for the DHG experiments in this research.

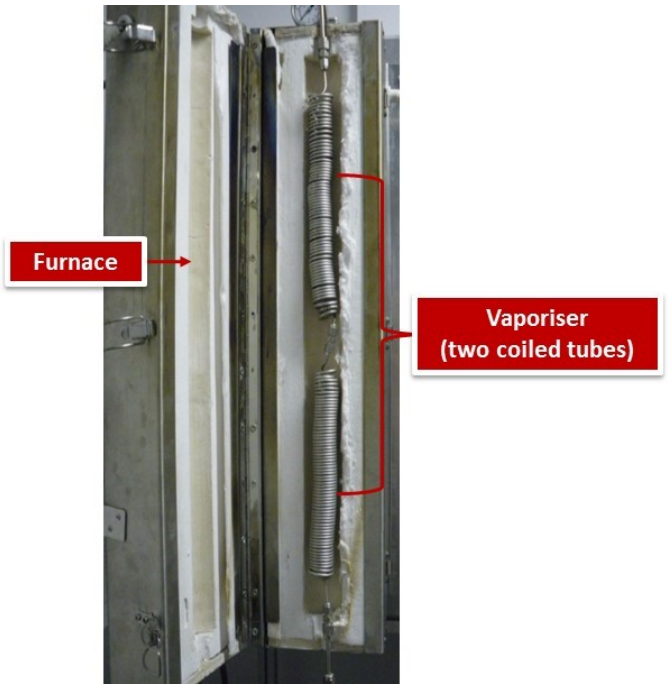

Figure 3.14 Revamped vaporiser reactor.

In theory, a longer and thinner vaporiser tube increases residence time and heat transfer which favours the vaporisation process (Fogler, 2006). A new commissioning test to validate this was carried out once all the series of modification and optimisations were completed (Test B1).

A heating tape and new isolation system on the connecting tube between vaporisation and gasification-reforming sections: To reduce heat loss from the connecting tube, it was decided to install: a heating tape, a thermocouple to monitor the temperature required in the tube if necessary and a new isolation system which was made of thermal ceramic fibre covered by aluminium sheets. Figure 3.15 shows these improvements.

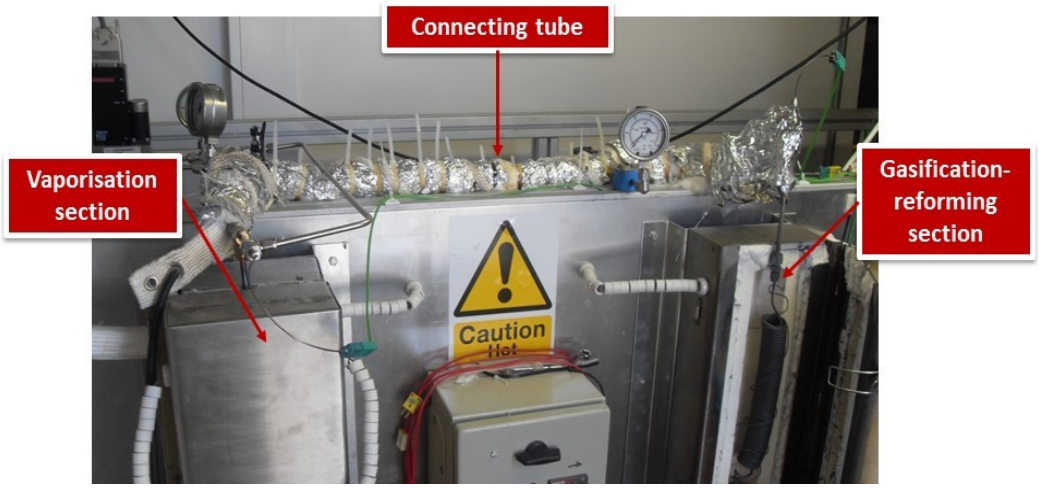

Figure 3.15 Connecting tube between vaporiser and gasification-reforming sections with heating tape and new isolation system.

The heating tape temperature was regulated and monitored during the DHG experiments to avoid coke formation and to maintain the conditions of steam saturation.

A commissioning test (Test B1) was carried out to evaluate these modifications. Figure 3.16 shows the result. The operating conditions were the same as those used in test A5. The heating tape was regulated at 360 ºC. The rig was previously pressurised with nitrogen (N_2) at 180 bar. Table 3.2 shows the operating conditions used in Test B1.

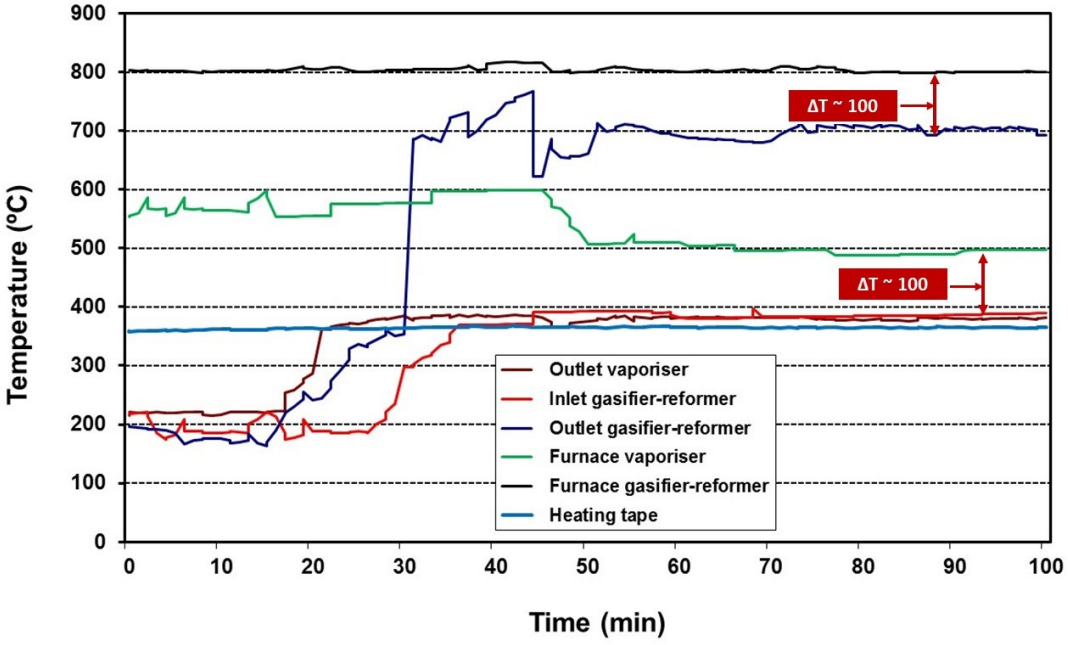

Figure 3.16 Test B1: Temperature during water injection into rig already pressurised with nitrogen (N_2) at 180 bar.

Results indicated a drastic reduction of required furnace temperature: 500 ºC instead of the 600 ºC previously required to reach the same outlet vaporiser temperature. The temperature gradient with the new vaporiser design was 100 ºC, thereby validating the efficiency of this new design. It is possible that the higher residence time and greater contact area favoured the heat transfer.

In the case of the connecting tube, heating tape and isolation system, these performed favourably. There was no important difference between the outlet vaporiser temperature and the inlet gasifier-reformer temperature. Hence, both modifications were used for the DHG experiments.

In the case of the methane feedstock, DHG experiments based on these modifications were performed with no major inconveniences; the results are discussed in chapter 5. However, when the first trials of the DHG experiments using naphtha feedstock were started, we did find some difficulties at some points:

- Interferences at the mixing (entry) point in the injection system between the water and naphtha prior to the vaporisation section.
- Coke formation in the pre-heating unit prior to the gasifier-reformer reactor in the gasification-reforming section.

At the second stage of trials, further optimisations were carried out and are discussed below.

New location of mixing (entry) point of water/naphtha injection in the vaporisation section: The mixing (entry) point is the point where the water inlet flow rate and the naphtha inlet flow rate are mixed. The original rig design located this entry prior to the vaporisation furnace and the mixing process occurred at lab room conditions in liquid phase, 20 ºC and 1 bar approximately.

Greaves et al., (2004) reported some interferences when pentane and water were co injected to the rig. To avoid these, this research allocated the mixing (entry) entry point in the vaporisation section connected between the coiled tubes which the vaporiser reactor is comprised of. Figure 3.17 shows the optimisation.

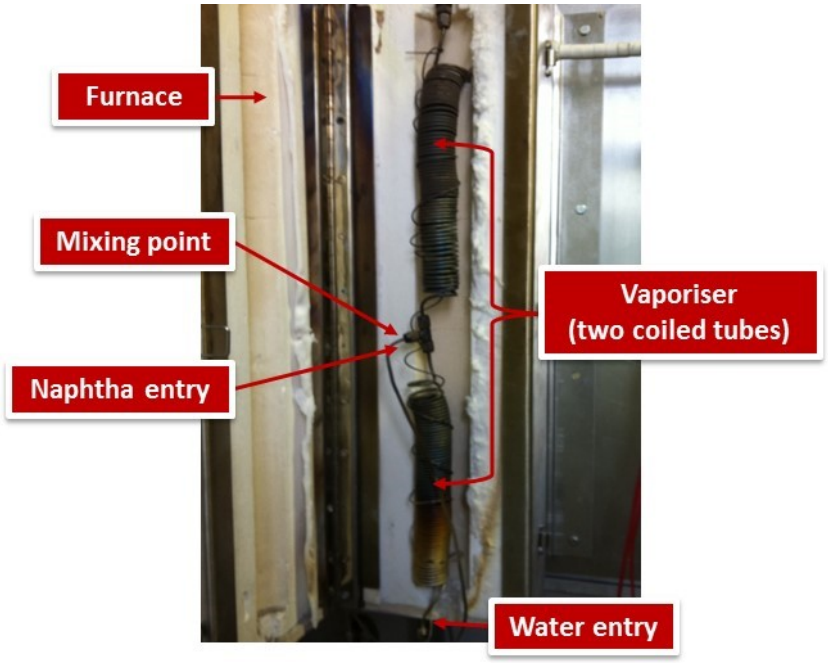

Figure 3.17 Mixing (entry) point in vaporisation section.

The water fluid enters the vaporiser from the bottom while the naphtha (with lower boiling temperature) enters at the mixing point. This permitted the mixing to occur at a higher temperature with the presence of steam favouring the total vaporisation of the water/naphtha. The design was based on Eiler's (2010) research where steam reforming studies in a micro channel reactor were carried out using an optimised mixing process of water/liquid hydrocarbons prior to the reactor. This arrangement was used for DHG experiments using the naphtha feedstock.

Removal of pre-heating unit prior to gasifier-reformer reactor in DHG experiments using naphtha feedstock: This optimisation was realised to avoid coke formation in the gasification-reforming section when naphtha was used as feedstock. In the first trial of the DHG experiments using naphtha (Run 20-01) which will be discussed and analysed in chapter 6 (section 6.2.2), the gasification-reforming section was unexpectedly blocked by carbon deposits just a short time after the naphtha injection.

Table 3.3 shows the operating conditions during the DHG test and Figure 3.18 shows the pressure curves indicative of coking; a drastic pressure drop after 300 minutes was observed between the inlet and outlet pressure of the gasifier-reformer.

Table 3.3 Run 20-01: Operating conditions during DHG test using naphtha feedstock (Catalyst C11-PR).

Run	20-01 (DHG test)
Reformer tube dimensions	Φ ½ -inch x 30 cm
Catalyst type	C11-PR
Catalyst loading (g)	15.2
Catalyst size (mm)	6 x 6 x 2
Pressure (bar) *	10
Outlet gasifier-reformer temperature (ºC) *	650
Steam to carbon molar ratio (Naphtha) *	6
Total inlet flow rate ($L.min^{-1}$) *	0.0110
Naphtha inlet flow rate ($L.min^{-1}$) *	0.0020
Water inlet flow rate ($L.min^{-1}$) *	0.0090
(*) Average values	

On disconnecting the gasification-reforming section, inspection showed that the pre-heating unit prior to the gasifier-reformer reactor was totally blocked by coke deposits while the reactor remained unchanged: no coke deposits or disintegration of the catalyst.

This is technically possible as a consequence of the high temperature in the gasification-reforming furnace, no catalyst presence and a higher tendency or affinity of higher hydrocarbons like naphtha to form coke. To avoid this, the pre-heating section dimension was modified and based on the results (coke formation regardless of the pre-heating dimensions, see appendices, section A.7 for details), it was decided to remove it entirely. In consequence, the gasifier-reformer itself also acted as the preheating unit.

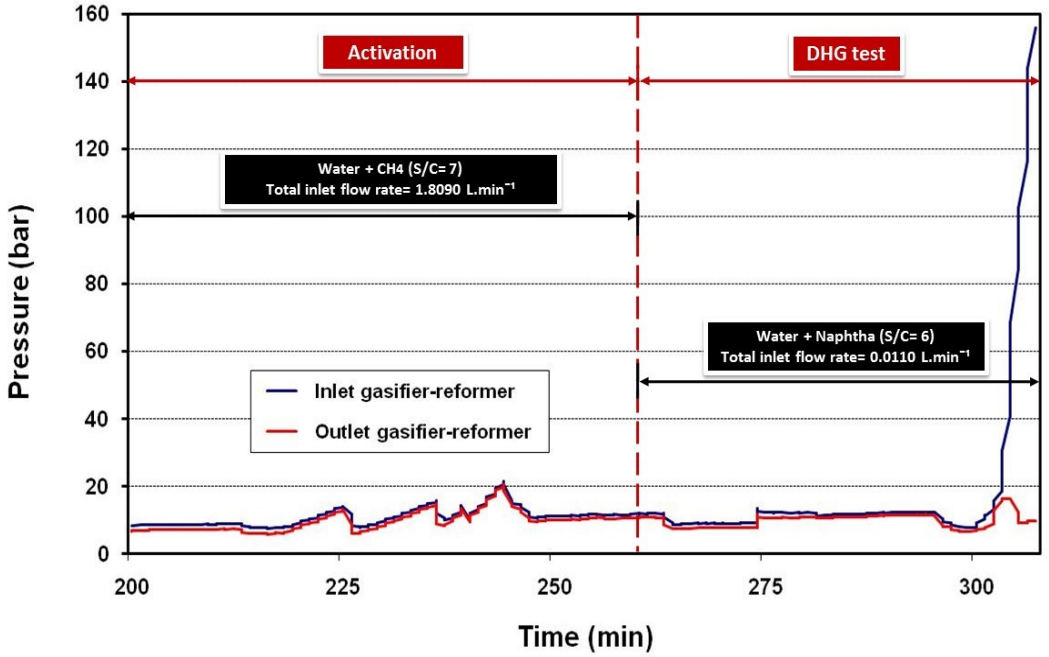

Figure 3.18 Run 20-01: Inlet and outlet pressure of gasifier-reformer during DHG test using naphtha feedstock (Catalyst C11-PR).

A pre-heating section enables the feedstock to be heated up reducing thermal shocks or temperature drop once it enters into contact with the catalyst in the gasifier-reformer. This gradient influences enormously the conversions obtained and the mechanical properties of the catalyst (Shayegan et al., 2008, Lee et al., 2008).

Figure 3.19 shows the final gasification-reforming section used for the DHG experiments using naphtha feedstock where the pre-heating section was removed. For the DHG experiments using methane feedstock, the original design was used (see Figure 3.7, section 3.3.2).

The unit consists of a 316L stainless steel tube, ½ -inch in diameter, 0.083 inch in tube wall thickness and 30 cm in length as the gasifier-reformer reactor.

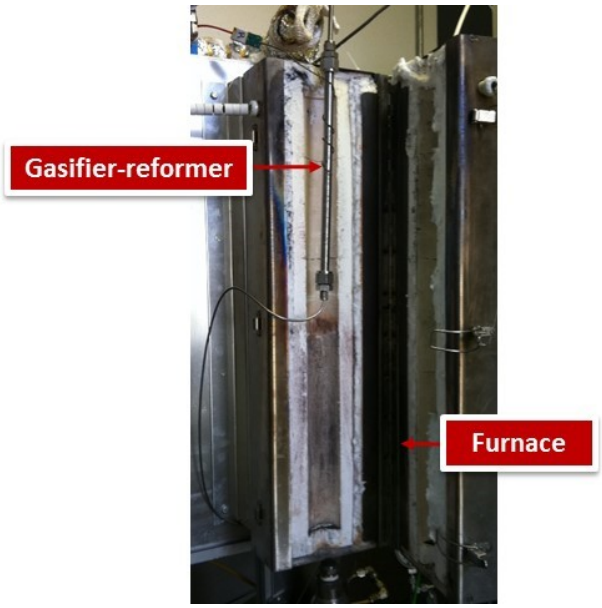

Figure 3.19 Revamped gasification-reforming section design used for DHG experiments (naphtha feedstock).

Increasing gasifier-reformer reactor length and catalyst loading in DHG experiments using naphtha feedstock: Some DHG experiments to be discussed in Chapter 6, section 6.3 and 6.4, were realised with a new gasifier-reformer reactor length, which was increased to study its effect on conversions and the quantity of hydrogen in produced dry gas at values of pressure higher than 130 bar.

The new reactor configuration is shown in Figure 3.20. The gasifier-reformer reactor diameter was kept the same but the tubing length was increased to 72 cm, from the previous value, 30 cm.

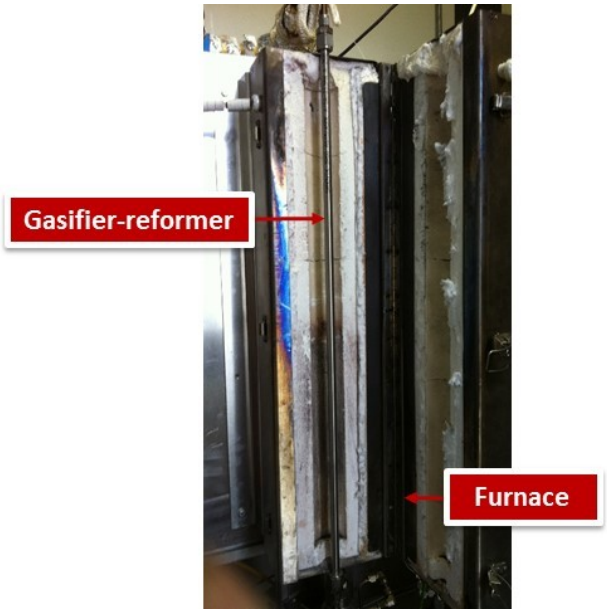

Figure 3.20 Gasifier-reformer reactor. Tube length 72 cm.

Cooling circulating bath for condenser: In the gas-liquid separation, the condenser unit which enables the cooling down of the produced gas from the gasifier-reformer reactor after the reaction, was optimised from the original design.

A cooling circulating bath with ethylene glycol at -5 ºC was connected to the jacket of the condenser to increase the efficiency of gas-liquid separation. Dry gas composed of H_2, CO, CO_2 and CH_4 would pass through the section to be analysed while any liquid residue, water and unreacted naphtha would be sent into the liquid residue accumulator.

Figure 3.21 shows the condenser connected to cooling circulating bath. This optimisation was used for the DHG experiments using both methane and naphtha feedstock.

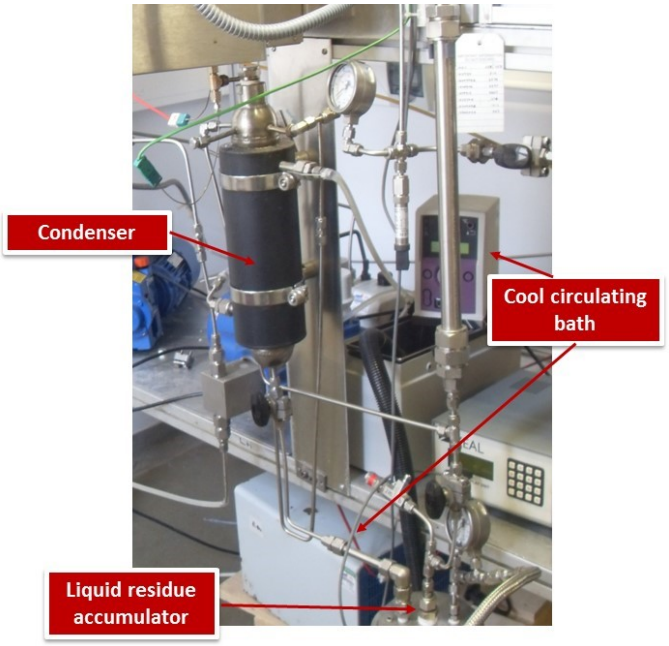

Figure 3.21 Condenser connected to cooling circulating bath.

3.4 Downhole gasification (DHG) rig: Revised design

Once the further modifications and optimisations were completed, the final design was generated and assembled to conduct the DHG experiments using methane and naphtha feedstock in a safe manner.

The final DHG design permitted the maximisation of rig efficiency in terms of the energy consumption, conversion, H_2 percentage in produced dry gas composition as the main gas of interest, and also in terms of the technical reliability in our experimental results as will be discussed in the analysis in the next chapters, 5, 6 and 7.

H_2 is considered to be the most important gas to generate. This is because in the DHG oil recovery techniques, it forms a more efficient gas cap than other gases to displace the oil from reservoir to surface. H_2 is more efficient than CO, CO_2 and CH_4 in this respect because it is less soluble in the hydrocarbons and the water from the reservoir according to Lake et al., (2008). Additionally, the H_2 generated in the reservoir is a very valuable gas and it can be sold once the oil recoverable economically has been displaced.

3.4.1 Flowsheet and assembly

Figure 3.22 and 3.23 show vaporisation and gasification-reforming as the main sections of the rig used for our DHG experiments with methane and naphtha feedstock.

Figure 3.22 Revamped vaporiser design for (a) methane feedstock, (b) naphtha feedstock.

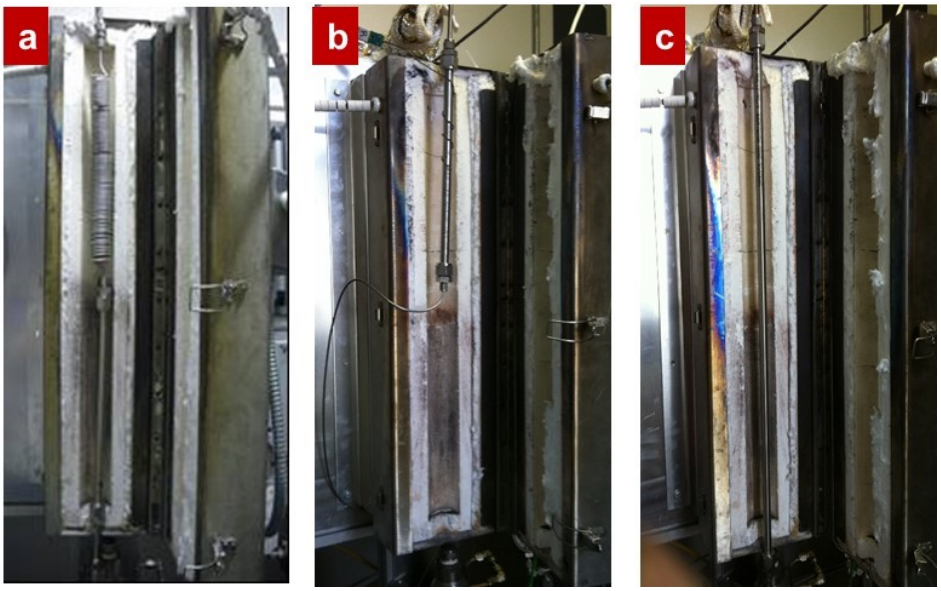

Figure 3.23 Revamped gasifier-reformer design used for DHG experiments using (a) methane feedstock, (b) and (c) naphtha feedstock.

The revised DHG flowsheet is shown in Figure 3.24. Every original section remained, although several modifications and optimisations were realised in some of them.

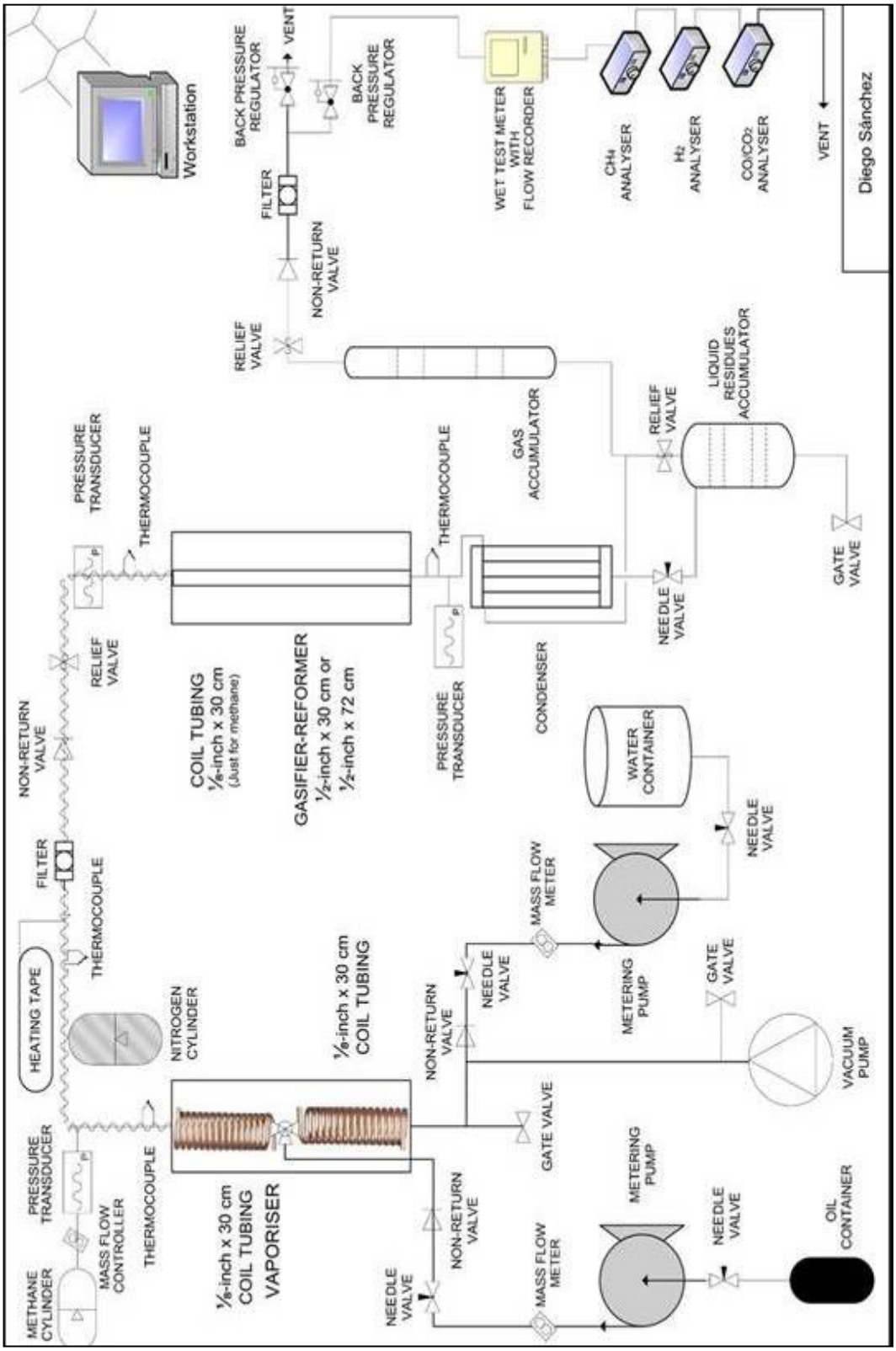

Figure 3.24 Revised flowsheet of downhole gasification (DHG) rig.

3.4.2 Equipments, instruments and lab tubing

A summary of equipments, instruments and tubing used for the final DHG assembly are listed here.

Equipments:

Item	Description	Quantity
Vacuum pump	Fisher Maxima. Code 13-880-14	1
Liquid pump	MPL. Maximum pressure 200 bar Flow injection rate (0-0.03) $L.min^{-1}$	2
Glass container	Pyrex. Capacity 2L	2
Needle valve	Swagelok SS-316L-¼-inch	5
Gate valve	Swagelok SS-316L-¼-inch	3
Non-return valve	Swagelok SS-316L-¼-inch	4
Relief valve	Swagelok SS-316L-¼-inch	3
Filter	Swagelok SS-316L-¼-inch Particulates filter 0.5 μm	2
Heating tape	Samox. Code EW-36115. Length 72 cm Maximum temperature 760 ºC	1
Furnace	Lenton vertical split tube furnace with temperature controller Watlow Series 96 Maximum temperature 1200 ºC	2
Gas accumulator	Swagelok SS-316L-1-inch. Length 45 cm	1
Condenser	Homemade design. SS-316L. Cap. 1L Maximum pressure 230 bar	1
Liquid residues accumulator	Homemade design. SS-316L. Cap 4L Maximum pressure 230 bar	1
Back pressure regulator	Tescom 26-1700 Series Maximum pressure 1034 bar	2
Cooling circulating bath	Cole Parmer. Code EW-12122 Bath capacity 6.5L with ethylene glycol Temperature range (-20 to 100) ºC Maximum flow pump 17 $L.min^{-1}$	1
Vials	Fisher scientific clear glass black caps Capacity 15 mL	15
RS232 cable	Belden EIA-232. PVC Jacket. 300V	4
RS485 cable	Belden EIA-232. PVC Jacket. 300V	3
USB interface module	Adam 4561. 1-port Isolated USB to RS-232/422/485 Converter	1
USB interface module	Adam 4562. 1-port Isolated USB to RS-232 Converter	1
PC (workstation)	Compaq T6500 2.10 GHz. Windows XP	1
LABVIEW	Version 8.5	1

Instruments:

Item	Model	Range	Reading accuracy (%)*
1 Mass flow meter (calibration with n-heptane)	Brooks QMBM2L1A2	(0-0.0100) $L.min^{-1}$ Min. flow rate 0.0002 $L.min^{-1}$	± 0.02
1 Mass flow meter (calibration with n-heptane)	Brooks QMBM2L1A2	(0-0.0100) $L.min^{-1}$ Min. flow rate 0.0002 $L.min^{-1}$	± 0.02
1 Mass flow controller (calibration with CH_4)	Brooks 5850TR	(0-2.0000) $L.min^{-1}$ Min. flow rate 0.0002 $L.min^{-1}$	± 0.02
4 Thermocouples	Omega Type K KMTXL062U12	(0-1335) ºC Min. temp. 1 ºC	± 1
3 Pressure transducers	Validyne DP15 with Carrier Demodulator Validyne CD15	(0-230) bar Min. pressure 1 bar	± 1
1 Wet test meter with flow recorder	A. Wright DM3C	(0-10.00) $L.min^{-1}$ Min. flow rate 0.01 $L.min^{-1}$	± 0.15
1 CH_4 analyser	HiTech IR150	0-100 % Min. detection 0.01 %	± 2
1 H_2 analyser	HiTech KIR150	0-100 % Min. detection 0.01 %	± 2
1 CO/CO_2 analyser	Servomex 1440C	0-100 % Min. detection 0.01 %	± 2
1 Portable O_2 analyser	Servomex 570A	0-100 % Min. detection 0.1 %	± 1
1 A/D input module	Adam 4017	8-channel 0-10 V	± 0.1
1 A/D input module	Adam 4018	8-channel 0-20mA	± 0.2

(*) Standard temperature and pressure

Lab tubing:

Item	Description	Wall thickness (inch)	Dimensions (inch x cm)
Connections	Swagelok Stainless steel 316L	0.035	¼ x 90
Vaporiser	Swagelok Stainless steel 316L-coiled	0.028	⅛ x 30 (2 units)
Pre-heating unit prior to the gasifier-reformer (CH_4 feedstock)	Swagelok Stainless steel 316L-coiled	0.028	⅛ x 30
Gasifier-reformer (CH_4 feedstock)	Swagelok Stainless steel 316L	0.083	½ x 30
Gasifier-reformer (Naphtha feedstock)	Swagelok Stainless steel 316L	0.083	½ x 30 (design 1)
	Swagelok Stainless steel 316L	0.083	½ x 72 (design 2)

References

AFANDIZADEH, S. AND FOUMENY, E.A, 2000. Design of packed bed reactors: guides to catalyst shape, size and loading selection. *Applied thermal engineering,* 21, pp. 669-682.

ASME, 2008. *Metals handbook: Properties and selection of iron, steels and high-performance alloys volume 1.* Washington: ASM International Press.

CALLAHAN, F.J., 1993. *Tube fitter's manual.* U.S.: Swagelok Co.

EILERS, B.J., 2010. *Microchannel steam-methane reforming under constant and variable surface temperature distributions.*

FOGLER, H.S., 2006. *Elements of chemical reaction engineering.* 4th edition. New York: Pearson Education, Inc.

GREAVES, M., RATHBONE, R., XIA, T., BENTHAHER, A., DUGGAN, S., 2004. *Downhole gasification for improved oil recovery and gas production (phase 1) experimental studies (1 Nov 2002 – 31 Oct 2004).* United Kingdom: University of Bath, (Confidential internal report).

GREAVES, M., XIA, T., RATHBONE, R. AND BENTAHER, A., 2005. Underground gasification for improved oil recovery. *Canadian international petroleum conference,* 7-9 June 2005 Calgary. Calgary: Petroleum Society Canadian Institute of Mining, Metallurgy & Petroleum, pp. 38-48.

GREAVES, M., RATHBONE, R., XIA, T., BENTHAHER, A., 2006. Experimental study of a novel In situ gasification technique for improved oil recovery from light oil reservoirs. *JCPT,* 45(8), pp. 41-47.

GREAVES, M. AND XIA, T.X., 2008. Producing hydrogen and incremental oil from light oil reservoirs using downhole gasification. *Canadian international petroleum conference,* 17-19 June 2008 Calgary. Calgary: Petroleum Society Canadian Institute of Mining, Metallurgy & Petroleum, pp. 14-24.

LAKE, L.W., WALSH, M.P., 2008. Enhanced oil recovery (EOR) field data: literature search. U.S.: University of Texas.

LEE, S., JOONGMYEON B.B., SUNGKWANG L.C. AND JOONGUEN P., 2008. Improved configuration of supported nickel catalysts in a steam reformer for effective hydrogen production from methane. *Journal of power sources,* 180, pp. 506–515.

PERRY, R.H. AND GREEN, D., 1984. *Chemical Engineers Handbook*. 6th edition. New York: McGraw-Hill.

PINKWART, K., BAYHA, T., LUTTER, W. AND KRAUSA, M., 2004. Gasification of diesel oil in supercritical water for fuel cells. *Journal power sources,* 136, pp. 211-214.

REID, R.C., PRANSUITZ, J.M. AND POLING, B.E., 1987. *The properties of gases and liquids.* New York: McGraw-Hill.

SHAYEGAN, J., YOUSEF MOTAMED HASHEMI, M. M. AND VAKHSHOURI, K., 2008. Operation of an industrial steam reformer under severe condition: A simulation study. *The canadian journal of chemical engineering,* 86, pp. 747–755.

SUSANTI, R., NUGROHO, A., LEE, J., KIM, Y. AND KIM, J., 2011. Noncatalytic gasification of isooctane in supercritical water: A strategy for high-yield hydrogen production. *International journal of hydrogen energy,* 36, pp. 3895-3906.
VISWANATHAN, R., 1989. *Damage mechanisms and life assessment of high temperature components.* Washington: ASM International Press.

CHAPTER 4: EXPERIMENTAL PROCEDURE, DATA ANALYSIS AND CHARACTERISATION OF SAMPLES

4.1 Introduction

This section shows details related to the DHG experimental phase where procedures utilised, data processing and characterisation of samples will be discussed. The technical reliability of our experimental results was vital; therefore, special attention was paid to the facts of: how to run a DHG experiment in a safe manner, how to take samples for analysis, how to process data once the experiment has finished and how reliable technically our results are.

In this respect, the data analysis involved a series of preliminary tests to minimise uncertainties in our direct readings from experiments and further calculations for analysis. Calibration of equipments, stability of signals, right equations to process data were all taken in consideration and are described and examined here.

4.2 Experimental procedure

Before starting a DHG experiment, the rig was always purged and tested using N_2 gas at different pressures and furnace temperatures to detect gas leaks. Every relief valve as well as every piece of equipment in the system was previously calibrated at desired operating conditions (section 4.3.1). The laboratory safety system was always checked.

4.2.1 Operation technique

It usually took about 10 hours on average to run a DHG experiment, with variations depending on what variable was under study and the number of test periods that the particular DHG experiment involved.

In our investigation, the term ´DHG experiment´ refers to a complete run. The ´test period´ term refers to a period during the experiment or run during which certain operating conditions are being evaluated in the rig, more specifically in the gasifier-reformer reactor, in terms of pressure, temperature, produced dry gas composition (vol. %) and dry gas outlet flow rate (total volume of dry gas generated per time unit).

Using methane feedstock (Chapter 5), the DHG experiments involved 3 test periods: (1) catalyst activation treatment to prepare the catalytic surface for the chemical reactions of interest, (2) the DHG test proper where our operating conditions and chemical reactions were studied and, (3) catalyst reactivation treatment to evaluate the possibility of catalytic activity restoration to initial conditions before the DHG test.

Using naphtha feedstock (Chapter 6) the DHG experiments involved 2 test

periods: (1) catalyst activation treatment and (2) the DHG test proper on the basis of the results obtained.

Before starting, the gasifier-reformer reactor tube was packed with the catalyst under study to be connected to the rig subsequently. Every piece of equipment and instrument was powered on. Levels of naphtha and water in the glass cylinders were revised and filled or replaced if necessary. The pressure in the methane cylinder was also checked.

To minimize the margin for error by the operator during the experiments, the following steps about how to run a DHG experiment were generated and repeated every time a new experiment was performed:

- Turn-on the computer and run the homemade software for the data acquisition and control (LABVIEW). Check that all inputs are being received properly
- Turn on the gas analysers (O_2, H_2, CO, CO_2, CH_4) and the wet test meter
- Turn on the power of the mass flow meters and controllers
- Turn on the power of the furnaces
- Turn on the power of the cooling circulating bath for the condenser
- Check the data displayed on the computer screen
- Check gas delivery system, gas cylinder pressure level, water and naphtha levels in the glass containers

Start-up procedure items:

- Air extraction by using a vacuum pump. Turn on the vacuum pump already connected to the DHG rig in order to extract air contained in the tubing. Period: couple of minutes and turn off the vacuum pump afterwards.
- Pressurising the system using nitrogen (N_2). Open the valve of the gas cylinder and let the rig be pressurised. Adjust the rig at the required pressure regulating the back pressure controller installed in the vent section at the end of the rig (see final DHG rig flowsheet, Figure 3.32 in chapter 3). The required pressure depended on the DHG experiment and variable under study. Keep purging the system until the reading of the portable oxygen analyser connected temporally to the vent section is zero. Shut off the valve of the N_2 cylinder and the back pressure controller in the vent section.
- Heating up the vaporiser and gasifier-reformer furnaces. Set the furnace power controllers to the desired temperatures and turn on the cooling circulating bath with ethylene glycol.
- Injection of water. Set the desired flow rate of injection pump through the mass flow meter. Start water injection into the system.
- Injection of methane. Set the required flow rate through the mass flow controller and start the injection process.

- Injection of naphtha. In DHG experiments where naphtha was the feedstock, set the desired flow rate through the mass flow meter and start injecting into the rig.
- Maintain the injection process of water and methane or naphtha for a certain period until the desired pressure is reached. Regulate back pressure controller in the vent section to keep the pressure value relatively constant. In the meantime, make sure that data acquisition and monitoring is completely operable and that data is being completely logged and saved.
- Slowly open the back pressure controller connected to the wet test meter and gas analysers to initiate the produced dry gas analysis of the DHG experiment. Regulate and adjust the back pressure controller to keep the analysis online and the desired pressure constant. To avoid abrupt pressure changes, shut down the controller if necessary.

Shut down procedure items:

- Shut down the back pressure regulator connected to the wet test meter and gas analysers.
- Turn off the computer and program for the data acquisition and control (LABVIEW). Once more, check that all data was logged and saved.
- Turn off the gas analysers (O_2, H_2, CO, CO_2, CH_4) and the wet test meter.
- Turn off the power of the mass flow meters and controllers.
- Turn off the power of the furnaces.
- Turn off the power of the cooling circulating bath for the condenser.
- Stop methane or naphtha injection.
- Shut down gas delivery to the system.
- Discharge the naphtha still in container.
- Stop water injection.
- Reduce the system pressure by slowly opening the back pressure controller from the vent section.
- Once rig is cooled down, purge the rig using N_2.
- Collect the solid and liquid sample from the rig. For details see the sampling procedure in section 4.2.4.
- Make sure that all the electrical power supplies are switched off once a run has finished.

4.2.2 Safety considerations

The DHG experiments used methane and naphtha as feedstock. Both are highly flammable and considerable amounts were consumed during experiments; this certainly required a high level of diligence to successfully perform the runs at high pressure and temperature in a completely safe manner.

The DHG rig was located inside a lab room with an installed gas extraction system and a vent system that discharged the gas directly out of the room. Further safety considerations during every run were:

- In the event that the naphtha in the container (2 litre) is evaporated into the air, the concentration of the flammable material is less than 0.01 vol. %, which is far below the LEL of light oil (LEL 0.9 and UEL 7.0, see material safety data sheet in Appendices, section B.1 and ref. Perry and Green, 1984, Reid et al., 1987).
- Once the DHG experiment has been carried out, the naphtha is immediately taken to the solvent store. This significantly reduced the risk of fire and explosion caused by leakage.
- The lab room is equipped with a fire extinguishing device which provided an additional safety item.
- During the run, a 4-gas monitor was used to detect the concentration of CH_4, CO, H_2 and O_2 in the lab room. If the detected level of flammable gas was above the limit, the alarm would go off.
- Constant observation by the operator was always carried out.

4.2.3 Risk assessment

During the experimental phase risk assessments were always observed. The most important rule is that no naked flames and electrical source of ignition are allowed in the lab room and only authorised people have access.

Details on risk assessment is reported in Appendices, section B.2.

4.2.4 Sampling procedure

Apart from the produced dry gas monitored and analysed online, liquid and solid samples were also analysed subsequent to the run. To that end, a short sampling procedure was carried out and replicated for every DHG experiment.

Solid samples: Basically, these were the catalysts and any solid particles present in the gasifier-reformer. Once the run had finished, the reactor was disconnected and solids were collected into clear glass vials sealed with black caps. They were labelled by reactor tube section: top, medium or bottom. The vials were taken into a desiccator until analysis. For comparisons, original catalyst samples were also taken into a desiccator.

In one determined run (Run 20-07 described in chapter 6, section 6.4.3), the gasifier-reformer reactor tube was analysed. This permitted the evaluation of any damage suffered by the reactor tube under the operating conditions of pressure and temperature. In that case, the tube was cut and the sample was preserved in resin until analysis.

Liquid samples: Liquid residue in the liquid residue accumulator consisted mainly of unreacted water and naphtha. The high pressure accumulator had a gate valve for discharge, the samples were collected after runs into clear glass vials sealed with black caps previously labelled with the run code. Due to the fact that the liquid sample might have contained two immiscible phases, oil and water, a centrifugal process was always carried out. However, no two phases were observed in this research. Hence, the one phase-liquid samples were stored in a lab fridge until analysis.

4.3 Data analysis

In this section, calibration procedures are outlined and the stabilities of the salient measurements or readings: inlet flow rates ($L.min^{-1}$), pressure (bar), temperature (ºC), produced dry gas composition (vol. %) and dry gas outlet flow rate ($L.min^{-1}$) are analysed. Additionally, the equations used in the further analysis of data are identified followed by an uncertainty analysis of the readings and calculated parameters.

Repeatability was also important, at least one second repeat of every DHG experiment was always carried out to confirm the result and increase technical reliability.

4.3.1 Calibration

Calibrations were conducted on two (2) liquid injection pumps, two (2) mass flow meters, one (1) mass flow controller, four (4) thermocouples, three (3) pressure transducers, three (3) relief valves, three (3) gas analysers and one (1) wet test meter.

Some calibrations were directly carried out by the corresponding manufacturer such as in the case of the mass flow meters, mass flow controller, pressure transducers, relief valves and thermocouples. The rest, including the liquid injection pumps to feed the rig and the gas analysers were carried out directly by the operator with the support of technical specialists.

Calibrations were repeated periodically to validate the measurements and technical reliability.

Liquid injection pumps: The existing pumps for water and naphtha were equipped with metering valves to provide variable flow rates monitored online through mass flow meters installed between pumps and the rig (see final DHG rig flowsheet, Figure 3.32 in chapter 3).

For calibrations, it was decided to inject the liquid, water or naphtha depending on the pump, at different flow rates varying the speed on the pump. The pump (already connected to mass flow meter) was

disconnected temporally from the rig and the end tube was situated over a 50 mL beaker to collect the liquid. Initial weight of the beaker was measured and recorded.

Once the liquid flow started the valve was adjusted at different ranges. Mass flow meter readings were recorded for 10 minutes at a time at each calibration flow rate. Equally, the mass of the water collected over the time period of 10 minutes was measured and divided by 10 to produce an average flow rate measurement in litres per minute. This process was repeated for six calibration points between (0.0002-0.0100) $L.min^{-1}$ for water and (0.0002-0.0030) $L.min^{-1}$ for naphtha. Those ranges were chosen based on the range of inlet flow rates to be used in the DHG experiments.

Average flow rates calculated by the mass of the water collected were compared to average flow rates measured by the mass flow meter. Every point of coincidence represented a scale measurement from the pump valve and from all these data, a calibration curve per liquid, water and naphtha was generated. As example mode, Figure 4.1 shows one of the graphs for water and naphtha injection pumps calibration.

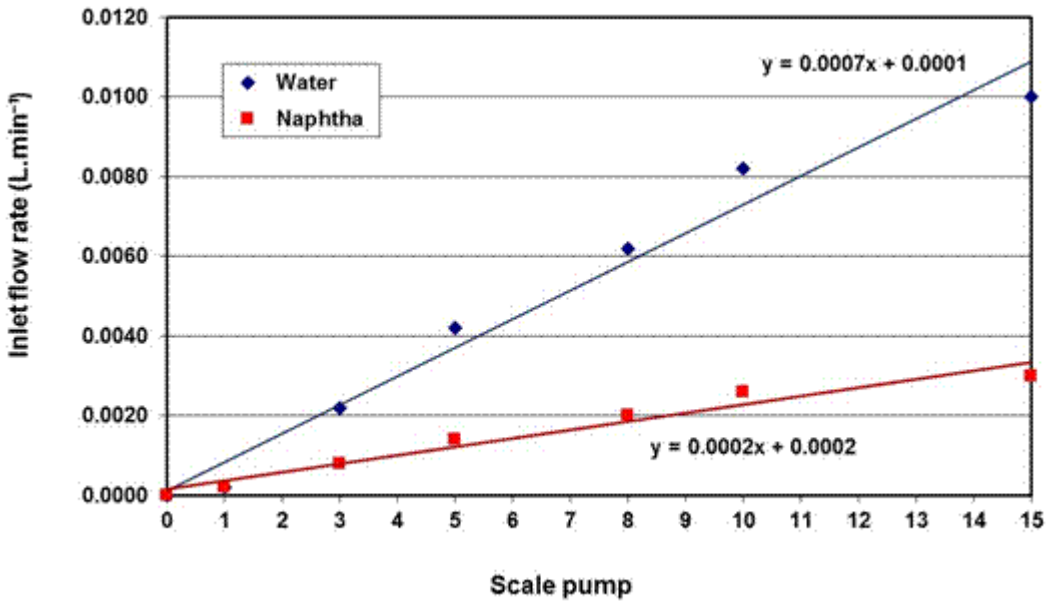

Figure 4.1 Water/naphtha injection pumps calibration.

The accuracy of the scale used in the measurements were listed as 0.0001 $L.min^{-1}$ for water and 0.0002 $L.min^{-1}$ methane flow which was acceptable within our engineering environment.

Wet test meter: For this calibration, gas methane (CH_4) at high purity (99.9999 %), high pressure (200 bar) supplied by BOC gases and, the mass flow controller BROOKS 5850TR previously calibrated with methane (± 0.02 %) were used.

The methane gas cylinder with the mass flow controller were disconnected from the rig to be reconnected to a back pressure regulator which reduced the pressure to nearly 1 bar as the wet test meter manual required. The preliminary test was carried out for 10 minutes.

The values obtained from the mass flow controller were compared to those measured from the wet test meter despite the latter being more sensitive to the variation of gas flow rates. However, this was carried out for calibration purposes. Figure 4.2 shows the obtained results.

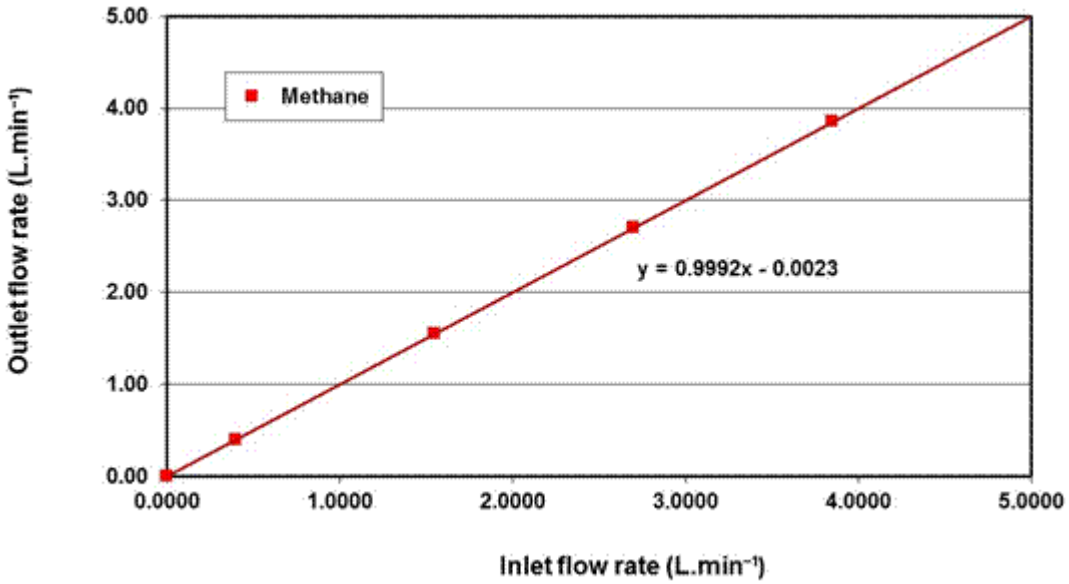

Figure 4.2 Wet test meter calibration.

The discrepancies observed between calibrations were below ± 0.5 % which was acceptable.

Gas analysers: Calibration of the gas analysers for H_2, CO, CO_2 and CH_4 was performed periodically every 2-3 weeks prior to a DHG experiment. For these calibrations, an analytical gas mixture obtained from BOC gases was used as calibration gas. The gas contained 50.00 vol. % H_2, 15.00 vol. % CO, 20.00 vol. % CO_2 and 15.00 vol. % CH_4 (± 0.02 %).

The analytical gas mixture was transferred at reduced pressure below 2 bar with help of a back pressure regulator connected previously to the gas analysers. The values read from gas analysers were compared to the calibration gas mixture. Table 4.1 shows one of the comparisons carried out.

Table 4.1 Gas analysers calibration.

Gases	Composition from supplier (vol. %)	Composition from gas analysers (vol. %)
H_2	50.00	50.08
CO	15.00	15.39
CO_2	20.00	21.00
CH_4	15.00	14.00

The discrepancies observed in the gas analysers calibrations were below 5 % which was acceptable.

4.3.2 Stability

The signal stability from every reading: inlet flow rates, pressure, temperature, produced dry gas composition and dry gas outlet flow rate was targeted towards achieving a steady-state operation to make sure that any variation monitored was entirely attributable to the gasification-reforming reactions.

The signal stability tests were performed over 15 minutes while the repeatability of the gas analysis measurements were performed. They were conducted analysing a sample (analytical gas mixture) from three readings. Deviations were generally below 10 %.

Water and naphtha inlet flow rates: The signal stabilities of water and naphtha flow rates during these 15 minutes are shown in Figures 4.3 and 4.4. The standard deviation of the water flow rate was 0.0001 $L.min^{-1}$ from the setpoint value. In the case of naphtha, the standard deviation was also 0.0001 $L.min^{-1}$ of the setpoint value.

During the DHG experiments, the flow rates used for water were between (0.0044-0.0090) $L.min^{-1}$ while for naphtha they were between (0.0004-0.0020) $L.min^{-1}$. The magnitude of the variation was relatively stable as the values of flow rates increased. The maximum standard deviation was 9.8 % with naphtha being produced at an average flow rate of 0.0004 $L.min^{-1}$.

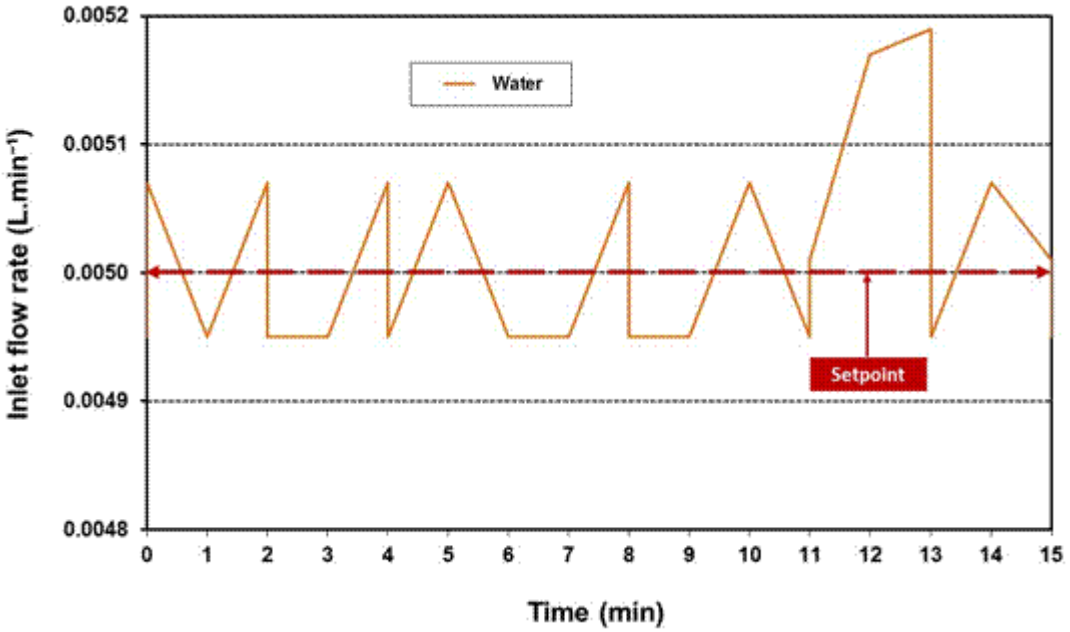

Figure 4.3 Signal stability of water inlet flow rate.

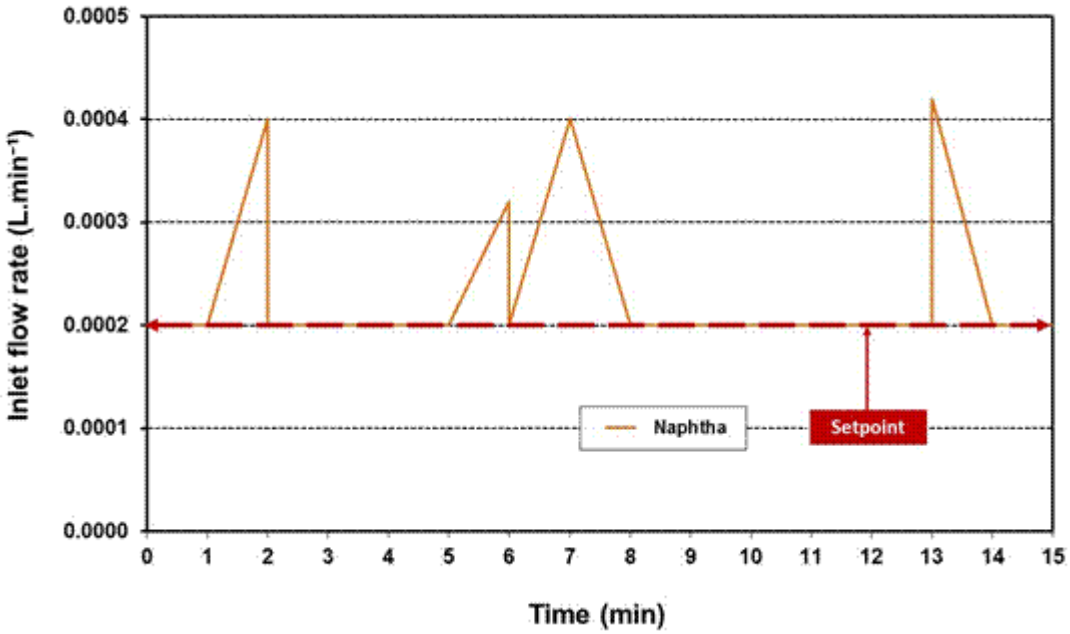

Figure 4.4 Signal stability of naphtha inlet flow rate.

Methane inlet flow rate: The methane flow rate was controlled by a Brooks mass flow controller including an internal proportional valve which maintained the flow rate at the setpoint. As has been mentioned, this instrument was previously calibrated with methane directly by the manufacturer.

Standard deviation was relatively low, 0.0186 $L.min^{-1}$ of the desired value as is seen in Figure 4.5. The setpoint was 1.0000 $L.min^{-1}$ which

corresponded to the minimum value used during the DHG experiments. The methane flow rate used in experimental phase was between (0.4000-2.0000) $L.min^{-1}$.

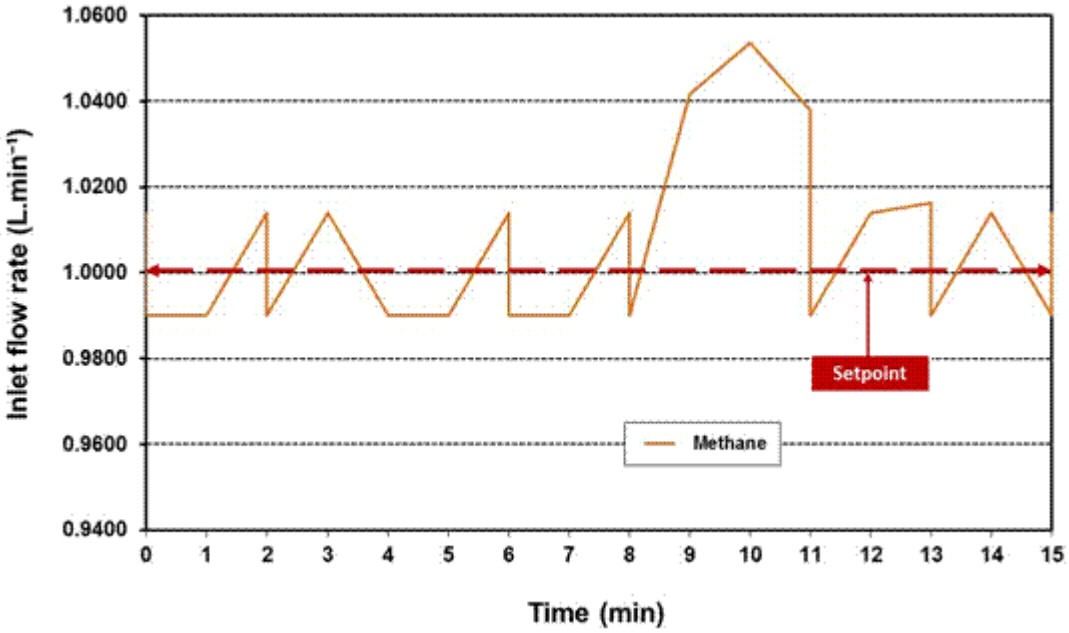

Figure 4.5 Signal stability of methane inlet flow rate.

Temperature: Thermocouple temperatures were monitored in 4 points of the rig: outlet vaporiser, heating tape, inlet gasifier-reformer and outlet gasifier-reformer. All of those temperature readings would oscillate in time due mainly to three variables: (1) operating conditions, (2) experimentation itself, steam reforming reactions in the gasifier-reformer and (3) any automatic adjustment realised by the program from the furnaces temperature controllers. The program was necessary to maintain the desired temperature of the fluid in the exits of the vaporisation and gasification-reforming sections.

At example mode, Figure 4.6 shows a temperature profile generated by the thermocouples whose signal stability was analysed for 30 minutes with their respective setpoints. The signals corresponded to one of the DHG experiments using naphtha feedstock (Run 20-02). See Chapter 6, section 6.2.3.

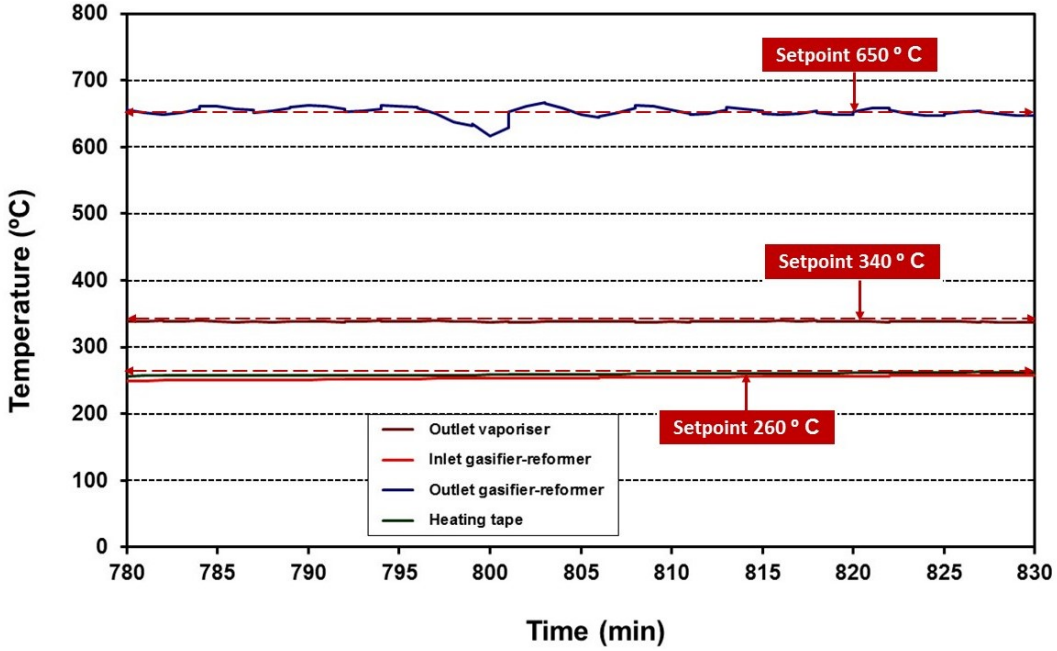

Figure 4.6 Signal stability of temperature. DHG experiment using naphtha feedstock Run 20-02.

As it can be seen in Figure 4.6, it was not difficult to achieve relatively stable temperature values during the experiment as a consequence of the three variables previously mentioned. The standard deviation from the setpoint was: outlet vaporiser 0.6 % (5 ºC), heating tape 0.4 % (3 ºC), inlet gasifier-reformer 0.6 % (5 ºC), and outlet gasifier-reformer 0.7 % (6 ºC).

Pressure: the pressure of the rig was monitored using pressure transducers in three points: (1) methane injection, (2) inlet gasifier-reformer and (3) outlet gasifier-reformer.

The signal stability of the pressure readings is shown in Figure 4.7 as example mode and corresponds to a DHG experiment using naphtha feedstock, Run 20-02 (for details, see Chapter 6, section 6.2.3). The standard deviation of the pressure over a 30 minute period was 0.7034 for the inlet gasifier-reformer and 0.6374 for the outlet gasifier-reformer.

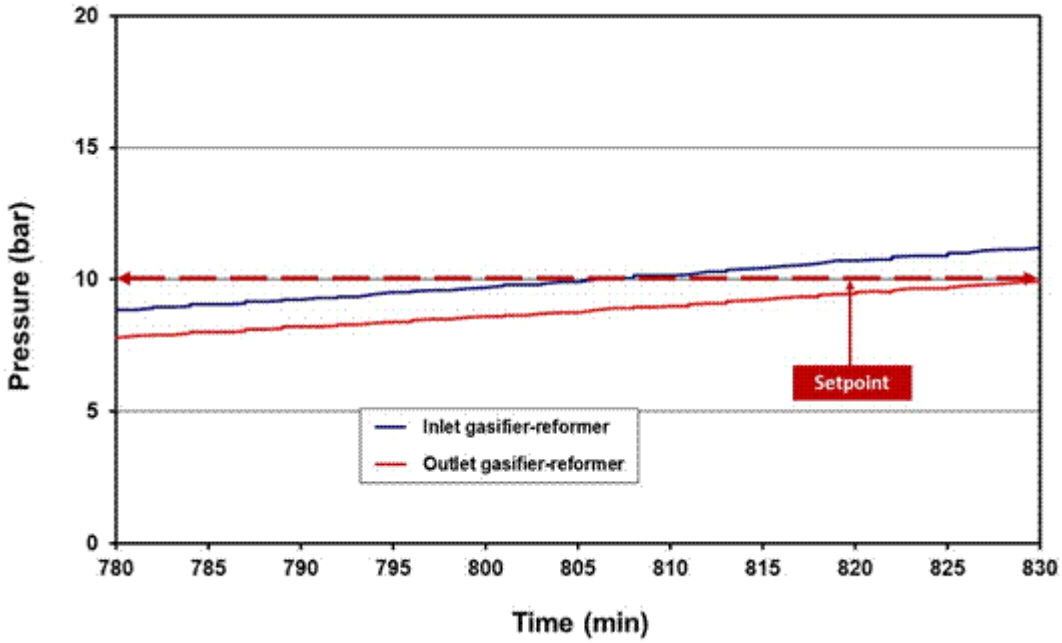

Figure 4.7 Signal stability of pressure. DHG experiment using naphtha feedstock Run20-02.

Dry gas outlet flow rate: A wet test meter with flow recorder was used to measure the produced dry gas flow rate generated in the gasifier-reformer once water and any liquid hydrocarbon residue had been separated in the gas-liquid separation section.

The wet test meter is a very sensitive instrument with accuracy of ± 0.15 %, at Standard temperature pressure. To analyse signal stability, the same arrangement for calibration was used (Previous section 4.3.1): the methane cylinder connected to the mass flow controller followed by back pressure regulator and then, the wet test meter.

The test was for 45 minutes and inlet flow rate was 5.0000 $L.min^{-1}$ which is in the range of the dry gas outlet flow rate to be generated in DHG experiments using naphtha feedstock (Chapter 6). Figure 4.8 shows the results.

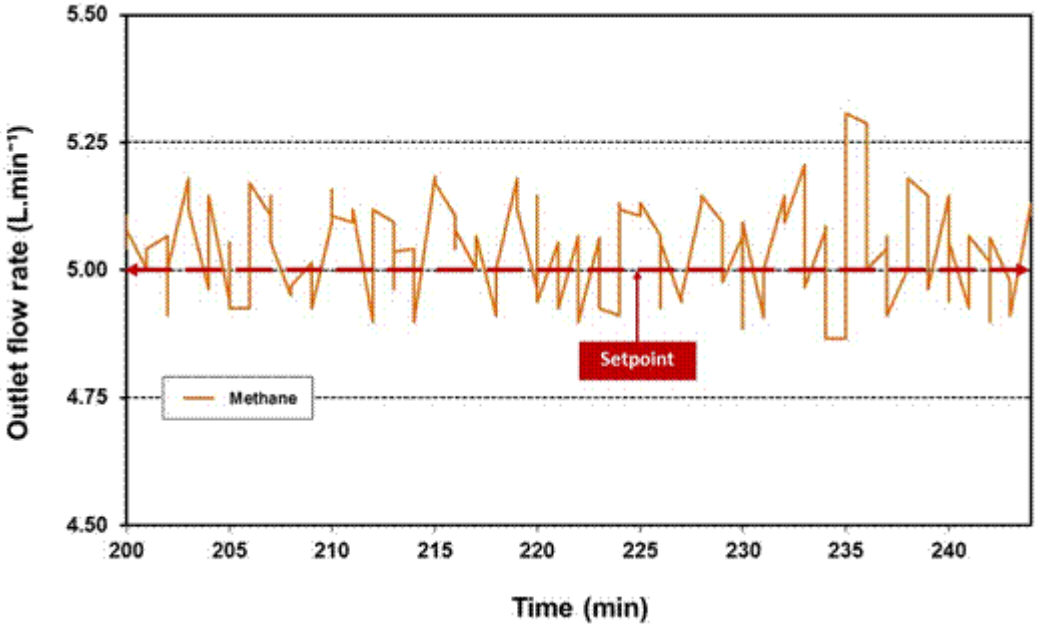

Figure 4.8 Signal stability of wet test meter.

The standard deviation is around 0.0952 which is very positive and reliable. However, a DHG experiment using naphtha feedstock, Run 20-07, showed severe oscillations throughout (see Chapter 6, section 6.4.3), mainly attributed to the deficient control of the back pressure regulator at higher pressure in the system (155-160) bar rather than signal stability from the instrument itself.

Outlet flow rate measured will be named dry gas outlet flow rate since is referred to the gas once water is separated after DHG reactions.

Gas analysis repeatability: Using the analytical gas mixture for calibration, the sample was analysed per triplicate by the gas analysers. The results of standard deviation (± SD) of gases are listed in Table 4.2 and were calculated using the equation reported by Eilers (2010).

Table 4.2 Example gas measurement repeatability.

Sample	H_2 (vol. %)	CO (vol. %)	CO_2 (vol. %)	CH_4 (vol. %)
1	50.12	15.23	19.35	16.10
2	50.10	17.85	21.57	15.90
3	50.60	14.21	22.12	17.75
Standard deviation (± SD)	0.28	1.88	1.47	1.02

Average values of produced dry gas compositions are reported with a standard deviation ± 2 %.

4.3.3 Equations used for analysis

In the case of the DHG experiments using naphtha feedstock (Chapter 6),

a stage of data processing was carried out to analyse engineering parameters such as space velocity, residence time, Reynolds number and mass balance after the test. This supported the investigation and gave an insight into the results of conversion, H_2 concentration, no coke formation and disturbances in produced dry gas curves during the sampling observed throughout, all directed towards exploring the technical feasibility of DHG implementation at field scale.

In the following section, relevant equations are presented. The ideal gas law was fundamental to calculations, and the gasifier-reformer reactor was considered as a plug flow reactor packed with a catalyst bed tube. Further details of the data and calculations are in Appendix B, Sections B.4, B.5, B.6 and B.7.

For the DHG experiments using methane feedstock (Chapter 5), engineering parameters were not calculated since they were basic experiments and their results only served as a baseline and a benchmark of previous investigations using the experimental DHG rig (Greaves et al., 2004, Greaves et al., 2005).

Space velocity: Here, SV was calculated as the ratio of inlet flow rate at DHG operation of temperature and pressure in the gasifier-reformer $(T,P)_{DHG}$ to size of reactor (Fogler, 2006, Kandiyoti, 2009, Levenspiel, 1999):

$$Space\ velocity\ (h^{-1}) = \frac{Q_{mixture}}{V_{efective}} \tag{4.1}$$

Where $Q_{mixture}$ was the volumetric total inlet flow rate of water plus naphtha at DHG conditions taking into consideration molar change, since fluid expands modifying density in the reactor tube as steam reforming reactions occur (Greaves et al., 2006 and Greaves et al., 2008):

$$Q_{mixture} = (Total\ inlet\ Flow\ Rate).\left(\frac{P_o T_{DHG}}{T_o P_{DHG}}\right).(1 + \frac{Steam\ Moles}{Naphtha\ Moles}) \tag{4.2}$$

Where P_o is the initial pressure (1.01 bar), P_{DHG} is the pressure at DHG operating conditions, T_o is the initial temperature in kelvin (293.15 K) and T_{DHG} is the temperature at DHG operating conditions in Kelvin.

The volume of the reactor is 19.09 cm^3 (Length= 30 cm) and 45.80 cm^3 (Length= 72 cm). Since the catalyst bed was also taken into consideration, the effective volume of reactor was calculated as:

$$V_{effective} = (V_{reactor}) \,.\, (\varepsilon_{catalyst\ bed}) \tag{4.3}$$

Where $\varepsilon_{catalyst\ bed}$ is the voidage of the catalyst bed. For C11-PR the value was 0.66 and it was 0.51 for crushed HiFUEL R110, these values are estimated on the basis of the research of Afandizadeh and Foumeny (2000), Benyahia and O´neill (2005), Fogler (2006), Foumany and Benyahia (1991).

Residence time. This was calculated using the gasifier-reformer reactor dimensions and the inlet flow rate at the inlet of the gasifier-reformer as:

$$\mathrm{Re}\,sidence\,time\,(s) = \frac{V_{effective}}{Q_{mixture}} \tag{4.4}$$

Residence time is practically the inverse of space velocity. This parameter was important for comparisons with other investigations (Cheekatamarla et al., 2006, Krumplet et al., 2002, Pinkwart et al., 2004).

Reynolds number. The Reynolds number (Re) is a dimensionless number that is commonly used to characterise different flow regimes: laminar, transitional or turbulent and it is based on a ratio of inertial forces to viscous forces (Fogler, 2006, Kandiyoti, 2009, Levenspiel, 1999).

For <u>fluid flow through the catalyst packed tube</u> assuming spherical particles of diameter $D_{particle}$ in contact with the voidage, $\varepsilon_{catalyst\ bed}$, the Reynolds number can be defined as:

$$\mathrm{Re} = \left[\frac{\rho \,.\, Q}{\mu} \right]_{mixture} . \frac{1}{A} . \frac{D_{particle}}{(1 - \varepsilon_{catalyst\ bed})} \tag{4.5}$$

Where $\rho_{mixture}$ is the density of the mixture (water plus naphtha), μ mixture is the dynamic viscosity of the mixture, *A* is the tube cross sectional area and $D_{particle}$ is the average diameter of the catalyst. $\varepsilon_{catalyst\ bed}$ is the voidage of the catalyst bed which was estimated at 0.66 for C11-PR and at 0.51 for the crushed HiFUEL R110.

A mixture density, $\rho_{mixture}$, is calculated using an ideal gas equation given the molecular weight of mixture, $M_{mixture}$, at DHG operating conditions of pressure and temperature (Fogler, 2006, Kandiyoti, 2009, Levenspiel, 1999),

$$M_{mixture} = \sum Xi \,.\, Mi \tag{4.6}$$

$$\rho_{mixture} = \frac{P_{DHG} \,.\, M_{mixture}}{R \,.\, T_{DHG}} \tag{4.7}$$

Where *i* corresponds to each component (steam, methane or naphtha), *M*

is the molecular weight and *X* is the mole fraction. *P* is pressure, *R* is the gas constant and *T* is the temperature in Kelvin.

A viscosity of mixtures, $\mu_{mixture}$, can be calculated using the following semi-empirical equation (Fogler, 2006, Kandiyoti, 2009, Levenspiel, 1999),

$$\mu_{mixture} = \frac{\sum Xi \,.\, \mu i \,.\, (Mi)^{1/2}}{\sum Xi \,.\, (Mi)^{1/2}} \tag{4.8}$$

Where X_i is the mole fraction of component *i,* μ_i is the viscosity and M_i is the molecular weight. The *i* refers to each fluid: water, methane or naphtha.

The viscosities of each fluid, μ_i, were calculated extrapolating from graphs of steam at saturated conditions and methane reported at different temperatures by Perry and Green, (1984) and Reid et al., (1987) in *Chemical Engineer´s Handbook* and *The properties of Gases and Liquids* reference books respectively.

For the *Re* calculations, this investigation did not include technical factors such as: heat loss, pressure drop, diffusion coefficients, surface roughness, pipe vibrations and flow fluctuations. However, the calculations realised here were more than sufficient to shed some light on fluid patterns in the DHG process for further analysis.

Mass balance: This was calculated on the basis of differential volume per time unit using the following general equation (Fogler, 2006, Kandiyoti, 2009, Levenspiel, 1999),

$$Input = Output + Accumulation \tag{4.9}$$

Where *Input* is the mixture of water (H_2O) plus methane (CH_4) or naphtha, *Output* is the produced dry gas after reaction (H_2, CO, CO_2 and CH_4), *Accumulation* is any unreacted water (H_2O) and naphtha present in liquid phase after the reaction. For the DHG experiments, every term was calculated in terms of mass per minute since this was the time unit used to monitor the inlet and outlet flow rates and the total time period of experimentation.

The terms were calculated as,

$$Input = m_{CH_4/naphtha} + m_{H_2O} \tag{4.10}$$

$$Output = m_{H_2} + m_{CO} + m_{CO_2} + m_{CH_4} \tag{4.11}$$

$$Accumulation = m_{H_2O} + m_{naphtha} \tag{4.12}$$

Therefore,

$$Balance = Input - Output - Accumulation \quad (4.13)$$

4.3.4 Uncertainties

Uncertainties of all directly measured quantities are tabulated in Table 4.3. Total uncertainties were calculated using the root sum squared (RSS) of the calibration and stability uncertainties as follows:

$$U_{total} = \sqrt{U_{Cal}^2 + U_{Stab}^2} \quad (4.14)$$

Where U_{total} is total uncertainty, U_{cal} is calibration uncertainty, U_{stab} is stability uncertainty.

Table 4.3 Uncertainties of directly measured readings.

Reading	Calibration accuracy	Signal stability	Total uncertainty
Water inlet flow rate (L.min^{-1})	0.0001	0.0001	0.0001
Methane inlet flow rate (L.min^{-1})	0.0001	0.0189	0.0189
Naphtha inlet flow rate (L.min^{-1})	0.0002	0.0002	0.0003
Pressure (bar)	1	2	2.24
Temperature (ºC)	1	3	3.16
H_2 (vol. %)	0.02	0.28	0.28
CO (vol. %)	0.40	1.88	1.92
CO_2 (vol. %)	1.00	1.47	1.78
CH_4 (vol. %)	1.00	1.02	1.43
Outlet flow rate (L.min^{-1})	0.01	0.10	0.10

Sequential perturbation of dependant parameters by their corresponding uncertainties was used to generate uncertainties for the most important parameters of our research. The results are tabulated in Table 4.4.

Table 4.4 Uncertainties of calculated parameters.

Parameter	Uncertainty	Studied range
Steam to carbon (S/C) ratio	0.04	3-30
Space velocity (h^{-1})	0.05	18-24301
Residence time (s)	0.05	0.15-170
Reynolds number	0.06	8.80-972
Mass balance (kg.s^{-1})	1.00E-10	(9.10E-07)-(1.53E-04)

Details of the uncertainty analysis are available in Appendix B, section B.7. In summary, the uncertainties are below 6 % supporting the technical reliability of results which is positive. The uncertainties are associated mainly with the signal stability of measured readings rather than with the

calibrations and instruments themselves.

During the DHG experimental phase, uncertainties might have increased as a consequence of:

- Lower inlet flow rates of water, methane and naphtha due to absolute accuracy of the mass flow controller.
- Higher pressure values (> 130 bar) which affected the back pressure regulator control in some DHG experiments using naphtha feedstock, and hence affected the signal stability of the wet test meter (dry gas outlet flow rates) and the readings from the gas analysers.
- Steam reforming reactions in the gasifier-reformer (DHG experiments) from the experimentation which influenced temperature and pressure signal stability.

The uncertainties do not exceed 10 % in the worst case which is fairly acceptable in engineering environments.

4.4 Characterisation of solid samples

On disconnecting the gasifier-reformer reactor after DHG experiments, the catalysts or any solid particles existing inside were removed, analysed and compared to the original catalysts using scanning electronic microscopy (SEM) equipment. Equally, the gasifier-reformer tubes were scrutinised using this technique to evaluate damage occurring as a result of the DHG operating conditions of pressure and temperature to which they were submitted.

SEM images allow characterising surface samples to determine elements present on samples as well as topographic details: size, shape and texture (Greenwood, 1997). A wide range of configurations, techniques, resolutions and intensity signals of the instrument revealed important key points about the steam reforming reactions generated by the catalyst and their effect on the gasifier-reformer tube at DHG conditions of pressure and temperature.

The energy dispersive X-ray spectroscopy (EDX) combined with the SEM equipment was also applied to obtain more details of each studied sample as well as its elemental composition.

Characterisation was performed by specialists in the area using two scanning electronic microscopies, model JEOL JSM- 6480LV located in the Physics Department, University of Bath – England for catalyst samples and, QUANTA FEG 250 located in the Research Centre of PDVSA (Oil Company) from Venezuela for gasifier-reformer tube samples.

The SEM requires highly conductive samples; therefore, catalyst samples were coated with gold to increase their conductivity. In the case of the

carbon-containing and reactor tube samples, no gold coating was required or used since they were relatively conductive. The sample is placed inside the microscope vacuum column through air-tight doors.

Backscattered electron composition image (BEC), a special contrast technique (different detector) was considered for the analysis of some samples since high carbon deposition complicated the capture of images due to its low conductivity property. For this reason, a very thin gold layer was also spread on the catalyst samples.

4.5 Characterisation of liquid samples

One-phase liquid residue collected after the test was analysed to detect the possible presence of hydrocarbons in water using a standard test technique (ASTM D7678 – 11). The total hydrocarbons in the residue collected were firstly extracted with solvent for then, to be analysed using middle-infrared (mid-IR) laser spectroscopy in the region of (1370-1380) cm^{-1} (7.25 - 7.30 μm).

This technique covers the range of 0.5 to 1000 $mg.L^{-1}$ and may be extended to a lower or higher level depending on the volume extracted from the original sample volume collected after the test.

Middle-IR laser spectroscopy is based on strong fundamental rotational-vibrational molecular transitions generated in the middle-IR (2.5-10 μm) which is very useful for trace analysis. This spectra region is less congested allowing selective spectroscopic detection such as the strong vibrational bands associated with C-H stretching proper from hydrocarbons.

Liquid analyses were performed by specialists in the area using a Frontier spectrum 400 MIR/FIR spectrometer located in the Physics Department, University of Bath – England.

References

AFANDIZADEH, S. AND FOUMENY, E.A, 2000. Design of packed bed reactors: guides to catalyst shape, size and loading selection. *Applied thermal engineering,* 21, pp. 669-682.

BENYAHIA, F. AND O'NEILL, K.E., 2005. Enhanced voidage correlations for packed beds of various particle shapes and sizes. *Particulate science and technology,* 23, pp.169–177.

CALLAHAN, F.J., 1993. *Tube fitter's manual.* U.S.: Swagelok Co.

CHEEKATAMARLA, P., THOMSON, W., 2006. Hydrogen generation from 2,2,4 - trimethylpentane reforming over molybdenum carbide at low steam to carbon ratios. *Journal power sources,* 156, pp. 520-524.

EILERS, B.J., 2010. *Microchannel steam-methane reforming under constant and variable surface temperature distributions.*

FOGLER, H.S., 2006. *Elements of chemical reaction engineering.* 4th edition. New York: Pearson Education, Inc.

FOUMENY, E.A. AND BENYAHIA, F., 1991. Predictive characterization of mean voidage in packed beds. *Heat recovery systems & CHP,* 11(2-3), pp. 127-130.

GREAVES, M., RATHBONE, R., XIA, T., BENTHAHER, A., DUGGAN, S., 2004. *Downhole gasification for improved oil recovery and gas production (phase 1) experimental studies (1 Nov 2002 – 31 Oct 2004).* United Kingdom: University of Bath, (Confidential internal report).

GREAVES, M., XIA, T., RATHBONE, R. AND BENTAHER, A., 2005. Underground gasification for improved oil recovery. *Canadian international petroleum conference,* 7-9 June 2005 Calgary. Calgary: Petroleum Society Canadian Institute of Mining, Metallurgy & Petroleum, pp. 38-48.

GREAVES, M., RATHBONE, R., XIA, T., BENTHAHER, A., 2006. Experimental study of a novel In situ gasification technique for improved oil recovery from light oil reservoirs. *JCPT,* 45(8), pp. 41-47.

GREAVES, M. AND XIA, T.X., 2008. Producing hydrogen and incremental oil from light oil reservoirs using downhole gasification. *Canadian international petroleum conference,* 17-19 June 2008 Calgary. Calgary: Petroleum Society Canadian Institute of Mining, Metallurgy & Petroleum, pp. 14-24.

GREENWOOD, N. N. E., 1997. Chemistry of Elements, Elsevier, New York.

KANDIYOTI, R., 2009. *Fundamentals of reaction engineering.* London: Ventus Publishing ApS.

KRUMPELT, M., KRAUSE, T., CARTER, J., KOPASZ, J. AND AHMED, S., 2002. Fuel processing for fuel cell systems in transportation and portable power applications. *Catalysis today,* 77, pp. 3-16.

LEVENSPIEL, D., 1999. *Chemical reaction engineering.* 3rd edition. New York: Wiley Press.

PERRY, R.H. AND GREEN, D., 1984. *Chemical Engineers Handbook*. 6th edition. New York: McGraw-Hill.

PINKWART, K., BAYHA, T., LUTTER, W. AND KRAUSA, M., 2004. Gasification of diesel oil in supercritical water for fuel cells. *Journal power sources,* 136, pp. 211-214.
REID, R.C., PRANSUITZ, J.M. AND POLING, B.E., 1987. *The properties of gases and liquids.* New York: McGraw-Hill.
SUSANTI, R., NUGROHO, A., LEE, J., KIM, Y. AND KIM, J., 2011. Noncatalytic gasification of isooctane in supercritical water: A strategy for high-yield hydrogen production. *International journal of hydrogen energy,* 36, pp. 3895-3906.

CHAPTER 5: DHG PRODUCED DRY GAS COMPOSITION USING METHANE FEEDSTOCK

5.1 Introduction

In this chapter, a series of basic DHG experiments using methane feedstock are presented. These were used to verify the benchmark of previous investigations realised by Greaves et al. (2004), Greaves et al. (2005) using the rig and, at the same time, to provide a clear baseline of results. In addition, this precautionary approach prior to using naphtha feedstock was necessary in order to understand thoroughly the procedures for operating the DHG rig.

The experiments were conducted within a range of pressure from 50 bar up to 80 bar, a steam to carbon (S/C) ratio from 15 to 3 and values of temperature from 600 ºC to 750 ºC. The length of the gasifier-reformer reactor was 30 cm and the catalyst C11-PR was supplied by Sud Chemie. The investigation paid special attention to the catalyst treatment before and after the DHG test to enhance the conversion/H_2 concentration (H_2 being the main gas of interest), to minimise coke formation and to extend the survivability of the catalyst.

The sequence of a typical basic DHG experiment using methane feedstock included three test periods: (1) Catalyst activation treatment followed by (2) the DHG test proper where steam reforming reactions are studied in the gasifier-reformer reactor at DHG operating conditions, and (3) catalyst reactivation. To confirm results, at least one second repeat experiment was always carried out.

5.2 Experiments with catalyst C11-PR and gasifier-reformer length 30 cm

The main objective was to replicate the operating conditions of pressure and temperature, catalyst type and gasifier-reformer dimensions previously used by Greaves et al. (2004) and Greaves et al. (2005) to evaluate the operability/functionality of the experimental rig revamped in our investigation (for details, see chapter 3, section 3.3).

DHG experiments, Run 10-01, Run 10-02 and Run 10-03 were performed with a water inlet flow rate of 0.0044 $L.min^{-1}$ and based on this value the methane inlet flow rate was calculated at S/C ratio of interest.

5.2.1 Catalyst activation treatment prior to DHG tests

Every DHG experiment started with a prior period of catalyst activation to evaluate the operating conditions of interest for that part of our investigation named the DHG test period. The activation was always performed using the procedure reported by Twigg (1989) since it allows

the activation of catalysts ´on line´ and uses methane as feedstock. In practice, this procedure reduces costs and times of operation which would be important in the event of implementation at field scale. Previous investigations related to the DHG process did not report any catalyst activation treatments.

The activation treatment consisted firstly in injecting steam followed by the injection of methane at S/C ratio of 7 and an outlet temperature in the gasifier-reformer of 750 ºC. When methane concentration falls down to a low steady value at a rapid or slow rate, depending on the catalyst, it may indicate that catalyst activation or reduction is occurring. At that point, the operating conditions are extended for one hour at least before proceeding to the DHG test (Twigg, 1989).

The results of the activation periods from Run 10-01, Run 10-02 and Run 10-03 were similar in terms of curve behaviour and values of pressure, temperature, produced dry gas composition and outlet flow rate obtained. For that reason, just one of them (Run 10-01), corresponding to studies of temperature variation, is shown here as an example.

Table 5.1 shows the operating conditions used during the catalyst activation treatment in Run 20-01 with the catalyst C11-PR. Some values were average values during the time period of interest in the run. Figures 5.1, 5.2, and 5.3 show pressure, temperature, and produced dry gas composition obtained.

Table 5.1 Run 10-01: Operating conditions during catalyst activation using methane feedstock (Catalyst C11-PR).

Run	10-01 (activation)
Reformer tube dimensions	Φ ½-inch x 30 cm
Catalyst type	C11-PR
Catalyst loading (g)	15.2
Catalyst size (mm)	6 x 6 x 2
Pressure (bar) *	10
Outlet gasifier-reformer temperature (ºC) *	750
Steam to carbon molar ratio (CH_4) *	7
Total inlet flow rate ($L.min^{-1}$) *	0.8404
CH_4 inlet flow rate ($L.min^{-1}$) *	0.8360
Water inlet flow rate ($L.min^{-1}$) *	0.0044
(*) Average values	

Figure 5.1 shows the pressure curves for the catalyst activation beginning with steam only at 10 bar at 0.0044 $L.min^{-1}$. After 55 minutes approximately methane (CH_4) was also introduced at S/C of 7 for 150 minutes. During this time, the temperature was increased (Figure 5.2)

moderately up to 750 ºC. Complete steam saturation condition was always guaranteed by monitoring the inlet gasifier-reformer temperature. Saturated steam temperature at 10 bar of pressure is 179.9 ºC.

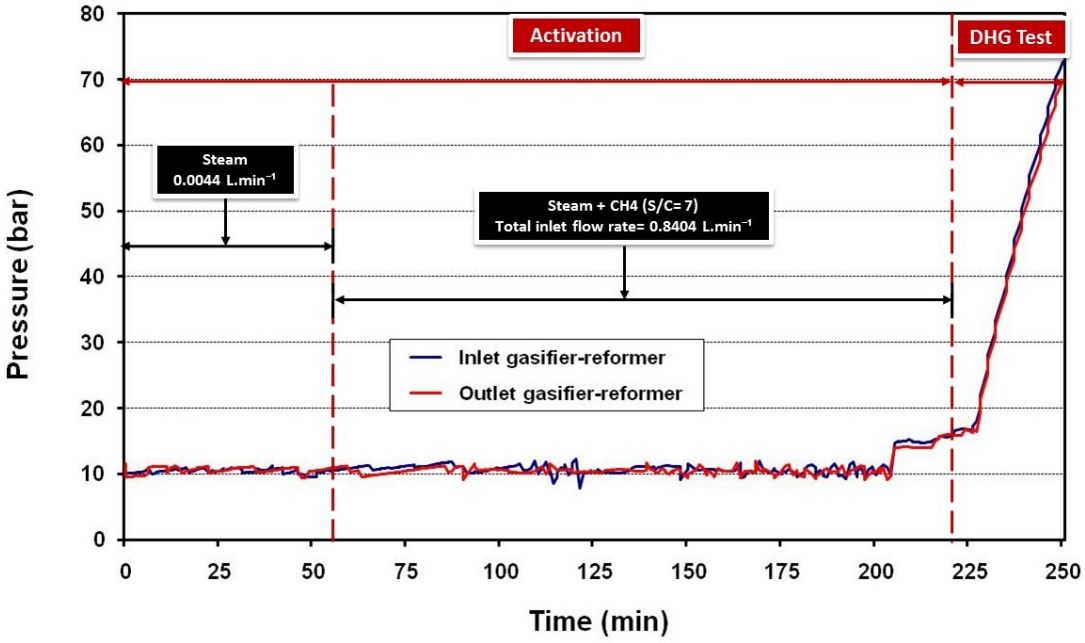

Figure 5.1 Run 10-01: Inlet and outlet pressure of gasifier-reformer during catalyst activation using methane feedstock (Catalyst C11-PR).

For 90 minutes, the gasifier-reformer maintained activation conditions, according to H_2 and CH_4 concentrations in the produced dry gas composition (vol. %) reported in Figure 5.3 from 125 minutes to 215 minutes. The condition of activation is higher at higher H_2 concentration values. After this, the DHG test started running.

At the start of the activation, the increase in the concentration of hydrogen occurs very rapidly, reaching nearly 76 % and is maintained during activation treatment. The concentrations of the other gases also level off at constant values: CO_2 (18 vol. %), CO (3 vol. %) and CH_4 (3 vol. %). This corresponds to an overall conversion of 97 %, which is considerable and acceptable in terms of having reached the activation condition.

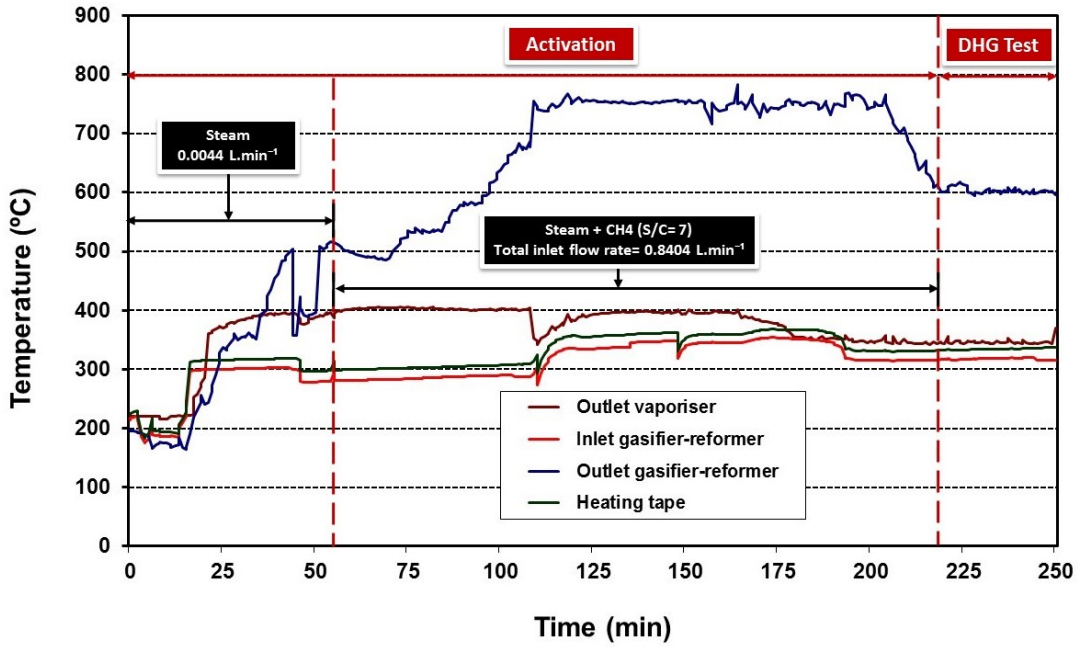

Figure 5.2 Run 10-01: Temperature profiles during catalyst activation using methane feedstock (Catalyst C11-PR).

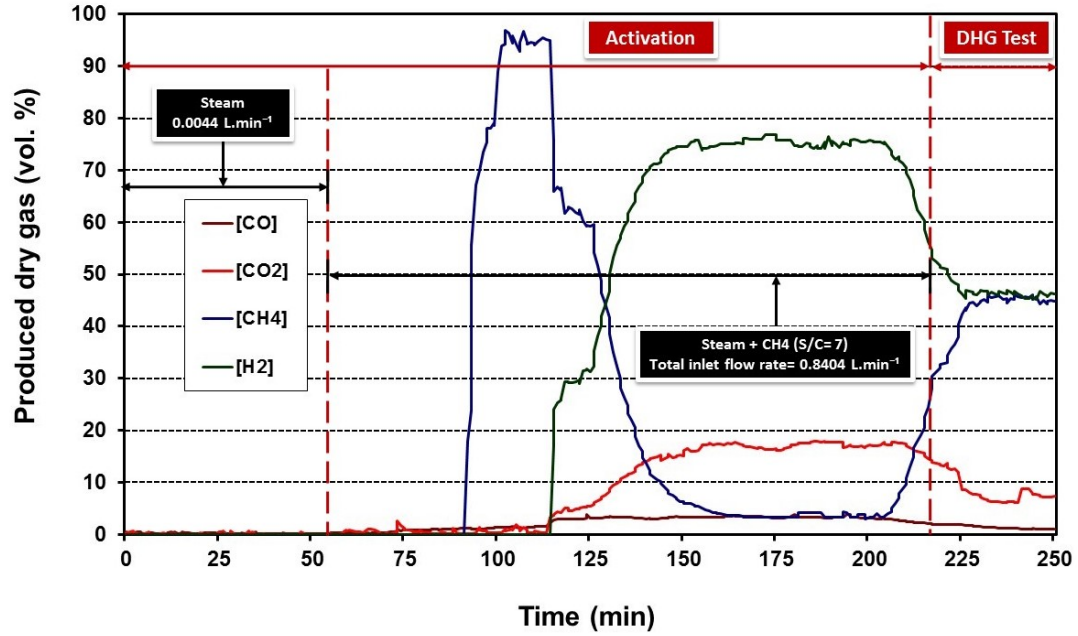

Figure 5.3 Run 10-01: Produced dry gas composition (vol. %) during catalyst activation using methane feedstock (Catalyst C11-PR).

The behaviour of the CH_4 and H_2 curves during activation has been described by Rashidi et al. (2013) in their studies with Nickel oxide and H_2 where metallic Ni particles are generated on the outer surface of NiO grains by nucleation into clusters. In our case, the process is slower since CH_4 is necessarily firstly adsorbed and decomposed on the active sites of

the catalyst. Methane as reducing agent could react as follows (Alizadeh et al., 2007):

$$NiO + CH_4 \Rightarrow Ni + 2H_2 \qquad \Delta H^0_{298} = 211.92\ kJ.mol^{-1} \qquad (5.1)$$

Ni contained in C11-PR might be dispersed as small crystallites on the refractory support which is sufficiently porous to allow access by the gas to the nickel surface. The presence of excess steam and the high temperature above 700 °C applied during activation procedure might result in a slight reduction of metallic nickel surface area due to the fact that steam favours the sintering process. However, results indicated a high activation grade and based on these, it leads us to suppose an almost negligible negative effect of steaming on nickel sintering.

The outlet dry gas flow rate from the gasifier-reformer was measured using the wet test meter (Figure 5.4). The average value was 1.92 L.min^{-1} which represented an important increase in comparison to the injection flow rate: 0.8404 L.min^{-1}.

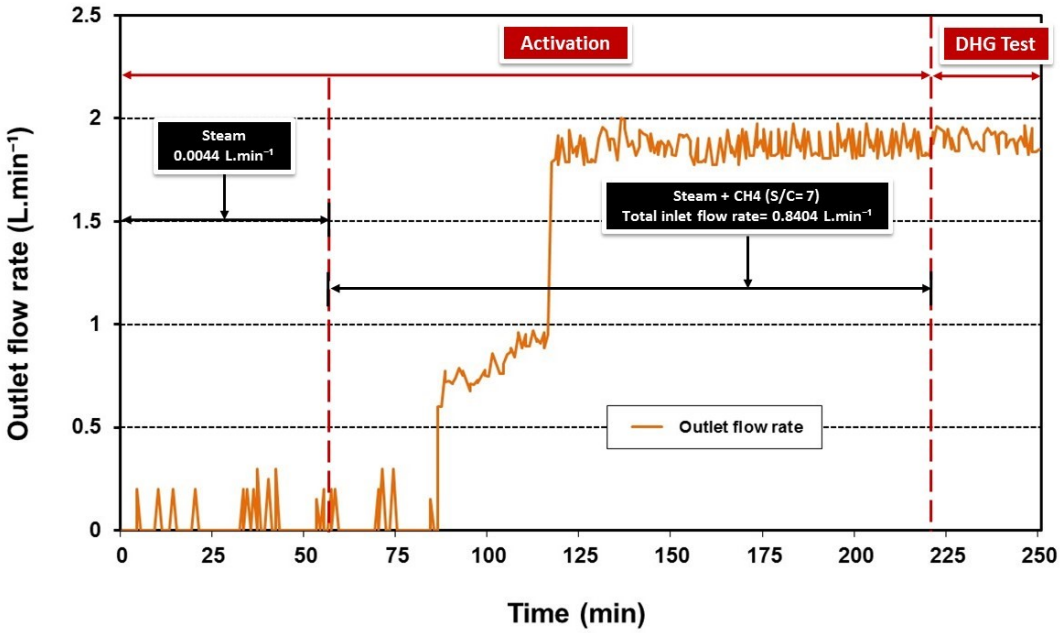

Figure 5.4 Run 10-01: Outlet flow rate from gasifier-reformer, produced dry gas, during catalyst activation using methane feedstock (Catalyst C11-PR).

The reason is attributed to the stoichiometry of steam reforming reactions: 4 moles of H_2 and 1 mole of CO_2 are produced in total per mole of CH_4 and 2 moles of H_2O. When just 1 mole of H_2O is consumed, the total produced is 1 mole of CO and 3 moles H_2 (Rostrup-Nielsen, 1984, Jones et al., 2008). This is represented in Figure 5.5.

Table 5.2 shows a summary of results obtained in Run 10-01 during the

activation treatment of C11-PR using methane feedstock.

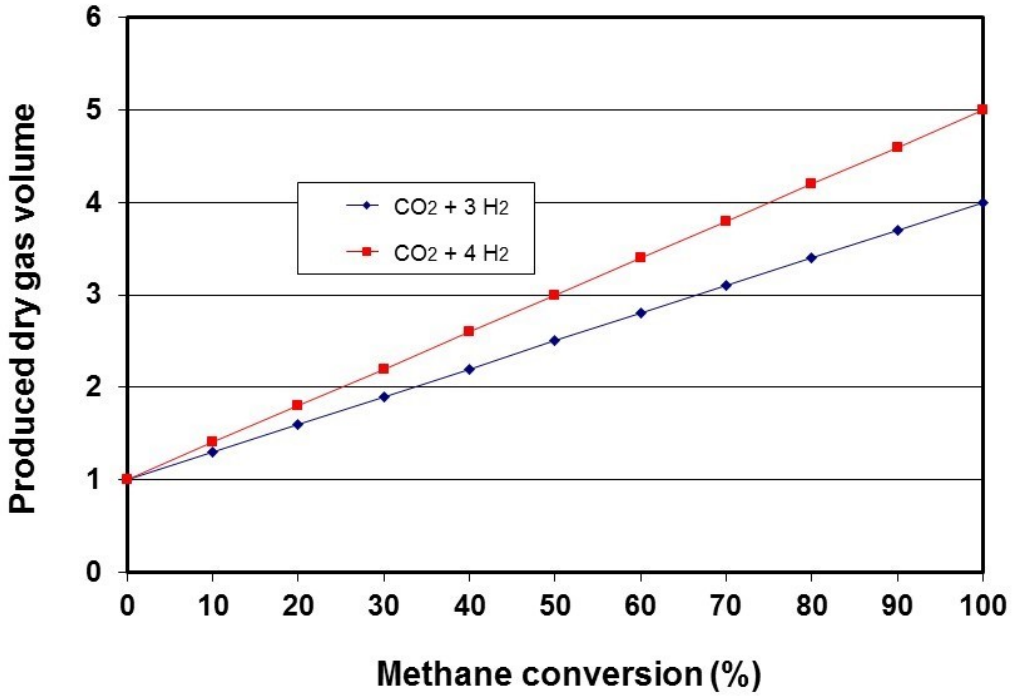

Figure 5.5 Produced dry gas in mole volume versus methane conversion.

Table 5.2 Run 10-01: Summary of operating conditions and results obtained in catalyst activation using methane feedstock (Catalyst C11-PR).

Run	10-01 (activation)
Reformer tube dimensions	Φ ½-inch x 30 cm
Catalyst type	C11-PR
Catalyst loading (g)	15.2
Catalyst size (mm)	6 x 6 x 2
Pressure (bar) *	10
Outlet gasifier-reformer temperature (°C) *	750
Steam to carbon molar ratio (CH_4) *	7
Total inlet flow rate ($L.min^{-1}$) *	0.8404
CH_4 inlet flow rate ($L.min^{-1}$) *	0.8360
Water inlet flow rate ($L.min^{-1}$) *	0.0044
Dry gas outlet flow rate ($L.min^{-1}$) *	1.92
Conversion (%) *	97
Produced dry gas composition (%) **	
H_2	75
CO	3
CO_2	18
CH_4	3
(*) Average values	
(**) Standard deviation of average values is ± 2 %	

Some values were average values obtained during the catalyst activation test period. In summary, no major inconveniences were observed in this Run, as for the activation treatments in Run 10-02 and Run 10-03. The first basic DHG test using methane feedstock at operating conditions of interest will be described in the next section.

5.2.2 Pressure (50 to 80 bar)

Once the C11-PR catalyst was activated, the DHG test started to run. In this test, Run 10-02, pressure was studied from 50 bar to 80 bar using methane feedstock. The operating conditions are shown in Table 5.3.

Figure 5.6 shows the pressure curves obtained in the run. The DHG test started after 180 minutes which was the duration of the catalyst activation treatment. To achieve the pressures under study (50, 65 and 80 bar), the rig was always pressurised, injecting steam and CH_4 at S/C ratio of 3 and total flow rate of 2.0044 $L.min^{-1}$. No major findings were observed until the 500 minute point when there occurred an important pressure drop in the gasifier-reformer as the consequence of coke formation.

On disconnecting the reactor tube, inspection detected coke deposits and drastic catalyst disintegration on the top section while the catalyst from the bottom section remained unchanged, just exhibiting a very thin brownish layer attributed to the chemical reactions of methane steam reforming.

Table 5.3 Run 10-02: Operating conditions during DHG test using methane feedstock (Catalyst C11-PR).

Run	**10-02 (DHG test)**		
Reformer tube dimensions	Φ ½ -inch x 30 cm		
Catalyst type	C11-PR		
Catalyst loading (g)	15.2		
Catalyst size (mm)	6 x 6 x 2		
Outlet gasifier-reformer temperature (ºC) *	650		
Steam to carbon molar ratio (CH_4) *	3		
Total inlet flow rate ($L.min^{-1}$) *	2.0044		
CH_4 inlet flow rate ($L.min^{-1}$) *	2.0000		
Water inlet flow rate ($L.min^{-1}$) *	0.0044		
Pressure (bar) *	52	65	80
(*) Average values			

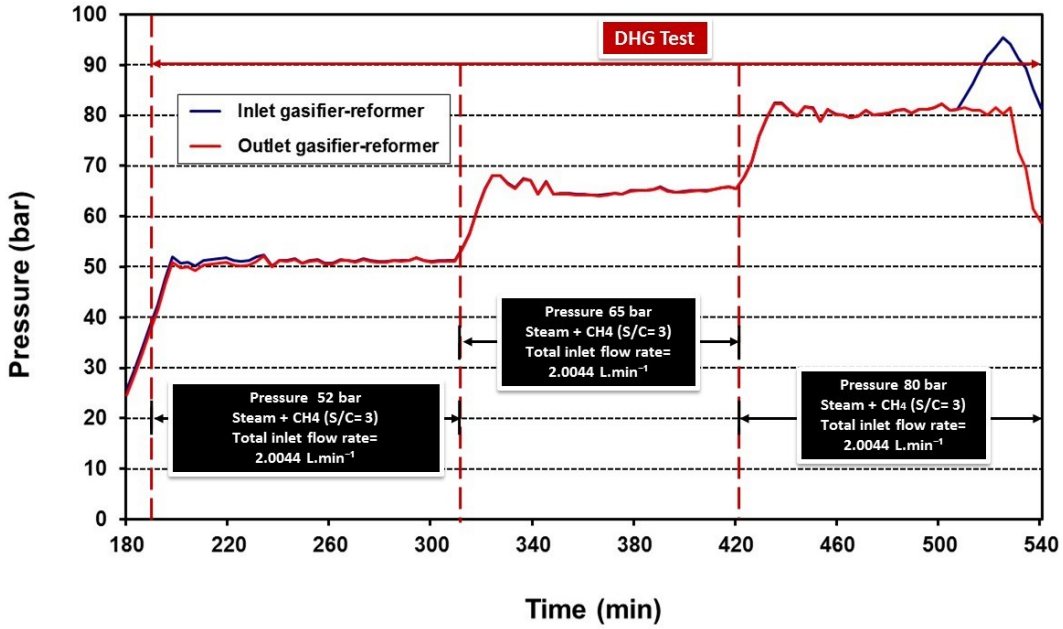

Figure 5.6 Run 10-02: Inlet and outlet pressure of gasifier-reformer during DHG test using methane feedstock (Catalyst C11-PR).

Figure 5.7 shows (a) the original catalyst, (b) the catalyst after the test from the bottom section of the gasifier-reformer and, (c) the catalyst after the test with coke deposits from the top section of the gasifier-reformer.

Certainly, coke formation in steam reforming is a factor to take into account especially at considerable values of pressure as in this case, 80 bar. In theory, thermodynamics principles indicate that important conversion and H_2 concentration in produced dry gas are favoured at high temperature (600-900 ºC), low pressure (< 30 bar) and S/C ratios 2-4 for methane (Rostrup-Nielsen et al., 1984, Twigg 1989, Christensen, 2005). However, values of pressure around 80 bar have a negative influence on the process so that an optimisation or adjustment of operating conditions is necessary.

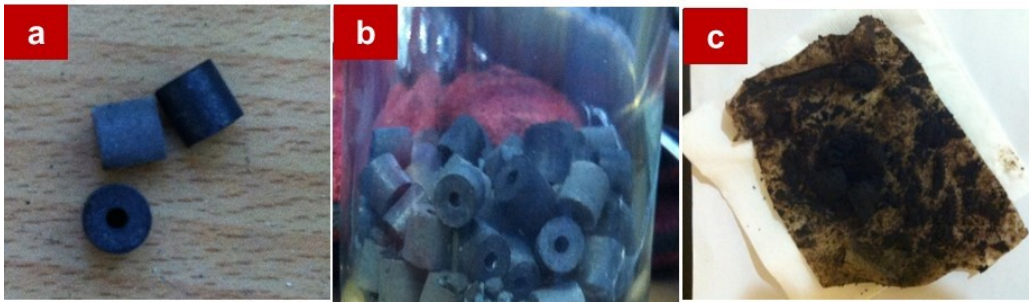

Figure 5.7 (a) original catalyst, (b) catalyst after test from bottom section of gasifier-reformer and, (c) catalyst after test with coke deposits from top section of gasifier-reformer.

Rostrup-Nielsen (1984) indicates that carbon deposits on Ni catalysts for

steam reforming may take place in different ways. Firstly, carbon formed directly by methane or by products recently generated, both being reversible reactions:

$$2\mathrm{CO} \Leftrightarrow C + CO_2 \quad \Delta H^{o}_{298} = -171.66\ kJ.mol^{-1} \tag{5.2}$$

$$CH_4 \Leftrightarrow C + 2\mathrm{H}_2 \quad \Delta H^{o}_{298} = 75.36\ kJ.mol^{-1} \tag{5.3}$$

This tendency has been reported by Greaves et al. (2004) and Greaves et al. (2005) who indicated that an increasing of S/C ratios compensates for the coke deposition on C11-PR when values of pressure higher than 50 are utilised in DHG experiments. They studied S/C ratios from 3 to 7 and observed relatively low values of coke. In the next section, experimental results associated with variation of this parameter (S/C) will be discussed and analysed.

Catalyst samples after the test from the top of the gasifier-reformer were analysed and compared to the original catalyst sample using a scanning electronic microscopy (SEM) model JEOL JSM-6480LV. Figure 5.8 shows the SEM images produced. A contrast technique, backscattered electron composition image (BEC) was utilised to detect carbon.

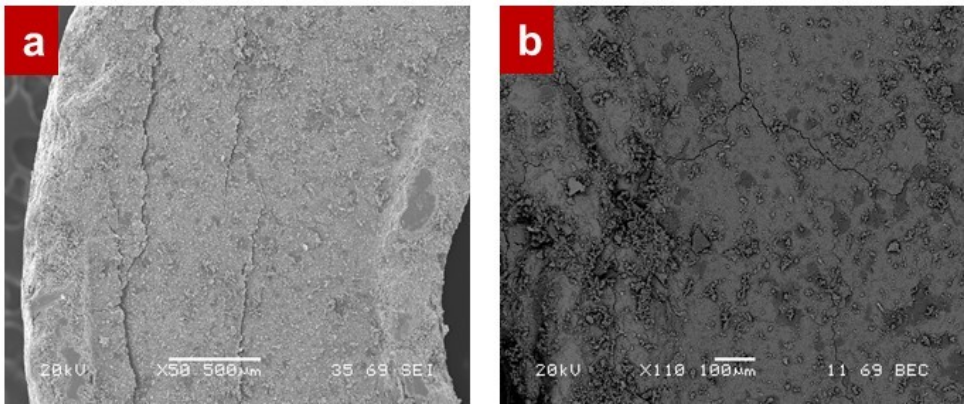

Figure 5.8 SEM images of C11 – PR catalyst (a) Original side view (20 KV, x50, 500 µm, SEI), (b) After DHG test Run 10-02, side view – top of reformer (20 KV, x110, 100 µm, BEC).

As seen in Figure 5.8, the presence of coke on catalyst is evident compared to the original sample. Darker spots on a surface apparently covered with coke might be indicative of two types of carbon formation on a catalytic surface. Helveg et al. (2011) reports on graphite and ´whisker´ carbon commonly formed in industrial steam reformer plants on Nickel, both of which are favoured thermodynamically by operating conditions. The ´whisker´ carbon type, unlike graphite, is able to disintegrate a catalyst mechanically, while graphite just deposits on its surface (Padban and Becher, 2005). This is commensurate with our case, it is possible therefore that both carbon types were present in our catalyst after the test.

Figure 5.9 shows the temperature profiles of the outlet vaporiser, heating tape, inlet and outlet gasifier-reformer used for this DHG test. No major findings were observed and steam saturation conditions were guaranteed regardless of the pressure value.

In the case of the produced dry gas composition (vol. %), Figure 5.10, shows the variations in H_2, CO, CO_2 and CH_4 affected by different values of pressure as has been reported by Greaves et al. (2004), Greaves et al. (2005). At 52 bar, H_2 concentration (as the main gas of interest for DHG process) was 48 vol. %, at 65 bar 43 vol. % and at 80 bar 39 vol. %. This represents a decrease by 9 % approximately when pressure increased from 52 bar to 80 bar which is considerable and totally commensurate with the reduction in conversion from 72 % to 63 %.

Pressure undoubtedly is one of the main factors influencing the effectiveness of the DHG process and for this reason it is the main parameter to be studied in our investigation using naphtha feedstock. Our results so far also indicate the importance of this factor. However, the conversion and H_2 concentration obtained in the current experiments are slightly higher than reported by previous researchers. Greaves et al. (2005) reports values of H_2 concentration around 33 vol. % at 80 bar and a conversion at around 58 vol. %. The main reason is attributed to the series of modifications and optimisations carried out to the experimental rig.

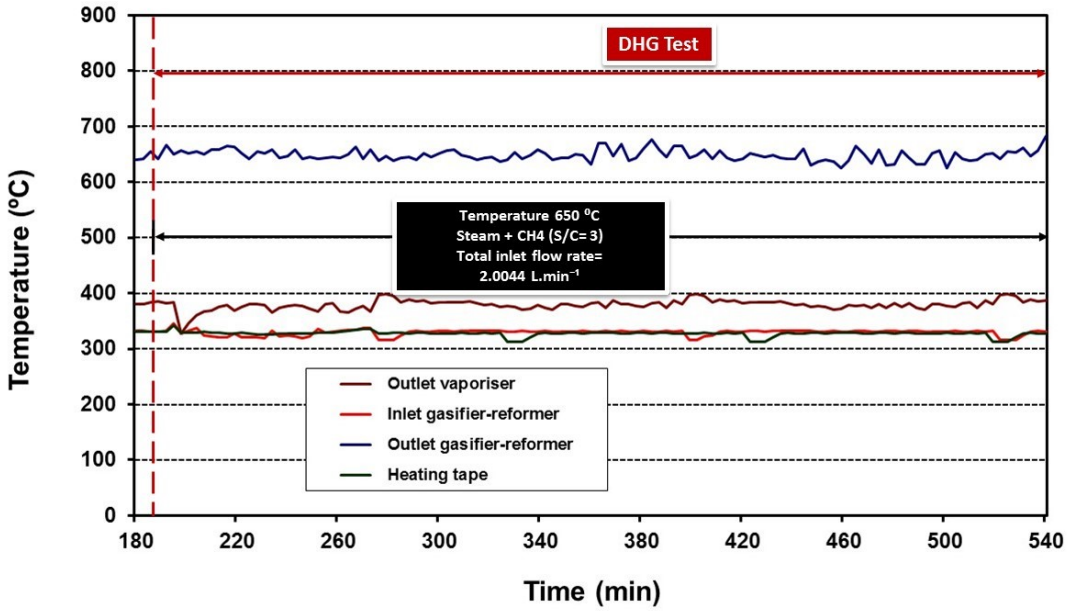

Figure 5.9 Run 10-02: Temperature profiles during DHG test using methane feedstock (Catalyst C11-PR).

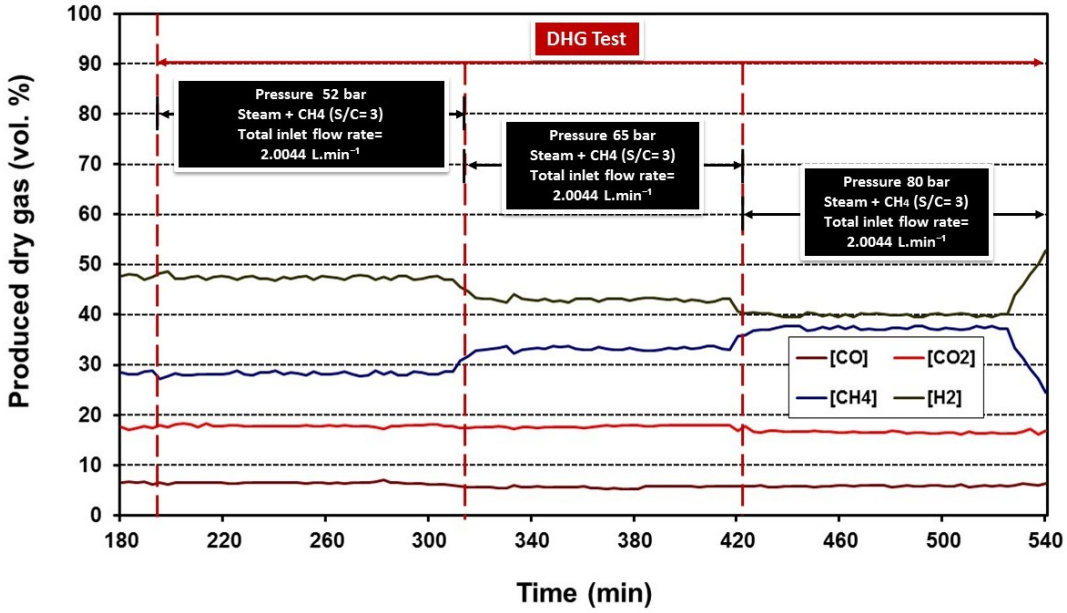

Figure 5.10 Run 10-02: Produced dry gas composition (vol. %) during DHG test using methane feedstock (Catalyst: C11-PR).

The dry gas outlet flow rates were registered manually and indicated a slight reduction as pressure increased: 3.67 $L.min^{-1}$ at 52 bar; 3.56 $L.min^{-1}$ at 65 bar and 3.49 $L.min^{-1}$ at 80 bar which represented a higher volumetric flow rate compared to the initial one. This was expected since chemical reactions in the gasifier-reformer generate more gases by 3-5 times per CH_4 mole (Jones et al., 2008) as it was explained in section 5.2.1 and Figure 5.5.

At higher pressure a lower flow rate is a consequence of the conversion obtained. A lower conversion means less gases generated and, therefore, lower total volumetric flow rate.

Overall, we may say that the results obtained are commensurate with previous investigations and tendencies reported in the literature. These results were sufficiently positive to continue our extensive programme of work via laboratory. The following Table 5.4 summarizes the experimental conditions and results of Run 10-02 for the DHG test period.

Repeatability of Run 10-02: A second repeat of every experiment was always carried out. The second repeat for Run 10-02 shows an almost identical trend for the DHG test period using methane feedstock based on pressure curves (Figure 5.11), temperature (Figure 5.12) and produced dry gas (Figure 5.13) shown below. This effectively confirms the consistency and reliability of our experimental results.

Table 5.4 Run 10-02: Summary of operating conditions and results obtained during DHG test using methane feedstock (Catalyst C11-PR).

Run	10-02 (DHG test)		
Reformer tube dimensions	Φ ½ -inch x 30 cm		
Catalyst type	C11-PR		
Catalyst loading (g)	15.2		
Catalyst size (mm)	6 x 6 x 2		
Outlet gasifier-reformer temperature (°C) *	650		
Steam to carbon molar ratio (CH_4) *	3		
Total inlet flow rate ($L.min^{-1}$) *	2.0044		
CH_4 inlet flow rate ($L.min^{-1}$) *	2.0000		
Water inlet flow rate ($L.min^{-1}$) *	0.0044		
Pressure (bar) *	52	65	80
Dry gas outlet flow rate ($L.min^{-1}$) *	3.67	3.56	3.49
Conversion (%) *	72	67	63
Produced dry gas composition (%) **			
H_2	47	43	39
CO	7	5	6
CO_2	18	18	17
CH_4	28	33	37
(*) Average values			
(**) Standard deviation of average values is ± 2 %			

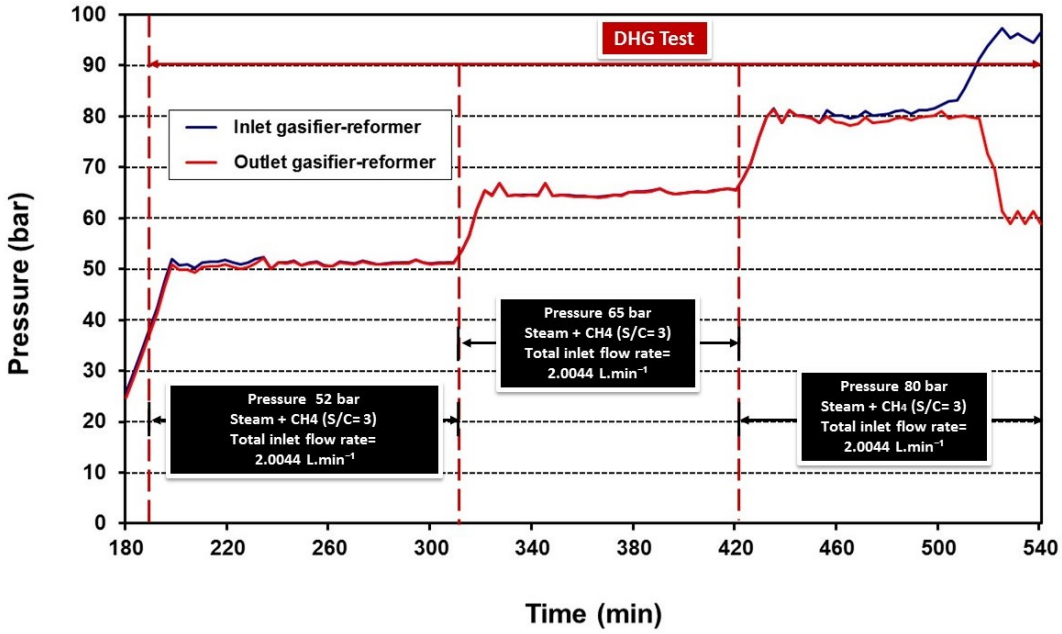

Figure 5.11 Repeat Run 10-02: Inlet and outlet pressure of gasifier-reformer (Catalyst C11-PR).

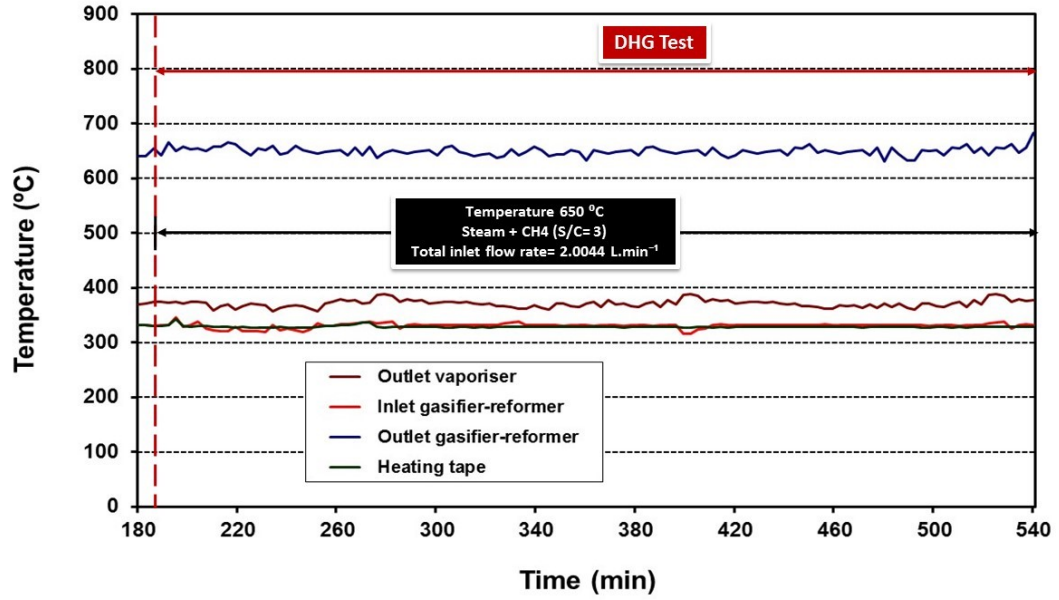

Figure 5.12 Repeat Run 10-02: Temperature profiles (Catalyst C11-PR).

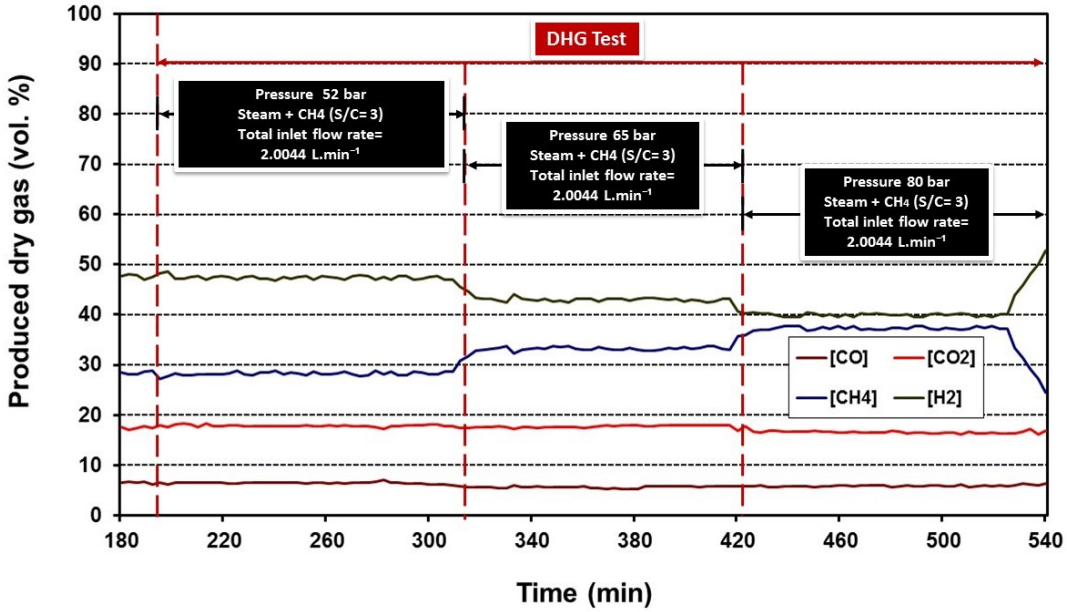

Figure 5.13 Repeat Run 10-02: Produced dry gas composition in vol. % (Catalyst C11-PR).

It is important to note that a divergence was also observed in Figure 5.6 corresponding to pressure curves specifically during the pressure drop beyond the 500 minute point. Curve behaviour is not identical since the degree of pressure drop is higher and more accentuated on the graph 5.11. However, in both cases the main cause is the same: suboptimal operating conditions.

5.2.3 Steam to carbon ratio (S/C= 15 to 3)

A relatively low S/C ratio of 3 at a pressure of 80 bar was determinant for coke formation in the previous Run 10-02 using methane feedstock. As this is a major concern, the investigation focused on exploring conditions that would avoid any serious effect of coking in future DHG experiments. Addressing this issue, Run 10-03 studied what S/C ratio might be used while maintaining pressure at 80 bar and temperature at 650 ºC.

Run 10-03 was conducted with a varying S/C ratio from 15 to 3 calculated on the basis of the water inlet flow rate (0.0044 $L.min^{-1}$).

Table 5.5 summarizes the operating conditions used in Run 10-03. Figure 5.14, 5.15 and 5.16 show the pressure, temperature and produced dry gas composition curves respectively obtained during the DHG test. The dry gas outlet flow rate was taken manually during the experiment.

Table 5.5 Run 10-03: Operating conditions during DHG test using methane feedstock (Catalyst C11-PR).

Run	10-03 (DHG test)					
Reformer tube dimensions	Φ ½ -inch x 30 cm					
Catalyst type	C11-PR					
Catalyst loading (g)	15.2					
Catalyst size (mm)	6 x 6 x 2					
Pressure (bar) *	80					
Outlet gasifier-reformer temperature (ºC) *	650					
Steam to carbon molar ratio (CH_4) *	15	10	8	6	4	3
Total inlet flow rate ($L.min^{-1}$) *	0.4044	0.6044	0.7544	1.0044	1.5044	2.0044
CH_4 inlet flow rate ($L.min^{-1}$) *	0.4000	0.6000	0.7500	1.0000	1.5000	2.0000
Water inlet flow rate ($L.min^{-1}$) *	0.0044	0.0044	0.0044	0.0044	0.0044	0.0044
(*) Average values						

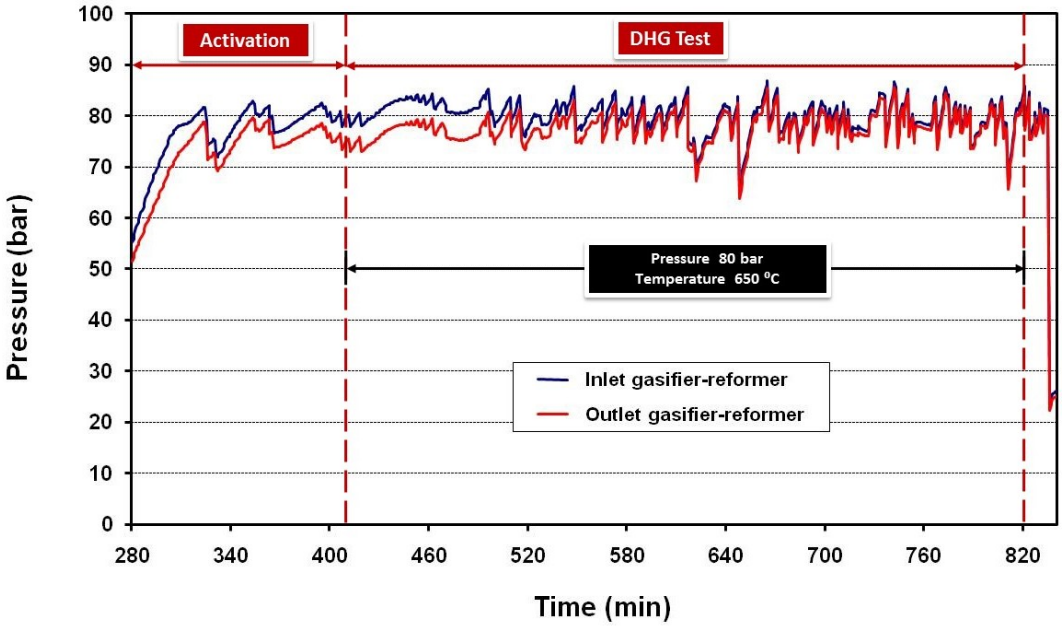

Figure 5.14 Run 10-03: Inlet and outlet pressure of gasifier-reformer during DHG test using methane feedstock (Catalyst C11-PR).

Figure 5.14 shows the inlet and outlet gasifier-reformer pressure in the DHG test period for Run 10-03, which started once the catalyst C11-PR was activated. No pressure drop was observed during the test although important disturbances or fluctuations were observed which reached values of 10 % standard deviation. This is attributed mainly to the pressure transducers rather than to the experimentation itself. Once Run 10-03 finished, a further calibration and checking of pressure transducers was carried out by the manufacturer before starting the next experiment.

To avoid coke formation at S/C= 3 as in the previous run (10-02), the gasifier-reformer was operated at the same S/C ratio as before for (20-40) minutes only since coke formation and pressure drop had been detected in Run 10-02 beyond the 80 minute point.

In regard to temperature profiles, Figure 5.15 shows the curves which indicated no major findings either, just a sudden and slight divergence in the outlet temperature of the vaporiser from the inlet temperature of the gasifier-reformer beyond the 725 minute point. This was due to a slight increase in the temperature of the heating tape to guarantee saturated steam conditions which are 295 ºC at 80 bar.

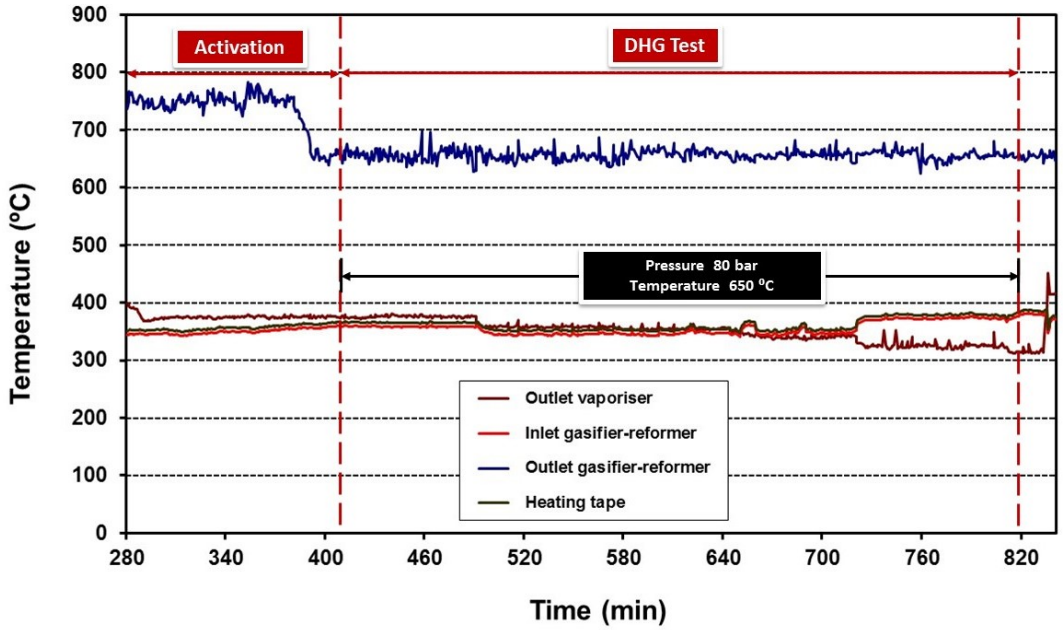

Figure 5.15 Run 10-03: Temperature profiles during DHG test using methane feedstock (Catalyst C11-PR).

Figure 5.16 shows the dry gas compositions in vol. % in the DHG test period, Run 10-03. The variation of H_2 and CH_4 concentration was sensitive to the changes in S/C ratios. The highest H_2 concentration (70.13 vol. %) was reached for S/C= 15 diminishing down to 63 %, 55 %, 50 %, 46 % and 40 % for S/C= 10, 8, 6, 4 and 3 respectively. The conversion was also affected, passing from 84 % at S/C= 15 to 48 % at S/C= 3.

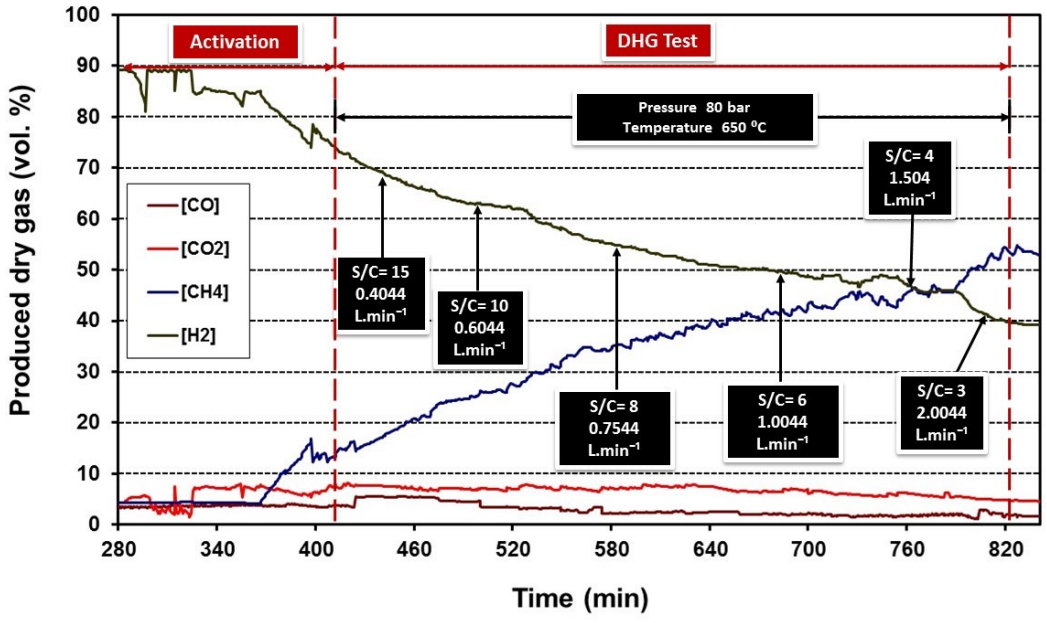

Figure 5.16 Run 10-03: Produced dry gas composition (vol. %) during DHG test using methane feedstock (Catalyst C11-PR).

The behaviour of the curves was compared to that of the curves reported by Greaves et al. (2004) and Greaves et al. (2005) and was found to be similar confirming the technical reliability of our results. However, our values of H_2 concentration and conversion were higher by 5-8 % which are attributed to the optimisations and modifications to the rig.

The dry gas outlet flow rates, whose average values were taken manually due to difficulties in the online recording, indicated that maximum values of dry gas outlet flow rates or total volume of dry gas per time unit (3.50 $L.min^{-1}$) were obtained when the S/C ratio was at its lowest (3). This is commensurate with stoichiometric principles since less hydrocarbon feedstock is reacting per unit time as the S/C ratio increases.

Table 5.6 shows how the dry gas outlet flow rate is dependent on the S/C ratio. This is a very important factor to consider in DHG implementation since an intermediate value that creates a high H_2 concentration in the produced dry gas, a high dry gas outlet flow rate (high volume per time unit) and no coke formation is the desired outcome.

We definitively need a DHG process in field operations enabling the formation of a significant volume of H_2 over a shorter time (high efficiency), while guaranteeing the survivability of the catalyst for 2 or more years.

Table 5.6 Run 10-03: Effect of S/C ratio on dry gas outlet flow rate and hydrogen in produced dry gas (vol. %) during DHG test using methane feedstock (Catalyst C11-PR).

Steam to carbon (S/C) ratio	Inlet methane flow rate ($L.min^{-1}$)	Inlet water flow rate ($L.min^{-1}$)	Total inlet flow rate ($L.min^{-1}$)	Dry gas outlet flow rate ($L.min^{-1}$)	Hydrogen in produced dry gas (vol. %)
3	2.0000	0.0044	2.0044	3.50	40.15
4	1.5000	0.0044	1.5044	2.84	45.90
6	1.0000	0.0044	1.0044	2.00	49.65
7	0.8360	0.0044	0.8404	1.92	75.47
8	0.7500	0.0044	0.7544	1.87	55.24
10	0.6000	0.0044	0.6044	1.56	62.75
15	0.4000	0.0044	0.4044	1.32	70.13

Addressing this point and based on our results, an intermediate value, S/C= 6, was selected beyond this run to perform the DHG tests. The next experiment will study the effects of temperature using methane feedstock.

In practice, the selection of the S/C ratio will tend to be the lowest possible, commensurate with its technical efficiency and economic performance. The suppression of coke formation on the catalyst surface due to an excess of steam is a very important fact to consider in this respect (Xu et al., 2008, Sperle et al., 2005, Li et al., 2010). Thus, both variables must be considered.

Catalyst reactivation treatment after the DHG test was carried out

successfully demonstrated by the fact that the same H_2 and CH_4 values obtained during the activation process were reached in the reactivation treatment, meaning a complete restoration of catalyst activity. This certainly suggests that the C11-PR catalyst can be operated over a longer period of time with no major problems. The details of the reactivation treatment will be described in section 5.2.5 in this chapter.

The following table summarizes the experimental conditions and results (Table 5.7) for the DHG test in Run 10-03.

Table 5.7 Run 10-03: Summary of operating conditions and results obtained during DHG test using methane feedstock (Catalyst C11-PR).

Run	10-03 (DHG test)					
Reformer tube dimensions	Φ ½ -inch x 30 cm					
Catalyst type	C11-PR					
Catalyst loading (g)	15.2					
Catalyst size (mm)	6 x 6 x 2					
Pressure (bar) *	80					
Outlet gasifier-reformer temperature (ºC) *	650					
Steam to carbon molar ratio (CH_4) *	15	10	8	6	4	3
Total inlet flow rate ($L.min^{-1}$) *	0.4044	0.6044	0.7544	1.0044	1.5044	2.0044
CH_4 inlet flow rate ($L.min^{-1}$) *	0.4000	0.6000	0.7500	1.0000	1.5000	2.0000
Water inlet flow rate ($L.min^{-1}$) *	0.0044	0.0044	0.0044	0.0044	0.0044	0.0044
Dry gas outlet flow rate ($L.min^{-1}$) *	1.32	1.56	1.87	2.00	2.84	3.50
Conversion (%) *	84	74	66	58	54	48
Produced dry gas composition (%) **						
H_2	70	63	55	50	46	40
CO	6	4	2	2	2	2
CO_2	8	7	7	6	6	5
CH_4	16	26	34	42	46	52
(*) Average values						
(**) Standard deviation of average values is ± 2 %						

5.2.4 Temperature (600 to 750 ºC)

Greaves et al. (2005) indicated the importance of temperature for conversion in the DHG process using methane feedstock. This run (10-01) is conducted at varying temperatures from 600 ºC to 750 ºC at 80 bar and S/C= 6. Table 5.8 summarizes the operating conditions used in the DHG test period once C11-PR was activated.

It is important to note that activation treatment curves obtained for this specific run were utilised to describe this treatment in section 5.2.1.

Figure 5.17, 5.18, 5.19 and 5.20 show the pressure, temperature, produced dry gas composition and the dry gas outlet flow rate curve obtained in the DHG test period of the Run 10-01.

Table 5.8 Run 10-01: Operating conditions during DHG test using methane feedstock (Catalyst C11-PR).

Run	10-01 (DHG test)			
Reformer tube dimensions	Φ ½ -inch x 30 cm			
Catalyst type	C11-PR			
Catalyst loading (g)	15.2			
Catalyst size (mm)	6 x 6 x 2			
Pressure (bar) *	80			
Steam to carbon molar ratio (CH_4) *	6			
Total inlet flow rate ($L.min^{-1}$) *	1.0044			
CH_4 inlet flow rate ($L.min^{-1}$) *	1.0000			
Water inlet flow rate ($L.min^{-1}$) *	0.0044			
Outlet gasifier-reformer temperature (ºC) *	600	650	700	750
(*) Average values				

Figure 5.17 shows the pressure curves. Fluctuations were still present after further calibration of the pressure transducers which minimised the level of disturbance calculated to below 8 % in standard deviation. No pressure drop was observed throughout, commensurate with the previous results (Run 10-03) and those reported by Greaves et al. (2005) where S/C= 6 was shown to be an acceptable value at 80 bar in terms of H_2 concentration and conversion of methane.

Figure 5.18 shows the temperature profiles during the DHG test where a temperature increase in the exit of the gasifier-reformer is observed with relative appreciable signal stability.

After 250 minutes, the outlet temperature of the gasifier-reformer was increased up to 600 ºC for 80 minutes, at which point, the temperature was increased again up to 650 ºC and for another 80 minutes, then increased up to 700 ºC and 750 ºC for another 80 minutes each approximately. To achieve this, the temperature controllers program required an adjustment of furnace temperature which required as its maximum value almost 870 ºC for 750 ºC. This indicated an acceptable heat transfer since a difference of 100-120 ºC was always present between the furnace temperature and the internal temperature of the fluid at the exit of the gasifier-reformer. Details of the furnace program temperature controllers is described in chapter 3, section 3.3.4.

Steam saturated conditions of fluids at the entrance of the gasifier-reformer were always guaranteed by adjusting the heating tape temperature if necessary.

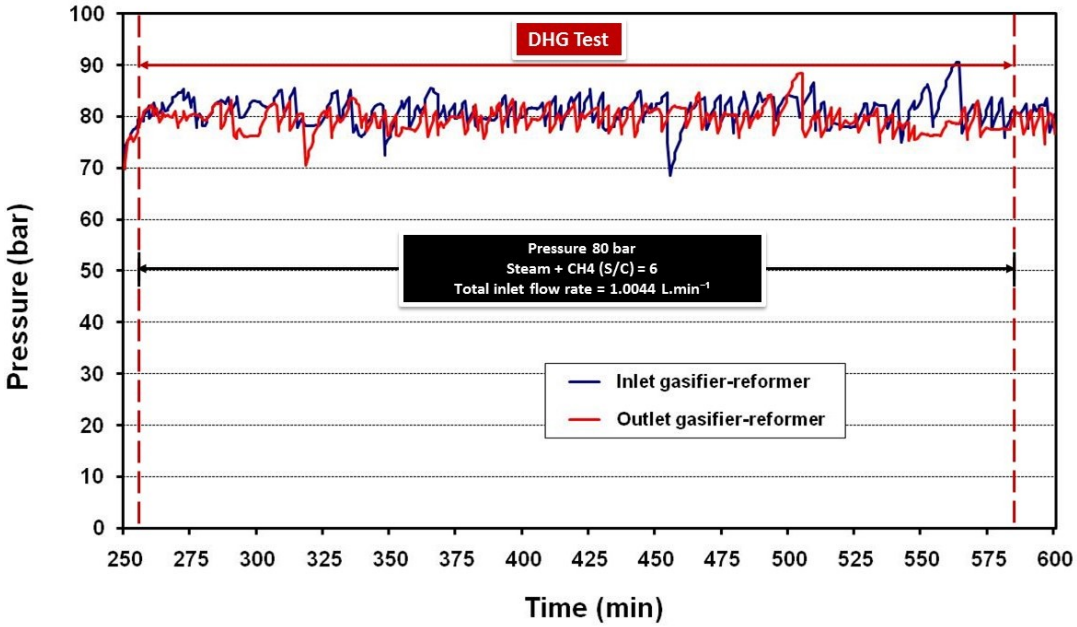

Figure 5.17 Run 10-01: Inlet and outlet pressure of gasifier-reformer during DHG test using methane feedstock (Catalyst C11-PR).

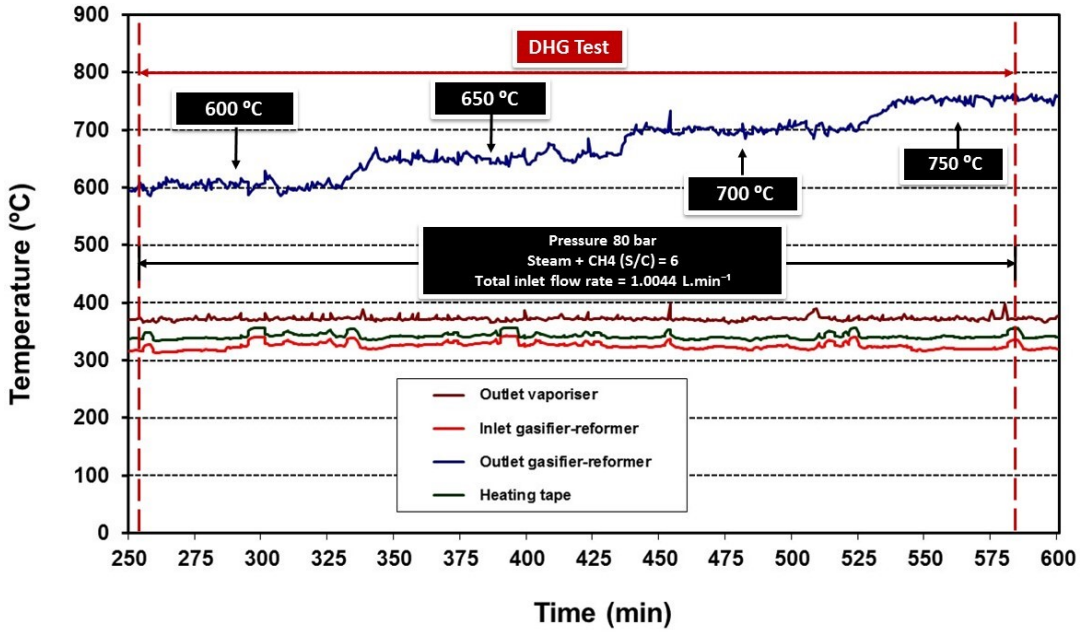

Figure 5.18 Run 10-01: Temperature profiles during DHG test using methane feedstock (Catalyst C11-PR).

Regarding the produced dry gas compositions (vol. %), Figure 5.19 indicates how H_2 concentration is improved as the reaction temperature in the gasifier-reformer was increased from 600 °C to 750 °C, and how at the same time CH_4 concentration decreased which is indicative of a higher conversion.

The H_2 concentration passed from 46 vol. % at 600 °C to 53 vol. % at

650 º C, 56 vol. % at 700 ºC and 60 vol. % at 750 ºC. This represented an increase by 3-6 % per 50 ºC approximately which is totally commensurate with values reported by Greaves et al. (2004) and Greaves et al. (2005) who indicated an increase of 2-6 % per 50 ºC at similar operating conditions. However, our values were slightly higher compared to their results, which is attributed to the revamped and optimised DHG rig.

The conversion of our results showed an inverse tendency when temperature increased, as expected. The conversion of CH_4 increased from 55 % at 600 ºC to 60 % at 650 ºC, 65 % at 700 ºC and 70 % at 750 ºC.

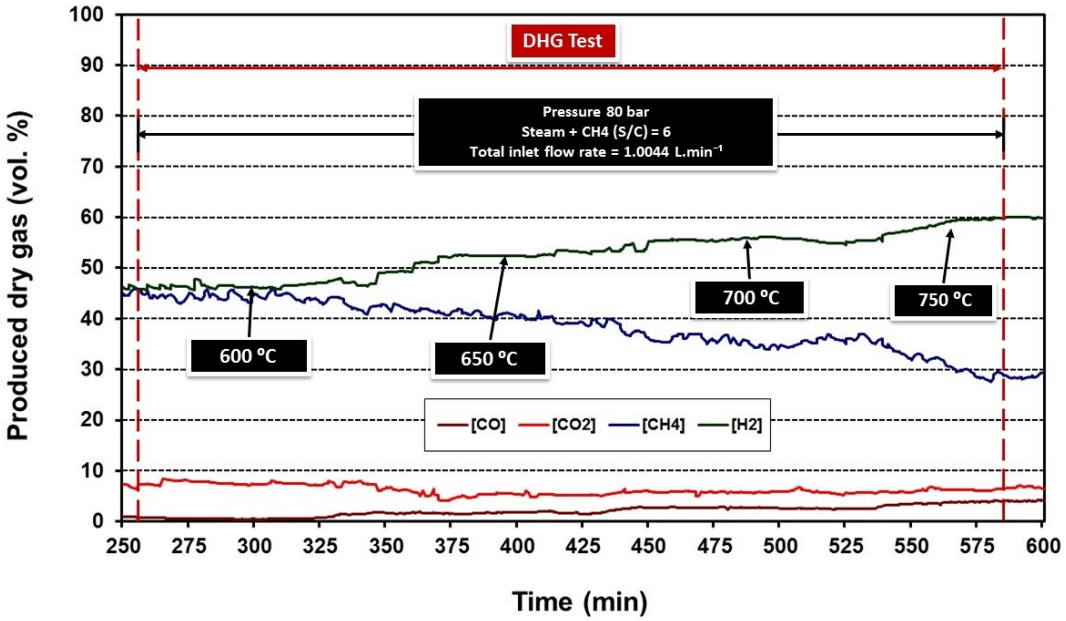

Figure 5.19 Run 10-01: Produced dry gas composition (vol. %) during DHG test using methane feedstock (Catalyst C11-PR).

In this run, fortunately the dry gas outlet flow rates were recorded online. Figure 5.20 shows the results with a relative signal stability below 5 % which is acceptable and justifiable for signal stability from an instrument. The average values for the dry gas outlet flow rates were: 1.67 $L.min^{-1}$ at 600 ºC; 2 $L.min^{-1}$ at 650 ºC; 2.28 $L.min^{-1}$ at 700 ºC and 2.5 $L.min^{-1}$ at 750 ºC, fairly similar to those reported by Greaves et al. (2005) at similar operating conditions. This is positive since it confirms the operability of the rig and the technical reliability of our experimental results.

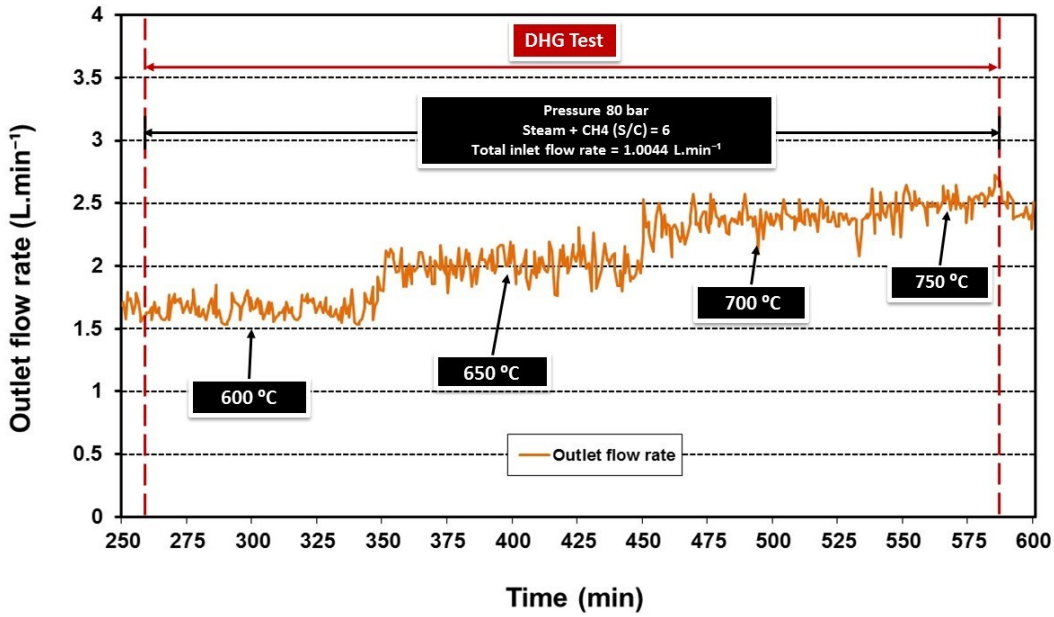

Figure 5.20 Run 10-01: Dry gas out let flow rate during DHG test using methane feedstock (Catalyst C11-PR).

Overall, the dry gas outlet flow rate increases when temperature is increased, which is completely feasible since temperature favours the conversion and H_2 concentration, representing a higher volume of gases per time unit. In theory, this parameter might compensate for any negative effect that pressure from an oil reservoir would have on the DHG process: more specifically, on the steam reforming reactions. However, its achievability is limited by operation costs, the need for higher energy and for an enhanced electrical supply quite apart from the chemical and mechanical constraints on the catalyst and gasifier-reformer reactor material respectively.

Stress generated by higher temperature means a nickel sintering process reducing catalytic activity in pores, favouring coke deposition and the collapse or breaking down of the catalyst itself (Trimm, 1997, Froment, 2008). The gasifier-reformer tube would be submitted to higher stress damaging irreversibly the material and, as a consequence, the overall process would be seriously affected (Viswanathan, 1989, Beyer et al., 2005, ASME, 2008, American petroleum institute, 2010).

An intermediate value that allows high H_2 concentration, a high conversion, minimum coke formation, the survivability of the catalyst for periods of 2 or more years in the event of DHG implementation in field operations with acceptable operation costs is what is desired. Thus, the search for those conditions of operation which would enable us to achieve a compromise between all those factors and parameters is necessarily part of an investigation which centres on the exploration of the technical feasibility of DHG using naphtha at pressures higher than 130 bar as typically found for watered oil reservoirs in mature oil fields. This is the

subject of the whole of the next chapter (chapter 6). The following table summarizes the experimental conditions and results (Table 5.9).

Table 5.9 Run 10-01: Summary of operating conditions and results obtained during DHG test using methane feedstock (Catalyst C11-PR).

Run	10-01 (DHG test)			
Reformer tube dimensions	Φ ½ -inch x 30 cm			
Catalyst type	C11-PR			
Catalyst loading (g)	15.2			
Catalyst size (mm)	6 x 6 x 2			
Pressure (bar) *	80			
Steam to carbon molar ratio (CH_4) *	6			
Total inlet flow rate ($L.min^{-1}$) *	1.0044			
CH_4 inlet flow rate ($L.min^{-1}$) *	1.0000			
Water inlet flow rate ($L.min^{-1}$) *	0.0044			
Outlet gasifier-reformer temperature (^0C) *	600	650	700	750
Dry gas outlet flow rate ($L.min^{-1}$) *	1.67	2.00	2.28	2.50
Conversion (%) *	55	60	65	70
Produced dry gas composition (%) **				
H_2	46	53	56	60
CO	0	2	3	4
CO_2	7	5	58	6
CH_4	45	40	35	30
(*) Average values				
(**) Standard deviation of average values is ± 2 %				

After 580 minutes of operation, catalyst reactivation treatment was carried out. To that end, the pressure was reduced to 10 bar and the S/C ratio was modified to 7. The H_2 generation and presence of CH_4 coincided with those values originally obtained during the activation process which leads to the supposition that the DHG test did not greatly affect the catalytic activity of C11-PR. This was confirmed when the reformer tube was opened since the catalyst was observed unchanged.

Further details of the reactivation procedure will be discussed in the next section using the curves obtained in this same run (10-01).

5.2.5 Catalyst reactivation treatment after DHG tests

As has been mentioned, the survivability of the catalyst for DHG is very important since once the process is being applied in field operations, it is necessary to allow for the conversion of hydrocarbons into oil wells for a period of 2 or more years. Thus, good performance and appearance after our DHG tests might be indicative of its operability in future implementation. This is why in this research activation and reactivation treatments were focussed on so greatly. In practice based on results, it seems that both should be considered as operational requirements to

extend the life of the catalyst.

This section shows the reactivation treatment of C11-PR performed once the DHG period within the experiment or run had finished. The operating conditions were same as those used for the activation treatment and are shown in Table 5.10 which corresponded to the Run 10-01. This procedure was applied to the Run 10-02 and Run 10-03 with favourable and similar results. For this reason, just one run is shown as an example. Appendix C shows a complete run or experiment corresponding to Run 10-01 including the three periods: activation, DHG test and reactivation.

Table 5.10 Run 10-01: Operating conditions during catalyst reactivation using methane feedstock (Catalyst C11-PR).

Run	10-01 (reactivation)
Reformer tube dimensions	Φ ½ -inch x 30 cm
Catalyst type	C11-PR
Catalyst loading (g)	15.2
Catalyst size (mm)	6 x 6 x 2
Pressure (bar) *	10
Outlet gasifier-reformer temperature (ºC) *	750
Steam to carbon molar ratio (CH_4) *	7
Total inlet flow rate ($L.min^{-1}$) *	0.8404
CH_4 inlet flow rate ($L.min^{-1}$) *	0.8360
Water inlet flow rate ($L.min^{-1}$) *	0.0044
(*) Average values	

Once the reduced catalyst is subjected to steam reforming reactions, excess steam and coke deposits negatively affect the catalyst. Full activity could be restored by applying the same activation procedure or a controlled steaming process that avoids the reoxidation of Nickel and favours, at the same time, the gasification of coke via a water gas shift reaction. Figure 5.21, 5.22 and 5.23 show the pressure, temperature and produced dry gas composition (vol. %) obtained.

Figure 5.21 shows the inlet and outlet pressure of the gasifier-reformer. Pressure was reduced from the 80 bar proper to the DHG test period to 10 bar with special care to avoid any mechanical damage to the catalyst. No major findings or pressure drop were observed throughout. The signal was also fairly stable, below 4 % which is positive.

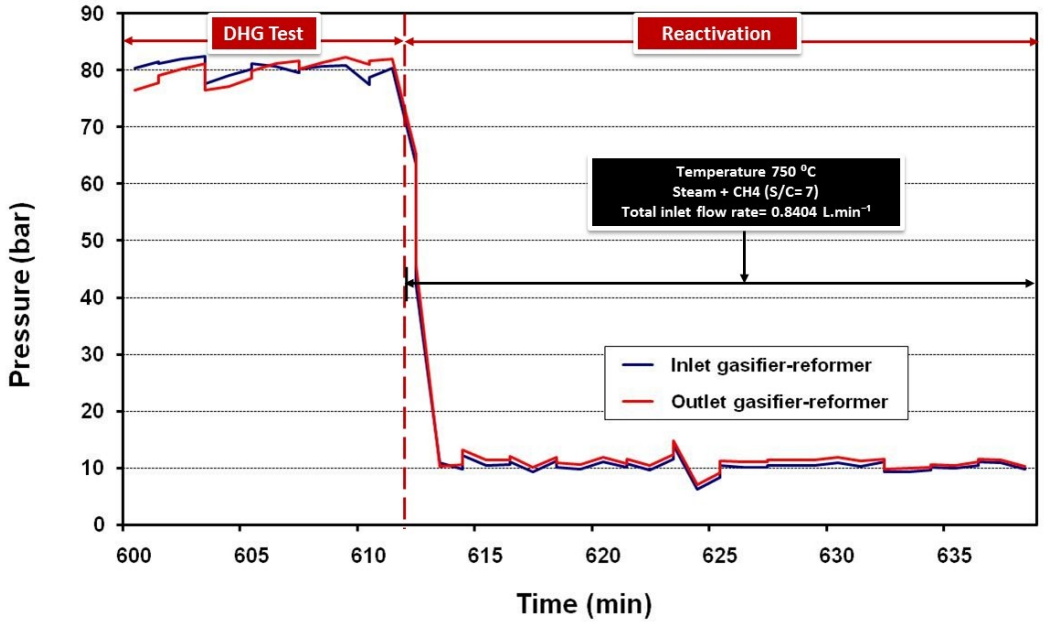

Figure 5.21 Run 10-01: Inlet and outlet pressure of gasifier-reformer during catalyst reactivation using methane feedstock (Catalyst C11-PR).

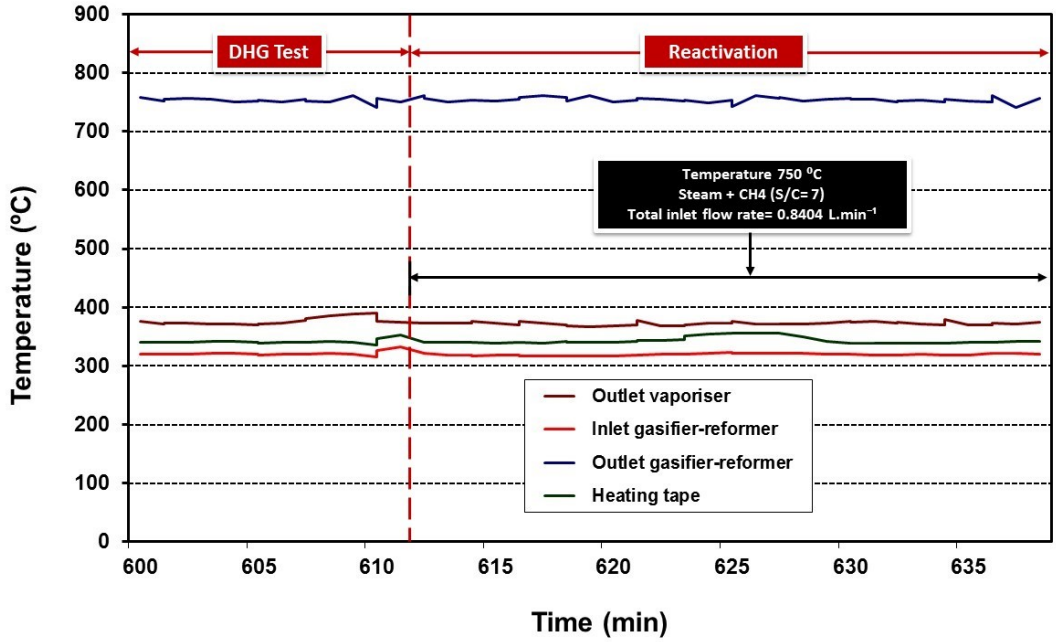

Figure 5.22 Run 10-01: Temperature profiles during catalyst reactivation using methane feedstock (Catalyst C11-PR).

The temperature profiles shown in Figure 5.22 did not show any major disturbances or points requiring attention, and no variation in the temperature of the gasifier-reformer was required since Run 10-01 performed at 750 ºC in the last stage of the DHG test.

In Figure 5.23 important changes in the H_2 and CH_4 curves were observed in the produced dry gas composition (vol. %). An increase of H_2 concentration was clearly detected parallel to a decrease in CH_4 level.

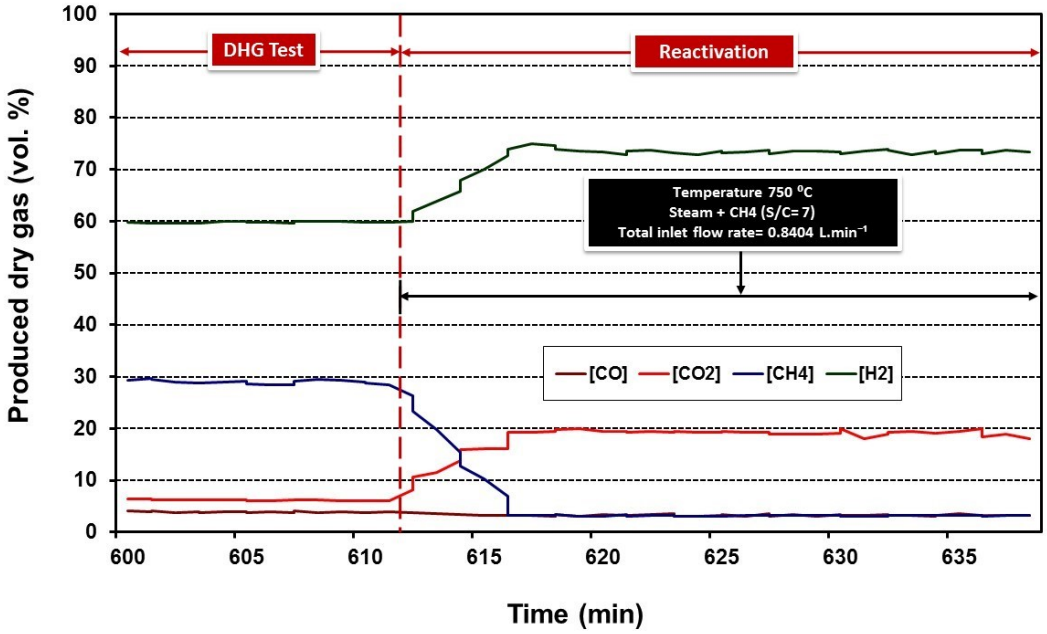

Figure 5.23 Run 10-01: Produced dry gas composition (vol. %) during catalyst reactivation using methane feedstock (Catalyst C11-PR).

The values of both almost reached the original values obtained during the activation treatment (discrepancies are below 3 %) which lead to the supposition of total restoration of catalytic activity after the DHG test. In practice, it also leads to the supposition that extending catalyst life in future DHG implementation might not be a problem. However, this is highly dependent on the hydrocarbon feedstock to be converted in the gasifier-reformer and the operating conditions to be applied in field operations.

DHG envisages the use of naphtha feedstock directly extracted and vaporised from the oil in the reservoir under conditions using (50-200) bar of pressure. Naphtha tends to produce more coke on the catalyst and higher pressure than 80 bar might favour the coking process. Thus, it is necessary to first carry out experimental results using naphtha before taking a decision on the feasibility of implementation of reactivation treatments, Chapter 6 will discuss the DHG experiments in relation to the use of naphtha feedstock.

A C11-PR catalyst sample was analysed after reactivation using scanning electronic microscopy (SEM). Figure 5.24 shows the SEM image. No coke deposits were observed and porosity seems to be appreciable and higher than the original without treatment shown in Figure 5.8. This is very supportive of the findings previously mentioned on the total restoration of

catalytic activity after the DHG test.

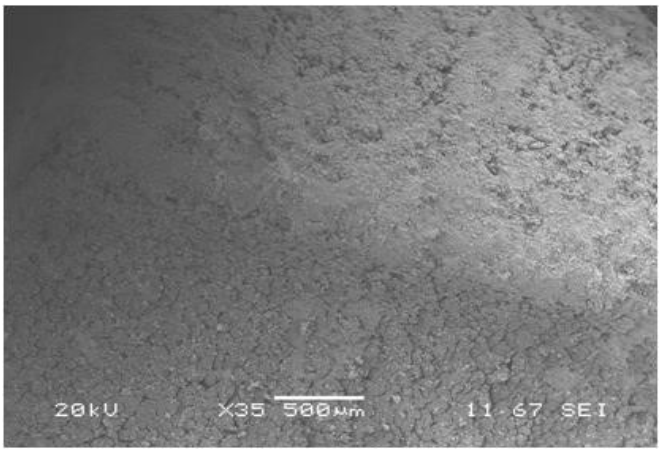

Figure 5.24 SEM image of C11–PR catalyst after reactivation treatment in Run 10-01. Side view (20 KV, x35, 500 µm, SEI).

Dry gas outlet flow rates (Average values) were very similar to those obtained in the catalyst activation treatment which was 1.92 $L.min^{-1}$, while that in the reactivation treatment was 1.87 $L.min^{-1}$, representing an almost negligible divergence.

The Table 5.11 summarizes the experimental conditions and the results of the C11-PR reactivation treatment corresponding to Run 10-01.

Table 5.11 Run 10-01: Summary of operating conditions and results in catalyst reactivation using methane feedstock (Catalyst C11-PR).

Run	10-01 (reactivation)
Reformer tube dimensions	Φ ½ -inch x 30 cm
Catalyst type	C11-PR
Catalyst loading (g)	15.2
Catalyst size (mm)	6 x 6 x 2
Pressure (bar) *	10
Outlet gasifier-reformer temperature (ºC) *	750
Steam to carbon molar ratio (CH_4) *	7
Total inlet flow rate ($L.min^{-1}$) *	0.8404
CH_4 inlet flow rate ($L.min^{-1}$) *	0.8360
Water inlet flow rate ($L.min^{-1}$) *	0.0044
Dry gas outlet flow rate ($L.min^{-1}$) *	1.87
Conversion (%) *	97
Produced dry gas composition (%) **	
H_2	74
CO	3
CO_2	20
CH_4	3
(*) Average values	
(**) Standard deviation of average values is ± 2 %	

5.3 Mass balance analysis

As example mode a mass balance analysis is shown in Table 5.12 which corresponds to Run 10-01. Equations and data are described in chapter 4, section 4.3.3 and Appendix B, Sections B.4, B.5, B.6 and B.7.

This mass balance analysis was carried out to ensure technical reliability of our experimental results and good performance of the experimental rig. As can be seen, no major inconveniences or negative findings were found. Discrepancies are below 8 % which is acceptable for the engineering environment. Uncertainties are detailed in chapter 4, section 4.3.4.

Table 5.12 Run 10-01: Mass balance.

RUN 10-01	IN Total inlet ($kg.s^{-1}$)		OUT Total outlet ($kg.s^{-1}$)						BALANCE ($kg.s^{-1}$)
			Produced dry gas				Liquid products		
	CH_4	Water	H_2	CO	CO_2	CH_4	CH_4	Water	
Catalyst activation	9.32E-06	7.48E-05	4.44E-06	4.70E-06	4.62E-05	3.17E-07	-	4.72E-05	-1.87E-05
DHG Test (600 °C)	1.11E-05	7.48E-05	2.37E-06	6.24E-07	1.66E-05	3.72E-06	-	4.72E-05	1.54E-05
DHG Test (650 °C)	1.11E-05	7.48E-05	3.21E-06	3.07E-06	1.43E-05	3.92E-06	-	4.71E-05	1.43E-05
DHG Test (700 °C)	1.11E-05	7.48E-05	3.90E-06	4.58E-06	1.79E-05	3.89E-06	-	4.71E-05	8.53E-06
DHG Test (750 °C)	1.11E-05	7.48E-05	4.55E-06	7.53E-06	2.10E-05	3.63E-06	-	4.71E-05	2.09E-06
Catalyst reactivation	9.32E-06	7.48E-05	4.20E-06	4.94E-06	4.90E-05	3.05E-07	-	4.72E-05	-2.15E-05
TOTAL	6.30E-05	4.49E-04	2.27E-05	2.54E-05	1.65E-04	1.58E-05	-	2.83E-04	4.40E-08

5.4 Concluding remarks

In previous work reported by Greaves at al. (2004) and Greaves et al. (2005), the DHG process was tested in experiments using methane feedstock to study the effect of pressure, S/C ratio and temperature on steam reforming reactions in the gasifier-reformer. In this chapter, these experiments were replicated as basic DHG experiments to verify the operability of the experimental rig commissioned and revamped in this investigation; thereby to understand the procedures for operating the rig and to generate a clear baseline of results. Failure to optimize these procedures could lead to rapid deterioration of catalyst activity, conversion, H_2 concentration as our main gas of interest and, possible cessation of operation due to coke blocking the action of the catalyst.

The experiments were conducted using methane feedstock in a range of pressure from 50 bar up to 80 bar, steam to carbon (S/C) ratio from 15 to 3, and values of temperature from 600 ºC to 750 ºC. The length of the gasifier-reformer reactor was 30 cm and the catalyst C11-PR was supplied by Sud Chemie. The investigation paid special attention to catalyst treatment: activation and reactivation procedures.

The experimental results of these basic DHG experiments using methane feedstock have led to the following conclusions:

1. Overall, the basic DHG experiments using methane feedstock and replicating the operating conditions of pressure (50-80 bar), S/C ratios (15 to 3) and temperature (600-750 ºC) with a gasifier-reformer tube length of 30 cm and C11-PR catalyst showed the same tendency and similar values of conversion and H_2 concentration in produced dry gas as that reported by Greaves et al., (2004) and Greaves et al., (2005). This provided confidence that the operability and functionality of the commissioned and revamped experimental rig were fit to carry out the main goal of this research – to carry out DHG experiments using naphtha feedstock extending the pressure up to 160 bar – with good performance, a clear baseline and technical reliability of results.

2. Basic DHG experiments using methane feedstock at 650 ºC, S/C= 3 and a reactor tube length of 30 cm showed that H_2 concentration in the produced dry gas decreased by 9 % approximately when pressure increased from 52 bar to 80 bar (48 vol. %, at 65 bar 43 vol. % and at 80 bar 40 vol. %) which is considerable and totally commensurate with the reduction in methane conversion that passed from 72 % to 63 %. This tendency was reported by Greaves et al. (2004) and Greaves et al. (2005) who indicated that the increasing of pressure is the main factor influencing the effectiveness of the DHG process. It is expected that such a decrease in H_2 concentration from the gasifier-reformer would continue at higher pressure values, and so values below 25 vol. % of H_2 concentration at 160 bar are projected.

3. The steam to carbon (S/C) ratio has a very significant influence on: the H_2 concentration in produced dry gas, the dry gas outlet flow rate or total volume of dry gases generated per time unit and coke formation on the catalyst. Basic DHG experiments using methane feedstock at 650 ºC, 80 bar, reactor tube length of 30 cm showed that the highest H_2 concentration (70 vol. %) was reached for S/C= 15 while the lowest was 40 % for S/C= 3. The conversion was also influenced passing from 84 % at S/C= 15 to 48 % at S/C= 3. However, the volume of produced dry gas was inverse: maximum values (3.50 $L.min^{-1}$) were obtained when S/C ratio was the lowest, 3 compared to 1.32 $L.min^{-1}$ at S/C= 15. This is commensurate with the results reported by Greaves et al (2004) and Greaves et al. (2005), and is attributed to the fact that less methane feedstock is reacting per time unit. In practice, an intermediate value that promotes technical efficiency, good economic performance and minimisation of coke formation on the catalyst surface is what is desired.

4. A higher temperature in the gasifier-reformer favours a higher H_2 concentration in produced dry gas and a higher methane conversion. Basic DHG experiments using methane feedstock, 80 bar, S/C= 6 indicated that H_2 concentration passed from 46 vol. % at 600 ºC to 53 vol. % at 650 ºC, 56 vol. % at 700 ºC and 60 vol. % at 750 ºC. This represented an increase of 3-6 % per 50 ºC approximately which is totally commensurate with the values reported by Greaves et al. (2004) and Greaves et al. (2005) who indicated an increase of 2-6 % per 50 ºC at similar operating conditions. However, temperature increase is limited by operation costs, higher energy consumption and electrical supply, apart from chemical and mechanical constraints on catalyst and gasifier-reformer reactor material.

5. The survivability of the catalyst is very important for DHG since if the process is to be applied successfully in field operations, it is necessary that hydrocarbons conversion is active for a period of 2 or more years. The favourable results obtained during the catalyst activation and reactivation performed during the experimentation using methane feedstock or controlled steaming leads to the recommendation that both procedures should be considered as operational requirements in order to preserve and extend the life of the catalyst beyond this point of the investigation.

References

ALIZADEH, R., JAMSHIDI, E. AND ALE-EBRAHIM, H., 2007. Kinetic study of nickel oxide reduction by methane. *Chemical engineering technology,* 30(8), pp. 1123–1128.

AMERICAN PETROLEUM INSTITUTE, 2010. *Damage mechanisms affecting fixed equipment in the refining industry.* 2nd edition. Washington: API Publishing Services.

ASME, 2008. *Metals handbook: Properties and selection of iron, steels and high-performance alloys volume 1.* Washington: ASM International Press.

BABADAGLI, T., 2007. Development of mature oil fields — A review. *Journal of petroleum science and engineering,* 57, pp. 221–246.

BEYER, F., BRIGHTLING, J., FARNELL, P., FOSTER, C., 2005. Steam reforming – 50 years of development and the challenges for the next 50 years. Proceedings of the *AIChe 50th Annual Safety in Ammonia Plants and Related Facilities Symposium,* 26-29 September 2005 Toronto. Canada, pp. 01-12.

CHRISTENSEN, K.O., 2005. Steam Reforming of Methane on Different Nickel Catalysts. Thesis (PhD). Norwegian University of Science and Technology, Trondheim.

FROMENT, G.F., 2008. Kinetic modelling of hydrocarbon processing and the effect of catalyst deactivation by coke formation. *Catalysis reviews,* 50, pp. 01-18.

GREAVES, M., RATHBONE, R., XIA, T., BENTHAHER, A., DUGGAN, S., 2004. *Downhole gasification for improved oil recovery and gas production (phase 1) experimental studies (1 Nov 2002 – 31 Oct 2004).* United Kingdom: University of Bath, (Confidential internal report).

GREAVES, M., XIA, T., RATHBONE, R. AND BENTAHER, A., 2005. Underground gasification for improved oil recovery. *Canadian international petroleum conference,* 7-9 June 2005 Calgary. Calgary: Petroleum Society Canadian Institute of Mining, Metallurgy & Petroleum, pp. 38-48.

GREEN, D.W., WILLHITE G.P., 1998. Enhanced Oil Recovery. *Society of Petroleum Engineers*, Texas.

HELVEG, S., SEHESTED, J. AND ROSTRUP-NIELSEN, J.R., 2011. Whisker carbon in perspective. *Catalysis today,* 178, pp. 42– 46.

HUTCHINSON, C. A., BRAUN, P.H., 1961. Phase Relations of Miscible Displacement in oil Recovery. *AIChE J.*, 7, pp. 64-72.

JONES, G., JAKOBSEN, J.G., SHIM, S.S., KLEIS, J., ANDERSSON, M.P., ROSSMEISL, J., PEDERSEN, F.A., BLIGAARD, T., HELVEG, S., 2008. First principles calculations and experimental insight into methane steam reforming over transition metal catalysts. *Journal of catalysis,* 259, pp. 147-160.

KULKARNI, M.M., 2005. *Multiphase mechanisms and fluid dynamics in gas injection enhanced oil recovery processes.* Dissertation (PhD). Louisiana State University, U.S.

LAKE, L.W., WALSH, M.P., 2008. *Enhanced oil recovery (EOR) field data: literature search.* U.S.: University of Texas.

LI, L., WANG, X.G., SHEN, K., ZOU, X.J., LU, X.G., DING, W.Z., 2010. Highly efficient $Ni/CeO_2/Al_2O_3$ catalyst for pre-reforming of liquefied petroleum gas under a low molar ratio of steam to carbon. *Chinese journal catalysis,* 31, pp. 525-527.

PADBAN, N. AND BECHER, V., 2005. *Literature and state-of-the-art review (Re: Methane Steam Reforming).* CHRISGAS, (October 2005_WP11_D89).

RASHIDI, H., EBRAHIM, H.A. AND DABIR, B., 2013. Reduction kinetics of nickel oxide by methane as reducing agent based on thermogravimetry. *Thermochimica acta,* 561(2013), pp. 41– 48.

ROSTRUP-NIELSEN, J.R., 1984. *Catalytic Steam Reforming volume 5.* New York: Springer-Verlag Press.

SCHUTLE, W.M., 2005. Challenges and strategy for increased oil recovery. Proceedings of the *International Petroleum Technology Conference,* 21-23 November 2005 Doha. Qatar: pp. 02-09.

SPERLE, T., CHEN, D., LODENG, R., HOLMEN, A., 2005. Pre-reforming of natural gas on a Ni catalyst Criteria for carbon free operation. *Applied Catalysis A: General,* 282, pp. 195–204.

TRIMM, D.L., 1997. Coke formation and minimisation during steam reforming reactions. *Catalysis today,* 37, pp. 233-238.

TWIGG, M.V., 1989. *Catalyst Handbook*. 2nd edition. England: Wolfe Press.

VISWANATHAN, R., 1989. *Damage mechanisms and life assessment of high temperature components.* Washington: ASM International Press.

XU, J., YEUNG, C.M., NI, J., MEUNIER, F., ACERBI, N., FOWLES, M., TSANG, S., 2008. Methane steam reforming for hydrogen production using low water-ratios without carbon formation over Ceria coated Ni catalysts. *Applied Catalysis A: General,* 345, pp. 119–127.

CHAPTER 6: DHG PRODUCED DRY GAS COMPOSITION USING NAPHTHA FEEDSTOCK

6.1 Introduction

In this chapter, results are presented for experiments carried out on a naphtha feedstock which was used to represent the naphtha fraction to be extracted and vaporised from oil into reservoirs in DHG implementation at field scale.

A series of experiments was conducted covering a range of pressure from 80 bar up to 160 bar. Initially, the investigations focused on exploring conditions that would avoid any serious effect of carbon deposition on the catalyst; special attention was also paid to what steam to carbon ratio (S/C) should be employed.

The length of the gasifier-reformer reactor was also increased by 100 % in order to increase the catalyst loading. Two different catalysts were used: C11-PR supplied by Sud Chemie and crushed HiFUEL R110 from Alfa Aesar (Johnson Matthey). Additionally, experiments of shutdown/start up cycles followed by variation of temperature (from 600 ºC to 750 ºC) were performed to simulate possible sudden electrical disruptions in field implementation.

The sequence of a typical DHG experiment using naphtha feedstock included two test periods: (1) Catalyst activation treatment followed by (2) the DHG test proper where steam reforming reactions were studied in the gasifier-reformer reactor at DHG operating conditions. To confirm results, at least one second repeat experiment was always carried out.

6.2 Experiments with catalyst C11-PR and gasifier-reformer length 30 cm

This section involved firstly experiments directed at selecting an optimal steam to carbon (S/C) ratio that avoided coke formation on the catalyst (Run 20-01 and Run 20-02). Subsequently, pressure was extended from 10 bar to 82 bar and then to 110 bar (Run 20-03).

The DHG experiments were performed with a water inlet flow rate of 0.0090 $L.min^{-1}$ instead of the 0.0044 $L.min^{-1}$ used in the DHG experiments with methane feedstock as detailed in chapter 5.

6.2.1 Catalyst activation treatment prior to DHG tests

A catalyst activation period was carried out prior to the DHG test period during every experiment and has been analysed separately. The treatment was performed using methane feedstock; the experimental procedures were the same as those used in chapter 5. The operation conditions were

same except for the inlet flow rates since the water inlet flow rate was increased by 104.6 %, and therefore, the methane inlet flow rate also increased maintaining the S/C ratio at 7.

The results of the activation periods from Run 20-01, Run 20-02 and Run 20-03 were similar in terms of curve behaviour and values of pressure, temperature, produced dry gas composition and outlet flow rate obtained. For that reason, just one of them (Run 20-01) is shown here as an example.

Table 6.1 shows the operating conditions used during the catalyst activation treatment in Run 20-01 with the catalyst C11-PR. Some values were average values over the time period of interest in the run. Figure 6.1, 6.2, 6.3 and 6.4 show pressure, temperature, produced dry gas composition and outlet flow rates curves obtained.

Table 6.1 Run 20-01: Operating conditions during catalyst activation using methane feedstock (Catalyst C11-PR).

Run	20-01 (activation)
Reformer tube dimensions	Φ ½ -inch x 30 cm
Catalyst type	C11-PR
Catalyst loading (g)	15.2
Catalyst size (mm)	6 x 6 x 2
Pressure (bar) *	10
Outlet gasifier-reformer temperature (ºC) *	750
Steam to carbon molar ratio (CH_4) *	7
Total inlet flow rate ($L.min^{-1}$) *	1.8090
CH_4 inlet flow rate ($L.min^{-1}$) *	1.8000
Water inlet flow rate ($L.min^{-1}$) *	0.0090
(*) Average values	

As shown in Figure 6.1, the gasifier-reformer was started up with steam only flowing through the catalyst bed. After 15 minutes, methane was also introduced at a reduced pressure of 10-15 bar to carry out activation of the catalyst at a steam to carbon ratio (S/C) of 7 and a temperature of 750 ºC (Figure 6.2). At the end of this treatment (265 minutes), the DHG test started with the injection of naphtha.

Figure 6.2 indicates the temperatures of: the outlet vaporiser, the inlet gasifier-reformer and the outlet gasifier-reformer (unfortunately the thermocouple on the inlet to the gasifier-reformer was broken). The outlet gasifier-reformer temperature decreases sharply from 700 ºC to 400 ºC when methane flow is started. It takes more than 1 hour to reach 750 ºC, the temperature required for catalyst activation.

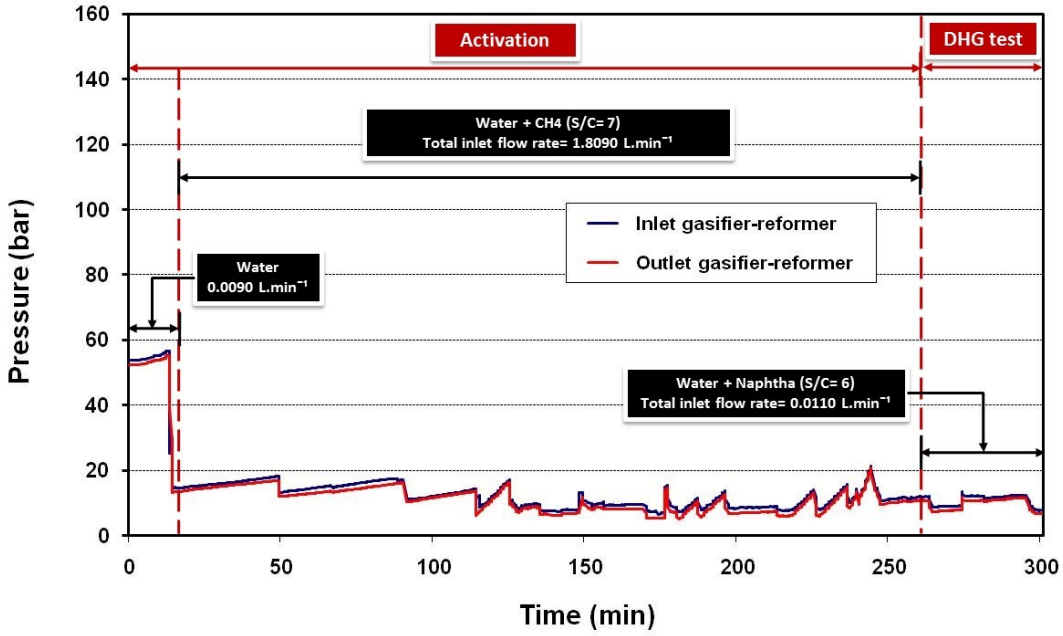

Figure 6.1 Run 20-01: Inlet and outlet pressure of gasifier-reformer during catalyst activation using methane feedstock (Catalyst C11-PR).

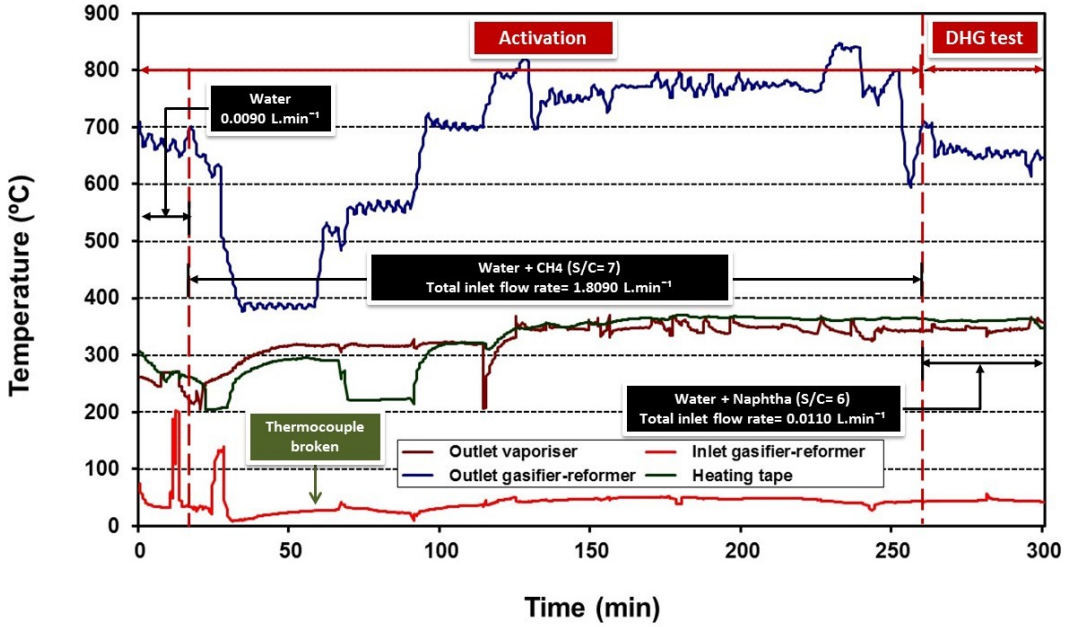

Figure 6.2 Run 20-01: Temperature profiles during catalyst activation using methane feedstock (Catalyst C11-PR).

Once the activation was completed, the furnace temperature was reduced in the gasification-reforming section using the temperature controller program to obtain a lower outlet temperature of 650 ºC, the desired temperature for the next period of the DHG test.

The furnace temperature controllers of the vaporisation and gasification-reforming sections have a program to adjust the furnace temperature to the desired outlet vaporiser and outlet gasifier-reformer temperature (For details, see chapter 3). The temperature of the furnaces is approximately 100 ºC above that needed to achieve the desired outlet temperature.

In relation to the gas compositions graph (Figure 6.3), for the period between 140 – 265 minutes when catalyst activation occurred, the curves associated with catalyst activation were observed to demonstrate the same behaviour seen in chapter 5 in Run 10-01. This confirms what previous research (Alizadeh et al., 2007, Rashidi et al., 2013) indicates: the behaviour of the H_2 and CH_4 curves during activation at similar operating conditions are dependent on catalyst type. After 265 minutes, the DHG test started to run.

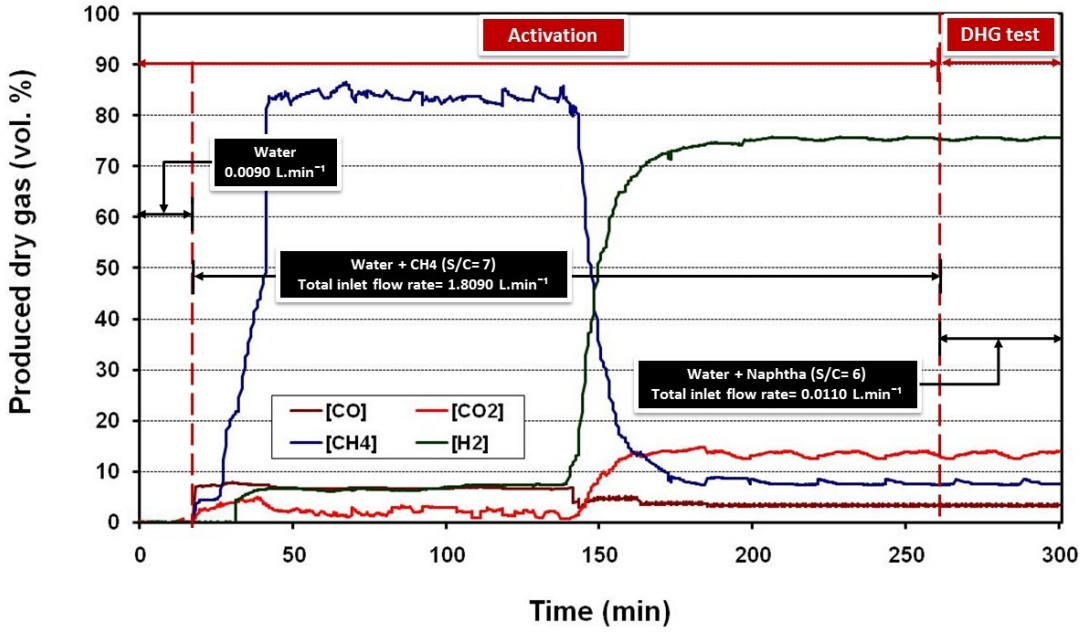

Figure 6.3 Run 20-01: Produced dry gas composition (vol. %) during catalyst activation using methane feedstock (Catalyst C11-PR).

At the start of the activation, the increase in the concentration of hydrogen occurs very rapidly, reaching nearly 76 % and this level is maintained during the activation treatment. The concentrations of the other gases also level-off at constant values: CO_2 (14 vol. %), CO (3 vol. %) and CH_4 (8 vol. %). This corresponds to an overall conversion of 92 %, which is consistent with the performance for the C11-PR catalyst obtained in chapter 5.

The dry gas outlet flow rate from the gasifier-reformer was measured by the wet test meter online and is shown in Figure 6.4. The average value during the activation period was 4.12 $L.min^{-1}$ which was over 100 % more than previously obtained in the catalyst activation treatments in chapter 5. This is logical due to the fact that the total inlet flow rate used here was

1.8090 L.min^{-1} instead of 0.8404 L.min^{-1}. The increment of the flow rate is based on stoichiometry and conversion: 1 mole of CH_4 with 1 mole H_2O produce 1 mole of CO and 3 moles H_2 while 1 mole of CH_4 with 2 moles H_2O produce 1 mole of CO_2 and 4 moles H_2 (see chapter 2, section 2.4.1 and chapter 5, Figure 5.5).

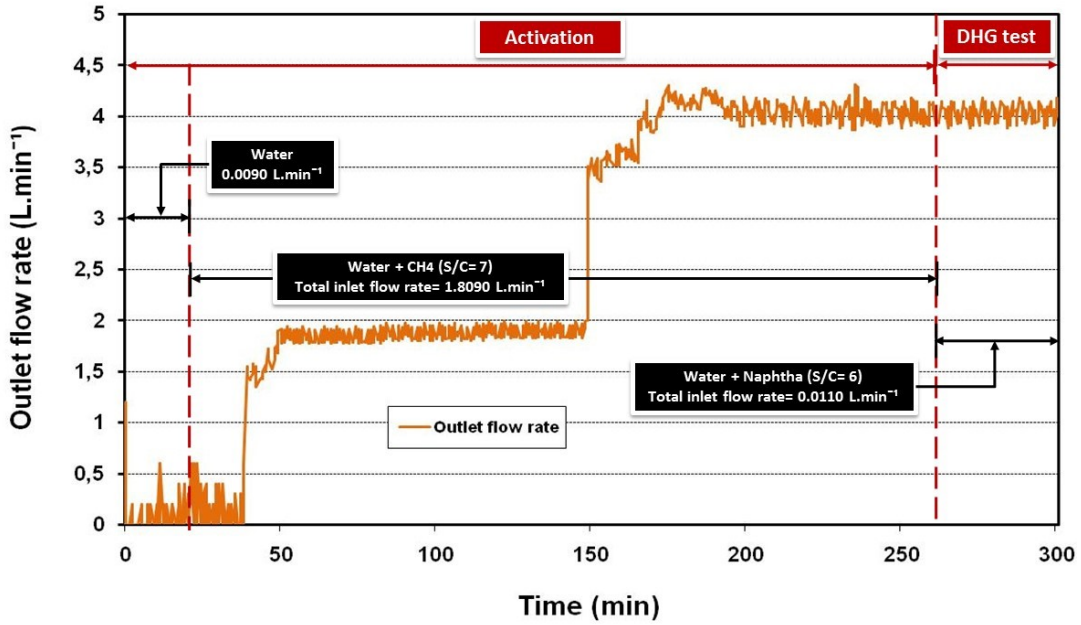

Figure 6.4 Run 20-01: Outlet flow rate from gasifier-reformer, produced dry gas, during catalyst activation using methane feedstock (Catalyst C11-PR).

Table 6.2 shows a summary of the results obtained in Run 20-01 during activation treatment of C11-PR using methane feedstock. Some values were average values over the time period of interest in the run. In the case of this table, these values are from the catalyst activation test period proper.

In summary, no major inconveniences were observed in this run, as in Run 20-02 and Run 20-03. The first trial of the DHG test using naphtha feedstock will be described in the next section.

Table 6.2 Run 20-01: Summary of operating conditions and results obtained in catalyst activation using methane feedstock (Catalyst C11-PR).

Run	20-01 (activation)
Reformer tube dimensions	Φ ½ -inch x 30 cm
Catalyst type	C11-PR
Catalyst loading (g)	15.2
Catalyst size (mm)	6 x 6 x 2
Pressure (bar) *	10
Outlet gasifier-reformer temperature (ºC) *	750
Steam to carbon molar ratio (CH_4) *	7
Total inlet flow rate ($L.min^{-1}$) *	1.8090
CH_4 inlet flow rate ($L.min^{-1}$) *	1.8000
Water inlet flow rate ($L.min^{-1}$) *	0.0090
Dry gas outlet flow rate ($L.min^{-1}$) *	4.12
Conversion (%) *	92
Produced dry gas composition (%) **	
H_2	76
CO	3
CO_2	14
CH_4	8
(*) Average values	
(**) Standard deviation of average values is ± 2 %	

6.2.2 First trial

In the first instance, the DHG rig used here was the original design for the DHG tests on methane in chapter 5, prior to the further modifications and optimisations described in chapter 3, section 3.3.5.

The naphtha fraction feedstock had an average boiling point of approximately 108 ºC and a density of 691 $Kg.m^{-3}$ (Details are in chapter 3, section 3.2.1 and Appendix A, section A.2). Twigg (1989) reports that naphtha fractions with a final boiling point of less than 220 ºC are generally considered suitable for steam reforming (chemical reactions which the DHG process is based on), demonstrated in a table with an analysis of naphtha detailing some ideal compositional specifications. These values were compared positively with our naphtha feedstock effectively demonstrating its technical suitability.

For comparison, n-heptane has a boiling point temperature of 100 ºC and a density of 689 $kg.m^{-3}$. Heptane was chosen as the model surrogate for naphtha in some calculations here and in the numerical modelling studies

in Chapter 7.

Run 20-01 (DHG test period): the operating conditions used are given in Table 6.3. This first trial started once the C11-PR catalyst had been activated. In Run 20-01 this activation occurred after 265 minutes. The results of the activation treatment have already been discussed in the previous section 6.2.1.

Table 6.3 Run 20-01: Operating conditions during DHG test using naphtha feedstock (Catalyst C11-PR).

Run	20-01 (DHG test)
Reformer tube dimensions	Φ ½ -inch x 30 cm
Catalyst type	C11-PR
Catalyst loading (g)	15.2
Catalyst size (mm)	6 x 6 x 2
Pressure (bar) *	10
Outlet gasifier-reformer temperature (⁰C) *	650
Steam to carbon molar ratio (Naphtha) *	6
Total inlet flow rate ($L.min^{-1}$) *	0.0110
Naphtha inlet flow rate ($L.min^{-1}$) *	0.0020
Water inlet flow rate ($L.min^{-1}$) *	0.0090
(*) Average values	

In Figure 6.5, after 265 minutes the naphtha flow injection was started at 0.0020 $L.min^{-1}$ with S/C= 6. The latter value was selected with reference to the previous tests on methane (see chapter 5, section 5.3.2), but the specific value was calculated assuming that naphtha can be approximated to n-heptane. The densities of the two are very similar as mentioned previously.

Of chief concern was the possibility that the catalyst could be deactivated by carbon fouling/coke deposition. It is apparent from the sudden rise in inlet pressure at 300 minutes that the catalyst bed was in fact totally blocked by carbon fouling. This was totally unexpected, since the operation with methane had been perfectly satisfactory under these conditions using a much lower S/C= 4 and lower inlet flow rates of water (0.0044 $L.min^{-1}$ instead of 0.0090 $L.min^{-1}$ used here in Run 20-01).

On disconnecting the reactor tube, inspection of the top and bottom sections of the gasifier-reformer revealed that the catalyst was not in fact blocked by carbon deposits. However, the coiled tube of the pre-heating unit (Fig. 6.6) was heavily, or totally, blocked by carbon deposits.

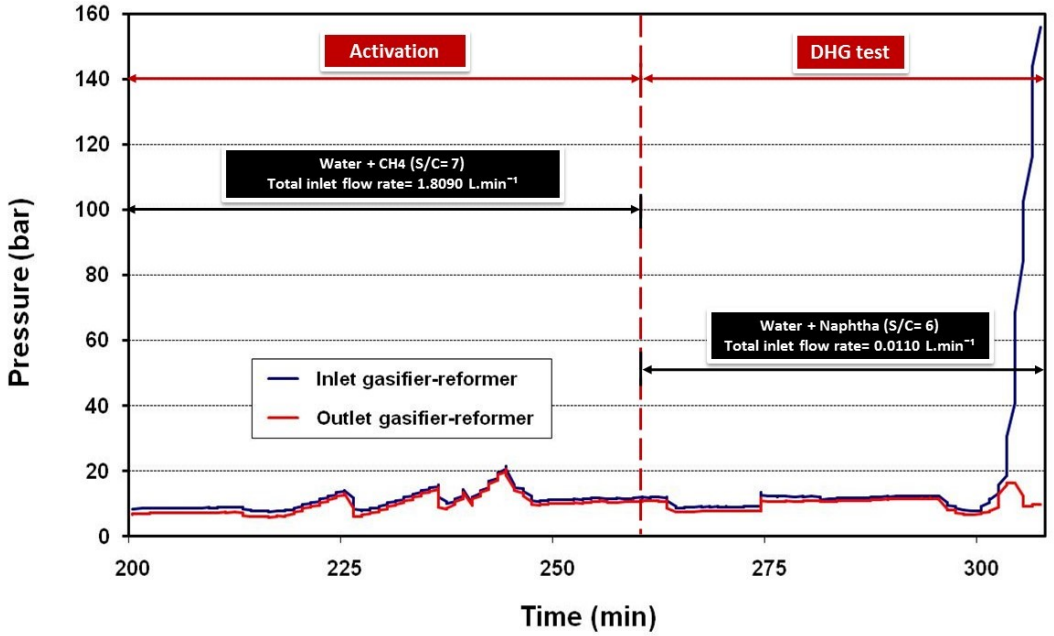

Figure 6.5 Run 20-01: Inlet and outlet pressure of gasifier-reformer during DHG test using naphtha feedstock (Catalyst C11-PR).

Previously in the DHG tests with methane in chapter 5, the gasifier-reformer unit itself included an entry length as the pre-heating unit to heat up the feed prior to the reactor, avoiding temperature shocks and therefore, mechanical failure of the catalyst. The unit consisted in a coiled tube of ⅛-inch diameter and 30 cm of coiled length.

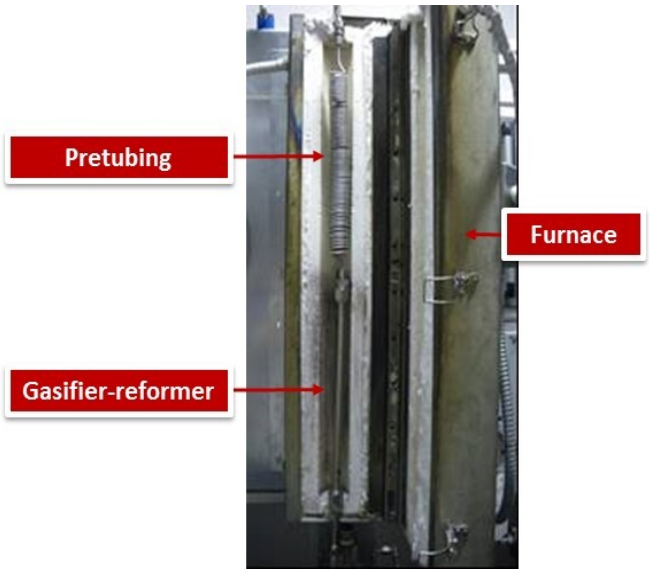

Figure 6.6 Gasification-reforming section used for methane feedstock in chapter 5.

To avoid this blockage, the unit was removed entirely for the final DHG rig assembly using naphtha feedstock (see final design, chapter 3, section 3.3.5) after this first trial, Figure 6.7.

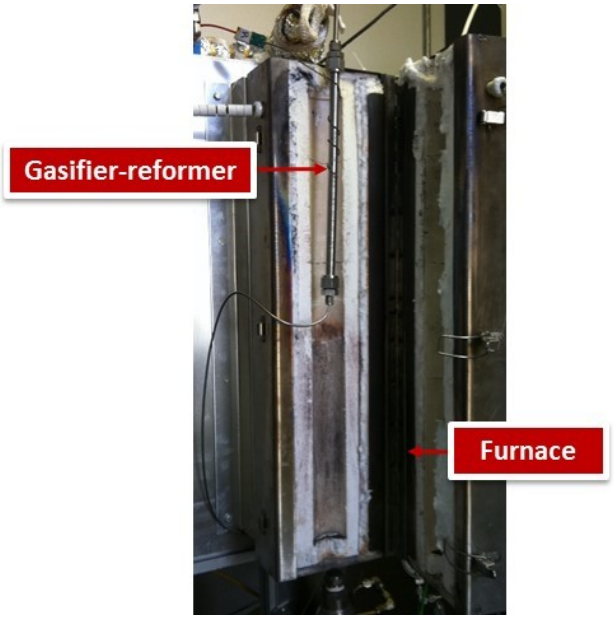

Figure 6.7 Revamped gasification-reforming section.

It is stated (Bartholomew, 1982, Bartholomew, 2001, Chen et al., 2004, Xu et al., 2008, Takenaka et al., 2008, Sperle et al., 2005) that coke in the pre-heating is formed by thermal pyrolysis (cracking) of the hydrocarbons contained in the naphtha according to:

$$C_n H_m \Rightarrow Polymers \Rightarrow nC(coke) + \frac{m}{2} H_2 \qquad (6.1)$$

For hydrocarbons higher than methane as in this case, the reaction is irreversible. Naphtha might have formed carbon in detriment of the reaction with steam due to the fact that its thermodynamic stability favours the accumulation of carbon. Therefore, the presence of catalysts is necessary to slow down the coking process rate or to increase selectivity for steam reforming reactions.

According to Rostrup-Nielsen (1984), this is the major difference between steam reforming of higher hydrocarbons like naphtha and steam reforming of methane.

Twigg (1989) comments on the complexity of coking from naphtha, showing a figure where multiple ways of forming coke are possible. One of them is certainly thermal cracking with steam, which is favoured enormously by the absence of a catalyst as was the case with the pre-heating unit. The chemical reactions involved are the disproportionation (6.2) and reduction of carbon monoxide (6.3), according to Twigg (1989) and Christensen (2005):

$$2\mathrm{CO} \Leftrightarrow C + CO_2 \quad \Delta H^{o}_{298} = -171.66\ kJ.mol^{-1} \qquad (6.2)$$

$$CO + H_2 \Leftrightarrow C + H_2O \quad \Delta H^{o}_{298} = -131\ kJ.mol^{-1} \tag{6.3}$$

Figure 6.8 shows the outlet temperature of the vaporiser, inlet gasifier-reformer and the outlet gasifier-reformer (unfortunately the thermocouple located on the inlet gasifier-reformer was broken as has been mentioned). Stable temperature curves were observed during the DHG test with no major inconveniences.

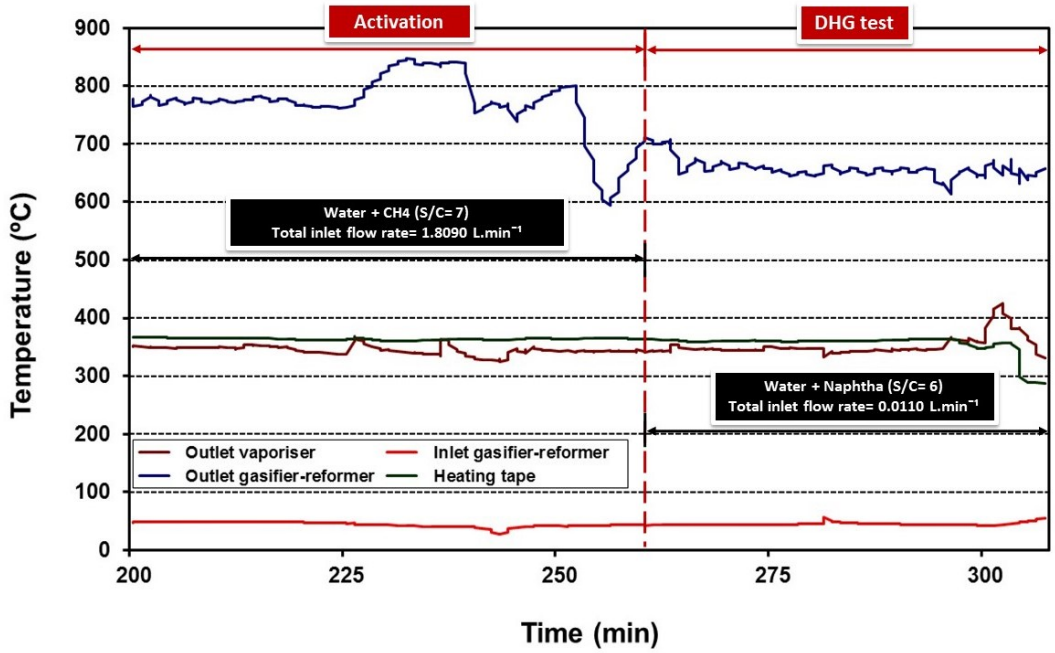

Figure 6.8 Run 20-01: Temperature profiles during DHG test using naphtha feedstock (Catalyst C11-PR).

In relation to the produced dry gas composition (vol. in %) from the gasifier-reformer, Figure 6.9 indicates that the levels of H_2, CO_2, CO and CH_4 remained almost identical to those obtained from the catalyst activation treatment: H_2 (76 %), CO_2 (14 %), CO (3 %) and CH_4 (8 %). Certainly those values might not have been the product just of the naphtha conversion but also of the methane conversion during the catalyst treatment since the blockage by coke and the concomitant drastic pressure drop occurred just 20 minutes after having injected the naphtha. This time is not enough to obtain values of dry gas composition (vol. %) stabilised and attributable completely to the new feedstock (naphtha) conversion. Hence, no produced dry gas composition by naphtha conversion is reported.

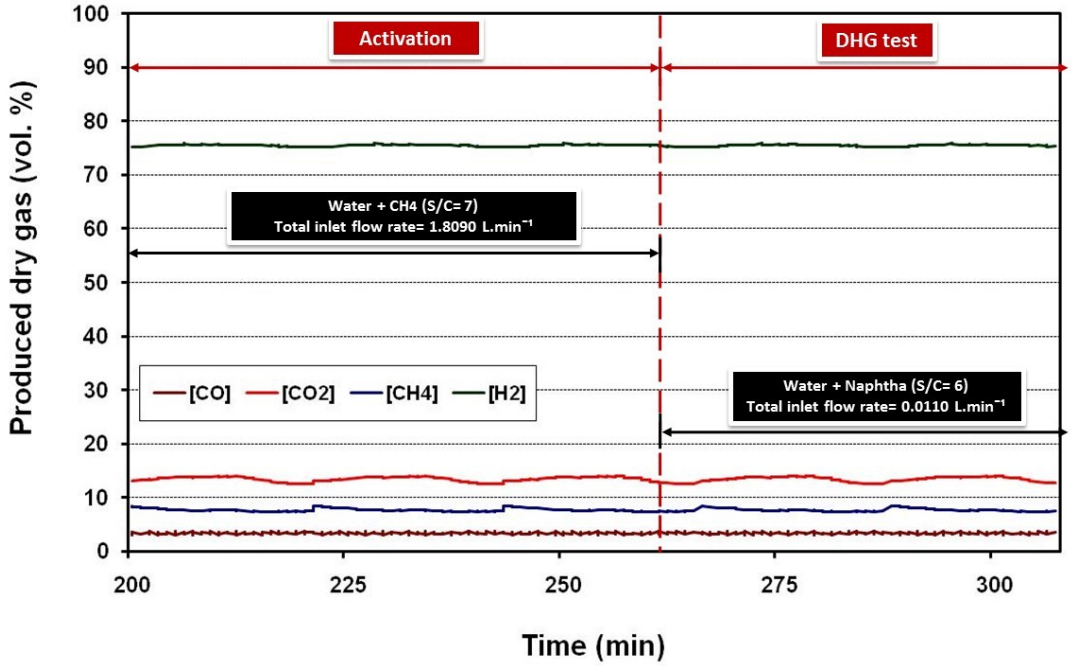

Figure 6.9 Run 20-01: Produced dry gas composition (vol. %) during DHG test using naphtha feedstock (Catalyst: C11-PR).

Figure 6.10 shows a graph of the dry gas outlet flow rate versus time in Run 20-01 during the DHG test. Signal stability is below 3.0 % which is acceptable. The average value was 5.06 $L.min^{-1,}$ which is very high in relation to the total inlet flow rate, 0.0110 $L.min^{-1,}$ and slightly higher than that obtained in the activation treatment using methane.

This is attributed to the high volume of gases generated by the naphtha conversion added to some gases still present which were generated by methane conversion from the previous test period during the catalyst activation treatment.

Stoichiometrically, higher volume of gas products from naphtha conversion is logical and can be explained through the chemical reactions involved in the DHG process (steam reforming), more specifically in the gasifier-reformer reactor (n- heptane as model surrogate of naphtha):

$$C_nH_m + nH_2O \Rightarrow nCO + (n + \frac{m}{2})H_2 \quad \Delta H^o_{298} > 0\text{, where n > 1} \qquad (6.4)$$

$$CO + 3H_2 \Leftrightarrow CH_4 + H_2O \quad \Delta H^o_{298} = 206\ kJ.mol^{-1} \qquad (6.5)$$

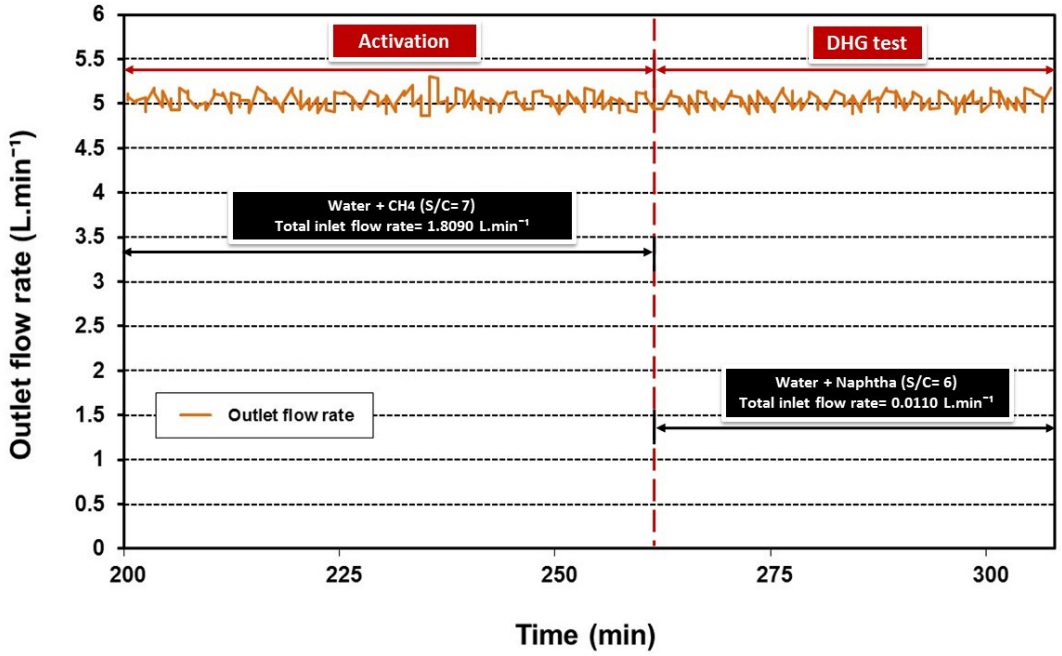

Figure 6.10 Run 20-01: Outlet flow rate, produced dry gas during DHG test using naphtha feedstock (Catalyst C11-PR).

$$CO + H_2O \Leftrightarrow CO_2 + H_2 \quad \Delta H^o_{298} = -41\ kJ.mol^{-1} \tag{6.6}$$

$$CH_4 + 2H_2O \Leftrightarrow CO_2 + 4H_2 \quad \Delta H^o_{298} = 165\ kJ.mol^{-1} \tag{6.7}$$

1 mole naphtha can be converted to 7 moles CO and 15 moles H_2 (22 total moles) or 7 moles CO_2 and 22 moles H_2 (29 total moles) depending on how many moles of H_2O are consumed.

This, compared to the 3-5 total moles generated by the methane feedstock, is effectively very high (see chapter 5, Figure 5.5). The relation between naphtha conversion and the produced dry gas in mole volume is shown in Figure 6.11.

Equally, in Figure 6.10 it can be seen that, at low pressure, the back pressure regulator controlling the exit gas from the gasifier-reformer appears to operate very well as do the curves from the produced dry gas compositions (Figure 6.9). All of them are very steady with no major fluctuations. They look very similar to those obtained using methane as feedstock.

Table 6.4 summarizes the experimental conditions and results.

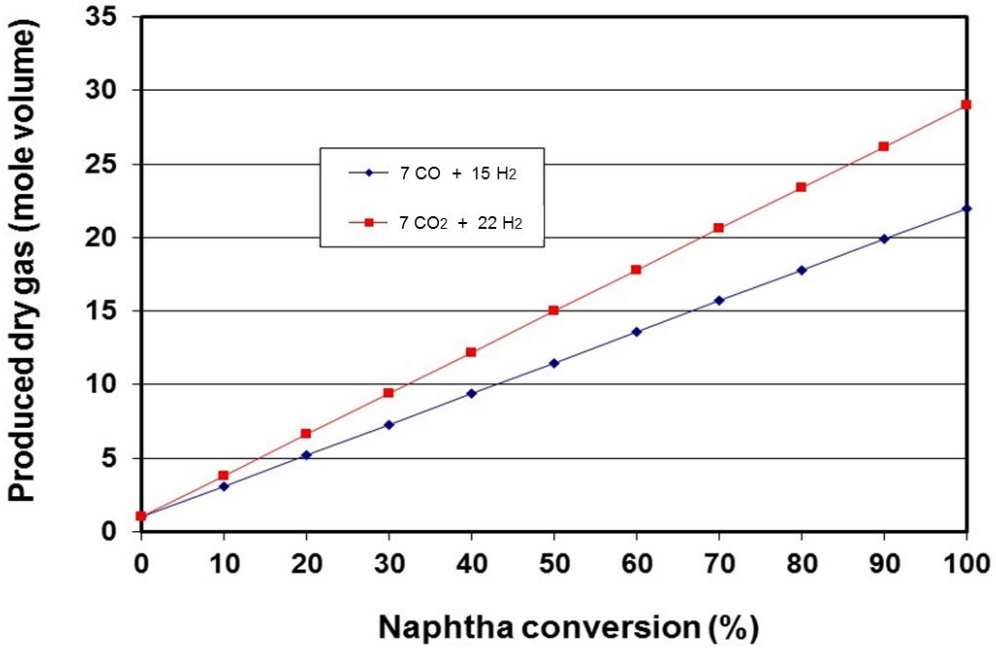

Figure 6.11 Produced dry gas in mole volume versus naphtha conversion.

Table 6.4 Run 20-01: Summary of operating conditions and results obtained during DHG test using naphtha feedstock (Catalyst C11-PR).

Run	20-01 (DHG test)
Reformer tube dimensions	Φ ½ -inch x 30 cm
Catalyst type	C11-PR
Catalyst loading (g)	15.2
Catalyst size (mm)	6 x 6 x 2
Pressure (bar) *	10
Outlet gasifier-reformer temperature (ºC) *	650
Steam to carbon molar ratio (Naphtha) *	6
Total inlet flow rate (L.min⁻¹) *	0.0110
Naphtha inlet flow rate (L.min⁻¹) *	0.0020
Water inlet flow rate (L.min⁻¹) *	0.0090
Dry gas outlet flow rate (L.min⁻¹) *	5.06
Produced dry gas composition (%) **	
H_2	Unavailable by coke formation
CO	
CO_2	
CH_4	
(*) Average values	
(**) Standard deviation of average values is ± 2 %	

Repeatability of Run 20-01: A second repeat of every experiment was always carried out. The second repeat for Run 20-01 shows an almost identical trend in both periods: the activation treatment and the DHG test using naphtha feedstock according to curves of pressure (Figure 6.12),

temperature (Figure 6.13), produced dry gas (Figure 6.14) and outlet flow rates (Figure 6.15). Therefore, this confirms the consistency and reliability of the experimental results.

It is important to mention that a coking process also was observed during the DHG test period. This clearly supported the idea of removing the pre-heating unit from the gasification-reforming section.

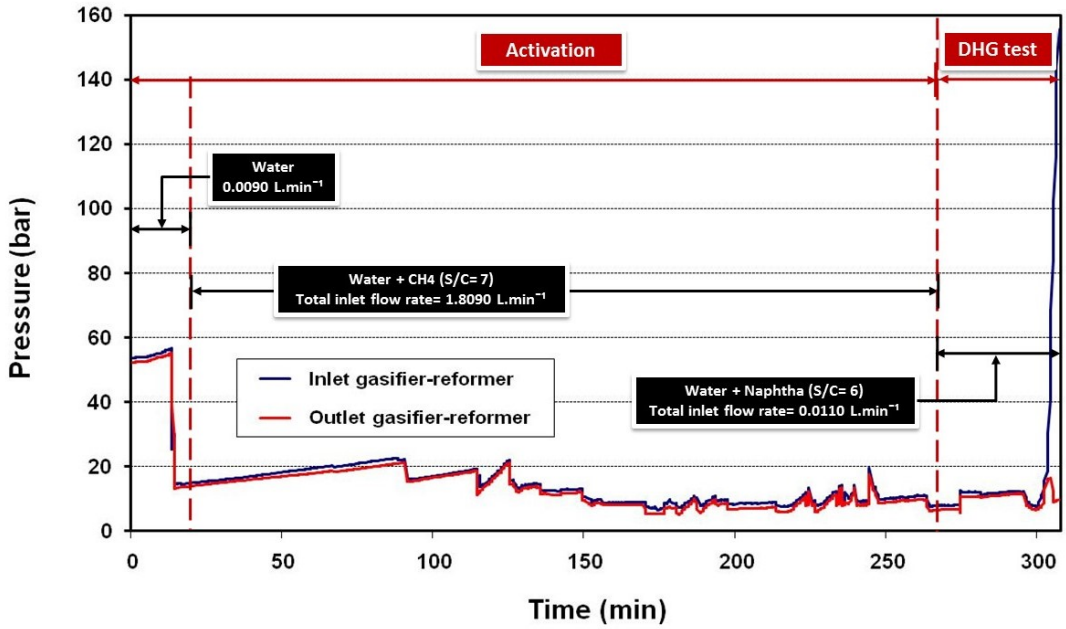

Figure 6.12 Repeat Run 20-01: Inlet and outlet pressure of gasifier-reformer (Catalyst C11-PR).

In the case of the produced dry gas composition (vol. %) from the gasifier-reformer, Figure 6.14, it is also important to mention that the levels of H_2, CO, CO_2 and CH_4 remained steady after the blockage by coke formation, the same phenomena that occurred in the first Run 20-01. Hence, it is effectively uncertain whether the produced dry gas composition was generated by naphtha conversion only: such values appear to have been the left over product of the methane conversion plus the naphtha conversion.

The dry gas outlet flow rate in Figure 6.15 does not present major differences in comparison to that for the first Run 20-01. However, the signal stability here is considerable, even slightly higher. The standard deviation was 2.4 % instead of 3.0 % from the first Run 20-01.

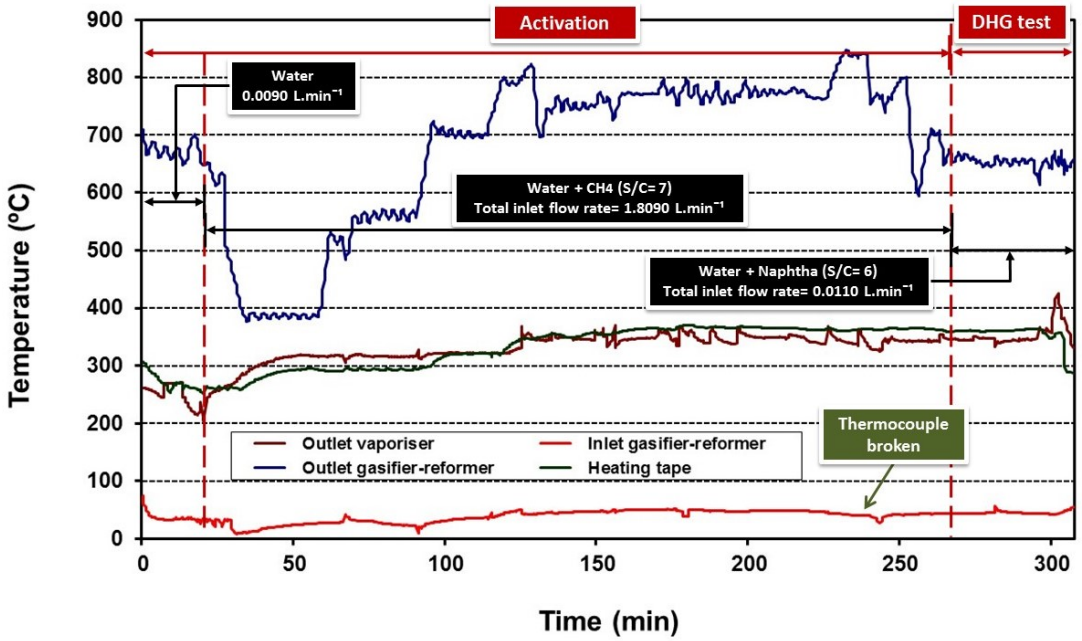

Figure 6.13 Repeat Run 20-01: Temperature profiles (Catalyst C11-PR).

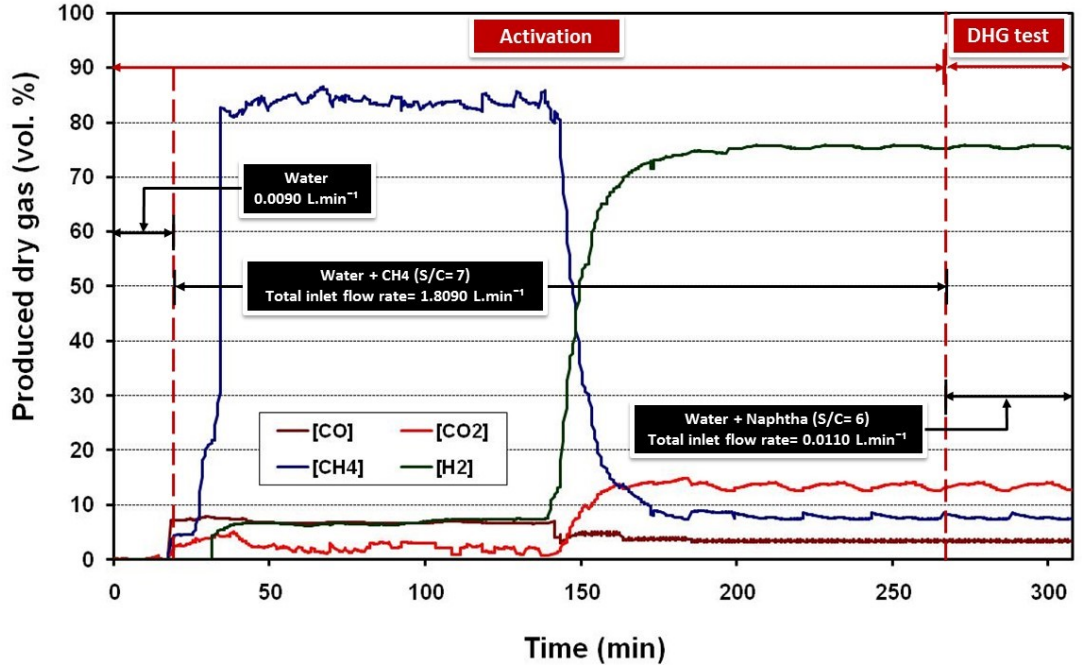

Figure 6.14 Repeat Run 20-01: Produced dry gas composition in vol. % (Catalyst C11-PR).

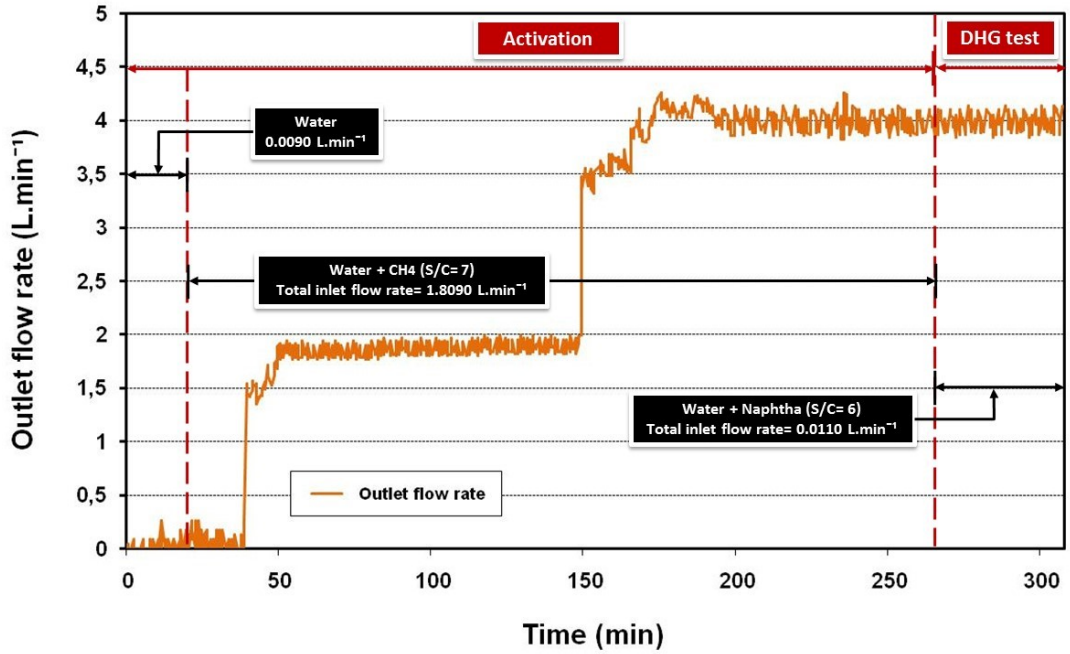

Figure 6.15 Repeat Run 20-01: Outlet flow rate, produced dry gas (Catalyst C11-PR).

6.2.3 Steam to carbon ratio (S/C= 30 to 6)

The effect of varying the steam to carbon (S/C) ratio was investigated in Run 20-02 using S/C = 30, 20, 15, 10 and 6 at 650 ºC and 10 bar as pressure. The water inlet flow rate remained at 0.0090 $L.min^{-1}$, an increase of 100 % in relation to that used in the DHG experiments with methane feedstock in chapter 5 (0.0044 $L.min^{-1}$).

This water inlet flow rate permitted the calculation of the naphtha inlet flow rates required to obtain the steam to carbon (S/C) ratios under study. n-Heptane was considered as the model surrogate for naphtha. It is important to take into account that S/C ratios are referred to carbon mole contained per molecule. For naphtha (n-heptane) in this investigation, 7 carbon moles are considered per molecule.

Beyond this Run 20-02, a new gasification-reforming section was used, namely the final design with no pre-heating unit. This has been shown previously in two points (Figure 3.26 in chapter 3, section 3.3.5 and Figure 6.7 in chapter 6, section 6.2.2).

Once the C11-PR catalyst was activated, the DHG test period started at the highest S/C ratio, to avoid carbon formation on the catalyst. Table 6.5 shows the operating conditions used during the DHG test period in Run 20-02. Some parameters are average values since they were taken over the time period during which they were in operation.

Table 6.5 Run 20-02: Operating conditions during DHG test using naphtha feedstock (Catalyst C11-PR).

Run	20-02 (DHG test)				
Reformer tube dimensions	Φ ½ -inch x 30 cm				
Catalyst type	C11-PR				
Catalyst loading (g)	15.2				
Catalyst size (mm)	6 x 6 x 2				
Pressure (bar) *	10				
Outlet gasifier-reformer temperature (ºC) *	650				
Steam to carbon molar ratio (Naphtha) *	30	20	15	10	6
Total inlet flow rate (L.min^{-1}) *	0.0094	0.0096	0.0098	0.0101	0.0110
Naphtha inlet flow rate (L.min^{-1}) *	0.0004	0.0006	0.0008	0.0011	0.0020
Water inlet flow rate (L.min^{-1}) *	0.0090	0.0090	0.0090	0.0090	0.0090
(*) Average values					

Figure 6.16, 6.17 and 6.18 show pressure, temperature and produced dry gas composition curves obtained during the DHG test.

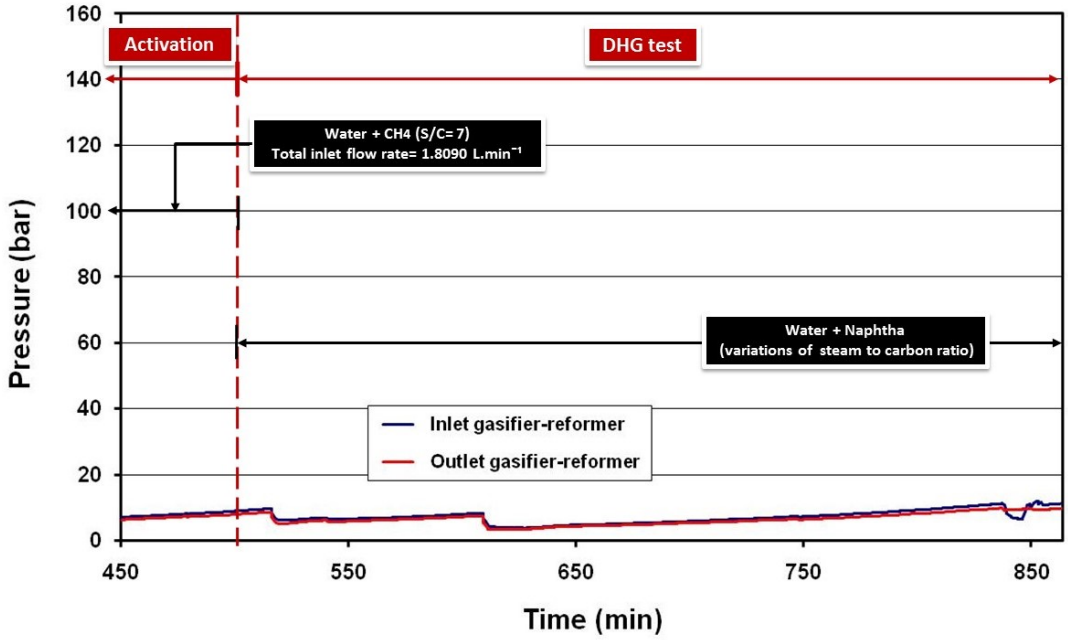

Figure 6.16 Run 20-02: Inlet and outlet pressure of gasifier-reformer during DHG test using naphtha feedstock (Catalyst C11-PR).

Figure 6.16 shows inlet and outlet gasifier-reformer pressure during the DHG test period, just a final stage of the activation treatment period is shown with no major findings. Pressure during the experiment showed certain stability and an average value of 10 bar. The DHG test started at 500 minutes with the injection of naphtha at 0.0004 L.min^{-1} creating a total inlet flow rate (water + naphtha) of 0.0094 L.min^{-1} (S/C= 30). No major inconveniences, no coke formation or pressure drop. This verifies that the performance of the new gasifier-reformer section was satisfactory.

In Figure 6.17, the outlet gasifier-reformer temperature was reduced from the 750 ºC used for catalyst activation to 650 ºC approximately for the DHG test period. It remained steady during the period (from 500 to 865 minutes). During the experiment, some inconveniences with the isolation system were present, and for that reason, there was important heat loss between the outlet vaporiser and the inlet gasifier-reformer. However, the value of temperature at the inlet gasifier-reformer (230 ºC) was over saturated steam temperature by 50-60 ºC. The saturated steam temperature is 184 ºC at 10 bar pressure.

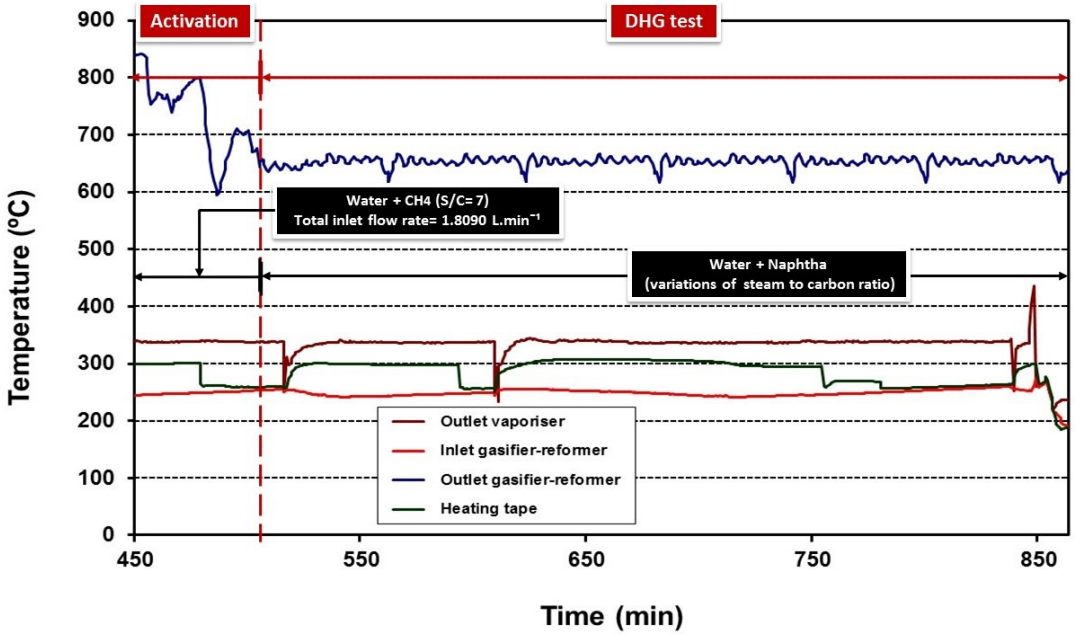

Figure 6.17 Run 20-02: Temperature profiles during DHG test using naphtha feedstock (Catalyst C11-PR).

The variation of produced dry gas composition (vol. %), as the S/C ratio was increased is shown in Figure 6.18. The highest hydrogen concentration (75 %) was achieved for S/C= 30 and 20. At lower S/C ratios, there is a falling trend of the hydrogen concentration, down to 70 %, 67 % and 65 %, for S/C = 15, 10, 6, respectively.

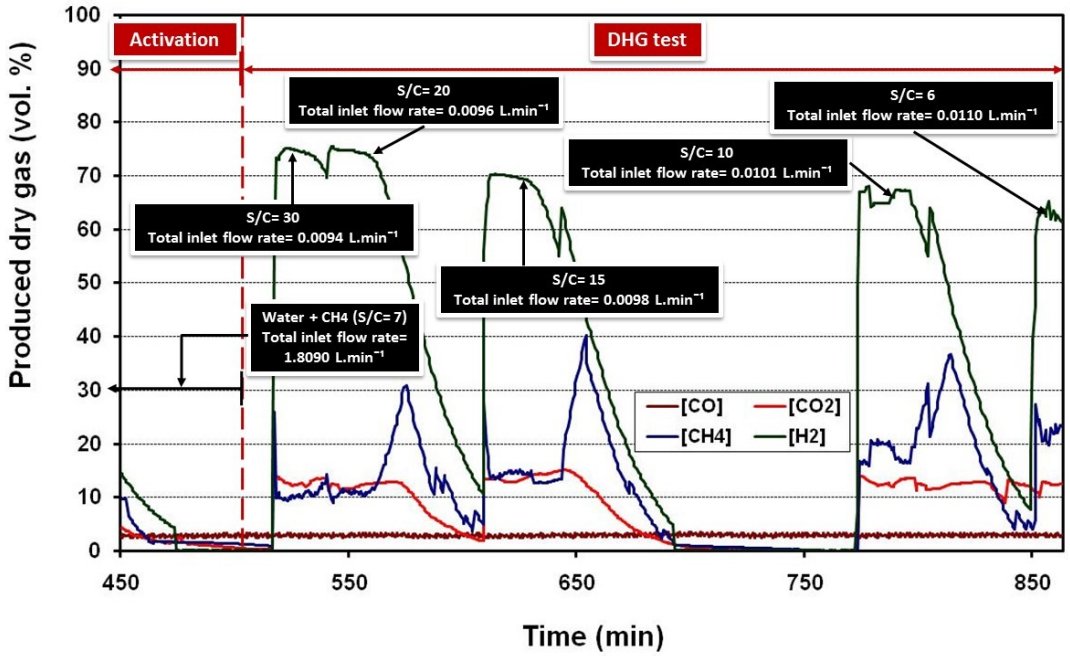

Figure 6.18 Run 20-02: Produced dry gas composition (vol. %) during DHG test using naphtha feedstock (Catalyst C11-PR).

In Figure 6.18, the fluctuations occurring during the DHG test period when the naphtha injection started, are attributable, part, to the necessity to shut in the rig to keep pressure values steady every time gas samples were taken. The relatively low flow rates through the system also mean that any loss of volume in the system, due to the taking of gas samples, would lead to a reduction in pressure, which did not instantly recover.

As has been mentioned, no blockage of the catalyst bed or pressure drop was observed despite the fact that the experiment was carried out for a total of nearly 900 minutes (400 minutes of DHG test approximately). Also, the clean physical appearance of the catalyst indicates that the catalyst activity could possibly be maintained for significantly longer periods, which is very positive. Equally, no liquid residue from the naphtha in the accumulator was detected after the test, meaning a complete naphtha conversion to ´inert´ gases occurred. This is certainly possible: it is indicated by the irreversibility of the first reaction associated with higher hydrocarbon steam reforming (see Chapter 2, section 2.4.1).

In relation to the outlet flow rates, average values in Run 20-02 indicated the same tendency observed in the DHG tests on methane (Chapter 5). As higher S/C ratios are used, lower dry gas outlet flow rates (less moles of products in total) are obtained, meaning less hydrocarbon feedstock reacting per time unit. Table 6.6 shows the tendency.

Table 6.6 Run 20-02: Effect of S/C ratio on dry gas outlet flow rate and hydrogen in produced dry gas (vol. %) during DHG test using naphtha feedstock (Catalyst C11-PR).

Steam to carbon (S/C) ratio	Inlet naphtha flow rate ($L.min^{-1}$)	Inlet water flow rate ($L.min^{-1}$)	Total inlet flow rate ($L.min^{-1}$)	Dry gas outlet flow rate ($L.min^{-1}$)	Hydrogen in produced dry gas (vol. %)
6	0.0020	0.0090	0.0110	5.09	65.10
10	0.0011	0.0090	0.0101	2.45	67.28
15	0.0008	0.0090	0.0098	1.80	70.18
20	0.0006	0.0090	0.0096	1.36	74.63
30	0.0004	0.0090	0.0094	0.86	75.00

Increasing the S/C ratio certainly improves the H_2 concentration in produced dry gas composition, but the improvement in yield is relatively small compared to the loss in process efficiency to form a gas cap enabled to displace oil into reservoirs, since less volume per time unit of dry gas is generated.

An intermediate value that allows high H_2 concentration in produced dry gas, a high dry gas outlet flow rate (high volume per time unit) and no coke formation is the desired outcome. For this reason, beyond this run, the DHG tests would be carried out using S/C= 6 as an intermediate value.

S/C= 6 is also a representative value of current industrial practice and this makes it convenient to compare its results with the results obtained previously with methane in chapter 5. Moreover, an S/C range of 6 to 8 is recommended by Sud-Chemie, C11-PR catalyst supplier, when naphtha is used as feedstock (see Appendices, section A.4).

In practice, the selection of the S/C ratio will tend to be the lowest possible, commensurate with its technical efficiency and economic performance. Suppression of coke formation rates on the catalyst surface due to an excess of steam is a very important fact to consider in this respect (Xu et al., 2008, Sperler et al., 2005, Li et al., 2010). Thus, both variables must be considered.

For safety reasons, the reactivation treatment was not carried out after the 900 minutes of operation. Based on the good performance and appearance of the catalyst after the experiment, it was presumed that the reactivation might not be a problem. In practice, certainly this step is one to consider and an operational requirement, which can be conducted in an 'off-line' manner.

In future development trials, i.e. full-scale pilot DHG tests, it would be necessary to establish that the catalyst could survive much longer periods, ca. 2 years or more, taking into account other factors that affect survivability of the catalyst. An example of these would be any dynamic operational adjustment, especially during shutdown/start up cycles of the DHG unit, due to loss of power by electrical failures or unexpected

disruptions. The above tests provide some indication that this may not be a problem either. In fact, experimental studies were carried out in relation to power disruptions and are discussed in more detail later (see Section 6.4.3).

Following table (6.7) summarizes the experimental conditions and results of Run 20-02, DHG test period.

Table 6.7 Run 20-02: Summary of operating conditions and results obtained during DHG test using naphtha feedstock (Catalyst C11-PR).

Run	20-02 (DHG test)				
Reformer tube dimensions	Φ ½ -inch x 30 cm				
Catalyst type	C11-PR				
Catalyst loading (g)	15.2				
Catalyst size (mm)	6 x 6 x 2				
Pressure (bar) *	10				
Outlet gasifier-reformer temperature (ºC) *	650				
Steam to carbon molar ratio (Naphtha) *	30	20	15	10	6
Total inlet flow rate ($L.min^{-1}$) *	0.0094	0.0096	0.0098	0.0101	0.0110
Naphtha inlet flow rate ($L.min^{-1}$) *	0.0004	0.0006	0.0008	0.0011	0.0020
Water inlet flow rate ($L.min^{-1}$) *	0.0090	0.0090	0.0090	0.0090	0.0090
Dry gas outlet flow rate ($L.min^{-1}$) *	0.86	1.36	1.80	2.45	5.09
Conversion (%) *	100	100	100	100	100
Produced dry gas composition (%) **					
H_2	75	75	70	67	65
CO	3	3	3	3	3
CO_2	13	12	13	13	13
CH_4	9	11	13	16	20
(*) Average values					
(**) Standard deviation of average values is ± 2 %					

6.2.4 Pressure (82 to 110 bar)

One of the **main objectives of the research** was to investigate if the DHG process based on steam reforming reactions of naphtha in the gasifier-reformer could be successful at significantly higher pressures than is normally selected for conventional steam reforming processes using naphtha feedstock. This is mainly because the application of DHG in watered–out, light oil reservoirs will necessarily have to operate in the range 50–200 bar whereas much of the data relevant to surface processes is generally limited to the range 10-30 bar or is referred to pressures higher than 221 bar as biomass gasification where steam reforming reactions occur with supercritical water (>221 bar, 374 ºC), whose properties are unique and very different from steam (Osada et al., 2007).

Importantly, therefore, the question to be answered is - can a DHG unit be operated at high pressure reservoir conditions, and still produce sufficient 'inert gases' (H_2, CO, CO_2) to achieve significant incremental oil recovery using an immiscible process like GSGI (Gravity stabilised gas injection) or WAG (Water alternating gas)? This investigation tried to answer this

question positively through a number of DHG experiments using naphtha feedstock.

Run 20-03: The C11-PR catalyst was activated prior to the DHG test. Operating conditions of S/C= 6 and 650 ºC approximately were used. Pressure was increased from 10 bar (activation treatment) to 82 bar initially and subsequently to 110 bar. Table 6.8 summarizes those operating conditions. Figure 6.19, 6.20 and 6.21 show pressure, temperature and produced dry gas compositions generated during the test period.

Table 6.8 Run 20-03: Operating conditions during DHG test using naphtha feedstock (Catalyst C11-PR).

Run	20-03 (DHG test)	
Reformer tube dimensions	Φ ½ -inch x 30 cm	
Catalyst type	C11-PR	
Catalyst loading (g)	15.2	
Catalyst size (mm)	6 x 6 x 2	
Outlet gasifier-reformer temperature (ºC) *	650	
Steam to carbon molar ratio (Naphtha) *	6	
Total inlet flow rate ($L.min^{-1}$) *	0.0110	
Naphtha inlet flow rate ($L.min^{-1}$) *	0.0020	
Water inlet flow rate ($L.min^{-1}$) *	0.0090	
Pressure (bar) *	82	110
(*) Average values		

After carrying out the catalyst activation (210–700) minutes, the pressure was increased in two stages: 82 bar for 110 minutes and 110 bar for another 120 minutes, approximately according to Figure 6.19. A slight pressure drop over the catalyst bed of about 2 bar can be observed which seems to be relatively constant over the whole experiment including both test periods: the catalyst activation and the DHG test proper, so that it is considered as a normal pressure drop across the catalyst bed.

The pressurisation was built up with methane and water up to 38 bar and after that, it was increased with naphtha and water. Special care was taken in the process to avoid any unnecessary disturbance from the introduction of naphtha feed that could affect the catalyst activity and hence conversion.

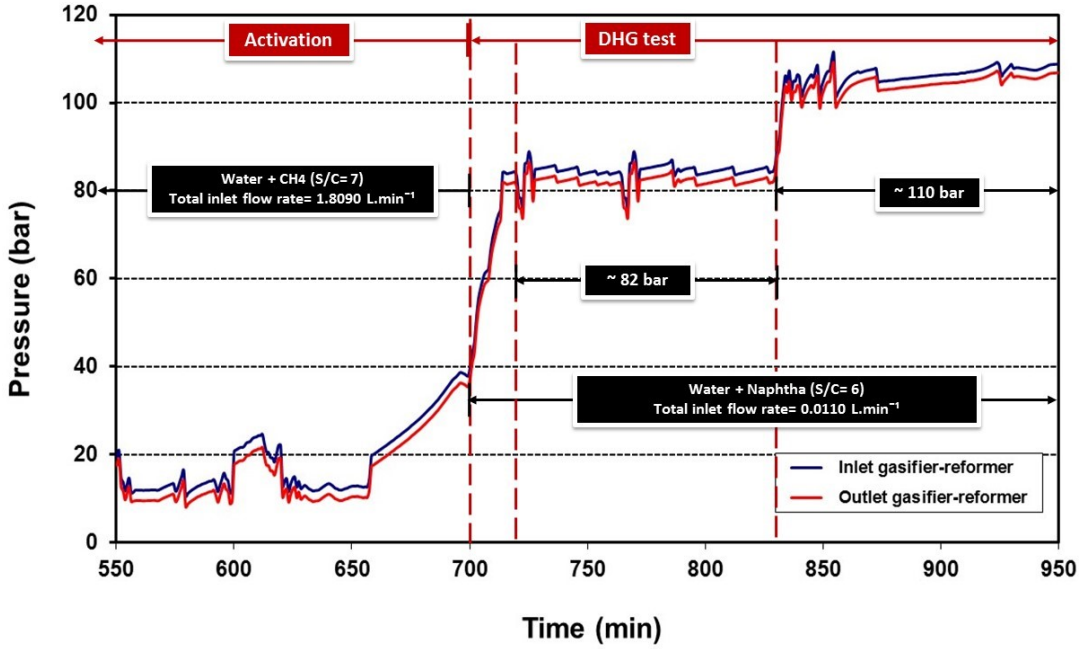

Figure 6.19 Run 20-03: Inlet and outlet pressure of gasifier-reformer during DHG test using naphtha feedstock (Catalyst C11-PR).

The pressure graph also shows some fluctuations attributable to slight variations of pressure suffered in the gas-liquid separation section and gas sampling. In parallel, the large volume of gas generated from the gasifier-reformer, the condensation process of important steam volume and the sampling of gas for analysis, opening and closing the back pressure regulator, irreversibly produce pressure disturbances in the rig as appear in Figure 6.19.

In practice or future field implementations, the water disposal would not be a problem: it might be reused or injected directly into the reservoir to try to replace the pore volume previously occupied by the displaced oil. In this way, DHG process efficiency would increase: displacing oil by gas generated in situ and, at the same time, injecting fresh water from the DHG reactor to replace rapidly the empty pore volume. More details of the technical feasibility of DHG implementation in oil reservoirs will be discussed in section 6.6 in this chapter.

Figure 6.20 shows the temperature profiles in Run 20-03 during the DHG test. The outlet gasifier-reformer temperature is maintained quite steady, at 650 ºC and no important heat loss between outlet vaporiser and inlet gasifier-reformer is observed. Fortunately, the inconveniences in the isolation system were resolved.

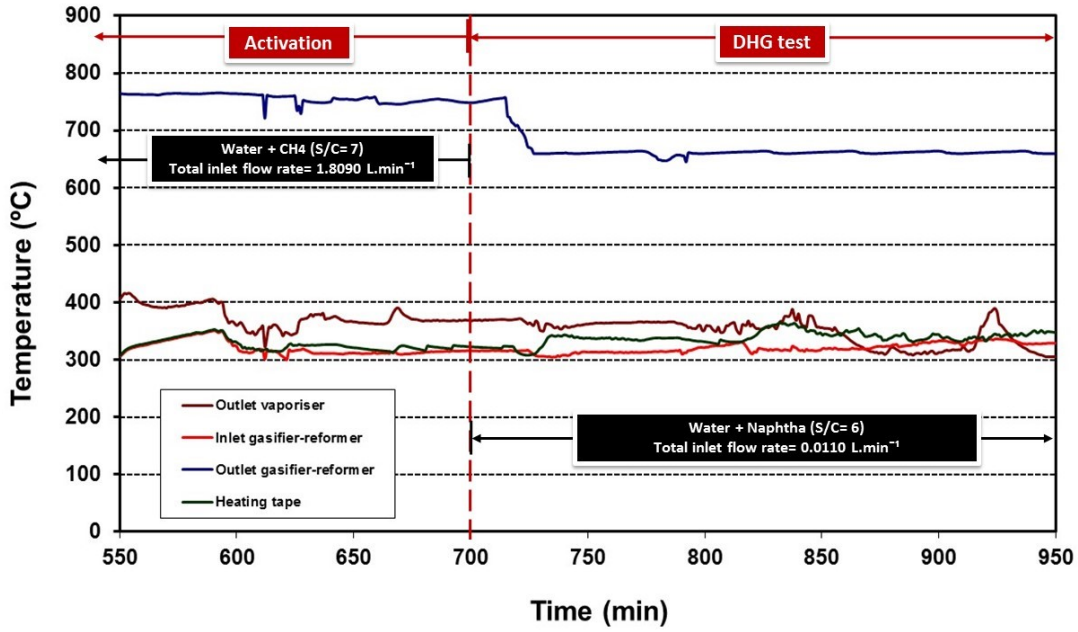

Figure 6.20 Run 20-03: Temperature profiles during DHG test using naphtha feedstock (Catalyst C11-PR).

When a gas sample was taken for analysis, a disturbance in the produced dry gas composition was always created as is shown in Fig. 6.21. This is very evident during the catalyst reduction period here as the hydrogen concentration first falls from around 73 vol. % down to 58 vol. %, but then recovers up to 78 vol. % when the sampling valve is closed again to maintain the desired pressure constant. The same effect is apparent during the 82 bar test period, but the decrease specifically in the hydrogen concentration is much larger. The second repeat of the run confirmed this behaviour.

In previous experiments, the disturbance created by gas sampling was also observed but the degree of variation in the produced dry gas graph was less pronounced. Certainly, these new operating conditions of higher pressure and naphtha as feedstock have had an influence.

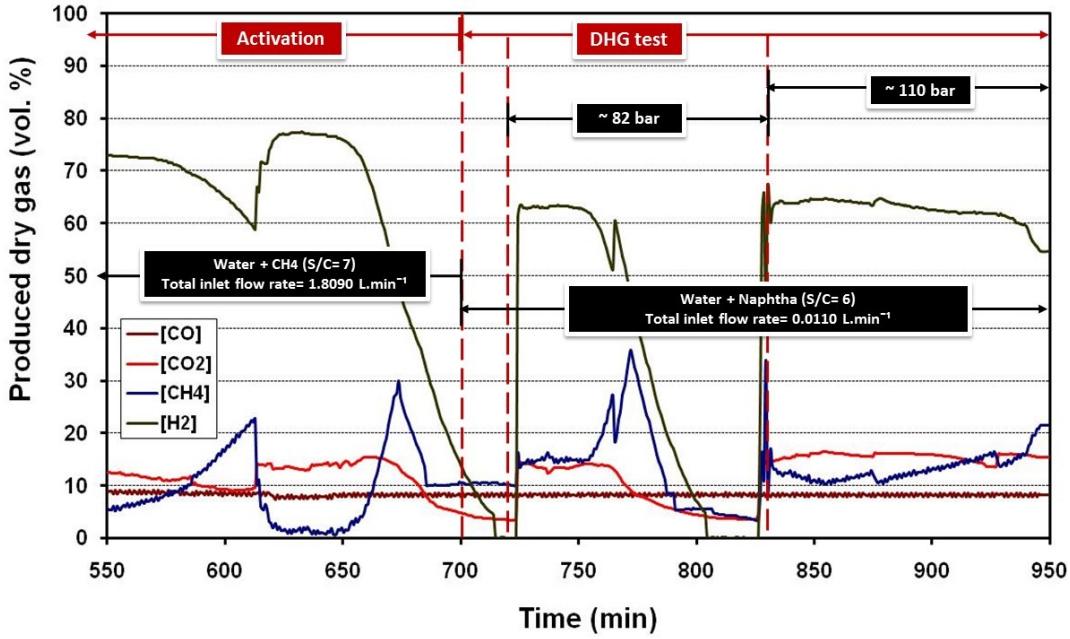

Figure 6.21 Run 20-03: Produced dry gas composition (vol. %) during DHG test using naphtha feedstock (Catalyst C11-PR).

Nevertheless, we can see that there is a good recovery in the concentration levels of the various components, especially for H_2. Thus, H_2 is maintained at a high level, 63-64 %, as the pressure increases up to 110 bar.

From previous work (Greaves et al., 2005) this was unexpected, since their results on methane showed a declining trend as pressure increases. When Greaves et al., (2008) utilised light naphtha plus reservoir gas as feedstock, their results showed H_2 concentration ranging from 35 % to 60 % operated at (710-760) ºC and pressures up to 130 bar. Also, they reported unconverted naphtha residue in the accumulator, not obtaining a 100 % conversion. The SEM images of the catalyst (C11-PR) indicated severe catalyst fouling.

Here in Run 20-03, instead, there was no unconverted naphtha residue and total naphtha conversion was obtained successfully. The main reasons for this are thought to be the series of modifications and optimisations carried out by this investigation on the existing rig.

Equally important is the fact that the recovery in H_2 concentration following a large disturbance is further evidence that the DHG process can recover from a sudden upset, or dynamic change in the reactor. This is a very important feature of the DHG process, if it is to operate continuously over long periods in the field.

In addition, the average dry gas outlet flow rates in the run, 5.07 $L.min^{-1}$ at 82 bar and 5.04 $L.min^{-1}$ at 110 bar (650 ºC, S/C= 6) show themselves to be very similar to those obtained in the previous Run 20-02, 5.09 $L.min^{-1}$ at

10 bar (650 ºC, S/C= 6). This is very positive since it means that the pressure increase does not affect drastically the volume of produced dry gas, especially the H_2 concentration.

In practice, the volume of produced dry gas and H_2 are the main drive factors in displacing oil from a reservoir using DHG by gas displacement in an immiscible process like GSGI (Gas stabilised gas injection) or WAG (water alternating gas). If the volume of the gases, in particular H_2, are only slightly affected by pressure, the DHG process would turn out to be more efficient than expected from previous investigation (Greaves et al., 2004, Greaves et al., 2005, Greaves et al., 2008).

Unfortunately, the flow meter recorder from the wet test meter presented some difficulties in recording online the outlet flow rates from this run so that measurements were taken manually. Details of equipment and the homemade software used as the interface between the instrument and the data acquisition and monitoring section are discussed in chapter 3, section 3.3.4.

The recommissioning of the flow meter recorder and software took a long time and therefore, it was decided to continue the experimental phase and make a special effort to record the outlet flow rates online in the main DHG experiments. Table 6.9 summarizes the operating conditions and results obtained in Run 20-03.

Table 6.9 Run 20-03: Summary of operating conditions and results obtained during DHG test using naphtha feedstock (Catalyst C11-PR).

Run	20-03 (DHG test)	
Reformer tube dimensions	Φ ½ -inch x 30 cm	
Catalyst type	C11-PR	
Catalyst loading (g)	15.2	
Catalyst size (mm)	6 x 6 x 2	
Outlet gasifier-reformer temperature (ºC) *	650	
Steam to carbon molar ratio (Naphtha) *	6	
Total inlet flow rate ($L.min^{-1}$) *	0.0110	
Naphtha inlet flow rate ($L.min^{-1}$) *	0.0020	
Water inlet flow rate ($L.min^{-1}$) *	0.0090	
Pressure (bar) *	82	110
Dry gas outlet flow rate ($L.min^{-1}$) *	5.07	5.04
Conversion (%) *	100	100
Produced dry gas composition (%) **		
H_2	63	64
CO	9	9
CO_2	13	16
CH_4	14	11
(*) Average values		
(**) Standard deviation of average values is ± 2 %		

When the reformer was opened, any conjecture as to whether slight variations in the pressure drop along the gasifier-reformer reactor were due to coke formation or to the disintegration of the catalyst was dismissed since no untoward effects were observed. The C11–PR was unchanged, just a thin brown layer on its surface, as observed in previous DHG experiments using the same catalyst and methane feedstock detailed in chapter 5 .

6.3 Experiments with catalyst C11-PR and gasifier-reformer length 72 cm

The new reactor configuration shown in Figure 6.22, is simply a tube Swagelok Stainless steel (SS) 316L, wall thickness 0.083 inch. The gasifier-reformer diameter stayed the same, ½-inch, but its length was increased to 72 cm, from the previous value, 30 cm. Catalyst loading passed from 15.2 g used previously to 36.1 grams. The water inlet flow rate was the same, 0.0090 $L.min^{-1}$ and naphtha remained as feedstock.

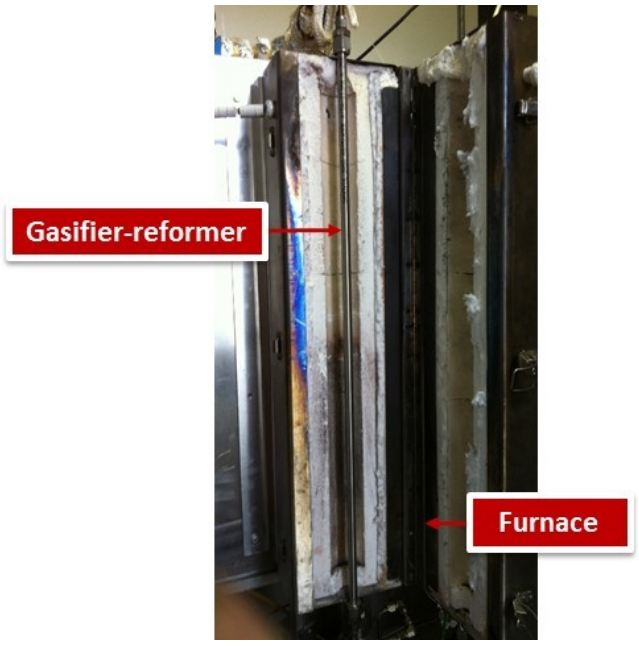

Figure 6.22 New gasifier-reformer reactor length 72 cm.

Increasing reactor length allows a higher catalyst loading and residence time. It is also possible that the length increase of the reactor is beneficial in reducing thermal shock or temperature drop between the temperature of naphtha/steam from the vaporiser and the internal temperature of the reactor/catalyst bed, affecting positively conversions and the mechanical properties of the catalyst (Shayegan et al., 2008, Lee et al., 2008).

The pre-heating section compensated for the temperature gradient when methane was used as feedstock. However, it was removed entirely for the DHG experiments using naphtha. Increasing the length of the reactor might reduce the gradient compensating for the function of the pre-heating

section and controlling the coke formation at the same time.

To extend the pressure range even more, up to (140-160) bar, was undoubtedly the main objective in this section. Additionally, the effect of the new length of the gasifier-reformer reactor was analysed and compared with Run 20-03 at the same operating conditions (650 ºC, S/C= 6 at 82 bar and 110 bar). A second repeat was always carried out to confirm the results.

6.3.1 Catalyst activation treatment prior to DHG tests

Catalyst activation using this new reactor length was realised prior to every DHG test as always. The same operating conditions and methane as feedstock were used. Curves of pressure-temperature-produced dry gas composition in the activation treatment periods corresponding to Run 20-04 and Run 20-05 from this section 6.3 showed clearly identical trends and values to those obtained in the previous section (6.2). This indicates that the new gasifier-reformer length and increased catalyst loading did not affect the catalyst activation period.

Equally, the catalyst activation treatments from both runs did not show any significant differences from each other so we took just one of them to be shown here as example mode. Table 6.10 shows the operating conditions during catalyst activation in Run 20-04 using methane feedstock.

Table 6.10 Run 20-04: Operating conditions during catalyst activation using methane feedstock (Catalyst C11-PR).

Run	20-04 (activation)
Reformer tube dimensions	Φ ½ -inch x 72 cm
Catalyst type	C11-PR
Catalyst loading (g)	36.1
Catalyst size (mm)	6 x 6 x 2
Pressure (bar) *	10
Outlet gasifier-reformer temperature (ºC) *	750
Steam to carbon molar ratio (CH_4) *	7
Total inlet flow rate ($L.min^{-1}$) *	1.8090
CH_4 inlet flow rate ($L.min^{-1}$) *	1.8000
Water inlet flow rate ($L.min^{-1}$) *	0.0090
(*) Average value	

Figure 6.23, 6.24 and 6.25 show the pressure, temperature and produced dry gas composition generated in the run. The average outlet flow rate values were taken manually. Figure 6.23 shows the inlet and outlet pressures. Curves are relatively stable when water and methane were co injected at S/C= 7 and the pressure value was about 10-13 bar. The activation period lasted 200 minutes approximately. No major findings were encountered. Just a slight pressure drop at the beginning, 0-50

minutes while water only was injected. After that, no further pressure drop was observed.

Once catalyst activation was completed, water only was injected into the rig at 0.0050 $L.min^{-1}$ to prepare the system for the next period of the DHG test using naphtha feedstock. This accelerated the purge from the rig, especially from the gasifier-reformer, of the produced dry gases generated during the activation (methane steam reforming) avoiding undesired mixtures of reactants, methane/naphtha or products generated by both gasification-reforming processes. Moreover, the water injection guaranteed the catalyst integrity during the purge, maintaining the activation of the catalyst surface.

For DHG implementation at field scale, this is an aspect to consider since cycles of steam on the catalyst would be beneficial, extending its useful life in the gasifier-reformer in the oil well. As has been mentioned, catalyst use should be extended for 2 or more years.

This investigation has reported on the injection of methane or water only as catalyst treatments prior or post DHG tests, which have been shown to be very useful in increasing and preserving catalyst activity. Previous works (Greaves et al., 2004, Greaves et al., 2005, Greaves et al., 2008) did not report studies on this aspect. However, no doubt they will be considered in case of DHG implementation. Figure 6.24 shows the temperature profiles. No major fluctuations can be seen here or in the produced dry gas composition curves in Figure 6.25.

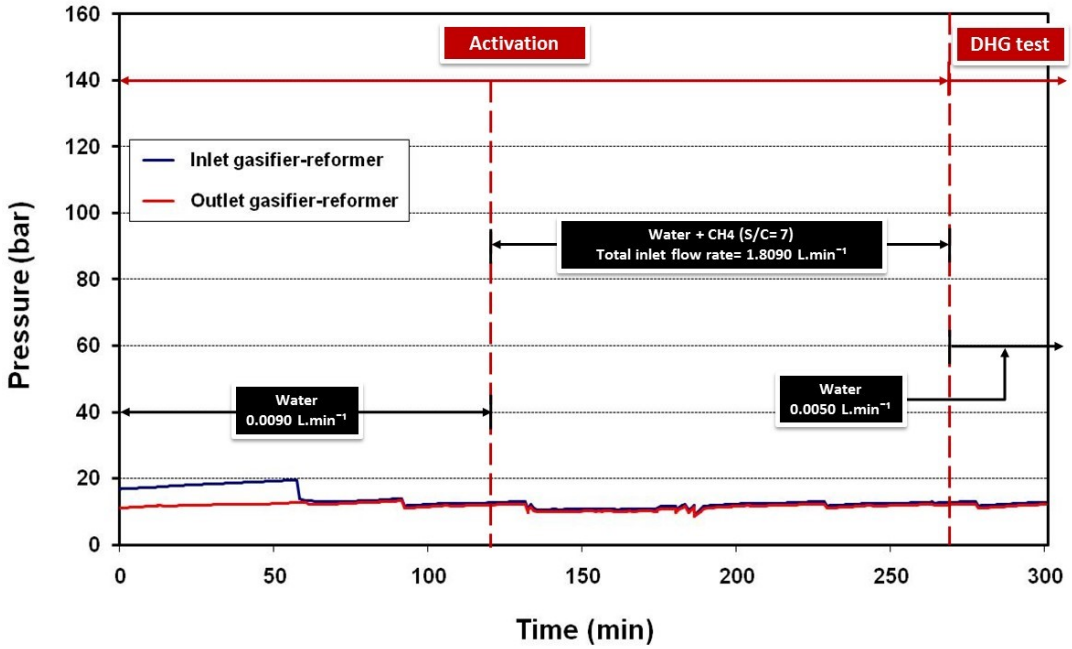

Figure 6.23 Run 20-04: Inlet and outlet pressure of gasifier-reformer during catalyst activation using methane feedstock (Catalyst C11-PR).

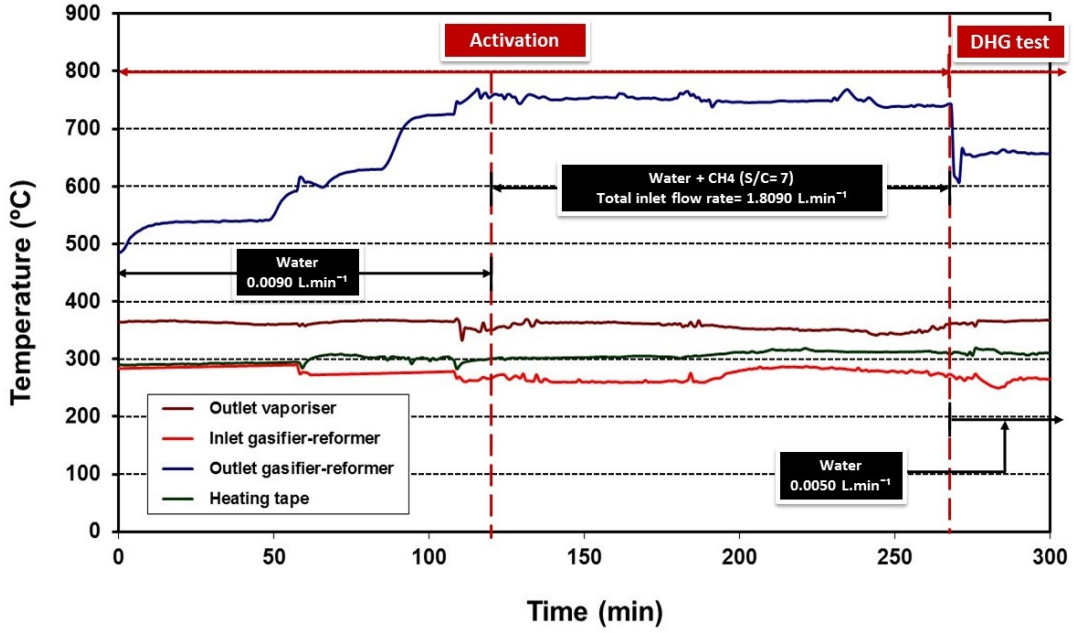

Figure 6.24 Run 20-04: Temperature profiles during catalyst activation using methane feedstock (Catalyst C11-PR).

The maximum conversion period was maintained for 40 minutes approximately to guarantee maximum reduction conditions (highest H_2 concentration) on the catalyst. This condition is vital for catalyst activation. The decrease in the produced dry gas curves occurred when the valve was closed progressively after 225 minutes.

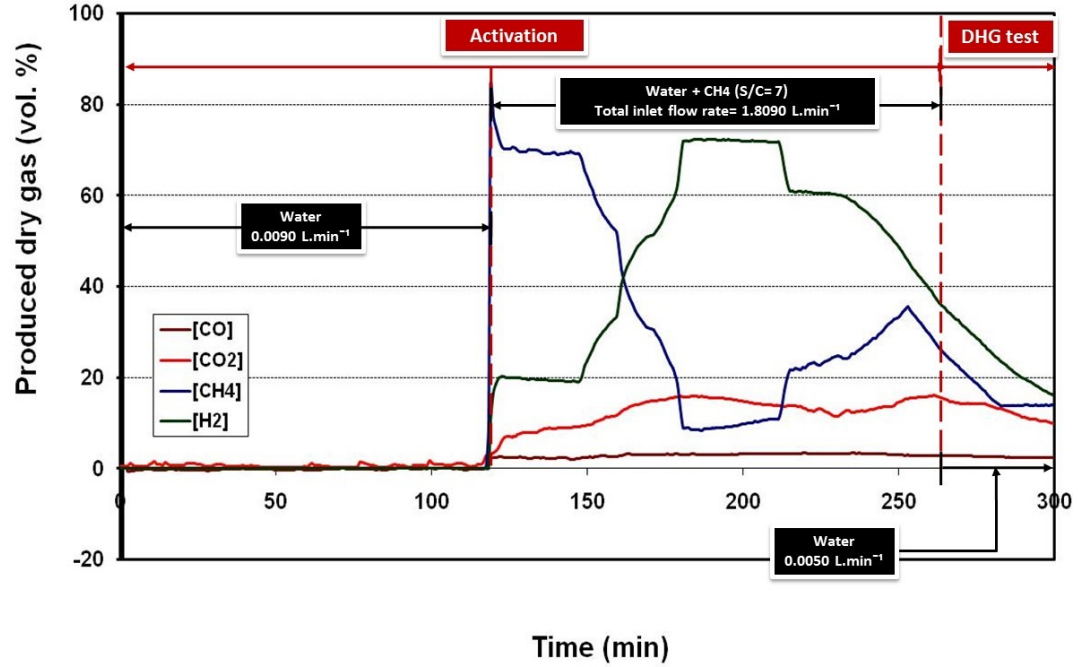

Figure 6.25 Run 20-04: Produced dry gas composition (vol. %) during catalyst activation using methane feedstock (Catalyst C11-PR).

The average values of outlet flow rates during the activation period in Run 20-04 were fairly similar (4.09 $L.min^{-1}$) to those obtained during the activation treatment period in previous runs. For instance, Table 6.2 reports an average of 4.12 $L.min^{-1}$ obtained during the catalyst activation treatment in Run 20-01 (see section 6.2.1). This is technically acceptable in basis of stoichiometry and the conversion demonstrated in chapter 5 which falls into range theoretically calculated.

The increasing of the length of the gasifier-reformer during the catalyst treatment did not affect greatly the conversions or the H_2 concentration. However, the activation process was slightly faster in the longer reactor tube. The CH_4 decrease and rapid H_2 formation in this case, Run 20-04, occurred approximately at 25 minutes, while in Run 20-01 using the 30 cm reactor tube length the activation lasted 50 minutes.

The reaction rate is directly influenced by a longer reactor tube since it allows a more efficient heat transfer process from the gasifier-reformer and provides a higher catalyst bed for the steam/naphtha mixture in order to reach ideal reaction conditions. The results are summarized in Table 6.11.

Table 6.11 Run 20-04: Summary of operating conditions and results obtained during catalyst activation using methane feedstock (Catalyst C11-PR).

Run	20-04 (activation)
Reformer tube dimensions	Φ ½ -inch x 72 cm
Catalyst type	C11-PR
Catalyst loading (g)	36.1
Catalyst size (mm)	6 x 6 x 2
Pressure (bar) *	10
Outlet gasifier-reformer temperature (ºC) *	750
Steam to carbon molar ratio (CH_4) *	7
Total inlet flow rate ($L.min^{-1}$) *	1.8090
CH_4 inlet flow rate ($L.min^{-1}$) *	1.8000
Water inlet flow rate ($L.min^{-1}$) *	0.0090
Dry gas outlet flow rate ($L.min^{-1}$) *	4.09
Conversion (%) *	90
Produced dry gas composition (%) **	
H_2	72
CO	3
CO_2	15
CH_4	10
(*) Average values	
(**) Standard deviation of average values is ± 2 %	

6.3.2 Pressure (82 to 130 bar)

Run 20-04: Table 6.12 summarizes the operating conditions used for this DHG test using naphtha feedstock, catalyst C11-PR and the longer gasifer-reformer reactor tube, 72 cm in length. The variable under study was pressure at three different values: 82, 110 and 130 bar.

The DHG test period started once the catalyst activation treatment was completed. Figure 6.26, 6.27 and 6.28 show the pressure, temperature and produced dry gas composition curves obtained during the run. Unfortunately, the dry gas outlet flow rate was taken manually. A second repeat was carried out confirming the result.

Table 6.12 Run 20-04: Operating conditions during DHG test using naphtha feedstock (Catalyst C11-PR).

Run	20-04 (DHG test)		
Reformer tube dimensions	Φ ½ -inch x 72 cm		
Catalyst type	C11-PR		
Catalyst loading (g)	36.1		
Catalyst size (mm)	6 x 6 x 2		
Outlet gasifier-reformer temperature (^{0}C) *	650		
Steam to carbon molar ratio (Naphtha) *	6		
Total inlet flow rate (L.min^{-1}) *	0.0110		
Naphtha inlet flow rate (L.min^{-1}) *	0.0020		
Water inlet flow rate (L.min^{-1}) *	0.0090		
Pressure (bar) *	82	110	130
(*) Average values			

Looking at the pressure curves of Figure 6.26, a fairly rapid increase in pressure can be observed up to 82 bar approximately from 500 minutes to 600 minutes. On achieving this pressure level, it is apparent that, as well as a continuing slight rising trend in the inlet and outlet pressures, there is a sustained pressure drop of about 11 bar across the gasifier-reformer.

The same effect can be observed at the two higher pressures, 110 bar and 130 bar. The condition of the catalyst was investigated following the test. It revealed that the catalyst suffered some slight mechanical failure in the inlet section of the reactor tube. A short section of the catalyst at the top of the reactor tube contained small, broken pieces of the catalyst extrudate. The rest of the catalyst remained unchanged, except for a light brown discolouring. There was no evidence of coke deposits.

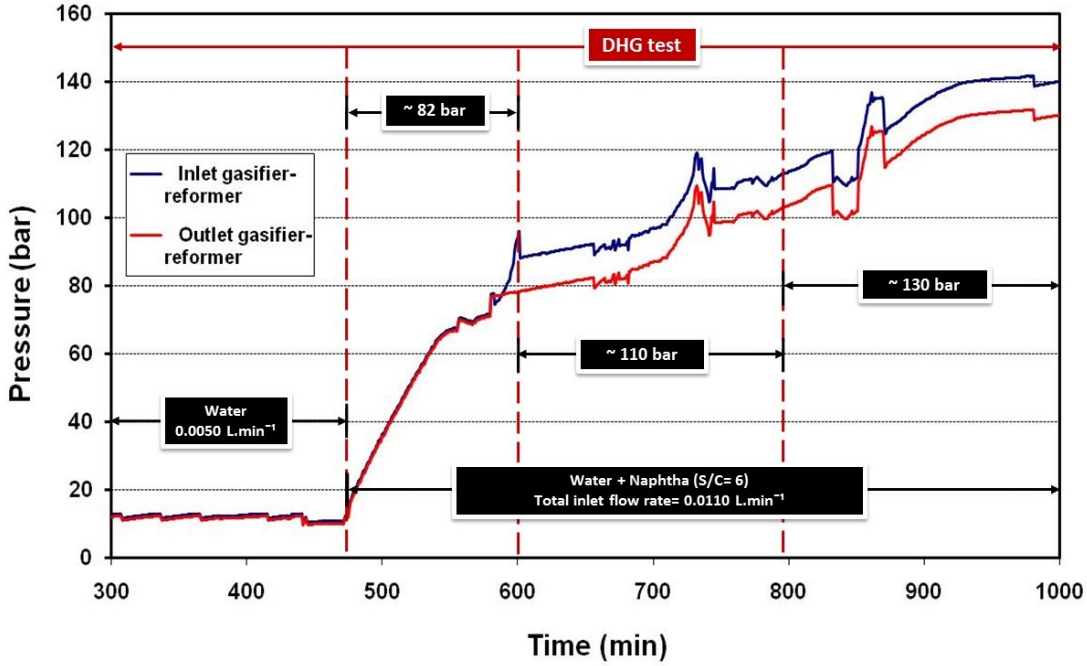

Figure 6.26 Run 20-04: Inlet and outlet pressure of gasifier-reformer during DHG test using naphtha feedstock (Catalyst C11-PR).

The broken catalyst had compacted, causing the 10 bar increase in pressure drop. The partial disintegration of the C11-PR catalyst was due to thermal shock at the entrance of the gasifier-reformer tubing.

In practice, therefore, it is recommended that the temperature gradient between the inlet flow from the vaporiser and the inlet to the gasifier-reformer needs to be more gradual – to preserve the catalyst from thermal shock. Alternatively, it may be possible to use different catalyst with better mechanical properties enabling it to tolerate higher pressure (50-200) bar and higher temperature (600-800) ºC.

The temperatures attained during the steaming (water injection only to the rig) and the test operation period is shown in Fig. 6.27.

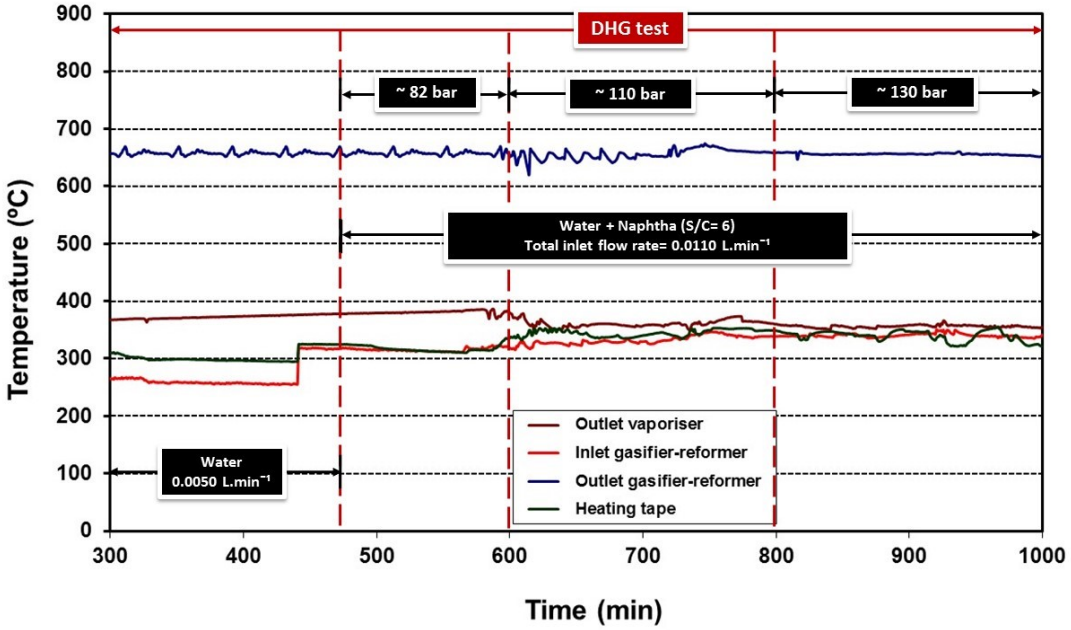

Figure 6.27 Run 20-04: Temperature profiles during DHG test using naphtha feedstock (Catalyst C11-PR).

The temperature at the inlet gasifier-reformer increases slightly during steaming and the 82 bar test: it reaches 310 ºC approximately. Later on, it increases slowly to 350 ºC to maintain an outlet gasifier-reformer temperature of 650 ºC during the DHG test, for the 82, 110 and 130 bar values.

The produced dry gas composition is shown in Figure 6.28. There is only a slight reduction, less than 5 %, in the H_2 concentration as the pressure increases by 48 bar. Likewise, CH_4 and CO_2 suffered a slight decrease, as pressure increased, of less than 8 % overall. However, there was a steady behaviour in the CO concentration during the DHG test in the three pressure values. These all represent no major variations in composition for the various components. H_2 is less affected and it did not reduce very greatly when the pressure was increased by nearly 60 %.

Hence, increased catalyst loading (more than double than that in Runs from section 6.2) appears to have contributed to maintaining the H_2 conversion. The higher catalyst loading may compensate for any reduction in the amount of H_2 concentration as a consequence of pressure increase. Higher catalyst loading provides more residence time and therefore longer contact of the reactants on the catalyst surface. Equally, a longer tube as reactor allows a more efficient heat transfer process from the gasifier-reformer to the feedstock needed to reach ideal reaction conditions.

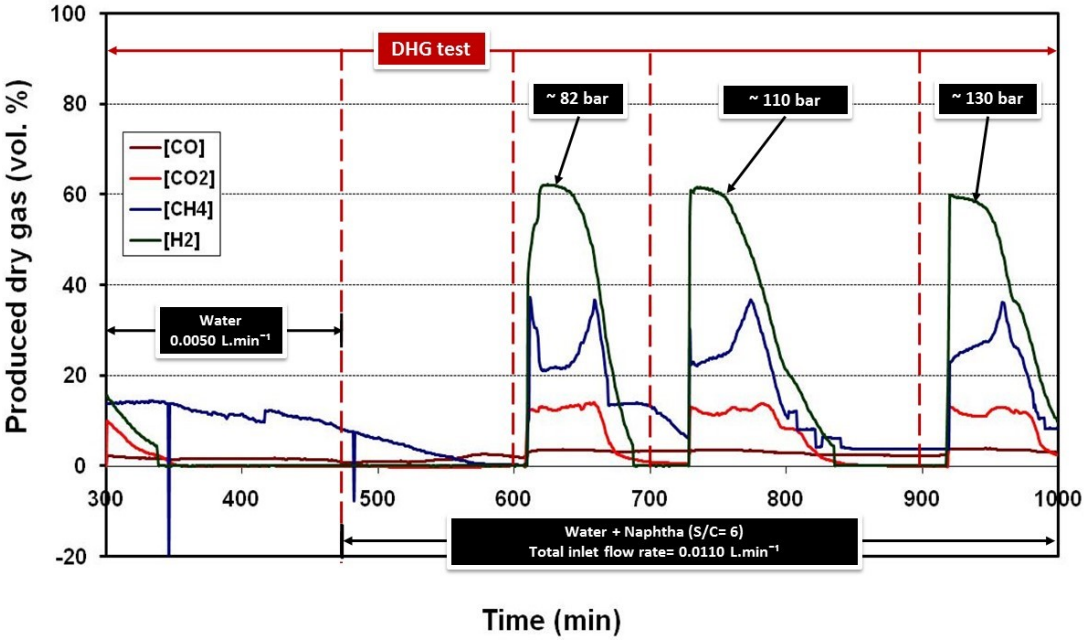

Figure 6.28 Run 20-04: Produced dry gas composition (vol. %) during DHG test using naphtha feedstock (Catalyst C11-PR).

This is commensurate with the maintenance of the dry gas outlet flow rate from the gasifier-reformer in accordance with the measured average values. At higher pressure, thermodynamics principles dictate that there should be less gas produced. This is indeed the case as is shown in Table 6.13. However, the difference is very low. For an increase of 48 bar pressure, the dry gas outlet flow rate reduces by 0.06 $L.min^{-1}$, from 5.17 $L.min^{-1}$. This represents a reduction of less than 2 %.

Hence, if this were projected onto, say, 200 bar pressure, typical of a some watered-out North Sea oil reservoir, we might expect a reduction in DHG produced gas of around 12 % compared to that produced at 80 bar.

At the end of the test, the gasifier-reformer was opened and the C11-PR remained almost identical to its original state. Just a slight brown layer on the catalyst was observed. In the same way, it seems that naphtha conversion to gases H_2, CO, CO_2 and CH_4 was maintained at 100 % as no unconverted naphtha residue in the accumulator was detected.

Table 6.13 summarizes operational conditions and results of Run 20-04.

Table 6.13 Run 20-04: Summary of operating conditions and results obtained during DHG test using naphtha feedstock (Catalyst C11-PR).

Run	20-04 (DHG test)		
Reformer tube dimensions	Φ ½ -inch x 72 cm		
Catalyst type	C11-PR		
Catalyst loading (g)	36.1		
Catalyst size (mm)	6 x 6 x 2		
Outlet gasifier-reformer temperature (⁰C) *	650		
Steam to carbon molar ratio (Naphtha) *	6		
Total inlet flow rate ($L.min^{-1}$) *	0.0110		
Naphtha inlet flow rate ($L.min^{-1}$) *	0.0020		
Water inlet flow rate ($L.min^{-1}$) *	0.0090		
Pressure (bar) *	82	110	130
Dry gas outlet flow rate ($L.min^{-1}$) *	5.17	5.11	5.06
Conversion (%) *	100	100	100
Produced dry gas composition (%) **			
H_2	62	61	60
CO	4	3	4
CO_2	13	12	12
CH_4	22	23	24
(*) Average values			
(**) Standard deviation of average values is ± 2 %			

6.3.3 Pressure (140 to 160 bar)

Run 20-05: In order to study steam reforming of naphtha in the gasifier-reformer (the chemical reactions on which DHG is based) at even higher pressure, 140 to 160 bar, Run 20-05 was carried out. Operating conditions of temperature, S/C ratio, water and naphtha inlet flow rates remained equal to those used in previous Run 20-04. Table 6.14 shows the details.

Table 6.14 Run 20-05: Operating conditions during DHG test using naphtha feedstock (Catalyst C11-PR).

Run	20-05 (DHG test)
Reformer tube dimensions	Φ ½ -inch x 72 cm
Catalyst type	C11-PR
Catalyst loading (g)	36.1
Catalyst size (mm)	6 x 6 x 2
Outlet gasifier-reformer temperature (⁰C) *	650
Steam to carbon molar ratio (Naphtha) *	6
Total inlet flow rate ($L.min^{-1}$) *	0.0110
Naphtha inlet flow rate ($L.min^{-1}$) *	0.0020
Water inlet flow rate ($L.min^{-1}$) *	0.0090
Pressure (bar) *	140 - 160
(*) Average values	

The graphs showing the variation of pressure and temperature during Run 20-05 are in Figures 6.29 and 6.30, respectively. The fluctuations in pressure in (140-160) bar are around 12 % so some disturbance to the catalyst bed must have occurred. The partial disintegration of the C11-PR catalyst as a consequence of thermal shock at the entrance of the reformer tubing might have been the main cause. However, the temperature remains very steady at 650 ºC during the same period (after 660 minutes).

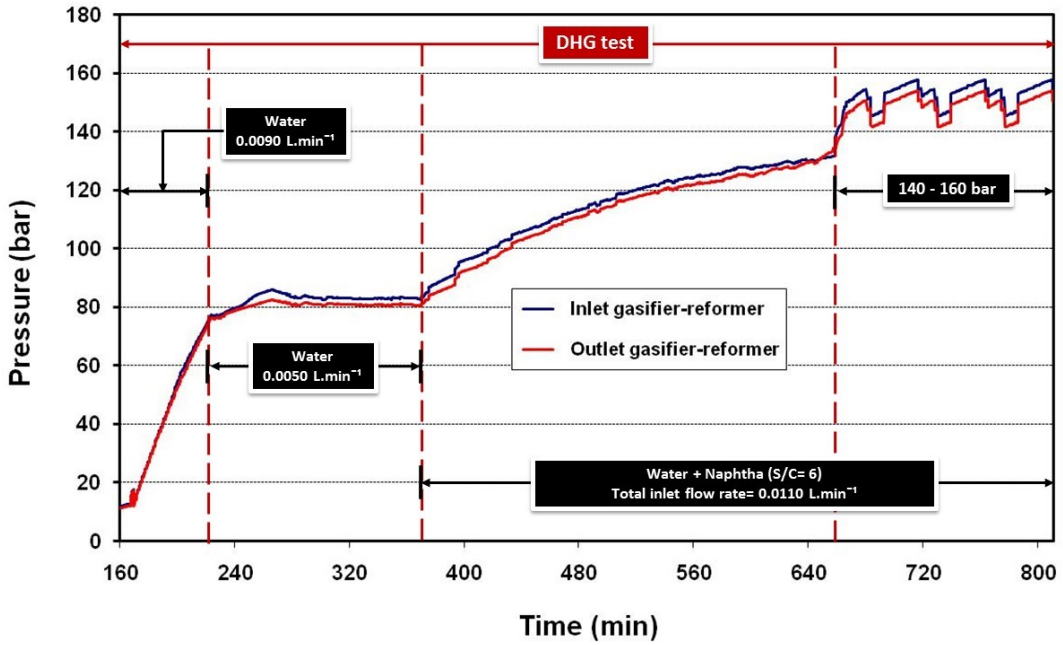

Figure 6.29 Run 20-05: Inlet and outlet pressure of gasifier-reformer during DHG test using naphtha feedstock (Catalyst C11-PR).

During the first stage of pressurization (steaming), two tendencies in the pressure curves were noticed: (1) a very sharp curve between (160 – 220) minutes with a water inlet flow rate of 0.0090 L.min^{-1}. The outlet gasifier-reformer temperature supported this increase (750 – 600) ºC since at a higher temperature a higher volume is occupied by gas, and the second tendency (2) was a steady curve where the outlet gasifier-reformer temperature was diminished down to 500 ºC as was the water inlet flow rate, down to 0.0050 L.min^{-1}.

This steaming procedure was carried out to minimise any thermal shock on the catalyst at the entrance of the gasifier-reformer and at the same time to purge the system of any dry gas generated by methane during the activation treatment. However, mechanical failures of the catalyst were present, as indicated by the slight pressure drop less of 2 %.

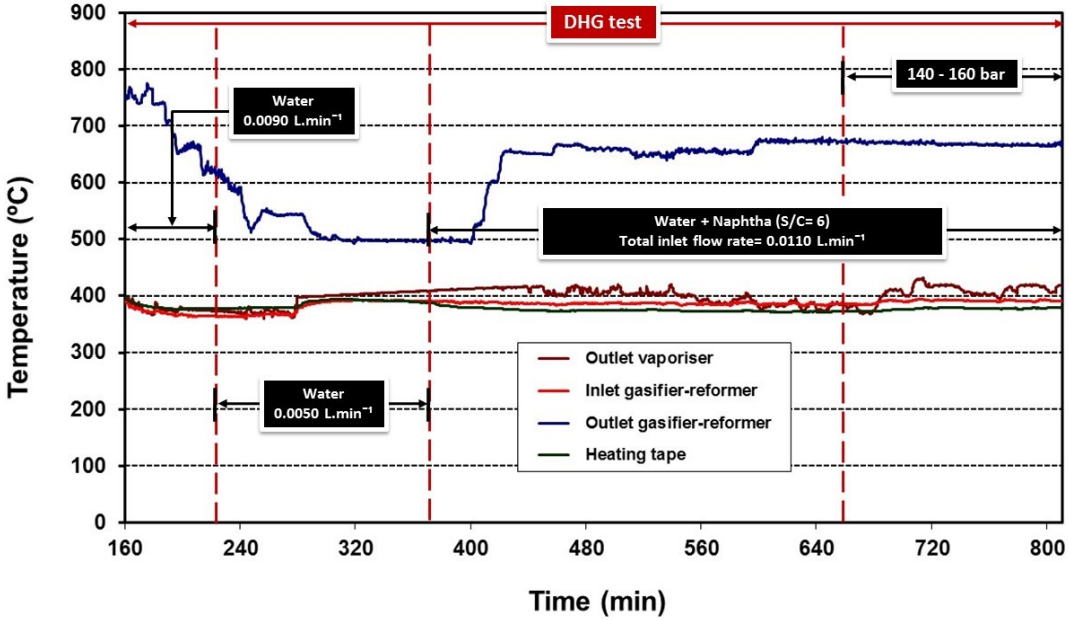

Figure 6.30 Run 20-05: Temperature profiles during DHG test using naphtha feedstock (Catalyst C11-PR).

Figure 6.31 shows the produced dry gas composition (vol. %). The average H_2 concentration is 56 vol. %, but varies from 47 vol. % to 55 vol. % as the pressure fluctuates between 140 and 160 bar. This value is not very different compared to those obtained previously in Run 20-04 at (110–130) bar, which is very positive for the DHG process.

The result certainly confirms that the effect of high pressure on produced dry gas, more specifically on H_2 concentration, is significantly less than occurred using methane as feedstock at lower pressure. Previously, it was believed that produced dry gas decreases as pressure increases along the whole pressure range for all hydrocarbons at the same tendency or level but this investigation demonstrates that this is not completely true.

Thermodynamically our result is possible since with higher hydrocarbons like our naphtha the first chemical reaction is irreversible, resulting in total conversion, unlike methane, which is attached to a chemical equilibrium (See Chapter 2, chemical reactions of steam reforming 2.4.1). The rest of the reactions associated with naphtha are the same as for methane: they are attached to an equilibrium highly influenced by pressure while the shift water reaction is unaffected.

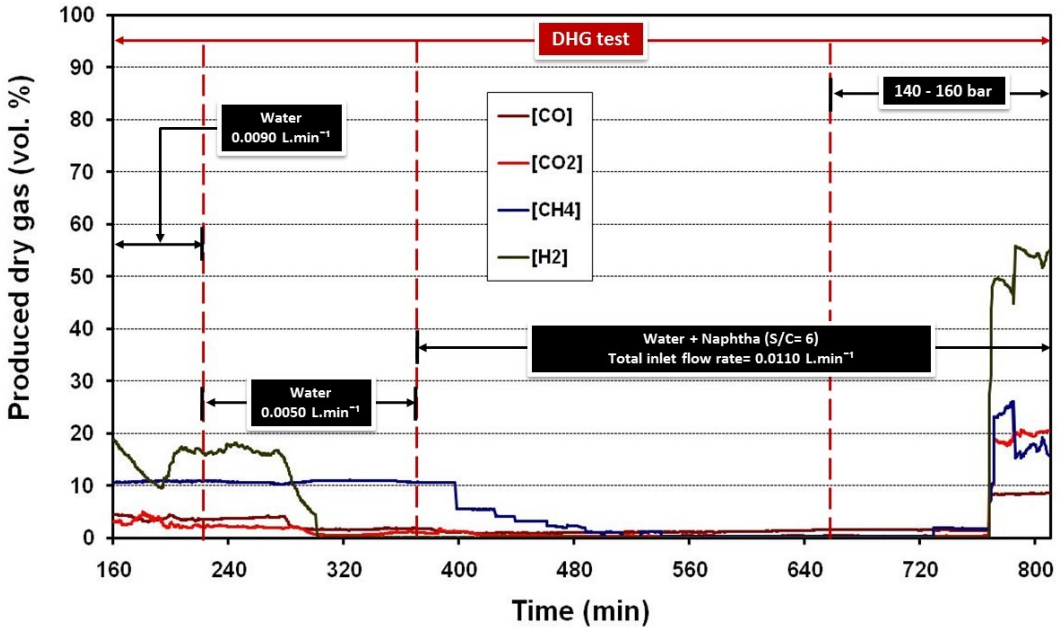

Figure 6.31 Run 20-05: Produced dry gas composition (vol. %) during DHG test using naphtha feedstock (Catalyst C11-PR).

However, the constraint here is the coke formation since higher hydrocarbons tend to form more coke than methane feedstock during steam reforming. Fortunately, this run did not demonstrate any coking on the disconnecting gasifier-reformer tube as the run ended and did not demonstrate any unconverted naphtha residue as liquid in the accumulator. Chemical analysis was carried out once the run had ended.

Thus, if coke formation is controlled catalytically at suitable operating conditions it is possible to obtain a 100 % conversion to gases as effectively occurred in this Run 20-05. This is very interesting since it demonstrates that in addition to the fact that H_2 concentration in produced dry gas is not too affected by pressure changes as methane is, that the feasibility of implementation of the DHG process at field scale is, in fact, enormous. Undoubtedly, this would represent an important advance in the knowledge and understanding of DHG obtained to date.

To summarize: there are two important facts picked up from Run 20-05 that require special attention and support: the complete conversion to gases from naphtha feedstock with no coke formation and no unconverted naphtha as residue, and less effect of pressure on the H_2 concentration and the rest of the gases at a higher pressure range using naphtha feedstock. Both are very positive developments in the implementation of DHG at field scale.

Abashar (2013) in their investigation of steam reforming of n-heptane (used here in this research as model surrogate for naphtha) reported similar effects, but over a lower range of pressure: complete conversion to gases and stronger reduction in H_2 concentration from 10 bar to 20 bar

than from 20 bar to 30 bar at S/C= 3.23.

To further investigate the effect of pressure, a numerical simulation study was also conducted here – see Chapter 7.

The dry gas outlet flow rates were again monitored manually and an average value was obtained very similar to that from the previous test, Run 20–04 which showed an outlet flow rate of 5.06 $L.min^{-1}$ at 130 bar while Run 20–05, outlet flow rate was 5.10 $L.min^{-1}$ at (140-160) bar.

As has been mentioned, the volume of produced dry gas per time unit is highly dependent on the conversion: logically, if the conversion did not vary greatly, the outlet flow rate would not change either.

Overall, the results from Run 20-05 were very important and positive. However, mechanical failures suffered by the catalyst like those observed in Run 20-04 lead to the supposition that the catalyst C11-PR is undergoing some difficulties in facing the new operating conditions of pressure (130-160 bar) not tested in previous research (Greaves et al., 2004, Greaves et al., 2005, Greaves et al., 2008) using naphtha feedstock.

The objective of the next section is to replace this catalyst by HiFUEL R110 which seems to be harder than C11-PR based on the fact that is has ceramic support and may possibly lead to better performance for the conversion due to a relative higher nickel oxide content (see chapter 3, section 3.2.2). The other areas of special interest in this section were to keep extending pressure or to simulate conditions at field scale, such as shutdown/start up cycles.

A second repeat was carried out confirming the results.

The following table summarizes the experimental conditions and results (Table 6.15).

Table 6.15 Run 20-05: Summary of operating conditions and results obtained during DHG test using naphtha feedstock (Catalyst C11-PR).

Run	20-05 (DHG test)
Reformer tube dimensions	Φ ½ -inch x 72 cm
Catalyst type	C11-PR
Catalyst loading (g)	36.1
Catalyst size (mm)	6 x 6 x 2
Outlet gasifier-reformer temperature (^{0}C) *	650
Steam to carbon molar ratio (Naphtha) *	6
Total inlet flow rate (L.min^{-1}) *	0.0110
Naphtha inlet flow rate (L.min^{-1}) *	0.0020
Water inlet flow rate (L.min^{-1}) *	0.0090
Pressure (bar) *	140 - 160
Dry gas outlet flow rate (L.min^{-1}) *	5.10
Conversion (%) *	100
Produced dry gas composition (%) **	
H_2	56
CO	8
CO_2	20
CH_4	16
(*) Average values	
(**) Standard deviation of average values is ± 2 %	

6.4 Experiments with crushed catalyst HiFUEL R110 and gasifier-reformer length 72 cm

The mechanical disintegration suffered by C11-PR during Run 20-04 and Run 20-05 led to the necessity of testing a new catalyst, HiFUEL R110 obtained from Alfa Aesar (Johnson Matthey), shown in Figure 6.32. This would be beneficial for the next stage of DHG experiments: minimal damage on catalyst, better conversion and minimisation of coke formation.

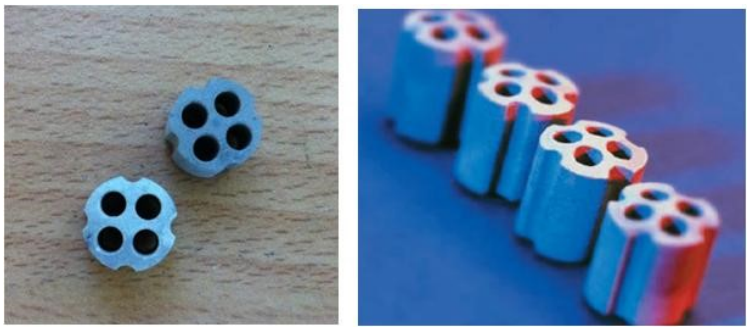

Figure 6.32 HiFUEL R110 catalyst from Alfa Aesar, 4 hole, 4 flute domed cylinders.

The new tests, Run 20-06 and Run 20-07 were performed in a reactor length of 72 cm, catalyst loading 36.5 g at 650 ºC and the same pressure range used previously in section 6.3, (140-160) bar, since our attention here was focused on the survivability of the catalyst and its performance and not at this stage on increasing the pressure range even more. Studies at (140-160) bar already represent an important advance in this investigation: no results have been reported in the literature so far associated with the DHG process using naphtha feedstock at that pressure range.

In future development trials, i.e. full-scale pilot DHG tests, it would be necessary to establish that the catalyst could survive much longer periods, ca. 2 years. Any effort to optimise or provide some idea or indication that this may not be a problem at (140-160) bar would have a similar importance and impact to increasing pressure beyond that range.

HiFUEL R110 catalyst: This catalyst contains 40-60 % nickel oxide on ceramic support, it comprises a 4-hole, 4 flute-domed cylinder geometry designed to compensate diffusional effects that are normally a feature of steam reforming reactors (Schwaab et al., 2009, Xu and Froment, 1989, Melo and Morlanes, 2008, Eduardo et al., 2009). Its ceramic support is made of calcium aluminates making it particular to steam reforming of light hydrocarbons like naphtha. The product bulletin (See Appendices, section A.5) mentions that pressure would have a minimal effect on approach to equilibrium and that its ideal activation treatment is very similar to that used in this research (S/C= 7, 750 ºC).

Unfortunately, the catalyst size was higher than that permitted by the internal diameter of the gasifier-reformer, so that it was decided to crush it into smaller pieces (Fig. 6.33) prior to every DHG experiment, Run 20-06 and Run 20-07. It is known that catalyst shape and size influence the conversion in reactors (Stefanescu et al., 2007, Hao, 1997, Somorjai, 1994), and that diffusional control is sensitive to the catalyst geometry and active surface area, which are all interconnected.

Figure 6.33 Crushed HiFUEL R110 catalyst.

Thus, the use of the catalyst in crushed form will certainly be sub-optimal

but the final shape-geometry to be selected for future work at lab or field scale will necessarily take into account the results obtained with the crushed form.

SEM images of crushed HiFUEL R110 were carried out before activation treatment. Figure 6.34 shows the images indicating that the catalyst has a higher porosity than C11–PR. Its ceramic catalyst support seems to be embedded with a very advanced synthesis technique since it exhibits a high purity of materials and it seems to be made of a mixture of aluminates and calcium. Ceramic support for catalysts according to references (Shinku et al., 2008, Christensen, 2005) reduces the effect of particulates contamination, hot spots and low pressure drops in tubular reformers. It also has a higher strength and hardness in relation to C11-PR catalyst according to the information supplied by the manufacturer (See appendices, section A.4 and A.5).

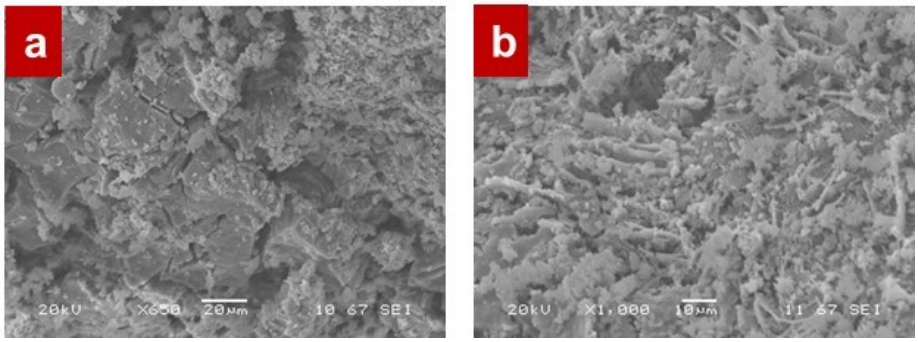

Figure 6.34 SEM images of crushed HiFUEL R110 before activation treatment (a) side view: 20 KV, x650, 20 µm, SEI (b) side view: 20 KV, x1000, 10 µm, SEI.

Chemical composition in the EDX analysis indicates a higher presence of nickel oxide (58 wt. %) than that existent in C11–PR (< 45 wt. %) and no signals associated with any other chemical element acting as promoter.

Repeats of every experiment from this section 6.4 were always carried out to confirm results. The activation treatment and DHG test period demonstrated the same tendency and produced dry gas composition/outlet flow rate values were very similar. As an example mode, the catalyst activation treatment period which corresponded to Run 20-06 will be discussed below.

6.4.1 Catalyst activation treatment prior to DHG tests

Catalyst activation using this new catalyst, crushed HiFUEL R110, was carried out prior to the DHG tests as always, at the same operating conditions using methane feedstock. Table 6.16 summarizes the operating conditions in Run 20-06 during catalyst activation. Figure 6.35, 6.36 and 6.37 show curves of pressure, temperature and produced dry gas composition (vol. %) obtained during the run.

Table 6.16 Run 20-06: Operating conditions during catalyst activation using methane feedstock (Catalyst crushed HiFUEL R110).

Run	20-06 (activation)
Reformer tube dimensions	Φ ½ -inch x 72 cm
Catalyst type	Crushed HiFUEL
Catalyst loading (g)	36.5
Original catalyst size	10 ½ -inch x 13 mm
Pressure (bar) *	10
Outlet gasifier-reformer temperature (⁰C) *	750
Steam to carbon molar ratio (CH_4) *	7
Total inlet flow rate ($L.min^{-1}$) *	1.8090
CH_4 inlet flow rate ($L.min^{-1}$) *	1.8000
Water inlet flow rate ($L.min^{-1}$) *	0.0090
(*) Average values	

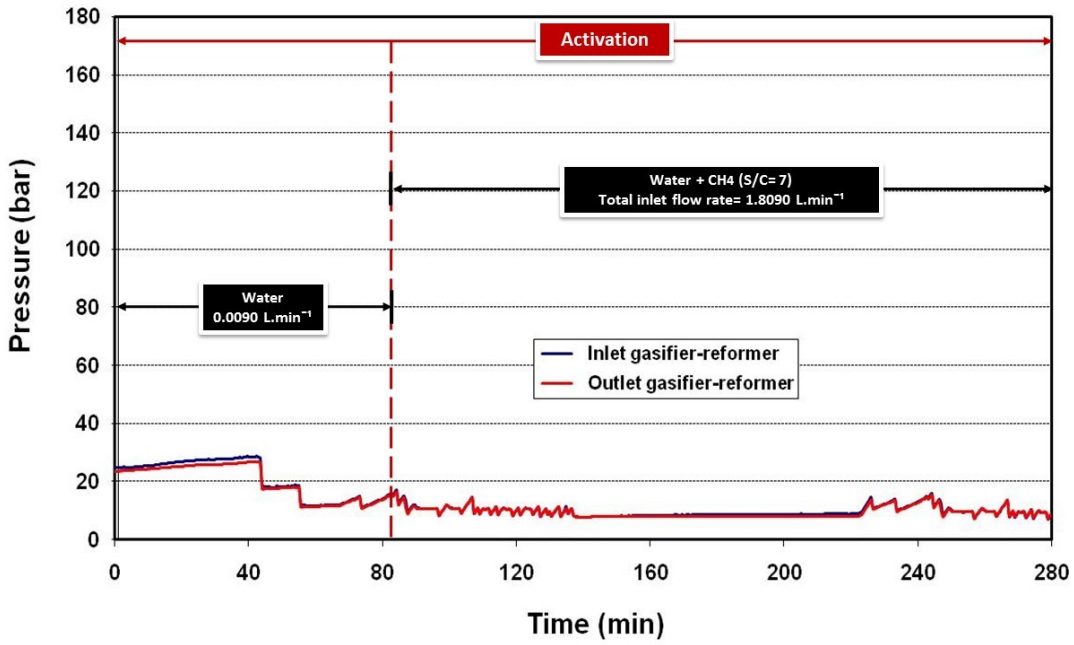

Figure 6.35 Run 20-06: Inlet and outlet pressure of gasifier-reformer during catalyst activation using methane feedstock (Catalyst crushed HiFUEL R110).

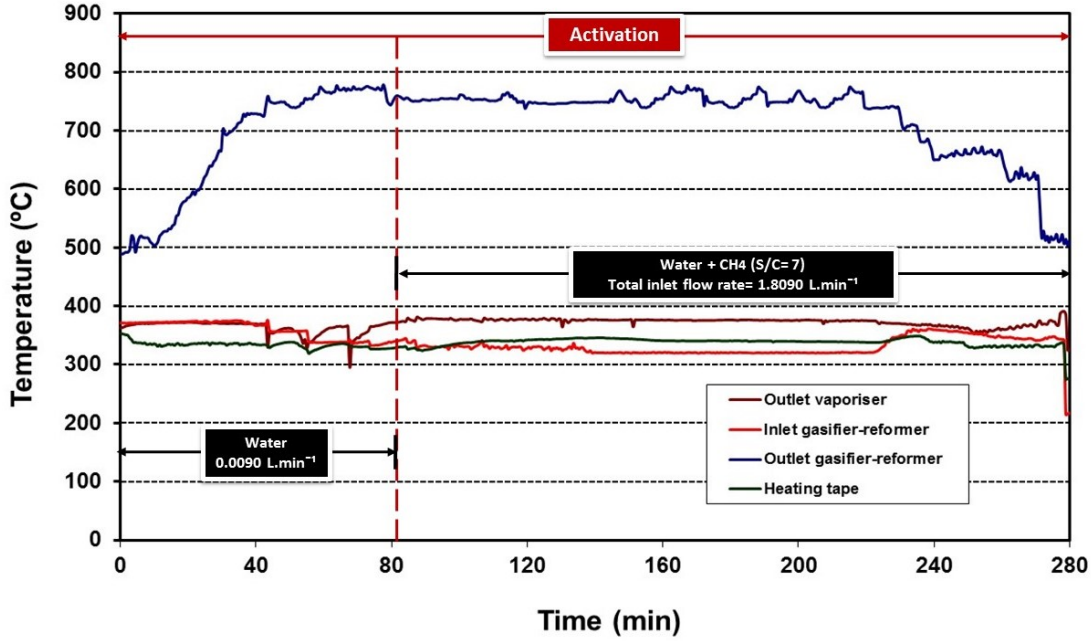

Figure 6.36 Run 20-06: Temperature profiles during catalyst activation using methane feedstock (Catalyst crushed HiFUEL R110).

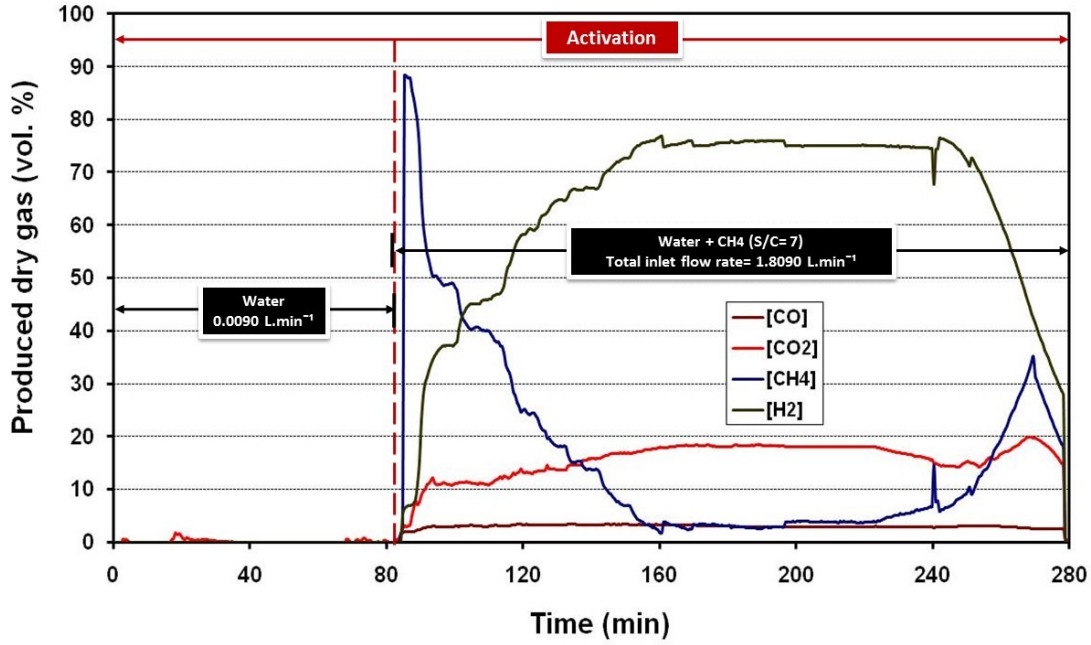

Figure 6.37 Run 20-06: Produced dry gas composition (vol. %) during catalyst activation using methane feedstock (Catalyst crushed HiFUEL R110).

Those curves showed an identical trend compared to previous sections 6.2 and 6.3 despite the fact that the catalyst used was different. This is logical: both catalysts are made of nickel oxide and differences between them are centred on the nature of the support and promoters. In addition,

the curves do not show higher fluctuations than previous activation curves and signal stability seems to be more stable. The main cause is attributed to the strength of the catalyst and its ceramic support despite its crushed state.

A slightly higher methane conversion (97 %) is observed in the produced dry gas composition graph (Figure 6.37). Previous sections 6.2 and 6.3 reported values in the range of 90-93 % on average. A higher H_2 concentration is also observed. In Run 20-06, H_2 concentration was 76 vol. % while the average values of H_2 in the activation period for Run 20-01, 20-02, 20-03, 20-04 and 20-05 were (72-74) vol. % and rarely reached 75 vol. %.

This undoubtedly is indicative of better catalyst performance by the crushed HiFUEL R110 during activation treatment using methane feedstock. It is significant that a rapid methane conversion and H_2 production occurred at 86 minutes meaning a more efficient heat transfer from the reactor to the feed, increasing in parallel with the conversion.

After 230 minutes, gas sampling for analysis was stopped and the furnace temperature was reduced to 650 ºC. After 280 minutes, water injection was started as the first step to prepare the system for the DHG test using naphtha feedstock.

In relation to the average values obtained manually of the dry gas outlet flow rates, it may be said that they were fairly stable, 4.11 $L.min^{-1}$ which was very similar to previous sections, 6.2 and 6.3. (4.12 $L.min^{-1}$ and 4.09 $L.min^{-1}$).

In theory, these average dry gas outlet flow rates are acceptable since they are under the limits calculated on stoichiometric principles and the conversion based on graph 5.5 shown in chapter 5.

A second repeat was carried out to confirm the results.

In practice, this kind of catalyst activation treatment might also be useful to monitor (by means of pressure and produced dry gas composition (vol. %) curve analysis) the performance of a catalyst in DHG at field scale in order to determine how long it would be able to last in the reservoir.

Table 6.17 summarizes the operating conditions and results in the activation treatment in Run 20-06 using methane as feedstock.

Table 6.17 Run 20-06: Summary of operating conditions and results obtained during catalyst activation using methane feedstock (Catalyst crushed HiFUEL R110).

Run	20-06 (activation)
Reformer tube dimensions	Φ ½ -inch x 72 cm
Catalyst type	Crushed HiFUEL
Catalyst loading (g)	36.5
Original catalyst size	10 ½ -inch x 13 mm
Pressure (bar) *	10
Outlet gasifier-reformer temperature (^{0}C) *	750
Steam to carbon molar ratio (CH_4) *	7
Total inlet flow rate ($L.min^{-1}$) *	1.8090
CH_4 inlet flow rate ($L.min^{-1}$) *	1.8000
Water inlet flow rate ($L.min^{-1}$) *	0.0090
Dry gas outlet flow rate ($L.min^{-1}$) *	4.11
Conversion (%) *	97
Produced dry gas composition (%) **	
H_2	76
CO	3
CO_2	18
CH_4	3
(*) Average values	
(**) Standard deviation of average values is ± 2 %	

6.4.2 Pressure (140 to 160 bar)

Run 20-06: Once the catalyst was activated, the DHG test period started using naphtha feedstock. This particular test was carried out with the goal of comparing its results with those obtained in Run 20-05 at the same pressure range, (140-160) bar, analysing any changes occurring as a consequence of the new catalyst.

In general terms, the results from Run 20-05 were very positive and represented an advance in DHG investigation. However, catalyst mechanical properties at operating conditions were relatively poor: the presence of a pressure drop was observed, and fluctuations in the pressure and produced dry gas curves were considerable.

With this new catalyst in Run 20-06, pressure drop and fluctuations should be reduced; the results will be analysed and discussed. To confirm the results, a second repeat was carried out. Table 6.18 summarizes the operating conditions.

Table 6.18 Run 20-06: Operating conditions during DHG test using naphtha feedstock (Catalyst crushed HiFUEL R110).

Run	20-06 (DHG test)
Reformer tube dimensions	Φ ½ -inch x 72 cm
Catalyst type	Crushed HiFUEL
Catalyst loading (g)	36.5
Original catalyst size	10 ½ -inch x 13 mm
Outlet gasifier-reformer temperature (ºC) *	650
Steam to carbon molar ratio (Naphtha) *	6
Total inlet flow rate ($L.min^{-1}$) *	0.0110
Naphtha inlet flow rate ($L.min^{-1}$) *	0.0020
Water inlet flow rate ($L.min^{-1}$) *	0.0090
Pressure (bar) *	155
(*) Average values	

The DHG test in Run 20-06 started with a pressurization and purge of the rig using water at 0.0180 $L.min^{-1}$ (steaming) followed by co-injection of water and naphtha (total inlet flow rate= 0.0110 $L.min^{-1}$) at S/C= 6. Figure 6.38 shows the pressure curves.

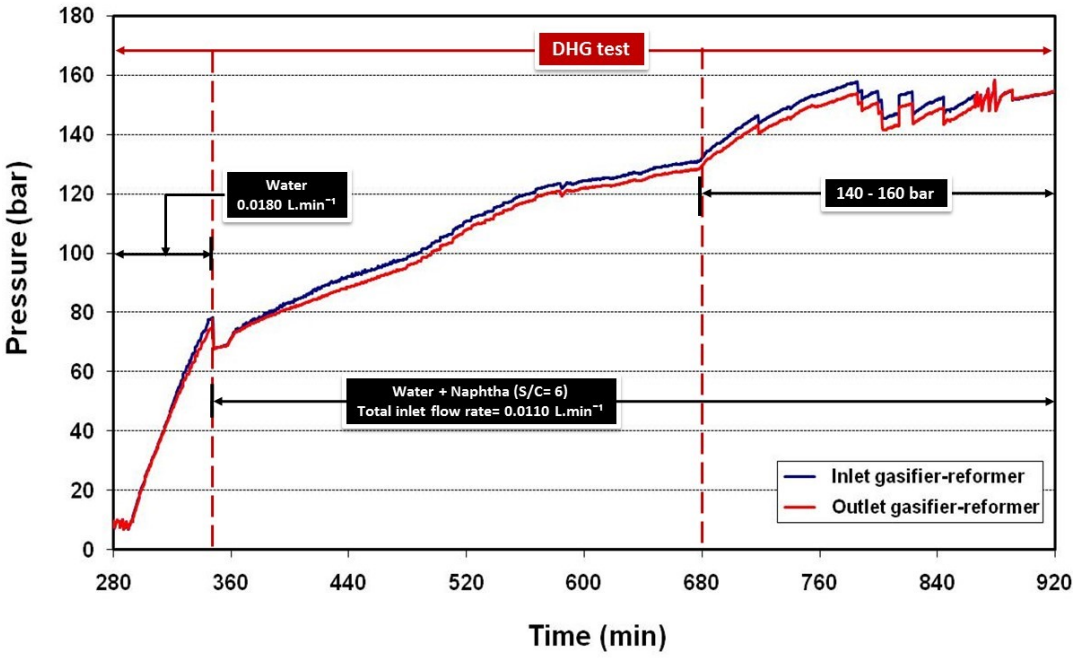

Figure 6.38 Run 20-06: Inlet and outlet pressure of gasifier-reformer during DHG test using naphtha feedstock (Catalyst crushed HiFUEL R110).

Both curves are relatively sharp despite the fact that the outlet gasifier-reformer temperature was only 500 ºC according to Figure 6.39. This temperature value was selected to avoid mechanical damage to the catalyst before the DHG test.

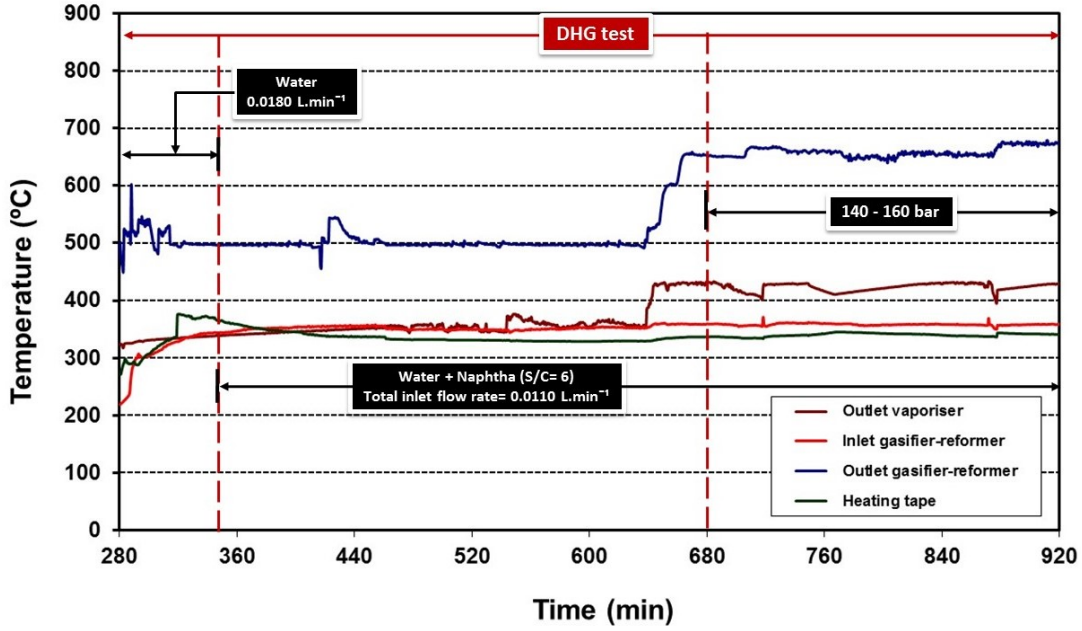

Figure 6.39 Run 20-06: Temperature profiles during DHG test using naphtha feedstock (Catalyst crushed HiFUEL R110).

Once 140–160 bar was reached, it may be observed that a lower level of fluctuations were present compared to the previous Run 20-05. The discrepancy was only 2 % approximately here in Run 20-06 where it was over 10 % in Run 20-05. The pressure curves also showed a gradual signal stabilisation after 860 minutes with a significant reduction of pressure drop. This suggests, in the first instance, that the new catalyst HiFUEL R110 had a positive effect in the gasifier-reformer. On disconnecting the reactor tube once the test was completed, no mechanical disintegration or brown layer was observed on its surface, confirming the positive analysis.

In practice, when looking at selecting a catalyst for the DHG process, Richardson (1989) and Batholomew and Farrauto (2006), indicate that catalytic, chemico-physical and morphological/mechanical properties should be considered (Figure 6.40). So far, there have been only limited studies focused on enhancing the catalyst for DHG. Our results with C11-PR and crushed HiFUEL R110 provide some understanding about how important and close the relationship between those three properties are, concluding that it is vital that catalysts in DHG at field scale have considerable conversion and preserving mechanical properties that will guarantee the survivability of the catalyst over a period, for 2 years.

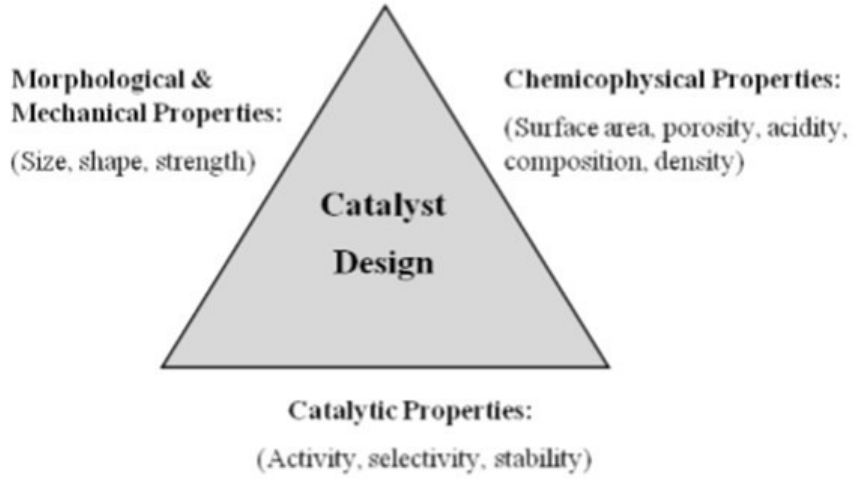

Figure 6.40 Catalyst design triangle (Original from Richardson, 1989, but taken from Azadi and Farnood, 2011).

The temperature curves from Figure 6.39 show no major findings: A slight increase of outlet vaporiser temperature was obtained as a consequence of the activity of the furnace temperature controller program which increased the temperature after 650 minutes. In general terms, the temperature curves show the typical behaviour observed in the previous Run 20-05. In relation to signal stability, standard deviation was below 6 % which is acceptable. The isolation system seems to have worked satisfactorily: no major difference between the outlet vaporiser and inlet gasifier-reformer temperatures was observed.

The H_2 concentration in Figure 6.41 remained relatively steady at (140–160) bar and its value was approximately 10 % higher than that obtained in Run 20-05 using the C11-PR catalyst (55.50 vol. % in H_2). H_2 production was 61 vol. % (theoretical maximum 70 %), CO 4 vol. %, CO_2 12 vol. % and CH_4 23 vol. % at 155 bar in Run 20-06.

This indicates that HiFUEL R110 effectively demonstrated a better performance in the gasification-reforming reaction (steam reforming) at (140-160) bar compared to C11-PR despite the fact that the HiFUEL R110 was in a crushed state. In addition, total naphtha conversion to gases occurred since no unconverted naphtha was detected in the accumulator after the test neither was there any coke formation on the HiFUEL R110 catalyst.

The high conversion and level of H_2 concentration show the same tendency as in Run 20-04 and Run 20-05: the sensitivity to pressure increase seems to be less than observed in the much lower (<80 bar) pressure range using methane.

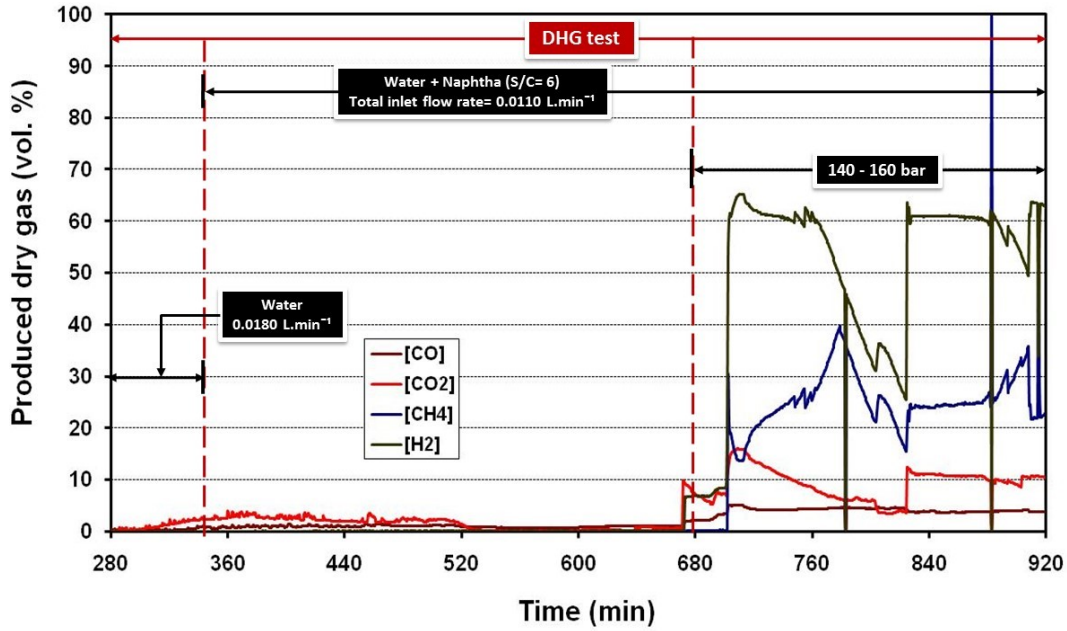

Figure 6.41 Run 20-06: Produced dry gas composition (vol. %) during DHG test using naphtha feedstock (Catalyst crushed HiFUEL R110).

Despite the fact that there are no studies of DHG using naphtha feedstock at such a pressure range, the review of literature on steam reforming reactions for other purposes using catalysts and similar organic feedstock might support our results. Azadi et al., (2010) reported glucose ($C_6H_{12}O_6$) steam reforming at 200 bar, 450 ºC and S/C= 15 with a ruthenium catalyst indicating a H_2 concentration in the produced dry gas composition of 34 % on a theoretical maximum of 60 %. Byrd et al., (2007) and Papadias et al., (2010) reported steam reforming of ethanol at 70 bar and 210 bar respectively and 600-700 ºC obtaining 50 and 58 vol. % of H_2 with different catalysts.

In the above cases, H_2 concentrations are considerable at such temperatures and certainly higher than expected for a lineal H_2 decrease as an effect of pressure, since such a decrease would mean 20 % or less instead of the actual results achieved. Implicitly, this leads to the supposition that such linearity does not occur.

Other research is described in Table 6.19 and some of them refer to pressures higher than 221 bar for biomass gasification with super critical water whose properties are unique and very different from steam (Osada et al., 2007). Abashar (2013) reported heptane steam reforming reactions at lower pressure (<30 bar) and presented some preliminary studies on the sensibility of H_2 to pressure. He reported that a more accentuated decrease was observed between (10-20) bar than between (20-30) bar, mentioning the possibility that that tendency might continue beyond 30 bar.

Table 6.19 Research review of steam reforming at similar DHG conditions using organic feedstock.

Feedstock	Application	Reactor type	Operating conditions	Catalyst	Hydrogen in produced dry gas (%)	Space velocity (h^{-1})*	Residence time (s)*	References
Methane	Hydrogen production	Tubular	P= 13 bar, T= 790 ºC, S/C= 2-4	Ni	> 85 in volume	3000	5.40	Rase, 1977
n- Decane	Biomass gasification	Tubular	P= 250 bar, T= 550 ºC 20 vol. %	Ni	< 15 in volume	360.00	10.00	Pinkwart et al., 2004
Methane	Fuel cell	Tubular	P= 246 bar, T= 600 ºC 2-18 wt %	Ni	8 in volume	60.00	60.00	Lachance, 2005
Isooctane + inert gas	Hydrogen production	Tubular	P= 1 bar, T= 1000 ºC S/C= 1.3	Mo	78 in volume	15000	0.24	Cheekatamarla and Thomson, 2006a
Hexadecane + inert gas	Hydrogen production	Tubular	P= 1 bar, T= 965 ºC S/C= 1.7	Mo	93 in volume	4000	0.90	Cheekatamarla and Thomson, 2006b
Pentane + reservoir gas	DHG	Tubular	P= 98 bar, T= 680 ºC S/HC= 3.9	Ni	51 in volume	3000	14.00	Greaves et al., 2006
Ethanol + inert gas	Fuel cell	Tubular	P= 210 bar, T= 600 ºC 10 wt %	Ru	57.5 in volume	200.00	18.00	Byrd et al., 2007
Light naphtha + reservoir gas	DHG	Tubular	P= 97 bar, T= 760 ºC S/HC= 5.4	Ni	56.2 in volume	5000	24.00	Greaves et al., 2008
Aviation fuel ($C_{12}H_{26}$)	Fuel cell	Tubular	P= 240 bar, T= 767 ºC 6.25 wt %	Ni	32 in volume	23.84	151.00	Picou et al., 2009
Acetic acid	Biomass gasification	Tubular	P= 1 bar, T= 600 ºC S/C= 5.8	Ni	74 in volume	16.00	225.00	Chen et al., 2009
Glucose	Biomass gasification	Tubular	P= 200 bar, T= 450 ºC S/C= 15	Ru	34 in volume	24.00	150.00	Azadi et al., 2010
Ethanol + inert gas	Fuel cell	Membrane	P= 70 bar, T= 700 ºC S/C= 3	Ni	50 in volume	8500	0.42	Papadias et al., 2010
Isooctane	Biomass gasification	Tubular	P= 250 bar, T= 637 ºC 9.9 wt % Oxidant (2 mol %)	Ni	59.5 in mole	200.00	18.00	Susanti et al., 2010
Isooctane	Biomass gasification	Inclined tubular	P= 240 bar, T= 767 ºC 6.25 wt %	Ni	68 in mole	33.96	106.00	Susanti et al., 2011
Light naphtha	DHG	Tubular	P= 155 bar, T= 650 ºC S/C= 6	Ni	61.13 in volume	23.19	155.24	This research (Run 20-06)

(*) Calculated on data reported
S/HC= Steam to hydrocarbon molar ratio

Fluctuations in the produced dry gas curves remained similar to those observed previously with C11-PR. Therefore, we concluded that this fact is entirely attributable to deficiencies in the back pressure regulator which controls higher pressures, added to the relatively low inlet flow rates used in the runs, which made difficult a rapid volume replacement when the produced dry gases were being sampled and analysed.

Calculations of space velocity, residence time and Reynolds number which will be reported in Table 6.23 supported the hypothesis about the use of relatively low inlet flow rates during Run 20-06. Further details will be discussed in section 6.5.

Unfortunately, the flow rate recorder continued to present some problems and the dry gas outlet flow rates were taken manually. Their average values indicated a slight increase in relation to Run 20-05 as a consequence of the higher conversion which represented 28-32 times (in mole terms) per naphtha mole. This is commensurate with the theoretical values discussed previously and shown in Figure 6.11, section 6.2.2.

In practice, the minimization of fluctuations during runs might be carried out on the basis of reactor size and design for implementation at field scale. Some ideas about this will be discussed in section 6.6. Table 6.20 summarizes the results obtained in Run 20-06.

Table 6.20 Run 20-06: Summary of operating conditions and results obtained during DHG test using naphtha feedstock (Catalyst crushed HiFUEL R110).

Run	**20-06 (DHG test)**
Reformer tube dimensions	Φ ½ -inch x 72 cm
Catalyst type	Crushed HiFUEL
Catalyst loading (g)	36.5
Original catalyst size	10 ½ -inch x 13 mm
Outlet gasifier-reformer temperature (^{0}C) *	650
Steam to carbon molar ratio (Naphtha) *	6
Total inlet flow rate (L.min^{-1}) *	0.0110
Naphtha inlet flow rate (L.min^{-1}) *	0.0020
Water inlet flow rate (L.min^{-1}) *	0.0090
Pressure (bar) *	155
Dry gas outlet flow rate (L.min^{-1}) *	5.12
Conversion (%) *	100
Produced dry gas composition (%) **	
H_2	61
CO	4
CO_2	12
CH_4	23
(*) Average values	
(**) Standard deviation of average values is ± 2 %	

Overall, results from Run 20-06 confirm the improved performance of HiFUEL R110 in comparison to C11-PR despite its suboptimal condition (crushed state) which might give an idea of how efficient it might be when using an adequate size and shape in future work. Hence, it is recommended that further studies are carried out on this catalyst aimed at optimising conversions, the H_2 concentration in produced dry gas and catalyst survivability in the medium/long term.

6.4.3 Shutdown/start up cycles followed by variation of temperature (600 to 750 ºC) at higher pressure (140-160) bar

Field operations often face electrical failures which would seriously impact the gasifier-reformer performance. A new run was carried out with shut down/start up cycles followed by temperature variations from 600 ºC to 750 ºC and extending the total time of the test.

A pressure range of (140-160) bar was under study here for comparison reasons since the previous runs, 20-05 and 20-06, were carried out at the same pressure range for both. Thus, our intention in general terms was: to extend pressure to a range not reported before for DHG using naphtha feedstock, to optimise the conversion through catalyst replacement and now with Run 20-07, to determine possible DHG behaviour in a future implementation facing sudden electrical disruptions. A second repeat was performed to confirm the results. Fortunately the outlet flow rates were able to be recorded online using the homemade software (chapter 3, section 3.3).

Run 20-07: The DHG test period started once the catalyst activation treatment had been completed followed by steaming and pressurization with water injection (0.090 $L.min^{-1}$) for 200 minutes in total. The DHG test started with the injection of water and naphtha, 0.0110 $L.min^{-1}$ at S/C= 6 and (140–160) bar for 300 minutes. During the cycle, data acquisition and monitoring, injection pumps and gas analysers remained on. After this, a sudden electrical shut down was simulated safely over a cycle by switching off the naphtha/water injection pumps, furnaces and heating tape for 300 minutes each.

The procedure was repeated three times for named cycles and during the last shut down cycle, at night time, the DHG rig was maintained with water injection, 0.0020 $L.min^{-1}$ at 120 ºC for 450 minutes to continue the test next day. The test was retaken at varying temperatures from 600 ºC to 750 ºC. The total time period of Run 20-07 was 1719 minutes. Temperature variation was carried out to study its effect on the catalyst surface and on the conversion in the steam reforming reactions, simulating any operational adjustment of temperature in future DHG implementation trials. Table 6.21 details the operating conditions used in Run 20-07. Figures 6.42, 6.43, 6.44 and 6.45 show the pressure, temperature,

produced dry gas composition and outlet dry gas curves obtained.

The pressure curves in Figure 6.42 presented no major fluctuations or pressure drops except for the first cycle between (207–507) minutes, where the pressure value oscillated from 140 bar to 158 bar meaning a standard deviation of 9 %. This is attributed to the system pressurisation by naphtha conversion/produced dry gases, the deficiency in the back pressure regulator to control the high values of pressure generated and, certainly, to the relatively low inlet flow rates that made rapid volume restoration in the rig difficult every time a gas sample was taken.

Table 6.21 Run 20-07: Operating conditions during DHG test using naphtha feedstock (Catalyst crushed HiFUEL R110).

Run	20-07 (DHG test)			
Reformer tube dimensions	Φ ½ -inch x 72 cm			
Catalyst type	Crushed HiFUEL			
Catalyst loading (g)	36.5			
Original catalyst size	10 ½ -inch x 13 mm			
Steam to carbon molar ratio (Naphtha) *	6			
Total inlet flow rate ($L.min^{-1}$) *	0.0110			
Naphtha inlet flow rate ($L.min^{-1}$) *	0.0020			
Water inlet flow rate ($L.min^{-1}$) *	0.0090			
Pressure (bar) *	155			160
Outlet gasifier-reformer temperature (ºC) *	650			(600 - 750)
Cycles	1	2	3	4
(*) Average values				

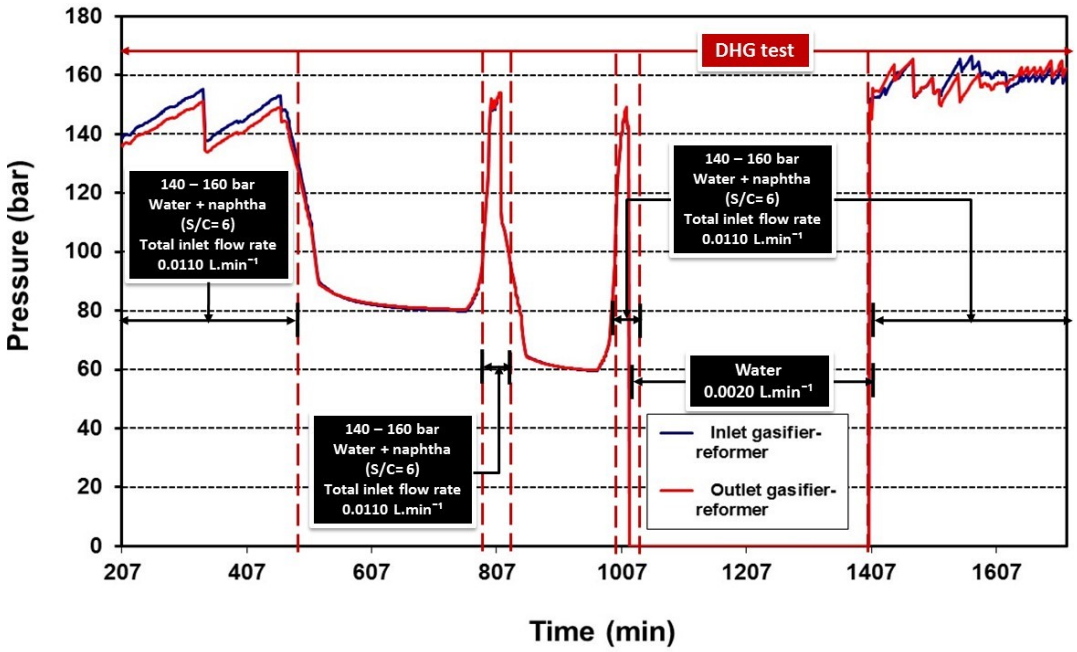

Figure 6.42 Run 20-07: Inlet and outlet pressure of gasifier-reformer during DHG test using naphtha feedstock (Catalyst crushed HiFUEL R110).

In regard to this run, the Reynolds numbers (*Re*) were calculated on the basis of the combined flow rates of naphtha and water indicating the presence of a laminar flow pattern (*Re* between 11-15) in the gasifier-reformer reactor (See details in section 6.5 and appendix B, section B.5). Certainly, the laminar pattern does not favour signal stability while gases are sampled and a rapid volume restoration is required, especially at higher pressure (140-160) bar. In addition, the laminar pattern does not favour the conversion either since steam reforming is mainly influenced by the external diffusion regime (Schwaab et al., 2009, Xu and Froment, 1989, Melo and Morlanes, 2008, Eduardo et al., 2009).

In future DHG implementation trials, increasing the intensity of mixing through higher inlet flow rates would make the fluid flow more turbulent and decrease the thickness of the boundary laminar layer, optimising even more the DHG process overall. The reaction rate would increase and it is possible that the external diffusion influence would become negligible, which would be a positive outcome. Moreover, higher inlet flow rates would make the DHG process more attractive economically, since a greater volume of dry gas per time unit would be produced, apart from the fact that coking would be less likely. Less residence time and more turbulence would reduce coke deposits on the catalyst bed (Trimm, 1997, Froment, 2008).

This might not be a problem. At field scale, higher naphtha injection rates are more easily handled and our DHG gasifier-reformer results have already demonstrated a considerable and positive conversion and produced dry gas volume per time unit. The technical feasibility of the DHG process based on our experimental results will be discussed in section 6.5 in this chapter.

Back to Figure 6.42, the rest of the cycles were steadier, pressure seemed to be more controlled, diminishing fluctuations to below 2 %, attributed mainly to deficiencies in the back pressure regulator to control pressure in the system. During the shutdown cycles, the pressure and temperature values in Figure 6.43 went down rapidly as far as a certain value and then they remained relatively steady. The temperature curves did not show marked fluctuations: these were below 1-2 %. Moreover, during the test period, the isolation system guaranteed a temperature over steam saturated temperature which is 352 ºC.

Once the injection pumps and furnaces started up, values of pressure and temperature were restored rapidly and according to Figure 6.44 did not affect the conversion and produced dry gas concentrations. The H_2, CO, CO_2 and CH_4 values remained almost identical to the initial ones. Figure 6.44 on produced dry gas composition (vol. %) shows this clearly. Variations of H_2, CO, CO_2 production were below 4 % while CH_4 was more sensitive, demonstrating a 10 % variation approximately.

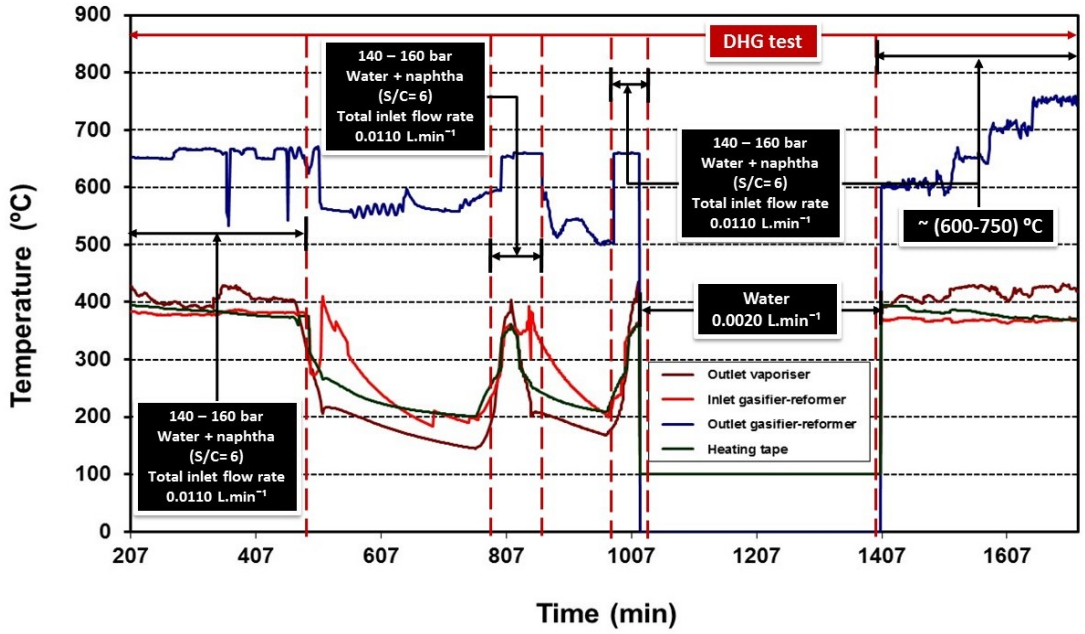

Figure 6.43 Run 20-07: Temperature profiles during DHG test using naphtha feedstock (Catalyst crushed HiFUEL R110).

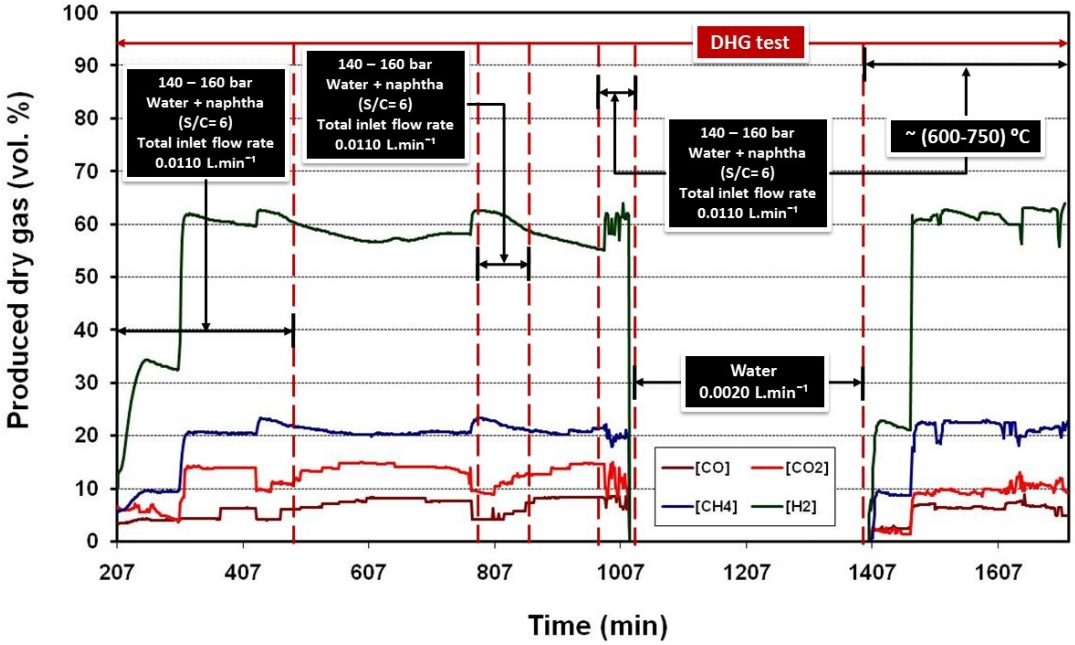

Figure 6.44 Run 20-07: Produced dry gas composition (vol. %) during DHG test using naphtha feedstock (Catalyst crushed HiFUEL R110).

In the temperature variation study realised the day after, pressure fluctuations were fairly moderate, standard deviation was below 4 %, lower than the first cycle (< 9 %), attributed to the influence of temperature: as temperature increases a faster volume replacement is favoured and hence, fluctuations are easier to regulate at the same pressure range, (140-160) bar.

The produced dry gas composition (vol. %) in Figure 6.44 shows that H_2, CO, CO_2 and CH_4 remained relatively steady despite the increase in temperature. It is possible that changes in produced dry gases through temperature increase are less sensitive to higher pressures as Papadias et al., (2010) concluded. They carried out studies on the effect of temperature in ethanol steam reforming for vehicular purposes using fuel cells at 70 bar approximately, observing the same tendency.

Figure 6.45 shows the dry gas outlet flow rate monitored online during Run 20-07. Homemade software and a flow recorder from the wet test meter were specially commissioned for the Run. Fluctuations are very severe attributed mainly to back pressure regulator control at higher pressure in the system. It seems that, at low pressure, the back pressure regulator operated very well as is shown in the outlet flow rate graphs in Figures 6.4, 6.10 and 6.15. However, back pressure regulator control was less good at higher pressures affecting to a greater degree the stability of this signal (chapter 4, section 4.3.2).

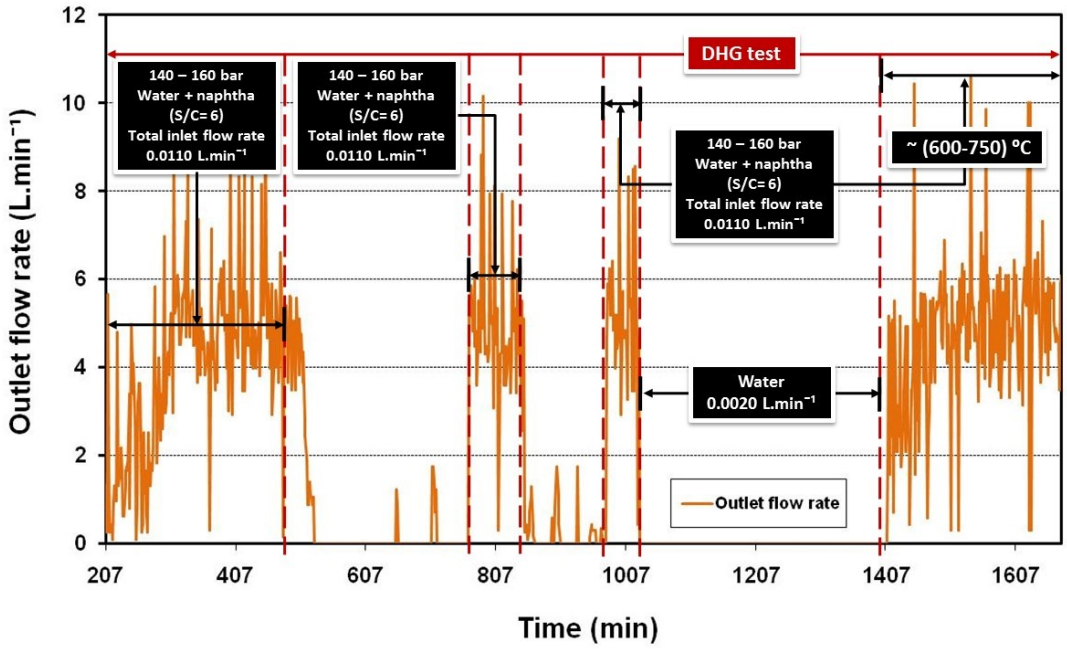

Figure 6.45 Run 20-07: Dry gas out let flow rate during DHG test using naphtha feedstock (Catalyst crushed HiFUEL R110).

Average values of outlet flow rates did not vary greatly between each cycle: 5.13 $L.min^{-1}$ for cycle 1, 5.09 $L.min^{-1}$ for cycle 2 and 5.11 $L.min^{-1}$ for cycle 3. Discrepancies were below 3 %. In the second part of the study, when temperature variation was present, the average value was 5.11 $L.min^{-1}$. Table 6.22 details the results obtained in Run 20-07.

Once Run 20-07 had finished, the gasifier-reformer reactor was opened and the catalyst examined: no major changes or physical damage were present. There was not even the brown layer on the catalyst which had

usually showed up on the C11-PR catalyst after DHG tests. In addition, no unconverted naphtha residue was detected in the accumulator meaning 100 % of naphtha conversion to ´inert´ gases despite the electrical disruptions and longer reaction time.

Overall, the results obtained in Run 20-07 are very favourable and bode well for a future DHG implementation at field scale, since factors usually present in field operations like electrical disruptions affecting pressure and temperature, plus a longer time reaction influencing the survivability of catalyst (crushed HiFUEL R110) seem to have had no major or negative consequences for the DHG reaction in the gasifier-reformer. There even occurred a rapid restoration of pressure and temperature to initial values after the cycle.

Table 6.22 Run 20-07: Summary of operating conditions and results obtained during DHG test using naphtha feedstock (Catalyst crushed HiFUEL R110).

Run	20-07 (DHG test)			
Reformer tube dimensions	Φ ½ -inch x 72 cm			
Catalyst type	Crushed HiFUEL			
Catalyst loading (g)	36.5			
Original catalyst size	10 ½ -inch x 13 mm			
Steam to carbon molar ratio (Naphtha) *	6			
Total inlet flow rate ($L.min^{-1}$) *	0.0110			
Naphtha inlet flow rate ($L.min^{-1}$) *	0.0020			
Water inlet flow rate ($L.min^{-1}$) *	0.0090			
Pressure (bar) *	155			160
Outlet gasifier-reformer temperature (ºC) *	650			(600 - 750)
Cycles	1	2	3	4
Dry gas outlet flow rate ($L.min^{-1}$) *	5.13	5.09	5.11	5.11
Conversion (%) *	100	100	100	100
Produced dry gas composition (%) **				
H_2	63	62	61	62
CO	4	4	7	6
CO_2	10	10	11	10
CH_4	23	23	20	22
(*) Average values				
(**) Standard deviation of average values is ± 2 %				

However, as a point to notice, a better and more efficient back pressure regulator at higher pressure is recommended to reduce fluctuations in the system, and further studies on increasing inlet flow rates to favour a transitional or turbulent flow pattern in the reactor would be beneficial despite the fact that the conversion obtained in this investigation are very positive and highly acceptable.

A higher inlet flow rate definitely is a variable to take into account since an optimal value would permit the reduction of fluctuations and a good relation of conversion to coke formation to dry gas outlet flow rate or an optimal volume of generated gases.

For safety reasons, the reactivation treatment was not carried out after the 1705 minutes of operation (over 28 hours). The reactor tube material does not permit a longer operation time safely as has been discussed, but based on the good performance and appearance of the catalyst after the experiment, it is presumed that crushed HiFUEL R110 reactivation might not be a problem. In practice, certainly this step is one to consider as an operational requirement, which can be conducted in an 'off-line' manner.

Constraint of gasifier-reformer reactor material under operating conditions used in Run 20-07: The final condition of the gasifier-reformer reactor material was not optimal when Run 20-07 culminated. Figure 6.46 shows the gasifier-reformer tubes utilised in repeat tests (2) and both of them exhibited some damage after the tests in the first section.

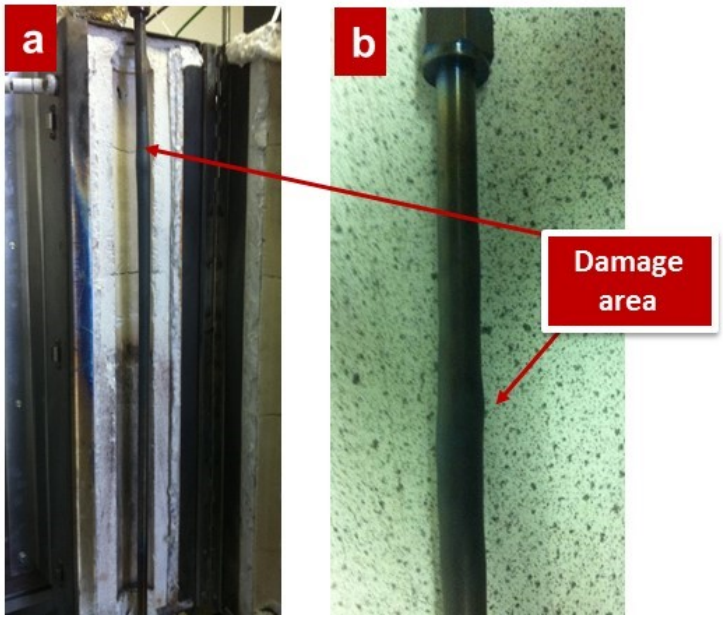

Figure 6.46 Final condition of gasifier-reformer used in Run 20-07 using naphtha feedstock (Catalyst crushed HiFUEL R110) (a) reactor tube in gasification-reforming furnace, (b) damage area.

Deformation was located in the first section of the tube (blended area) which is indicative since the main heat transfer and pressure changes occur in this region. Thermal shock between the entrance feed and internal reactor temperatures, irreversible conversion of naphtha on the catalyst bed and rapid increase of pressure by the produced gases are phenomena that generate considerable tension deforming the tube (Kemin et al., 2004, Pacheco et al., 2001, Shayegan et al., 2008).

SEM images and XDS analysis were carried out on this area in one of the tubes. For the analysis, an electronic microscopy FEI, model QUANTA FEG 250 in PDVSA Intevep, Venezuela, was used. Figure 6.47 shows the images.

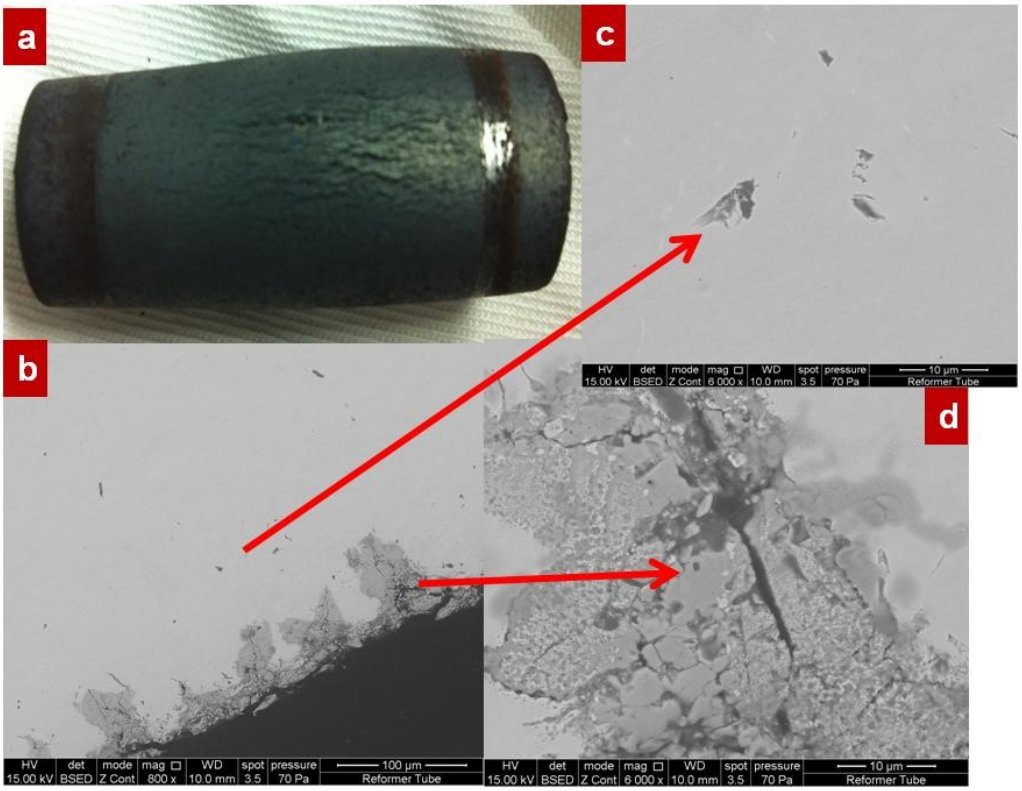

Figure 6.47 SEM images of the damage area from gasifier-reformer after Run 20-07 using naphtha feedstock (Catalyst crushed HiFUEL R110) (a) frontal view (b) frontal view: 15 KV, x800, 100 µm, BSED (c) zoom in: SEM image b - 15 KV, x6000, 10 µm, BSED (d) zoom in: SEM image b - 15 KV, x6000, 10 µm, BSED.

The damage exhibits severe creep and stress. API 571 (2010), on damage mechanisms affecting fixed equipment in the refining industry, mentions that this type of damage is caused by high temperature and pressure and normally occurs when material is operating above the creep limit or maximum pressure and temperature permitted for a specific material. SEM images (b), (c) and (d) showed the presence of some dark spots indicative of carbon inside the tube metal which can fall off the tube leaving those physical spaces empty which may lead to an eventual rupture. No coke presence was detected.

This occurred in Run 20-07: the severe operating conditions of pressure and temperature plus the longer test period led to the damage on the tube reactor. As was mentioned in chapter 3, section 3.3.3, this eventuality was always taken into consideration since the material selected was not the most adequate. However, this damage did not affect the DHG experimental phase and results.

In future work, a material replacement is recommended, especially if experimental studies involve higher pressure than 160 bar and longer durations. Several works (Azadi et al., 2010, Azadi and Farnood, 2011,

Castello, 2013, Papadias et al., 2010, Susanti et al., 2010, Susanti et al., 2011) have reported steam reforming studies carried out successfully at high pressure (>70 bar) and temperature (400-800 ºC) using Hastelloy as reactor material. This material is widely used in refineries and hydrogen production plants for steam reforming and biomass gasification.

Additional SEM images taken of the crushed HiFUEL R110 after Run 20-07 are shown in Figure 6.48. Results indicated that the crushed HiFUEL catalyst did not suffer any evident damage, coke deposition or the thin brown layer on the catalyst as had been usual for the C11–PR catalyst in previous runs.

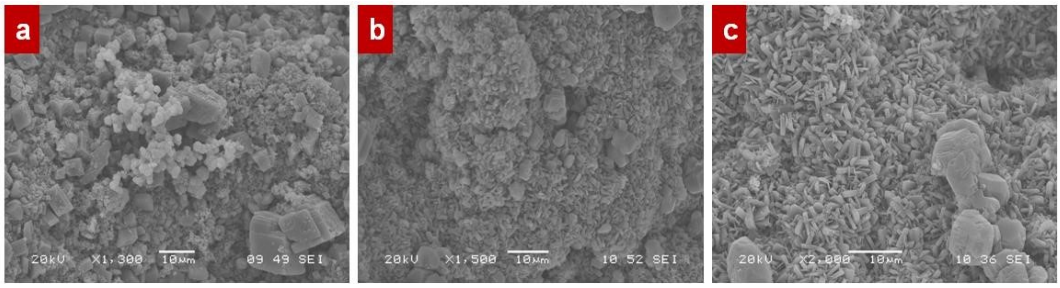

Figure 6.48 SEM images of crushed HiFUEL R110 catalyst after Run 20-07 using naphtha feedstock (a) side view: 20 KV, x1300, 10 µm, SEI (b) side view: 20 KV, x1500, 10 µm, SEI (c) side view: 20 KV, x2000, 10 µm, SEI.

Unexpectedly, the crushed HiFUEL R110 still showed a porosity similar to the original crushed catalyst prior to the DHG test (Figure 6.34, section 6.4) and no coke deposits. Some nickel and calcium crystals spread over the surface were even still observed. Due to the high pressure and temperature, apart from crystallization, some areas showed evidence of a sintering process. In general terms, the catalyst exhibited good performance indicative of good catalytic activity and mechanical properties.

It is interesting to mention that additional SEM images of the crushed HiFUEL R110 after the test were taken by the physics department in order to be shown in *Images of Research*, exhibition 2012 which took place at the Octagon, Milson Place in Central Bath. The reason was the unusual variety of forms and crystals found in just one surface sample on which just one type of feedstock (naphtha) was passed through in just run (20-07). Figure 6.49 exhibits the SEM images.

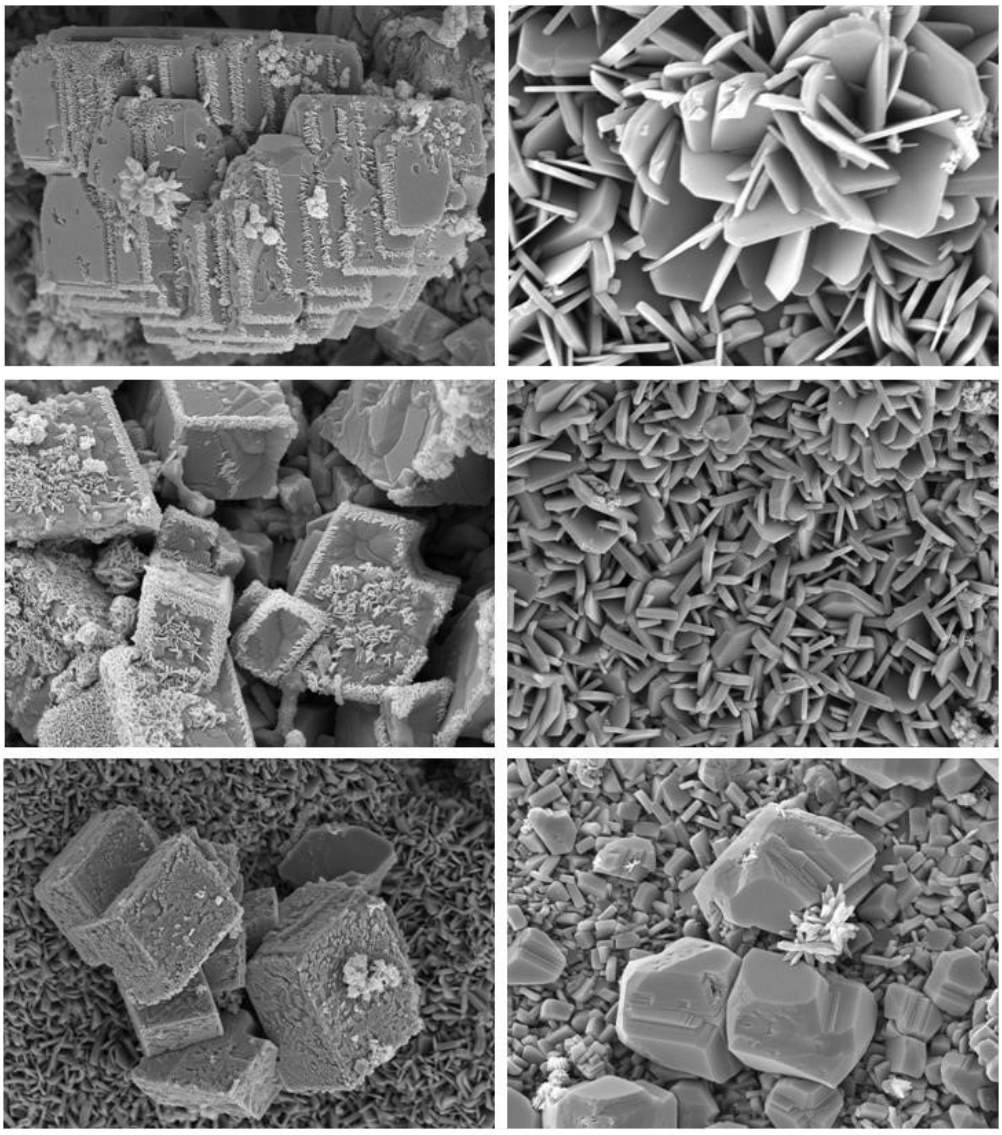

Figure 6.49 SEM images of crushed HiFUEL R110 after Run 20-07 using naphtha feedstock. Every image was taken at 20 KV, x8500, 10 μm, SEI on same sample in different areas (*Images of Research 2012*, Octagon Milson Place, Bath).

6.5 Space velocity, residence time, Reynolds number and mass balance analysis

As has been mentioned, the relatively low inlet flow rates used here certainly contributed to some disturbances: fluctuations in the signal stability of pressure and produced dry gas composition (vol. %) curves during the sampling procedure. To support this observation, space velocity (SV), residence time and Reynolds number (Re) were calculated and the values are showed in Table 6.23. Additionally, a mass balance corresponding to Run 20-07 is also showed as example mode (Table 6.24). Equations and data are described in chapter 4, section 4.3.3 and Appendix B, Sections B.4, B.5, B.6 and B.7.

Calculated space velocity and residence time are much lower in comparison to those reported by Greaves et al., (2006) and Greaves et al., (2008) in Table 6.19, section 6.4.2 despite the fact that we used the same inlet flow rate range for naphtha and water. This is attributed to their addition of reservoir gas to the hydrocarbon feedstock (pentane/naphtha). Our investigation did not add reservoir gas as part of the feedstock. In the reservoir, the crude oil is saturated with gas. When vaporised, the light end and gas are evaporated, therefore, it is important to have used methane as part of the naphtha feedstock. However, it is necessary first to evaluate if this is the best combination. If not, the vaporiser may have two sections: (1) low temperature to remove the gas, and (2) higher temperature to vaporise naphtha.

Our engineering parameters values, however, are indeed comparable to those reported by Picou et al., (2009), Alzadi et al., (2010) and Susanti et al., (2011) in Table 6.19 who performed steam reforming experiments over 200 bar at 450-770 ºC using only liquid organic feedstock with no gas presence. This is reasonable and it is also convenient at lab scale.

Higher inlet flow rates together with the relatively small reactor tube length via laboratory experiments would require very large quantities of feedstock to operate continuously and, in the case of tests of long duration, it would also mean a greater safety risk. In such a case, pilot scale or trials of implementation of DHG process at field scale would be ideal: any increase of inlet flow rates and reactor tube length would undoubtedly produce more produced dry gas volume (gas cap) enabling more oil to be displaced from a reservoir in a shorter time, meaning higher economic benefits.

Theoretically this is feasible since steam reforming reactions are relatively fast, so that higher inlet flow rates would lead to the increase of the mass transfer processes helping to transfer more reactants onto the catalytic surface and, at the same time, remove products recently formed (Daszkowskl and Eigenberger, 1992). In this regard, studies of the DHG process of flow rates, space velocity and residence time, and how these all influence the conversion and produced dry gas volume would be advantageous for future work and trials on a larger scale.

Regarding the Reynolds number, our calculations indicated relatively low values and a laminar flow pattern. Unfortunately, the literature review did not report values for comparison but studies like those carried out by Picou et al., (2009), Alzadi et al., (2010) and Susanti et al., (2011) which operated at similar operating conditions of pressure, temperature, reactor dimensions and catalyst bed to ours, therefore, they might have been performed under the same laminar flow pattern. In theory, this is not positive for steam reforming reactions.

Table 6.23 DHG tests using naphtha feedstock: Space velocity, residence time and Reynolds number.

	Run	Operating conditions *	Variable *	Flow rate (L.min⁻¹) *			Hydrogen in produced dry gas (vol. %) *	Space velocity (h^{-1})	Residence time (s)	Reynolds number, *Re*
				Total inlet	Inlet (feedstock)	Outlet (dry gas)				
C11 - PR [Loading: 15.2 g, (6 x 6 x 2) mm] Gasifier-reformer [Dimensions: Φ ¾ -inch x 30 cm]	20-01	750 ºC 10 bar S/C= 7	**Catalyst activation**	(water + CH4)	(CH4)	4.12	75.63	24300.23	0.15	971.45
				1.8090	1.8000					
	20-01	650 ºC 10 bar S/C= 6	**First trial**	(water + naphtha)	(naphtha)	5.06	Unavailable by coke formation	666.60	5.40	20.47
				0.0110	0.0020					
	20-02	650 ºC 10 bar	**Steam to carbon (S/C) ratio**	(water + naphtha)	(naphtha)					
			30	0.0094	0.0004	0.86	75.00	2497.40	1.22	127.20
			20	0.0096	0.0006	1.36	74.63	2007.08	1.79	82.14
			15	0.0098	0.0008	1.80	70.18	1544.10	2.33	60.25
			10	0.0101	0.0011	2.45	67.28	1101.71	3.27	39.78
			6	0.0110	0.0020	5.09	65.10	666.60	5.40	20.47
	20-03	650 ºC S/C= 6	**Pressure (bar)**	(water + naphtha)	(naphtha)					
			82	0.0110	0.0020	5.07	63.48	81.29	44.28	20.47
			110			5.04	64.40	60.60	59.41	20.47
C11 - PR [Loading: 36.1 g, (6 x 6 x 2) mm] Gasifier-reformer [Dimensions: Φ ¾ -inch x 72 cm]	20-04	750 ºC 10 bar S/C= 7	**Catalyst activation**	(water + CH4)	(CH4)	4.09	71.98	10125.10	0.36	971.45
				1.8090	1.8000					
	20-04	650 ºC S/C= 6	**Pressure (bar)**	(water + naphtha)	(naphtha)					
			82	0.0110	0.0020	5.17	61.88	33.87	106.28	20.47
			110			5.11	61.38	25.25	142.57	
			130			5.06	59.50	21.37	168.50	
	20-05	650 ºC S/C= 6	**Pressure (bar)**	(water + naphtha)	(naphtha)					
			(140-160)	0.0110	0.0020	5.10	55.50	18.52	194.42	20.47
Crushed HiFUEL [Loading: 36.5 g] Gasifier-reformer [Dimensions: Φ ¾ -inch x 72 cm]	20-06	750 ºC 10 bar S/C= 7	**Catalyst activation**	(water + CH4)	(CH4)	4.11	75.88	13103.07	0.27	490.68
				1.8090	1.8000					
	20-06	650 ºC S/C= 6	**Pressure (bar)**	(water + naphtha)	(naphtha)	5.12	61.13	23.19	155.24	10.34
			155	0.0110	0.0020					
	20-07	650 ºC 155 bar S/C= 6	**Shut down/ start up cycle**	(water + naphtha)	(naphtha)					
			1	0.0110	0.0020	5.13	62.63	23.19	155.24	10.67
			2			5.09	62.13			
			3			5.11	61.25			
		160 bar S/C= 6	**Temperature (ºC)**	(water + naphtha)	(naphtha)					
			600	0.0110	0.0020	5.11	61.88	21.25	169.42	11.26
			650					22.47	160.25	10.34
			700					23.68	152.01	10.11
			750					24.90	144.59	8.81

(*) Average values

Table 6.24 Run 20-07: Mass balance.

RUN 20-07 (DHG test)	IN Total inlet ($kg.s^{-1}$)		OUT Total outlet ($kg.s^{-1}$)						BALANCE ($kg.s^{-1}$)
			Produced dry gas				Liquid products		
	Naphtha	Water	H_2	CO	CO_2	CH_4	Naphtha	Water	
DHG Test (Cycle 1)	2.35E-05	1.53E-04	9.63E-06	1.61E-05	6.64E-05	5.61E-06	-	7.10E-05	7.76E-06
DHG Test (Cycle 2)	2.35E-05	1.53E-04	9.63E-06	1.65E-05	7.09E-05	5.66E-06	-	7.10E-05	2.81E-06
DHG Test (Cycle 3)	2.35E-05	1.53E-04	9.45E-06	2.58E-05	7.67E-05	5.04E-06	-	7.10E-05	-1.15E-05
DHG Test (Temperature variation)	2.35E-05	1.53E-04	9.57E-06	2.40E-05	6.55E-05	5.52E-06	-	7.10E-05	9.10E-07
TOTAL	9.40E-05	6.12E-04	3.83E-05	8.24E-05	2.80E-04	2.18E-05	-	2.84E-04	-1.00E-08

Studies on hydrogen production via steam reforming at industrial scale with pressures lower than 30 bar have reported that a turbulent flow pattern favours mass and heat transfer and, reduces the influence of external diffusion. That means higher conversions and easier removal of coke deposits from the catalyst (Daszkowskl and Eigenberger, 1992, Schwaab et al., 2009, Xu and Froment, 1989, Melo and Morlanes, 2008, Eduardo et al., 2009).

Extrapolating from this, our low Re values seem not to affect our experimental results at much higher pressures (110-160) bar. Total conversion and no coke formation were always observed. In the case of H_2 production, the values were also considerable. This leads to the supposition that the effect of the flow pattern is negligible or less sensitive as pressure increases up to 160 bar.

Mass balance was calculated for the DHG tests using naphtha feedstock to ensure technical reliability of the experimental results. No major inconveniences were found, discrepancies are below 10 % which is acceptable within the engineering environment. Uncertainties are detailed in chapter 4, section 4.3.4.

As has been mentioned, Table 6.24 showed a mass balance for Run 20-07 as an example.

6.6 Technical feasibility

Greaves et al., (2006) and Greaves et al., (2008) reported the general technical-economic feasibility of implementing DHG in light oil reservoirs. In this investigation, the experimental results demonstrate that a H_2 concentration over 60 % at (150-160) bar with total conversion of naphtha, no coke formation and a stable catalyst performance, despite suboptimal conditions (Run 20-06 and Run 20-07 with crushed HiFUEL R110).

The DHG process concept currently envisages a conversion of a fraction of the vaporised oil to provide the naphtha feedstock with the remainder fed into the production well. Once the DHG unit is started, the produced dry gas and unconverted water are injected into the reservoir. The expanding gas cap created at the top of the reservoir displaces the oil while unconverted water replaces some, or all, the displaced oil pore space. This would increase the efficiency of DHG since two fronts simultaneously act balancing viscous, gravity and capillary forces into reservoirs. In addition, catalyst activation/reactivation treatments via steaming or using reservoir gas feedstock are included to extend catalyst survivability within the reactor and these treatments would be carried out in an off line manner.

Previously, Greaves et al., (2006) and Greaves et al., (2008) considered the recycling of unconverted water into the DHG unit: however, the

injection of water directly to the reservoir is more beneficial. The continuous injection of fresh water from the surface to the DHG unit certainly requires higher operation costs but the incremental oil obtained undoubtedly compensates for this.

Recently, oil prices have increased to over $100/bbl which provides more incentive for future work to focus on an analysis of this new process design, the reservoir engineering parameters, electrical supply, the DHG unit design, heat recovery and other points to complete the picture of the feasibility of DHG implementation at field scale.

So far, the gasifier-reformer dimensions used here might be a starting point for a future pilot test. It would be feasible to use the same internal diameter with a considerable increase of reactor length and a more resistant tube material. Oil well completions support a tube length between (7-15) m depending on the reservoir depth and the type of well (horizontal or vertical). Materials like Hastelloys are already commercial and produced on a large scale for industrial purposes.

Renpu (2011) indicates that an average size of the internal casing diameter of devices (eg. Downhole pump) inserted into the producing area specifically of the oil well is between (0.18-0.25) m, so that 6-8 tubes disposed in parallel as gasifier-reformer reactors as minimum is an option: in this scenario, the volume of produced dry gas and disposal water per time unit would increase greatly. Greaves et al., (2006) reported 1.12 m^3 total gas volume generated at 150 bar per Kmol of n-butane and 50 % of conversion with just one gasifier-reformer reactor tube. If the number of tubes is increased as suggested above as a minimum value since the number of tubes might reach up to 15-18, we might work this out on a triangular pitch ca. (6-8) times that value instead, at least 7.89 m^3 approximately.

Using the experimental results from Run 20-07 (section 6.4.3) using naphtha feedstock at 160 bar, the volume would increase even more since total feedstock conversion was observed and, more importantly, hydrogen concentration was around 60 vol. %. If just hydrogen is considered, which is actually the effective displacing gas in DHG process, it is probable that over 10 % more of 7.89 m^3.could be included in the calculations. Even just this volume of hydrogen added to the unconverted water to be discharged into reservoir (new concept) undoubtedly represents a very considerable volume directed at displacing oil more efficiently to the surface.

Clearly this is very promising for future work. There are thousands of depleted light oil reservoirs around the world which fall into pressures less than 200 bar. Conversely, in oil reservoirs at pressures higher than 220 bar, DHG is also technically feasible using necessarily supercritical conditions of water (>221 bar, 374 ºC). Articles on biomass gasification have reported important H_2 production and feedstock conversion.

However, there might be limitations in economic terms and also on the survivability of the infrastructure due to the fact that water at those conditions is very corrosive.

The literature survey, chapter 2, described several advantages of DHG implementation in field operations, one of them being the idea of ´Hydrogen storage´ once the economically recoverable oil has been displaced. The hydrogen may be sold afterwards for the emerging ´Hydrogen economy´ extending the profits generated.

It may add that the potential for the DHG application for heavy oil reservoirs as a new technique of oil recovery coupled with chemicals in a WAG displacement looks interesting. This proposal is based on the study reported by Luo et al., (2013) where mixtures of $H_2/CO_2/N_2$ with polymers/surfactants are used in heavy oil recovery from reservoirs. Extrapolating from this study, using DHG would generate H_2 with other gases of $CO/CO_2/CH_4$ into heavy oil reservoirs using naphtha as feedstock, this being extracted and vaporised directly from the oil with only chemicals being added.

Certainly, the naphtha fraction percentage is lower in heavy oil than in light oil but the process is similarly feasible. In regards to the conversion and volume of produced dry gas composition, both might be optimised by adjusting variables such as catalyst loading, S/C ratio, gasifier-reformer temperature and reactor dimensions.

6.7 Concluding remarks

In the previous investigation carried out by Greaves et al. (2006) and Greaves et al., (2008), the DHG process was tested in experiments using a mixture of pentane, or naphtha and reservoir gas, at pressures up to 130 bar. In this investigation DHG experiments were performed using naphtha feedstock, extending the pressure up to 160 bar in a revamped small pilot scale rig. Using a wide range of S/C ratio, longer reactor tube, increased from 30 cm to 72 cm, higher catalyst loading, increased from 15.2 g to 36.5 g, were tested, together with two types of catalyst, C11-PR and HiFUEL R110.

Another advance on the previous investigations was the simulation of dynamic operational adjustments like electrical disruptions, through shutdown/start up cycles within the DHG experiments. These special tests showed the robustness of the DHG process, especially catalyst performance, when subjected to severe operational upsets.

The analysis of the experimental results in this chapter have led to the following conclusions:

1. Under DHG conditions, 650 ºC and 80 to 160 bar pressure as may exist in watered-out light oil reservoirs, the produced dry gas composition in the gasifier-reformer reactor was (56-63) vol. % of H_2 plus other inert gases, CO, CO_2 and CH_4 using S/C ratio of 6. The best result was obtained with the crushed HiFUEL R110 catalyst and a tube reactor length of 72 cm, but the results with the CP11-PR catalyst and a tube reactor length of 30 cm were also similarly favourable. In all cases, total conversion of naphtha was observed with no coke deposits on the catalyst. This indicates that the DHG process produces sufficient high concentrations of H_2 together with similar volumes of other inert gases to achieve significant incremental oil recovery using an immiscible process like GSGI (Gravity stabilised gas injection) or WAG (Water alternating gas).

2. Overall, the percentage of H_2 in the produced dry gas composition decreased by 8 % approximately in the DHG experiments at 650 ºC and S/C= 6 when the pressure increased from 80 bar to 160 bar, remaining at over 55 vol. %. From the previous DHG investigations (Greaves et al. 2005, Greaves et al. 2006, Greaves et al. 2008) this was unexpected, since their results with methane feedstock showed a more pronounced declining trend from over 60 % to less than 40 % in vol. as pressure was increased from 60 bar to 90 bar, and when they used naphtha plus reservoir gas as feedstock, their results showed the H_2 concentration ranging from 35 vol. % to 60 vol. % when operated at temperatures of (710-760) ºC and pressures from 60 to 130 bar.

3. The volume of produced dry gas decreased slightly (less than 5 %) as the pressure increased from 80 bar to 160 bar. This also contrasts with the previous results of Greaves et al., 2005, Greaves et al., 2008 where more severe declines in gas production were reported with increasing pressure up to 100-130 bar. However, volume of produced dry gas was very sensitive to the S/C ratio, beyond a value of 6. At higher S/C ratios, H_2 concentration increased but the volume of produced dry gas decreased. This affects the efficiency the DHG process in the rapid formation of a gas cap for the displacement of oil from reservoirs. In practice, the selection of the S/C ratio, will tend to be the lowest possible, commensurate with its technical efficiency and economic performance.

4. The DHG experiments with shutdown/start up cycles followed by variation of temperature (600 to 750 ºC) at higher pressure (140-160) bar indicated a rapid recovery. Although there was a large disturbance of the H_2 concentration, it quickly returned to its original level. Importantly, the crushed HiFUEL R110 showed a porosity similar to the original crushed catalyst and no coke deposit on its surface, after 1705 minutes of operation (over 28 h). This a very important feature of the DHG process, if it is to operate continuously over long periods in the field.

5. The relatively low inlet flow rates used in the DHG experiments contributed to some disturbances, and fluctuation of the pressure and produced dry gas composition (vol. %), especially during gas sampling. As a consequence, the space velocity, residence time and Reynolds number

were also low. In practice at field scale, higher inlet flow rates and a longer reactor tube length would be employed.

6. Instead of producing the unconverted water, it may be preferable in terms of oil recovery efficiency, to reinject the water into the reservoir.

References

ABASHAR, M.E.E., 2013. Steam reforming of n-heptane for production of hydrogen and syngas. *International journal of hydrogen source,* 38, pp. 861-869.

ALIZADEH, R., JAMSHIDI, E. AND ALE-EBRAHIM, H., 2007. Kinetic study of nickel oxide reduction by methane. *Chemical engineering technology,* 30(8), pp. 1123–1128.

AMERICAN PETROLEUM INSTITUTE, 2010. *Damage mechanisms affecting fixed equipment in the refining industry.* 2nd edition. Washington: API Publishing Services.

AZADI, P., OTOMO, J., HATANO, H., OSHIMA, Y. AND FARNOOD, R., 2010. Hydrogen production by catalytic near-critical water gasification and steam reforming of glucose.

AZADI, P. AND FARNOOD, R., 2011. Review of heterogeneous catalysts for sub- and supercritical water gasification of biomass and wastes. *International journal of hydrogen energy,* 36, pp. 9529-9541.

BARTHOLOMEW, C. AND FARRAUTO, R., 2006. *Fundamentals of industrial catalytic processes.* New York: Willey Press.

BYRD, A., PANT, K. AND GUPTA, R., 2007. Hydrogen production from ethanol by reforming in supercritical water using Ru/Al_2O_3 catalyst. *Energy fuels,* 21, pp. 3541-3547.

CASTELLO, D., 2013. *Supercritical water gasification of biomass.* Thesis (PhD). University of Trento, Trento.

CHEEKATAMARLA, P., THOMSON, W., 2006a. Hydrogen generation from 2,2,4 - trimethylpentane reforming over molybdenum carbide at low steam to carbon ratios. *Journal power sources,* 156, pp. 520-524.

CHEEKATAMARLA, P. AND THOMSON, W., 2006b. Catalytic activity of molybdenum carbide for hydrogen production generation via diesel reforming. *Journal of power sources,* 158, pp. 477-484.

CHEN, Y., YUAN, L., YE, T., ET AL., 2009. Effects of current upon hydrogen production from electrochemical catalytic reforming of acetic acid. *International journal hydrogen energy,* 34, pp. 1760-1770.

CHRISTENSEN, K.O., 2005. Steam Reforming of Methane on Different Nickel Catalysts. Thesis (PhD). Norwegian University of Science and Technology, Trondheim.

DASZKOWSKL, T. AND EIGENBERGER, G., 1992. A reevaluation of fluid flow, heat transfer and chemical reaction in catalyst filled tubes. *Society of chemical engineers,* 47, pp. 2245 2250.

EDUARDO, L.G., OLIVEIRA, C.A., GRANDE, A.L. AND RODRIGUES, E.R., 2009. Methane steam reforming in large pore catalyst. *Chemical engineering science,* 65(2010), pp. 1539–1550.

FROMENT, G.F., 2008. Kinetic modelling of hydrocarbon processing and the effect of catalyst deactivation by coke formation. *Catalysis reviews,* 50, pp. 01-18.

GREAVES, M., RATHBONE, R., XIA, T., BENTHAHER, A., DUGGAN, S., 2004. *Downhole gasification for improved oil recovery and gas production (phase 1) experimental studies (1 Nov 2002 – 31 Oct 2004).* United Kingdom: University of Bath, (Confidential internal report).

GREAVES, M., XIA, T., RATHBONE, R. AND BENTAHER, A., 2005. Underground gasification for improved oil recovery. *Canadian international petroleum conference,* 7-9 June 2005 Calgary. Calgary: Petroleum Society Canadian Institute of Mining, Metallurgy & Petroleum, pp. 38-48.

GREAVES, M., RATHBONE, R., XIA, T., BENTHAHER, A., 2006. Experimental study of a novel In situ gasification technique for improved oil recovery from light oil reservoirs. *JCPT,* 45(8), pp. 41-47.

GREAVES, M. AND XIA, T.X., 2008. Producing hydrogen and incremental oil from light oil reservoirs using downhole gasification. *Canadian international petroleum conference,* 17-19 June 2008 Calgary. Calgary: Petroleum Society Canadian Institute of Mining, Metallurgy & Petroleum, pp. 14-24.

HAO, S.R., 1997. Hydrocarbon steam-reforming process: feedstock and catalysts for hydrogen production in china. *International journal of hydrogen energy,* 23(5), pp. 315. 319.

HUTCHINSON, C. A., BRAUN, P.H., 1961. Phase Relations of Miscible Displacement in oil Recovery. *AIChE J.*, 7, pp. 64-72.

KEMIN, L., HAI-YAN, G., SHI-WEI, P., 2004. A study on naphtha catalytic reforming reactor simulation and analysis. *Journal of zhejiang university SCIENCE,* 6B(6), pp. 590-596.

KULKARNI, M.M., 2005. *Multiphase mechanisms and fluid dynamics in gas injection enhanced oil recovery processes.* Dissertation (PhD). Louisiana State University, U.S.

LAKE, L.W., WALSH, M.P., 2008. *Enhanced oil recovery (EOR) field data: literature search.* U.S.: University of Texas.

LACHANCE, R., 2005. *A fundamental study of model fuel conversion reactions in sub and supercritical water.* Thesis (PhD). Massachusetts Institute of Technology, Massachusetts.

LEE, S., JOONGMYEON B.B., SUNGKWANG L.C. AND JOONGUEN P., 2008. Improved configuration of supported nickel catalysts in a steam reformer for effective hydrogen production from methane. *Journal of power sources,* 180, pp. 506–515.

LI, L., WANG, X.G., SHEN, K., ZOU, X.J., LU, X.G., DING, W.Z., 2010. Highly efficient $Ni/CeO_2/Al_2O_3$ catalyst for pre-reforming of liquefied petroleum gas under a low molar ratio of steam to carbon. *Chinese journal catalysis,* 31, pp. 525-527.

LUO, P., ZHANG, Y. AND HUANG, S., 2013. A promising chemical augmented WAG process for enhanced heavy oil recovery. *Fuel,* 104, pp.333-341.

OSADA, M., SATO, T., WATANABE, M., SHIRAI, M. AND ARAI, K., 2007. Catalytic gasification of wood biomass in subcritical and supercritical water. *Combustion science and technology,* 178(1-3), pp. 537-552.

PACHECO, M., SIRA, J. AND KOPASZ, J., 2001. Reaction kinetics and reactor modelling for fuel processing of liquid hydrocarbons to produce hydrogen: isooctane reforming. *Applied catalysis A,* 250, pp.161–175.
PAPADIAS, D.D., LEE, S.H.D., FERRANDON, M. AND AHMED, S., 2010. An analytical and experimental investigation of high-pressure catalytic steam reforming of ethanol in a hydrogen selective membrane reactor. *International journal of hydrogen energy,* 35, pp. 2004–2017.
PICOU, J., WENZEL, J., LANTERMAN, H. AND LEE, S., 2009. Hydrogen production by noncatalytic autothermal reformation of aviation fuel using supercritical water. *Energy fuels,* 23, pp. 6089-6094.
PINKWART, K., BAYHA, T., LUTTER, W. AND KRAUSA, M., 2004. Gasification of diesel oil in supercritical water for fuel cells. *Journal power sources,* 136, pp. 211-214.
RASE, H., 1977. *Chemical reactor design for process plants vol.2: Case studies.* New York: John Wiley & Sons.
RASHIDI, H., EBRAHIM, H.A. AND DABIR, B., 2013. Reduction kinetics of nickel oxide by methane as reducing agent based on thermogravimetry. *Thermochimica acta,* 561(3), pp. 41– 48.
RENPU, W., 2011. *Advanced well completion engineering.* 3rd. edition, Oxford: Elsevier, Ltd.
RICHARDSON, J., 1989. *Principles of catalyst development.* New York: Plenum Press.
SHAYEGAN, J., YOUSEF MOTAMED HASHEMI, M. M. AND VAKHSHOURI, K., 2008. Operation of an industrial steam reformer under severe condition: A simulation study. *The Canadian journal of chemical engineering,* 86, pp. 747–755.
SHAYEGAN, J., YOUSEF MOTAMED HASHEMI, M. M. AND VAKHSHOURI, K., 2008. Operation of an industrial steam reformer under severe condition: A simulation study. *The canadian journal of chemical engineering,* 86, pp. 747–755.
SHINKU, L., JOONGMYEON B., SUNGKWANG L. AND JOONGUEN, P., 2008. Improved configuration of supported nickel catalysts in a steam reformer for effective hydrogen production from methane. *Journal of power sources,* 180, pp. 506–515.
SCHUTLE, W.M., 2005. Challenges and strategy for increased oil recovery. Proceedings of the *International Petroleum Technology Conference,* 21-23 November 2005 Doha. Qatar: pp. 02-09.
SCHWAAB, M., ALBERTON, A.L., FONTES, C.E., BITTENCOURT, R.C., PINTO, J.C., 2009. Hybrid modelling of methane reformers. 2. Modelling of the industrial reactors. *Ind. Eng. Chem. Res.,* pp. A-G.
STEFANESCU, A., VAN VEEN, A.C., DUVAL-BRUNEL, E., MIRODATOS, C., 2007. Investigation of a Ni-based steam reforming catalyst developed for the coating of microstructures. *Chemical engineering science,* 62, pp. 5092-5096.
SOMORJAI, G.A., 1994. *Principles of surface chemistry and catalysis.* New York: Willey Press.

SPERLE, T., CHEN, D., LODENG, R., HOLMEN, A., 2005. Pre-reforming of natural gas on a Ni catalyst Criteria for carbon free operation. *Applied Catalysis A: General,* 282, pp. 195–204.
SUSANTI, R., VERIANSYAH, B., KIM, J. AND LEE, Y., 2010. Continuous supercritical water gasification of isooctane: A promising reactor design. *International journal of hydrogen energy,* 35(5), pp. 1957-1970.
SUSANTI, R., NUGROHO, A., LEE, J., KIM, Y. AND KIM, J., 2011. Noncatalytic gasification of isooctane in supercritical water: A strategy for high-yield hydrogen production. *International journal of hydrogen energy,* 36, pp. 3895-3906.
TAKENAKA, S., ORITA, Y., UMEBAYASHI, H., MATSUNE, H., MASAHIRO, K., 2008. High resistance to carbon deposition of silica-coated Ni catalysts in propane stream reforming. *Applied catalysis A: General,* 351, pp. 189-194.
TRIMM, D.L., 1997. Coke formation and minimisation during steam reforming reactions. *Catalysis today,* 37, pp. 233-238.
XU, J., FROMENT, G.F., 1989. Methane steam reforming, methanation and water-gas shift: 1. Intrinsic kinetics. *AIChE journal,* 35(1), pp. 88-103.
XU, J., YEUNG, C.M., NI, J., MEUNIER, F., ACERBI, N., FOWLES, M., TSANG, S., 2008. Methane steam reforming for hydrogen production using low water-ratios without carbon formation over Ceria coated Ni catalysts. *Applied Catalysis A: General,* 345, pp. 119–127.

CHAPTER 7: THEORETICAL MAXIMUM OF DHG PRODUCED DRY GAS COMPOSITION USING METHANE AND NAPHTHA FEEDSTOCK

7.1 Introduction

In parallel with the experimental work, a basic numerical DHG model was developed to calculate the theoretical maximum of produced dry gas composition (in the equilibrium) to be compared with the experimental results to enable us to analyse any discrepancies and evaluate the overall performance of the DHG operation in the rig. For this purpose, hydrogen was taken as the main reference point for monitoring since it is the main gas of interest generated in the DHG process for gas displacement in depleted oil reservoirs.

In theory, the experimental results and the theoretical maximum should be comparable in steam reforming, since in this process reactions occur at a considerably high rate on the catalytic Nickel surface, reaching chemical equilibrium (Rostrup-Nielsen, 1984, Elnashaie at al., 1988, Twigg 1989, Kvamsdal et al., 1999, Gould et al., 2007, Wang et al., 2010). Thus, theoretical calculations would help to us understand which operating conditions or parameters should be optimised in the DHG process, and at which measure in order to obtain the desired dry gas composition.

So far, no numerical study for the DHG process has been reported in the literature. The literature only shows numerical studies for pressure values commonly used at industrial scale, below 30 bar; for steam reforming using different hydrocarbon feedstocks, just one exceptional study showed a numerical model at 70 bar approximately using ethanol feedstock with application in fuel cell vehicles (Papadias et al., 2010).

There have, however, been important advances in biomass gasification modelling where ASPEN PLUS, the commercial software, has been utilised to simulate the process with steam reforming reactions involved at pressure values around 221 bar and at temperatures higher than 374 ºC, in sub and super critical water conditions (Azadi et al., 2009, Azadi et al., 2010, Dermibar, 2010, Knezevic et al., 2010, Dermibas, 2010, Karamarkovic and Karamarkovic, 2010, Nahar and Madhani, 2010, Sadooghi and Rauch, 2012, Susanti et al., 2012, Sreejith et al., 2013).

In the current investigation, the commercial software ASPEN PLUS was also used. We simulated the DHG process using methane and naphtha (n-heptane as model surrogate) feedstocks and with the same operating conditions as in the experimental phase described in chapter 5 and chapter 6 for comparison purposes.

Additionally, sensitivity studies of pressure and temperature were carried out to predict DHG behaviour in terms of conversion and hydrogen concentration in equilibrium dry gas (vol. %) in a very wide range of

pressure (2-180) bar and temperatures (500-900) ºC using methane and naphtha (n-heptane as model surrogate).

7.2 Numerical model development

ASPEN PLUS is a problem-oriented software basically used to facilitate the calculation of chemical processes at steady state conditions where the system under study has reached the equilibrium. The literature contains several pieces of research on using this software for steam reforming reactions (Shirley, 2005, Azadi et al., 2009, Azadi et al., 2010, Dermibar, 2010, Knezevic et al., 2010, Susanti et al., 2012).

A study case of interest using this software was reported by Turpeinen et al., (2008) which carried out a theoretical study to calculate equilibrium dry gas composition in steam reforming. For that study, they used coke oven gas, refinery gas and bio gas feedstock at operating conditions normally existent in industrial plants. The numerical results were successfully validated from their experimental results and other chemical software demonstrating that ASPEN PLUS is adequate and reliable.

Aimed at increasing the technical reliability of our results, this investigation also verified manually that the numerical results from ASPEN PLUS are correct. For that purpose, calculations of equilibrium dry gas composition were carried out using methane feedstock and the procedure reported by Shirley´s PhD dissertation (2005). Our manual results were compared against Shirley´s results and ASPEN PLUS. The steps and manual calculations are detailed in Appendix D.

7.2.1 Manual calculation of equilibrium produced dry gas composition

A number of assumptions were made to simplify the calculations. All of the gases were considered ideal gases, which was reasonable since the compressibility factor of the steam/ methane mixture is approximately 0.99 at 500 ºC and 9.5 bar with a steam to carbon (S/C) ratio of 4. No carbon formation was assumed since the purpose of these calculations was to verify and validate ASPEN PLUS as a simulation tool for steam reforming reactions. The chemical species present in the system were CH_4, H_2O, CO, CO_2 and H_2.

The procedure consisted in determining the composition of a gas mixture at equilibrium minimising free Gibbs energy of the system. The technique used has been described by Smith et al. and referenced in Shirley (2005). It calculates the equilibrium constants for steam reforming reactions requiring the simultaneous solution of a smaller set of equations.

Some equations used for equilibrium constants (*K)* determination were:

Relationship between *K* and temperature,

$$\ln K = -\frac{\Delta G_R^o}{RT} \tag{7.1}$$

Van´t Hoff equation can be used to obtain *K* at other temperatures,

$$\ln\left(\frac{K_T}{K_{298}}\right) = \int_{298}^{T}\left(\frac{\Delta H_R^o}{RT^2}\right).dT \tag{7.2}$$

To calculate $\Delta H_{R,\,298}^{\circ}$ at different temperatures, the equation used by Smith et al., reported in Shirley´s PhD dissertation (2005) is related to the specific heat capacities of the various chemical species, Cp_i, as follows:

$$\Delta H_{R,T}^o = \Delta H_{R,298}^o + \frac{1}{\alpha_K}\left[\int_{298}^{T}\left(\sum_{products}\alpha_i.Cp - \sum_{reac\,tan\,ts}\alpha_i.Cp\right).dT\right] \tag{7.3}$$

Where specific heat capacity is given as a function of temperature,

$$\frac{Cp_i}{R} = A_i + B_iT + C_iT^2 + \frac{D_i}{T^2} \tag{7.4}$$

Based on the above equations, $\ln K_T$ calculated in this research is:

$$\begin{aligned}\ln K_T = &-24.92 - 2.278x10^4\,(T^{-1}) + 7.951\ln(T) - 4.354x10^{-3}\,(T)\\ &+ 3.6065x10^{-7}\,(T^2) + 4850(T^{-2})\end{aligned} \tag{7.5}$$

Now, for calculating the composition at equilibrium for steam reforming reactions the solution was performed using Newton´s technique where ε is the molar extent of reaction (moles change of each chemical species at equilibrium),

$$K_1 + \left[\frac{\partial K_1}{\partial \varepsilon_1}\right]\Delta\varepsilon_1 + \left[\frac{\partial K_1}{\partial \varepsilon_2}\right]\Delta\varepsilon_2 = 0 \tag{7.6}$$

$$K_2 + \left[\frac{\partial K_2}{\partial \varepsilon_1}\right]\Delta\varepsilon_1 + \left[\frac{\partial K_2}{\partial \varepsilon_2}\right]\Delta\varepsilon_2 = 0 \tag{7.7}$$

For a given temperature of 700 ºC and pressure of 6 bar with S/C= 2, the values here calculated are compared to those reported by Shirley (2005) and ASPEN PLUS in Table 7.1

The results indicate an almost identical agreement with the results calculated by ASPEN PLUS, effectively validating the use of ASPEN PLUS

in this research. The next step was to calculate the theoretical maximum of produced dry gas in the equilibrium described below.

Table 7.1 Equilibrium dry gas composition at T = 700 ºC, P = 6 bar and S/C= 2.

Component	Calculated mole fraction Shirley (2005)	Calculated mole fraction (This research)	Calculated mole fraction (ASPEN PLUS)
CH_4	0.106	0.103	0.105
H_2O	0.282	0.278	0.281
CO	0.069	0.071	0.070
CO_2	0.067	0.069	0.067
H_2	0.476	0.479	0.477
Total	**1.000**	**1.000**	**1.000**

7.2.2 Calculations of equilibrium produced dry gas composition using ASPEN PLUS

A simple model was set up using the RGibbs equilibrium reactor as is shown in Figure 7.1. This consists of three units or blocks and 5 streams. (1) Stream is designated for water which is vaporised in the HEATER, resulting in stream 2 (steam). This is mixed with methane or naphtha (3) in the MIXER block in the gas phase resulting in (4) stream. This mixture (4) is put into the RGIBBS block (DHG REACTOR) to determine the maximum values of each chemical species in equilibrium. The products are present in (5) stream.

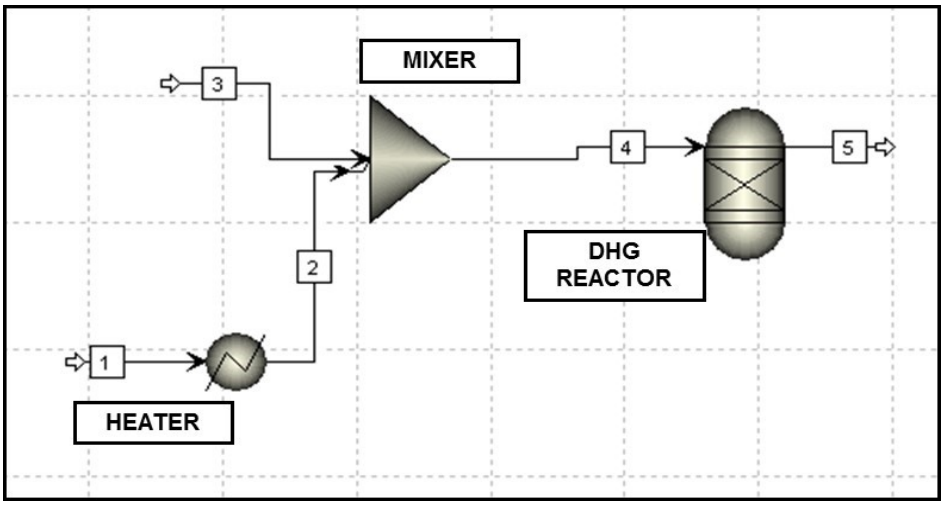

Figure 7.1 DHG reactor flowsheet (ASPEN PLUS).

No carbon deposits (coke) were taken into account in the DHG reactor based on our experimental results. As the RGibbs reactor minimises the Gibbs free energy to attain the equilibrium composition of the produced gases, it was necessary to add other chemical species. The selected

gases were CO, CO_2, H_2O, H_2, CH_4. n-Heptane was used as the model surrogate for naphtha feedstock to facilitate calculations.

Basically, every operating condition of pressure, temperature and steam to carbon (S/C) ratio was put in the DHG REACTOR block. The rest of the blocks were at 1 bar and at a vaporisation temperature of 350 ºC to ensure gas phase only. During numerical runs no major difficulties were found.

Once runs were made a result sheet was shown by ASPEN PLUS. Table 7.2 shows one as an example which corresponded to the catalyst activation treatment process; the operating conditions are 10 bar, 750 ºC and S/C= 7 using methane feedstock.

Table 7.2 Numerical results calculated by ASPEN PLUS. Operating conditions: 10 bar, 750 ºC, S/C= 7 using methane feedstock.

	Stream [1] H_2O (25 ºC, 1 bar)	Stream [2] H_2O (350 ºC, 1 bar)	Stream [3] CH_4 (25 ºC, 1 bar)	Stream [4] Inlet DHG reactor (S/C= 7, 1 bar)	Stream [5] Outlet DHG reactor (750 ºC, 10 bar)
Mole flow rate ($kmol.h^{-1}$)					
CH_4	0.00	0.00	1.00	1.00	0.05
H_2O	7.00	7.00	0.00	7.00	5.41
CO	0.00	0.00	0.00	0.00	0.31
H_2	0.00	0.00	0.00	0.00	3.48
CO_2	0.00	0.00	0.00	0.00	0.64
Total flow rate ($kmol.h^{-1}$)	7.00	7.00	1.00	8.00	9.90
Total flow rate ($kg.h^{-1}$)	126.11	126.11	16.04	142.15	142.15
Total flow rate ($L.min^{-1}$)	2.11	6044.59	413.15	6303.86	1403.41
Temperature (K)	298.15	623.15	298.15	576.18	1023.15
Pressure (bar)	1.00	1.00	1.00	1.00	10.00
Vapor fraction	0.00	1.00	1.00	1.00	1.00
Liquid fraction	1.00	0.00	0.00	0.00	0.00
Solid fraction	0.00	0.00	0.00	0.00	0.00

For comparison with our experimental results, additional calculations were carried out to obtain mole flow rates, the equilibrium dry gas mole fraction and equilibrium dry gas compositions in terms of moles and volume. Table 7.3 shows an example. The run corresponds to the same operating conditions and activation procedure: 10 bar, 750 ºC and S/C= 7 using methane feedstock.

Table 7.3 Equilibrium produced dry gas composition (vol %) calculated by ASPEN PLUS. Operating conditions: 10 bar, 750 ºC, S/C= 7 using methane feedstock.

	Mole flow rate ($kmol.h^{-1}$)	Equilibrium dry gas composition (vol. %)
CH_4	0.05	1.13
H_2	3.48	77.70
CO	0.31	6.97
CO_2	0.64	14.20
Total mole flow rate = 9.90 $kmol.h^{-1}$		
Water mole flow rate = 5.41 $kmol.h^{-1}$		
Total dry gas mole flow rate = 4.48 $kmol.h^{-1}$		

7.3 Numerical results in DHG

Once the numerical DHG model was completed, numerical results were obtained in two stages: (1) the equilibrium dry gas composition (theoretical maximum) at the same operating conditions and with the feedstocks used in the experimental stage in chapter 5 and 6, where the aim was to compare the results in terms of hydrogen concentration; and (2) studies of sensitivity at different temperatures and pressures to envisage the behaviour of the DHG system in terms of conversion and H_2 concentration.

As has been mentioned in chapter 6, hydrogen concentration in produced dry gas composition is used as reference gas since it would form a gas cap to displace oil more efficiently from reservoir to surface in case of DHG implementation at field scale. Under the mechanisms of oil recovery by gas displacement (immiscible process) within which DHG works, H_2 presence is highly desirable. Moreover, the H_2 generated is more valuable than the other gases, being able to be sold once the oil economically recoverable has been displaced and extracted.

The rest of the produced gas values are minorities and their relative solubilities in oil at reservoir conditions might affect the displacement efficiency of oil to surface to a degree which is highly dependent on oil reservoir conditions.

7.3.1 Numerical results at operating conditions used in DHG experimental phase

Table 7.4 and 7.5 show the obtained results. Differences in relation to the experimental results of hydrogen concentration are calculated as follows:

$$\%\ Difference = \frac{(Numerical\ result) - (Experimental\ result)}{Numerical\ result}\ x\ 100\% \qquad (7.8)$$

Table 7.4 and 7.5 show that the difference in the range of hydrogen concentration between the numerical and experimental results oscillates between 2.5 % to 12 % in all pressure ranges with methane and naphtha, an exception being the case of Run 20-05, using naphtha feedstock, whose difference was 17 % at (140-160) bar. This is attributed to mechanical failures of the catalyst suffered during the test which were reflected in a pressure drop (For details, see chapter 6, section 6.3.3). The theoretical conversion will be analysed in the next section 7.3.2.

In theory, the difference between our experimental values and the approach to equilibrium might be acceptable based on results reported by Shustorovich and Sellers (1998), Callaghan (2006) and Cengel and Boles (2008), who have studied and compared theoretical maximum (approach to the equilibrium) of steam reforming reactions on a catalytic surface of Nickel indicating differences below 20 %.

Overall, we may say that there is a relatively close approach to equilibrium, which was expected, given that steam reforming is a fast chemical process on a Nickel surface (Rostrup-Nielsen, 1984, Elnashaie at al., 1988, Twigg 1989, Kvamsdal et al., 1999, Gould et al., 2007, Wang et al., 2010). This is extremely positive since it is indicative of a good performance of our DHG experimental tests, most importantly at the higher pressure corresponding to Run 20-06 and Run 20-07 at (140-160) bar using naphtha feedstock.

Petrov (1998) mentioned that steam reforming reactions and their overall reaction rate are not connected with the reaction mechanism but are determined mainly by the rate of physical processes (diffusional control regime). That means heat and mass transfer might have had more influence on the conversion and H_2 concentration than did the chemical reactions themselves on the catalytic Nickel surface.

Table 7.4 Comparisons between experimental and numerical DHG results using methane feedstock.

Run	Operating conditions *	Variable *	Flow rate ($L.min^{-1}$) *			Conversion (%)	Hydrogen in produced dry gas (vol. %)		Difference (%)
			Total inlet (water + CH_4)	Inlet (CH_4)	Outlet (dry gas)		Experimental *	Numerical	
C11 - PR [Loading: 15.2 g, (6 x 6 x 2) mm] Gasifier-reformer [Dimensions: Φ ½ -inch x 30 cm]									
10-01	750 ºC 10 bar S/C= 7	Catalyst activation	0.8404	0.8360	1.92	96.64	75.47	77.70	2.87
10-02	650 ºC S/C= 3	Pressure (bar)							
		52	2.0044	2.0000	3.67	71.75	47.41	50.06	5.29
		65			3.56	67.00	43.26	47.60	9.12
		80			3.49	62.72	39.38	45.64	13.72
10-03	650 ºC 80 bar	Steam to carbon (S/C) ratio							
		15	0.4044	0.4000	1.32	84.00	70.13	70.76	0.89
		10	0.6044	0.6000	1.56	73.87	62.75	65.31	3.92
		8	0.7544	0.7500	1.87	65.75	55.24	61.94	10.82
		6	1.0044	1.0000	2.00	58.22	49.65	57.30	13.35
		4	1.5044	1.5000	2.84	54.35	45.90	50.48	9.07
		3	2.0044	2.0000	3.50	47.60	40.15	45.64	12.03
10-01	80 bar S/C= 6	Temperature (ºC)							
		600	1.0044	1.0000	1.67	54.62	46.35	50.80	8.76
		650			2.00	60.00	52.58	57.30	8.24
		700			2.28	65.25	55.95	62.82	10.94
		750			2.50	70.37	59.58	67.34	11.52
10-01	750 ºC 10 bar S/C= 7	Catalyst reactivation	0.8404	0.8360	1.87	96.67	73.78	77.70	5.05
(*) Average values									

Table 7.5 Comparisons between experimental and numerical DHG results using naphtha feedstock.

	Run	Operating conditions *	Variable *	Flow rate (L.min⁻¹) *			Conversion (%)	Hydrogen in produced dry gas (vol. %)		Difference (%)
				Total inlet	Inlet (feedstock)	Outlet (dry gas)		Experimental *	Numerical	
C11 - PR [Loading: 15.2 g, (6 x 6 x 2) mm] Gasifier-reformer [Dimensions: Φ ½ -inch x 30 cm]	20-01	750 ºC 10 bar S/C= 7	Catalyst activation	(water + CH4)	(CH4)	4.12	92.45	75.63	77.70	2.66
				1.8090	1.8000					
	20-01	650 ºC 10 bar S/C= 6	First trial	(water + naphtha)	(naphtha)	5.06	Unavailable by coke formation	Unavailable by coke formation	67.73	-
				0.0110	0.0020					
	20-02	650 ºC 10 bar	Steam to carbon (S/C) ratio	(water + naphtha)	(naphtha)		100.00			
			30	0.0094	0.0004	0.86		75.00	76.69	2.20
			20	0.0096	0.0006	1.36		74.63	75.63	1.32
			15	0.0098	0.0008	1.80		70.18	71.63	2.02
			10	0.0101	0.0011	2.45		67.28	69.91	3.76
			6	0.0110	0.0020	5.09		65.10	67.73	3.88
	20-03	650 ºC S/C= 6	Pressure (bar)	(water + naphtha)	(naphtha)					
			82	0.0110	0.0020	5.07	100.00	63.48	67.70	6.23
			110			5.04		64.40	67.35	4.38
C11 - PR [Loading: 36.1 g, (6 x 6 x 2) mm] Gasifier-reformer [Dimensions: Φ ½ -inch x 72 cm]	20-04	750 ºC 10 bar S/C= 7	Catalyst activation	(water + CH4)	(CH4)	4.09	90.05	71.98	77.70	7.36
				1.8090	1.8000					
	20-04	650 ºC S/C= 6	Pressure (bar)	(water + naphtha)	(naphtha)					
			82	0.0110	0.0020	5.17	100.00	61.88	67.70	8.60
			110			5.11		61.38	67.35	8.86
			130			5.06		59.50	67.04	11.25
	20-05	650 ºC S/C= 6	Pressure (bar)	(water + naphtha)	(naphtha)	5.10	100.00	55.50	66.75	16.85
			(140-160)	0.0110	0.0020					
Crushed HIFUEL [Loading: 36.5 g] Gasifier-reformer [Dimensions: Φ ½ -inch x 72 cm]	20-06	750 ºC 10 bar S/C= 7	Catalyst activation	(water + CH4)	(CH4)	4.11	97.13	75.88	77.70	2.34
				1.8090	1.8000					
	20-06	650 ºC S/C= 6	Pressure (bar)	(water + naphtha)	(naphtha)	5.12	100.00	61.13	66.86	8.57
			155	0.0110	0.0020					
	20-07	650 ºC 155 bar S/C= 6	Shut down/ start up cycle	(water + naphtha)	(naphtha)					
			1	0.0110	0.0020	5.13	100.00	62.63	66.75	6.17
			2			5.09		62.13		6.92
			3			5.11		61.25		8.24
		160 bar S/C= 6	Temperature (ºC)	(water + naphtha)	(naphtha)					
			600	0.0110	0.0020	5.11	100.00	61.88	66.03	9.32
			650						66.57	10.06
			700						67.05	10.70
			750						67.32	11.06

(*) Average values

Based on the low difference (%) between the experimental and numerical results in Table 7.4 and 7.5, we may say that heat and mass transfer in our case seem to be favourable at higher pressure (130- 160) bar using a gasifier-reformer reactor tube. In practice, this suggests that the DHG process design described in chapter 6, section 6.6 may certainly be considered for a pilot test or a new experimentation stage on a larger scale. However, increasing the number of tubes to 6 in parallel into the oil well might affect heat and mass transfer. Future work addressed to enhancing these parameters concerning the arrangement of DHG reactor tubes is recommendable.

To analyse more specifically the discrepancies between the experimental and numerical results, Figure 7.2, 7.3 and 7.4 compare values under similar conditions of pressure, steam to carbon (S/C) ratio and temperature respectively. For that comparison, the results obtained with methane (chapter 5) and naphtha (chapter 6) feedstock were both considered. As has been mentioned, no numerical studies in DHG have so far been reported in the literature; therefore, graphs comparing experimental results with methane and naphtha feedstock with their theoretical maximum might be very supportive and illustrative for a better understanding of the process.

In Figure 7.2, DHG results versus pressure, there is a reasonable agreement between the experimental and numerical values at (50-160) bar. That means a close approach to the equilibrium; just a slight divergence beyond 140 bar when C11-PR was used. However, the replacement of C11-PR by the HIFUEL R110 catalyst seems to have compensated for this divergence. This undoubtedly supports the positive evaluation of this latter catalyst mentioned in chapter 6 (section 6.4.2) and the importance that its mechanical properties take on when pressure increases in the DHG process.

Figure 7.2 also shows how H_2 concentration in produced dry gas from naphtha is also significantly higher at (80-160) bar compared to H_2 concentration from methane feedstock at the lower pressure range (50-80) bar. As has been discussed in chapter 6, section 6.3 and 6.4, the main reason is that conversion of naphtha is less affected by increasing pressure than conversion of methane due to the irreversibility of the first reaction in the steam reforming reactions scheme (Chen et al., 2004a, Abashar, 2013).

The significant decline for methane using C11-PR catalyst was 22 % overall (50-80) bar in the experimental results while the theoretical maximum was 12 %. This is commensurate with the experimental results reported by Greaves et al., (2005) with methane who reported approximately 15-30 % in the same range of pressure and with C11-PR as catalyst. For naphtha, the decline in H_2 production at (130-160) bar is about 6 % overall with the same catalyst, C11-PR, and when the catalyst

was changed to HIFUEL R110, the decline was < 3 %. This is indicative of this latter catalyst's ability to maintain conversion at high pressure, which is vitally important in the case of the DHG process. The numerical results or theoretical maximum only show a decline below 2 %.

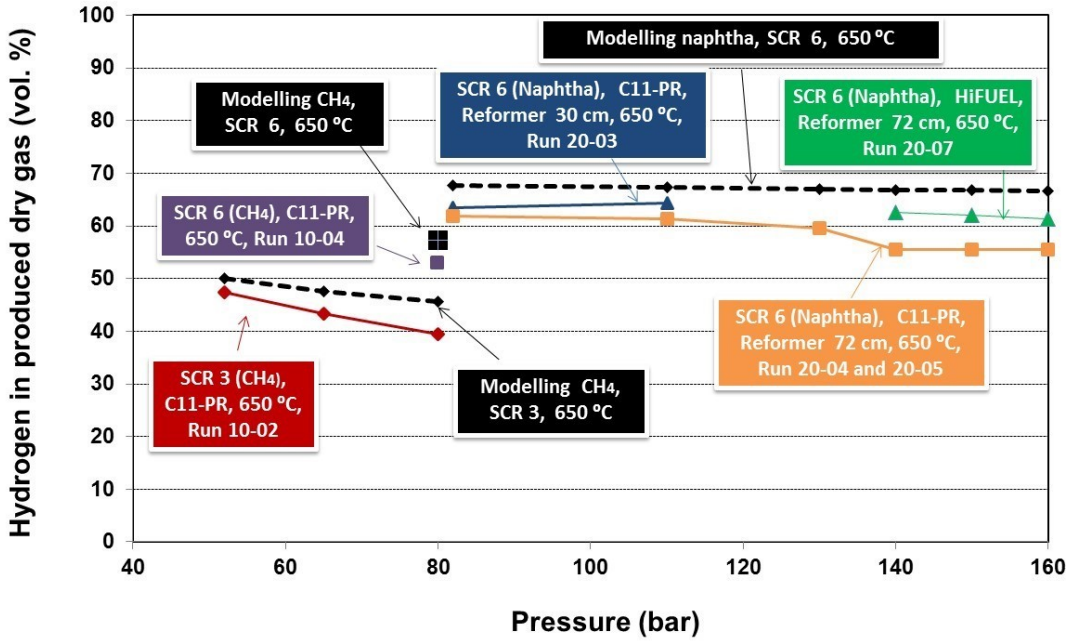

Figure 7.2 Experimental and numerical DHG results versus pressure.

Figure 7.3, DHG results versus S/C ratio, shows an increase of H_2 concentration in the produced dry gas composition when the S/C ratio was increased. The experimental results approach the equilibrium value (numerical results) very closely up to S/C= 20. Beyond S/C= 20, the conversion of naphtha obtained experimentally starts to diverge from the theoretical maximum which is curious and of academic interest. In practice, such S/C values are too high to be considered in DHG implementation since they are uneconomic and not beneficial. As has been discussed in chapter 6, section 6.2.3, the total volume generated of dry gas decreases when the S/C ratio increases at the same total inlet flow rate value.

In Figure 7.4, DHG results versus temperature, the influence of this parameter seems to be constant, demonstrating about 10 % discrepancy between the experimental and numerical results; there was just a higher difference in the case of methane at 750 ºC where our hydrogen value obtained in the laboratory diverged a bit more from the theoretical maximum. However, the effect of this is negligible since it represents less than 15 % (Shustorovich and Sellers, 1998, Callaghan, 2006, Cengel and Boles, 2008).

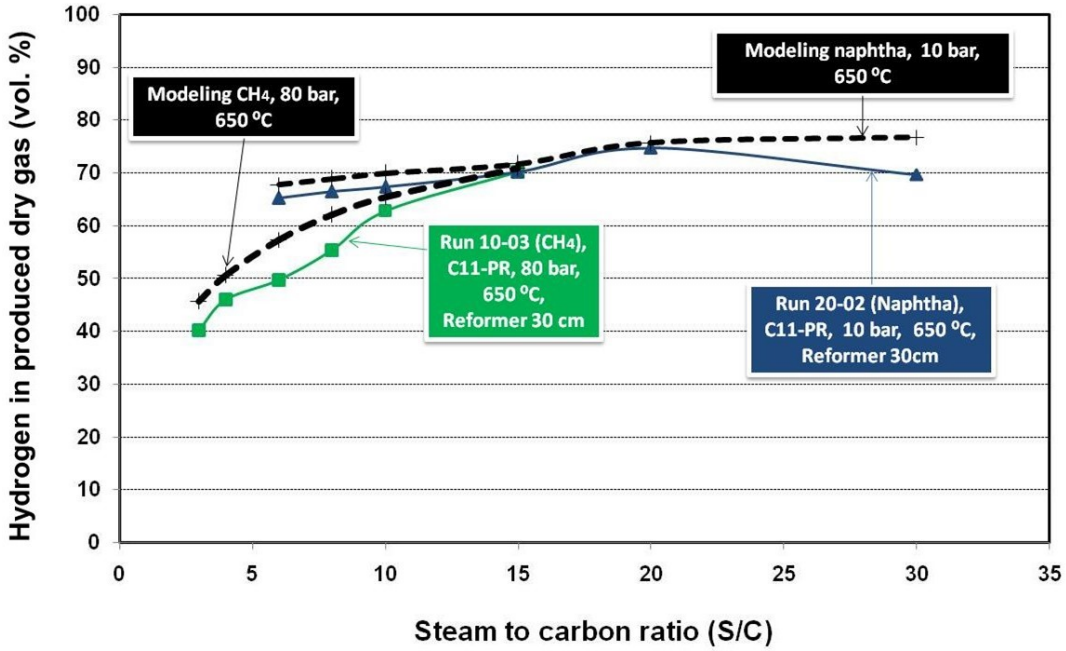

Figure 7.3 Experimental and numerical DHG results versus S/C ratio.

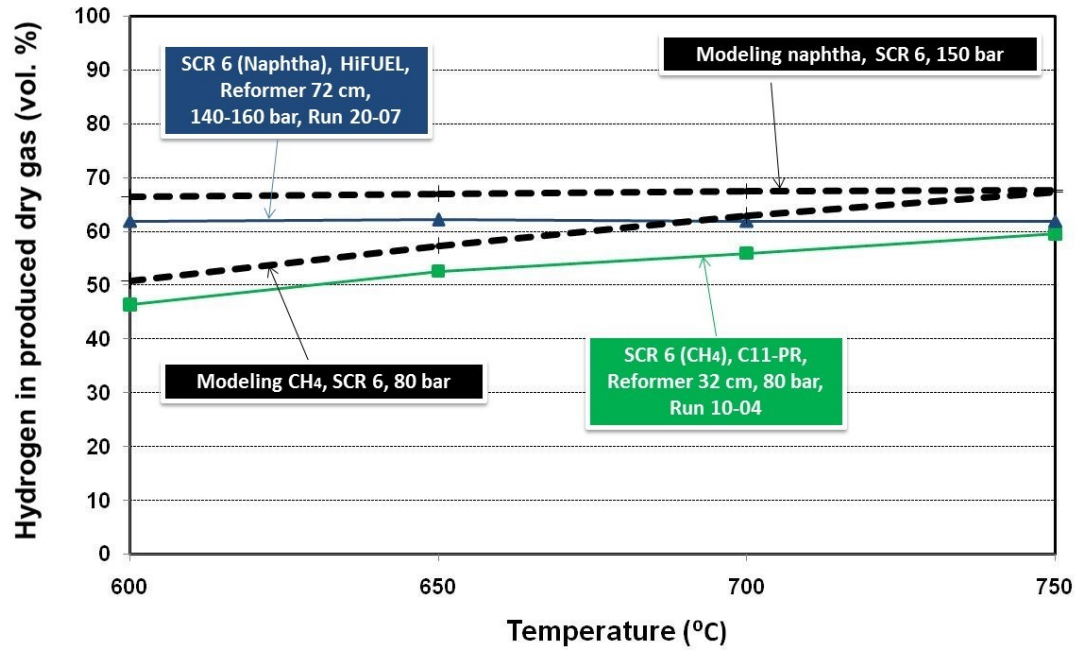

Figure 7.4 Experimental and numerical DHG results versus temperature.

It is also important to note that numerical values in the equilibrium for naphtha appear to be less influenced by the temperature increase from 600 ºC to 750 ºC than methane feedstock in terms of H_2 concentration in the produced dry gas. This observation is supported by Papadias et al., (2010) who reported the same tendency with ethanol steam reforming at 70 bar, and concluded that the irreversibility of the first steam reforming

reaction is the main reason. Certainly, ethanol is an oxygenate and not a hydrocarbon. However, ethanol steam reforming reactions are very similar to reactions with hydrocarbons higher than methane such as naphtha.

In practice, this phenomena is positive since it indicates that no considerable temperature increase within the range (600-750) ºC at (140-160) bar would be required to obtain important H_2 concentration from naphtha. In the case of DHG implementation where we want to optimise conditions using naphtha feedstock, temperature values within this range need not necessarily be increased because the impact of this increase on H_2 concentration would be relatively low. Other variables as S/C ratio, catalyst loading, reactor tube length or type of catalyst would have a greater impact.

7.3.2 Sensitivity studies of pressure and temperature

Since ASPEN PLUS was able to simulate very closely our experimental results of hydrogen concentration with no major problems, we decided to carry out sensitivity studies of methane and naphtha conversion in the equilibrium. For those studies, we ran curves of pressure from 2 bar to 180 bar, increasing the temperature from 500 ºC to 900 ºC with a S/C ratio of 6. Figure 7.5 shows the curves of methane and naphtha respectively where it is important to note that n-heptane is the model surrogate for naphtha in these studies.

Theoretical conversions were totally in accordance with our experimental results with discrepancies below 5 %. However, the shape of the curves is not similar for both feedstocks as was expected from previous DHG work (Greaves et al. 2005, Greaves et al. 2006, Greaves et al. 2008).

Methane behaves very differently from naphtha. Methane seems to be strongly affected by increasing pressure since it does not present full conversion at most pressure and temperature values. Naphtha is instead fully converted to gases from 600 ºC to 900 ºC at all pressure values. There was just a small area where the conversion was affected: below 600 ºC at pressures higher than 70 bar. In practice, it is not feasible to use this temperature since it is too low to gasify any carbon deposit on the catalyst with steam and H_2.

Crossing a vertical lane at 650 ºC on the graphs, we may observe that the effect of pressure on methane conversion is marked beyond 50 bar compared to the conversion obtained at pressures below 10 bar. Naphtha is instead always at 100 % conversion which is positive for the DHG process. Chen et al. (2004b) observed the same tendency with heptane using a numerical model. They compared n-heptane with methane conversion at different S/C ratios and reaction temperatures determining that n-heptane is fully converted by steam reforming for most operating conditions.

However, full conversion does not mean complete conversion to gases because the rest of the steam reforming reactions such as methanation and water gas shift are reversible (see chapter 2, section 2.4.1), and higher hydrocarbons like naphtha have a strong tendency towards carbon formation on the nickel catalyst causing significant catalyst deactivation if operating conditions are not controlled.

Figure 7.6 shows the hydrogen in equilibrium dry gas, where the theoretical maximum is represented in mole dry gas per mole of naphtha versus temperature (S/C= 6). On the graph, specifically at (82-180) bar, our range of interest, theoretical maximums were over 0.65 mole fraction (equivalent to 67.32 vol. %), which is considerable.

Extrapolating, it is possible that such values would be maintained within a similar range up to 221 bar. Overall, we may say then that DHG may produce significant H_2 concentrations from naphtha. This was unexpected, and means a very important advance towards DHG implementation and an incentive for future work since previous reports realised by Greaves research group only estimated values below 50 % up to 150 bar.

The DHG process is also feasible at pressures higher than 221 bar but steam reforming reactions would occur under super critical water conditions which have their own unique properties (Osada et al., 2007). Based on information from the biomass gasification articles discussed in chapter 6 (Table 6.19, section 6.4.2), H_2 concentration would still continue to be significant. Susanti et al., (2010) and Susanti et al., (2011) reported values of (59-68) vol. % in H_2 using isooctane feedstock at (240-250) bar and (637-767) ºC. However, as was mentioned in chapter 6, in field operations water at super critical conditions is very corrosive to infrastructure and well completion, affecting operation costs and materials survivability. Thus, a study of its economic impact might be necessary.

It is also important to note in Figure 7.6 how pressure influence predominates over temperature influence on hydrogen concentration from naphtha feedstock. Despite the fact that temperature was increased from 500 °C to 900 °C which should favour H_2 concentration, the graph shows an almost negligible effect. This is commensurate with the previous discussion in section 7.3.1, where no considerable temperature increase beyond 600 ºC at higher pressure, for example (140-160) bar would be required to obtain significant H_2 concentration from naphtha.

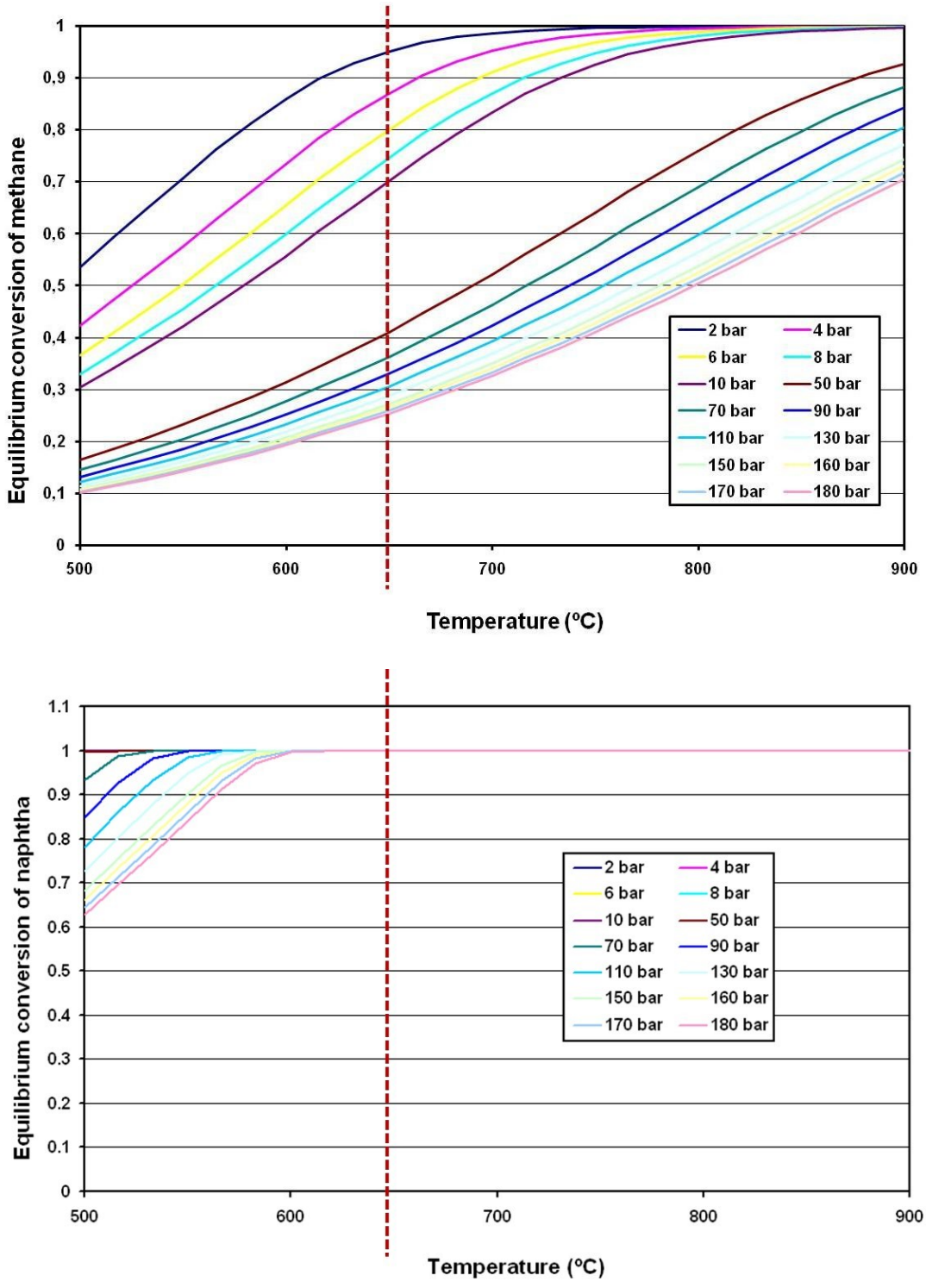

Figure 7.5 DHG sensitivity studies: Curves of methane and naphtha equilibrium conversion versus temperature (S/C= 6).

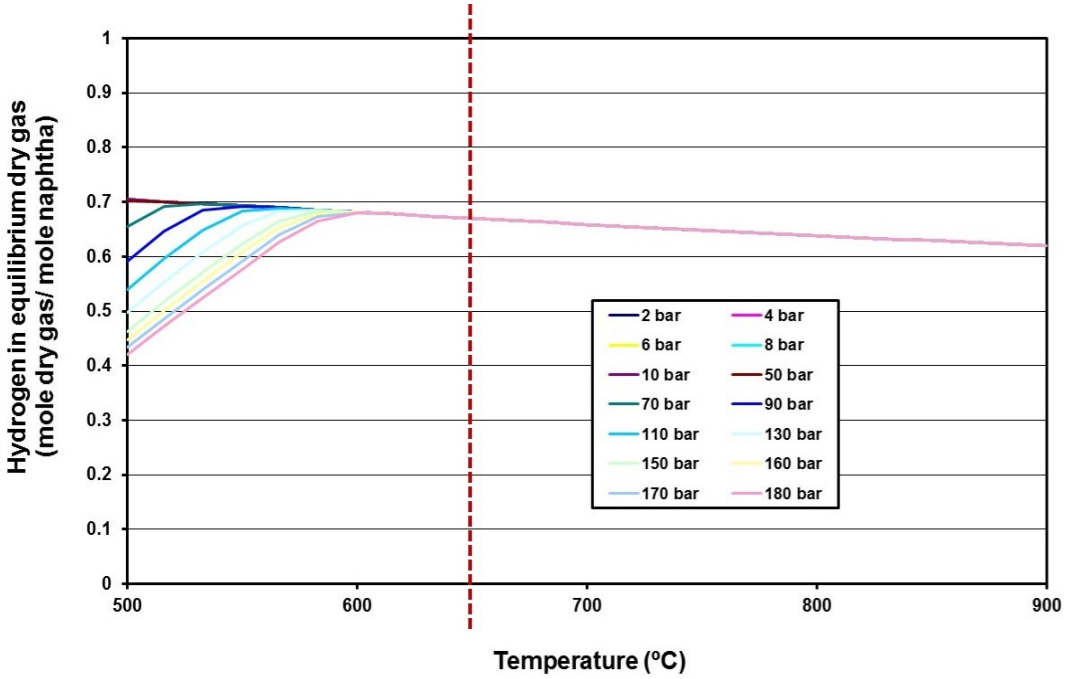

Figure 7.6 DHG sensitivity studies: Hydrogen in equilibrium dry gas (mole dry gas/ mole naphtha) versus temperature (S/C= 6).

To summarize this section's results, it has been stated here that the numerical model undoubtedly supports the idea of the use of naphtha feedstock for the DHG process instead of methane, and justifies the experimental results reported so far by Greaves et al. (2005), Greaves et al. (2006), Greaves et al., (2008) and by our investigation. It thereby provides an incentive to keep using numerical models for the DHG process in future work.

There is, however, an important constraint that this numerical model does not take into account: the strong tendency for hydrocarbons to create carbon deposition on a nickel catalyst. Fortunately, our experimental results were not affected by coke formation; however, numerical models which enable us to analyse limits and sensitivities in this respect might be useful.

Likewise, it might be useful to consider the effect of the kinetic reactions of steam reforming on hydrogen concentration and feedstock conversion during the DHG operation. This kind of study could support studies on the technical economic feasibility of the DHG process on a larger scale, i.e. a pilot test.

7.4 Concluding remarks

No numerical study for the DHG process had been reported in the literature so far up to the date of this research. Our investigation permitted us to develop a numerical DHG model which was able to calculate the theoretical maximum of produced dry gas composition (in the equilibrium). In terms of hydrogen concentration, the numerical and experimental results were compared at the same operating conditions used in chapter 5 (methane feedstock) and chapter 6 (naphtha feedstock); discrepancies were analysed.

Another advance in a numerical DHG model was the sensitivity studies undertaken in a very wide range of pressure (2-180) bar and temperature (500-900) ºC using the same methane and naphtha (n-heptane as model surrogate) feedstock at S/C= 6. The theoretical maximums of the feedstock conversion and hydrogen concentration in equilibrium dry gas in graph form provided an insight into the influence of pressure/temperature on the DHG operation.

The results of the numerical DHG model have led to the following conclusions:

1. The theoretical maximum of hydrogen concentration in the produced dry gas composition (in the equilibrium) in the DHG operation determined that our experimental results from methane (chapter 5) and naphtha (chapter 6) feedstock approached the equilibrium relatively closely with a difference of below 12 %. Importantly, the discrepancy at higher pressure (140-160) bar using naphtha feedstock was about 7 % on average. The theoretical maximum was around 67 vol. % of H_2 while the experimental value was about 61 vol. %. Overall, this is indicative of the good performance of the DHG experimental tests where factors such as catalyst type, catalyst loading, reactor tube length, heat and mass transfer were favourable. Hence, the commissioned and revamped small pilot scale rig is optimal for future DHG experimentation via laboratory on a more advanced scale. Additionally, this supports the idea outlined in chapter 6, section 6.6 (technical feasibility considerations) on the DHG design recommended for use for a pilot test.

2. Sensitivity studies of methane and naphtha (n-heptane as model surrogate) feedstock in the equilibrium carried out at S/C ratio of 6 indicated a full conversion of naphtha (100 %) to gases in temperatures ranging from 600 ºC to 900 ºC at pressures of (2-180) bar, unlike methane which showed a marked pressure effect beyond 50 bar. This is completely commensurate with the experimental results obtained in this research. For the DHG process this is an important advance since it confirms that total conversion of naphtha as feedstock to H_2 (mainly, along with other gases) is achievable at high pressures (up to 180 bar), and that the tendency towards total conversion and high H_2 concentration can continue up to 221

bar within an acceptable range. The result contrasts with the understanding from previous DHG investigations (Greaves et al., 2005, Greaves et al., 2006, Greaves et al., 2008) where H_2 concentration in produced dry gas composition was expected to continue falling more drastically as pressure increases.

3. Sensitivity studies of naphtha feedstock (n-heptane as model surrogate) in the equilibrium carried out at S/C ratio of 6 indicate that no major influences on H_2 concentration from naphtha are observed within the range (600-750) ºC at pressures values up to 180 bar. Additionally, sensitivity studies suggest that such tendency can continue up to 221 bar within an acceptable range. In practice, if we want to optimise conditions using naphtha feedstock for DHG implementation, temperature values within this range do not necessarily need to be increased since the impact on H_2 concentration is relatively low. Other variables like the S/C ratio, catalyst loading, reactor tube length or type of catalyst would have a higher impact. Hence, this factor may represent a reduction of operation costs in energy consumption for future DHG implementation.

4. It is expected that the DHG process using naphtha feedstock would also be feasible at pressures higher than 221 bar, but steam reforming reactions would occur under conditions using super critical water (>221 bar, 374 ºC) which has unique properties whose chemical mechanism is totally different (Osada et al., 2007). Despite the fact that super critical water can be favourable to naphtha conversion and H_2 in produced dry gas, the process under such conditions is very corrosive to infrastructure and well completion in future applications in field operations, affecting operation costs and the survivability of materials.

5. This study recommends using numerical models that take into account coke formation, operational parameters and the kinetics of steam reforming reactions in terms of their effect on hydrogen concentration and conversion in the DHG operation.

References

ABASHAR, M.E.E., 2013. Steam reforming of n-heptane for production of hydrogen and syngas. *International journal of hydrogen source,* 38, pp. 861-869.

AZADI, P., SYED, K.M. AND FARNOOD, R., 2009. Catalytic gasification of biomass model compound in near-critical water. *Applied catalysis A,* 358, pp. 65-72.

AZADI, P., OTOMO, J., HATANO, H., OSHIMA, Y. AND FARNOOD, R., 2010. Hydrogen production by catalytic near-critical water gasification and steam reforming of glucose. *International journal of hydrogen energy,* 35, pp. 3406-3414.

BARTHOLOMEW, C.H., 2001. Mechanisms of catalyst deactivation. *Applied catalysis A,* 212, pp. 17–60.

BHATTA, K.S.M. AND DIXON, G.M., 1967. Catalytic Steam Reforming of n-Butane at High Pressure. *Transactions of the faraday society,* 63, pp. 2217-2224.

BORKINK, J. G. AND WESTERTERP, K. R., 1992. Influence of tube and particle diameter on heat transfer in packed beds. *American institute of chemical engineers journal,* 38, pp. 703–715.

CALLAGHAN, C., 2006. *Kinetics and catalysis of the water-gas-shift reaction: a microkinetic and graph theoretic approach.* Thesis (PhD). Worcester Polytechnic Institute, Worcester.

CENGEL, Y.A. AND BOLES, M.A., 2008. *Thermodynamics—an engineering approach.* 6th edition. New Delhi: McGraw-Hill.

CHEN, Z, Y.Y. AND ELNASHAIE, S.S.E.H., 2004a. Hydrogen production and carbon formation during the steam reformer of heptane in a novel circulating fluidized bed membrane reformer. *Engineering chemical journal,* 43, pp. 1323-33.

CHEN, Z., YAN, Y., SAID, S.E. AND ELNASHAIE, H., 2004b. Catalyst deactivation and engineering control for steam reforming of higher hydrocarbons in a novel membrane reformer. *Chemical engineering science,* 59, pp. 1965 – 1978.

DASZKOWSKL, T. AND EIGENBERGER, G., 1992. A reevaluation of fluid flow, heat transfer and chemical reaction in catalyst filled tubes. *Society of chemical engineers,* 47, pp. 2245 2250.

DEMIRBAS, A., 2010. Hydrogen production from biomass via supercritical water gasification. *Energy sources, part A: Recovery, utilization and environmental effects,* 32(14), pp. 1342-1354.

ELNASHAIE, S.S.E.H., AL-UBAID, A.S., SOLIMAN, M.A. AND ADRIS, A.M., 1988. On the kinetics and reactor modelling of the steam reforming of methane - A review. *Journal of engineering sciences,* 14(2), pp. 247-273.

GALLUCI, F., PATURZO, L. AND BASILE, A., 2004. A simulation study of the steam reforming of methane in a dense tubular membrane reactor. *International journal of hydrogen energy,* 29, pp. 611-617.

GOULD, B.D., CHEN, X., SCHWANK, J.W., 2007. Dodecane reforming over nickel-based monolith catalysts. *Journal of catalysis,* 250, pp. 209-221.

GREAVES, M., XIA, T., RATHBONE, R.R. AND BENTAHER, A., 2005. Downhole gasification for improved oil recovery. *Paper D16, in proceedings to the 13th European symposium on improved oil recovery.* April 25-27, 2005. Budapest (Hungary).

GREAVES, M., RATHBONE, R., XIA, T., BENTHAHER, A., 2006. Experimental study of a novel In situ gasification technique for improved oil recovery from light oil reservoirs. *JCPT,* 45(8), pp. 41-47.

GREAVES, M. AND XIA, T.X., 2008. Producing hydrogen and incremental oil from light oil reservoirs using downhole gasification. *Canadian international petroleum conference,* 17-19 June 2008 Calgary. Calgary: Petroleum Society Canadian Institute of Mining, Metallurgy & Petroleum, pp. 14-24.

HOU, K. AND HUGHES, R., 2001. The kinetics of methane steam reforming over a Ni/a-Al_2O catalyst. *Chemical engineering journal,* 82, pp. 311-328.

KARAMARKOVIC, R. AND KARAMARKOVIC, V., 2010. Energy analysis of biomass gasification at different temperatures. *Energy*, 35, pp. 537–549.

KNEZEVIC, D., VAN SWAAIJ, W. AND KERSTEN, S., 2010. Hydrothemal conversion of biomass II: Conversion of wood, pyrolysis oil and glucose in hot compressed water. *Industrial & engineering chemistry research,* 49, pp. 104-112.

KVAMSDAL, H. M., SVENDSEN H. F. AND OLSVIK O., 1999. Dynamic simulation and optimization of a catalytic steam reformer. *Chemical engineering science,* 54, pp. 2697–2706.

NAHAR, G.A. AND MADHANI, S.S., 2010. Thermodynamics of hydrogen production by steam reforming of butanol: analysis of inorganic gases and light hydrocarbons. *International journal of hydrogen energy,* 35(1), pp. 98–109.

OSADA, M., SATO, T., WATANABE, M., SHIRAI, M. AND ARAI, K., 2007. Catalytic gasification of wood biomass in subcritical and supercritical water. *Combustion science and technology,* 178(1-3), pp. 537-552.

PAPADIAS, D.D., LEE, S.H.D., FERRANDON, M. AND AHMED, S., 2010. An analytical and experimental investigation of high-pressure catalytic steam reforming of ethanol in a hydrogen selective membrane reactor. *International journal of hydrogen energy,* 35, pp. 2004–2017.

PETROV, L., 1998. Present state and prospects for development of industrial catalysis. *Bulgarian chemistry industry,* 69, pp. 65 – 72.

ROSTRUP-NIELSEN, J.R., 1984. *Catalytic Steam Reforming volume 5.* New York: Springer-Verlag Press.

SADOOGHI, P. AND RAUCH, R., 2012. Sulphur deactivation effects on catalytic steam reforming of methane produced by biomass gasification. Proceedings of the *2012 COMSOL conference*. 2012 Milan.

SHIRLEY, A., 2005. *A transient steam reforming process to produce hydrogen from methane for use in fuel cells.* Thesis (PhD). University of Bath, Bath.
SHUSTOROVICH, E. AND SELLERS, H., 1998. The UBI-QEP technique: A practical theoretical approach to understanding chemistry on transition metal surfaces. *Surface science reports,* 31(1-3), pp. 1-119.
SOMORJAI, G.A., 1994. *Principles of surface chemistry and catalysis.* New York: Willey Press.
SUSANTI, R., DIANNINGRUM, L., YUM, T., KIM, Y., LEE, B. AND KIM, J., 2012. High-yield hydrogen production from glucose by supercritical water gasification without added catalyst. *International journal of hydrogen energy,* 37, pp. 11677-11690.
SREEJITH, C.C., MURALEEDHARAN, A.C. AND ARUN, P., 2013. Performance prediction of steam gasification of wood using an ASPEN PLUS thermodynamic equilibrium model. *International journal of sustainable energy.*
TURPEINEN, E., RAUDASKOSKI, R., PONGRA, E. AND KEISKI, R.L., 2008. Thermodynamic analysis of conversion of alternative hydrocarbon-based feedstocks to hydrogen. *International journal of hydrogen energy,* 33, pp. 6635-6643.
TWIGG, M.V., 1989. *Catalyst Handbook*. 2nd edition. England: Wolfe Press.
WALAS, E., 1990. *Chemical process equipment selection and design.* New York: Butterworth-Heinemann Press.
WANG, W. AND WANG, Y., 2010. Steam reforming of ethanol to hydrogen over nickel metal catalysts. *International journal of energy research,* 34, pp.1285–1290.
YAWS, C.L., 2007. *Yaw's handbook of thermodynamic properties for hydrocarbons and chemicals compounds.* U.S.: Elsevier.

CHAPTER 8: CONCLUSIONS AND RECOMMENDATIONS FOR FUTURE WORK

8.1 Introduction

This chapter summarizes the most important findings of the research reported in the thesis.

8.2 Conclusions

1. The DHG experiments carried out on naphtha feedstock conducted from 80 to 160 bar in a small pilot scale rig operated at 650 ºC, S/C= 6, achieved total feedstock conversion, no coke deposits on the catalyst and most importantly, a high H_2 concentration in the produced dry gas of (55 to 63) vol. %. The best result was obtained with crushed HiFUEL R110 catalyst and a reactor tube length of 72 cm. However, the results obtained with the C11-PR catalyst and a reactor tube length of 30 cm were also similar. These findings are in close agreement with numerical model predictions, which used n-heptane as a surrogate for naphtha.

2. Overall, the percentage of H_2 in the produced dry gas decreased by 8 % approximately, when the pressure was increased from 80 bar to 160 bar. The hydrogen content remained at over 55 vol. % compared to over 66 vol. % of H_2 calculated by the numerical model.

3. The volume of dry gas produced decreased by nearly 5 %, when the pressure was increased from 80 bar to 160 bar. This was very sensitive to the S/C ratio. Beyond a value of S/C = 6, the volume of produced dry gas decreased.

4. During shutdown/start up cycles, at high pressure (140-160) bar, there was a rapid recovery to original H_2 concentration levels. This resilience of the process to sudden upsets, e.g resulting from a power failure, is an important issue for sustained field operation.

5. The crushed HiFUEL R110 showed a porosity similar to the original crushed catalyst with no coke deposits on its surface after 1705 minutes of operation (over 28 h).

6. Within the temperature range investigated (600-750) ºC, there was no significant effect on the level of produced H_2. A similar result was predicted by the numerical model.

7. Reinjection of unconverted water from the DHG process into the reservoir instead of recycling it back to the gasifier-reformer reactor, is expected to increase the overall efficiency of the process.

8.3 Recommendations for future work

1. Higher flow rates of reactant (naphtha) and hence higher reactor space velocities, should be investigated, since this would reflect more closely what will be needed in field scale operation. Likewise, to evaluate if naphtha combined with gas or not is the best combination for future implementation.

2. DHG optimisation should be conducted by developing a dynamic process model of the DHG reactor assembly, representing all of the elements in the process flowsheet. This should be done for a single tube design, so that relevant experimental data can be incorporated, and also for expanded, multi-tube assemblies, up prototype level. Further, optimisation, will need to be integrate process and reservoir modelling, in order to determine the effect of reservoir parameters, such as oil layer thickness, gas cap expansion, oil composition, DHG module spacing, etc. on DHG performance.

3. The equilibrium model of the DHG process (in-situ catalytic reforming of naphtha) needs to be extended to include kinetic effects - of catalyst deactivation (coking), as well as reforming kinetics.

4. The production of hydrogen versus storage of hydrogen in the reservoir, as produced by the DHG process, should be investigated using the developed (from 2 above) process-reservoir simulation model, n-order to determine likely operational strategies.

5. Finally, more detailed technical-economic studies of the DHG process for pilot testing and implementation at field scale is required.

APPENDICES

APPENDIX A: MATERIALS AND EXPERIMENTAL DOWNHOLE GASIFICATION (DHG) RIG

A.1 Methane feedstock

Information on basic physical and chemical properties of methane was supplied by BOC gases through safety data sheet (SDS) No. 8321.

Appearance/Colour: Colourless gas
Odour: None
Melting point: -182 °C
Boiling point: -161 °C
Flash point: Not applicable for gases and gas mixtures
Flammability range: (4.4-15) vol. %
Vapour pressure 20 °C: Not applicable
Relative density, gas (Air=1): 0.6
Solubility in water: 26 $mg.L^{-1}$
Partition coefficient: n-octanol/water: 1.09 logPow
Autoignition temperature: 595 °C
Explosive acc. EU legislation: Not explosive
Explosive acc. transp. reg.: Not explosive
Oxidising properties: Not applicable
Molecular weight: 16 $g.mol^{-1}$
Critical temperature: -82 °C
Relative density, liquid (water=1): 0.42

A.2 Naphtha feedstock

Characterisation of naphtha was supplied directly by analytical services from Chevron Pembroke refinery. PONA and simulated distillation analysis are attached.

PONA analysis:

Data FileName	: C:\HPCHEM\1\DATA\D100122\RM305108.D		
Operator	: Admin		
Acquired On	: 22/01/2010 13:50:22	Vial	: 101
Processed On	:	Inj Volume	: 0,1 µl
Sample Name	: 183840 nap tk103		
SampleGroup	: PONA		
Sample Type	: PONA_AC		
Instrument Method	: PONA0001		

Analysis Conditions

A	3.3	OlefinSep	165
B	4		
E	7.5		

Normalized weight percent results

C-nr	Naph.	Paraf.	Cycl Ol.	i-Olef.	Olef.	Arom.	Other	Total
4		0.88						0.88
5	0.83	11.43		0.03	0.02			12.30
6	7.36	12.86			0.01	1.75		21.98
7	11.32	11.62				4.00		26.95
8	8.10	10.45				4.78		23.33
9	4.04	6.55				1.73		12.31
10	0.52	1.07				0.33		1.92
11	0.07	0.19						0.26
12+		0.06						0.06
Poly							0.02	0.02
Total	32.24	55.09		0.03	0.03	12.59	0.02	100.00

Normalized volume percent results

C-nr	Naph.	Paraf.	Cycl Ol.	i-Olef.	Olef.	Arom.	Other	Total
4		1.11						1.11
5	0.80	13.22		0.03	0.02			14.07
6	7.02	14.08			0.01	1.43		22.54
7	10.77	12.23				3.33		26.34
8	7.53	10.69				3.98		22.20
9	3.70	6.52				1.43		11.64
10	0.46	1.06				0.27		1.79
11	0.06	0.18						0.24
12+		0.05						0.05
Poly							0.01	0.01
Total	30.34	59.15		0.03	0.04	10.43	0.01	100.00

Simulated distillation:

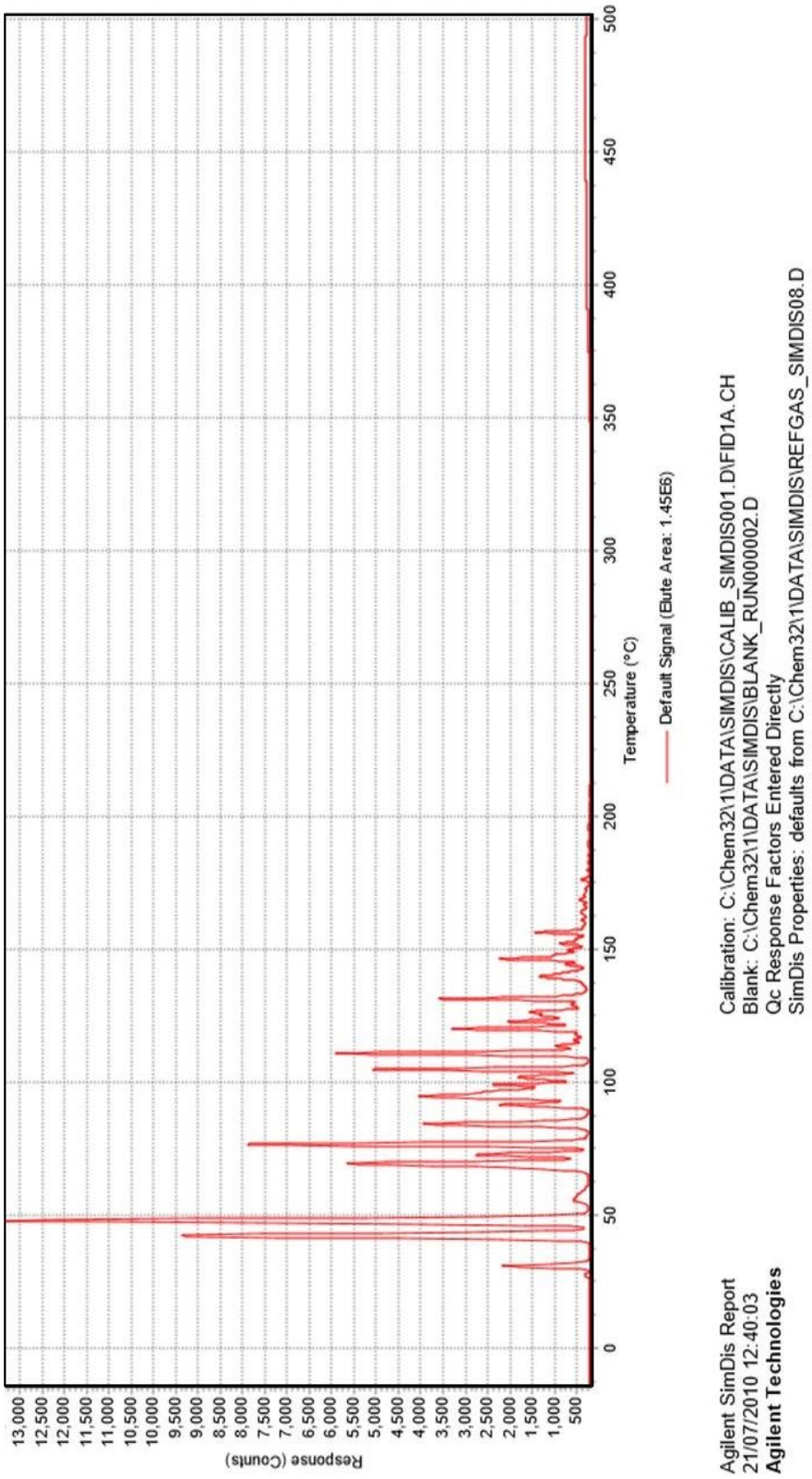

A.3 Nitrogen

Information on basic physical and chemical properties of methane was supplied by BOC gases through safety data sheet (SDS) No. 8347.

Appearance/Colour: Colourless gas
Odour: None
Melting point: -210 °C
Boiling point: -196 °C
Flash point: Not applicable for gases and gas mixtures
Flammability range: Non flammable
Vapour pressure 20 °C: Not applicable
Relative density, gas: 0.97
Solubility in water: 20 $mg.L^{-1}$
Autoignition temperature: Not applicable
Explosive acc. EU legislation: Not explosive
Explosive acc. transp. reg.: Not explosive
Oxidising properties: Not applicable
Molecular weight: 28 $g.mol^{-1}$
Critical temperature: -147 °C
Relative density, liquid: 0.8

A.4 C11-PR catalyst properties

This information has been supplied by SudChemie directly.

Form: Rig
Dimensions: (6 x 6 x 2) mm
Bulk Density: (1.0 ± 0.1) $kg.L^{-1}$
Min. average crushing strength: 10 kg.Dwl
Nickel (Min.): 45 wt. %
MgO (Min.): 10 wt. %
Promoter: Confidential
Al_2O_3: 10 wt. %

A.5 HiFUEL R110 catalyst properties

This information has been supplied by Alfa Aesar (A Johnson Matthey Company) directly. Stock No. 45465.

Form: Four-hole quadralobe
Dimensions: (10.5 x 13) mm. The hole ID is 2.7 mm
Bulk Density: (0.951) $kg.L^{-1}$
Min. average crushing strength: 52 kg.Dwl
Nickel (Min.): 45 wt. %
SiO_2 (Min.): 2 wt. %
Ceramic support

A.6 Wet test meter (DM3C model)

Technical data shown below was supplied by Alexander Wright Company (G H Zeal Ltd) sent by email (scientific@zeal.co.uk). The operating principle of the "Hyde" type of Meter is illustrated in Figure A1.

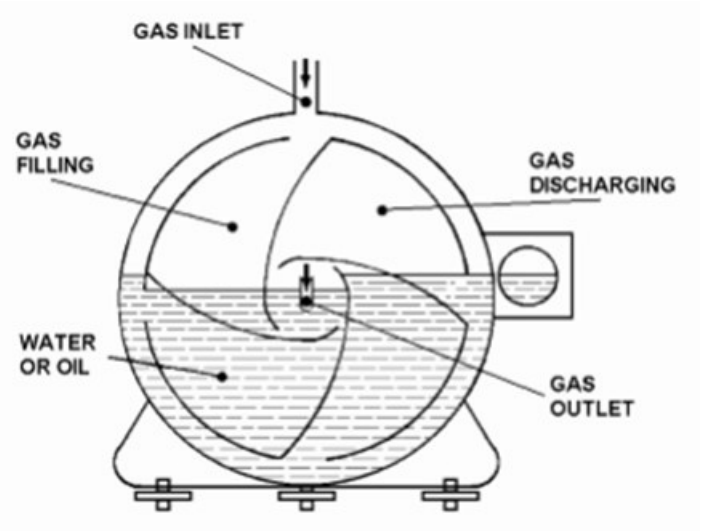

Figure A1 DM3C: Operating principle (Technical data sent by Alexander Wright Company).

The supplier indicated that the meter is suitable for use under pressure conditions not exceeding 0.085 bar positive or negative. Table A1 shows referential flow rates of meters from supplier.

Table A1 Referential flow rates (Technical data sent by Alexander Wright Company).

Model Ref. No.	Measuring Drum Capacity	Dial Capacity per Rev.	Minimum Dial Division	Maximum Registration	Normal hourly rate accuracy within ± 0.25% fsd	Minimum* hourly rate accuracy within ± 0.5% fsd	Maximum* hourly rate accuracy within ± 0.5% fsd
DM3A	0.5 dm^3	0.25 dm^3	0.005 dm^3	99,999.9 dm^3	60 dm^3	30 dm^3	90 dm^3
DM3B	1.0 dm^3	1.0 dm^3	0.01 dm^3	99,999 dm^3	120 dm^3	60 dm^3	180 dm^3
DM3C	2.0 dm^3	1.0 dm^3	0.01 dm^3	3 Dial cumulative index 10 dm^3, 100 dm^3, 1m^3	240 dm^3	120 dm^3	360 dm^3
DM3C 2.5	2.5 dm^3	2.5 dm^3	0.02 dm^3	3 Dial cumulative index 25 dm^3, 250 dm^3, 2.5m^3	300 dm^3	150 dm^3	450 dm^3
DM3D	5.0 dm^3	10.0 dm^3	0.1 dm^3	3 Dial cumulative index 100 dm^3, 1m^3, 10 m^3	600 dm^3	300 dm^3	900 dm^3
DM3E	10.0 dm^3	10.0 dm^3	0.1 dm^3	3 Dial cumulative index 100 dm^3, 1m^3, 10 m^3	1.2 m^3	600 dm^3	1.8 M^3
DM3F	20.0 dm^3	10.0 dm^3	0.1 dm^3	3 Dial cumulative index 100 dm^3, 1 m^3, 10 m^3	2.4 m^3	1.2 m^3	3.6 M^3
DM3G	50.0 dm^3	100.0 dm^3	1.0 dm^3	3 Dial cumulative index 1 m^3, 10 m^3, 100 m^3	6.0 m^3	3.0 m^3	9.0 M^3

(*) Maximum & minimum rates are intended as a guide only. All meters can be calibrated outside these values.

A.7 Removal of pre-heating unit prior to gasifier-reformer reactor in DHG experiments using naphtha feedstock

A series of experiments were carried out before to decide the entire removal of pre-heating unit. Figure A2 shows two (2) pre-heating unit designs used. Results indicated coke formation in both cases.

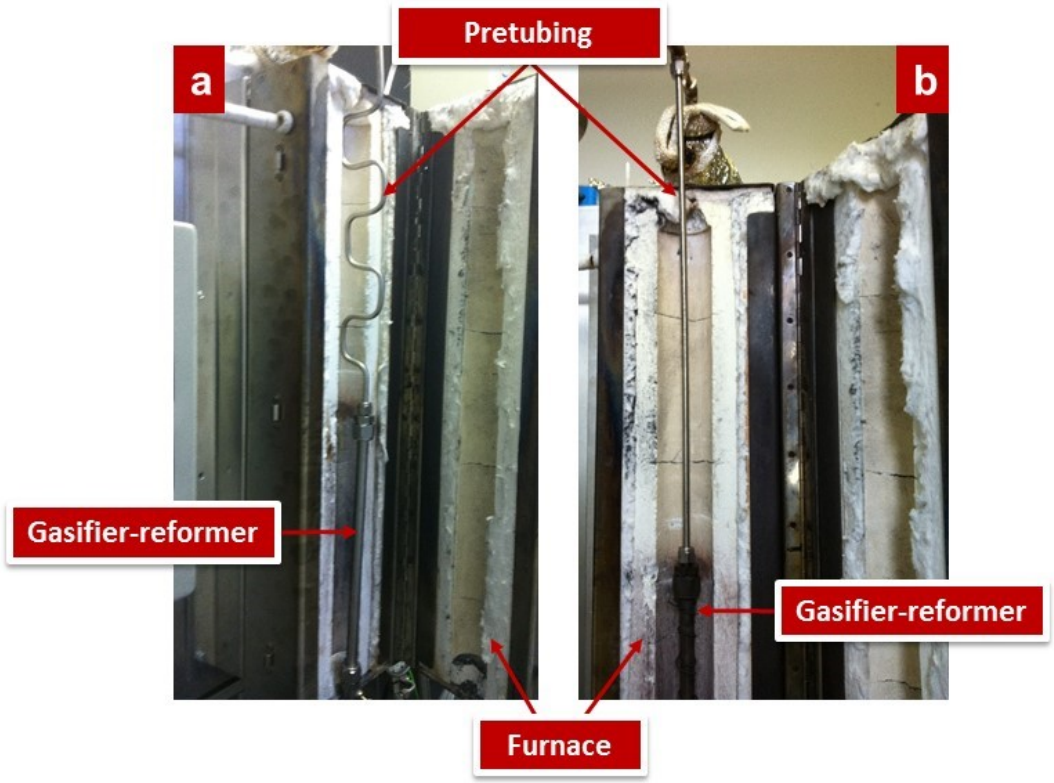

Figure A2 Pre-heating unit designs: (a) spiral tube, (b) straight tube. Swagelok SS-316L-¼-inch.

APPENDIX B: EXPERIMENTAL PROCEDURE, DATA ANALYSIS AND CHARACTERISATION OF SAMPLES

B.1 Naphtha firefighting measures

Information on basic physical and chemical properties of naphtha, material safety data sheet, MSDS No. 888100004450.

Form: Liquid
Flash point typical: -21.7 ºC (-7.1 ºF)
Auto ignition temperature: 225 ºC (437 ºF)
Lower explosive limit (LEL): 0.9 vol. %
Upper explosive limit (UEL): 7.0 vol. %
Suitable extinguishing media: Use water spray, alcohol-resistant foam, dry chemical or carbon dioxide. Do not use a solid water stream as it may scatter and spread fire.

Specific hazards during fire fighting: SMALL FIRES: Any extinguisher suitable for Class B fires, dry chemical, CO_2, water spray, fire fighting foam, or Halon. LARGE FIRES: Water spray, fog or fire fighting foam. Water may be ineffective for fighting the fire, but may be used to cool fire-exposed containers.
Special protective equipment for fire fighters: Fire fighters should wear positive pressure self-contained breathing apparatus (SCBA) and full turnout gear. Firefighters' protective clothing will provide limited protection.
Further information: Isolate area around container involved in fire. Cool tanks, shells, and containers exposed to fire and excessive heat with water. For massive fires the use of unmanned hose holders or monitor nozzles may be advantageous to further minimize personnel exposure. Major fires may require withdrawal, allowing the tank to burn. Large storage tank fires typically require specially trained personnel and equipment to extinguish the fire, often including the need for properly applied fire fighting foam. Exposure to decomposition products may be a hazard to health. Use extinguishing measures that are appropriate to local circumstances and the surrounding environment. Use water spray to cool unopened containers. Fire residues and contaminated fire extinguishing water must be disposed of in accordance with local regulations.

B.2 Detailed risk assessment: Fire and flammable materials

Table A2 shows risk assessment of the DHG experiments carried out in this investigation.

Table A2 Detailed risk assessment: Fire and flammable materials.

HAZARD	WHO MIGHT BE HARMED?	IS THE RISK ADEQUATELY CONTROLLED?	WHAT FURTHER ACTION IS NECESSARY TO CONTROL THE RISK?
Fire: Naphtha	All personnel present in laboratory	During DHG experiments, the most of naphtha is contained in accumulators. Only small amount (~20 ml) of naphtha is flowing inside of the stainless tubing and vaporiser and gasifier-reformer. The equipment is completely housed inside a fire-protected room. Smoke detector in the fume cupboard is activated to sound alarm.	None
Rupture of Vaporiser	All personnel present in laboratory	The vaporiser is contained inside an insulation box (furnace), which also traps some leaking. The release of combustion products (smoke) activates a smoke detector alarm, shutting off the electrical supply, terminating test.	None
Rupture of Gasifier-reformer	All personnel present in laboratory	The gasifier-reformer is contained inside an insulation box (furnace), which also traps some leaking oil. The release of combustion products (smoke) activates a smoke detector alarm, shutting off the electrical supply, terminating test.	None

Table A2 Detailed risk assessment: Fire and flammable materials (cont.).

HAZARD	WHO MIGHT BE HARMED?	IS THE RISK ADEQUATELY CONTROLLED?	WHAT FURTHER ACTION IS NECESSARY TO CONTROL THE RISK?
Rupture of exit production line	All personnel present in laboratory	Pressure detector activates alarm. Shutting off the electrical supply, terminating test.	None
Rupture of naphtha injection line	All personnel present in laboratory	Pressure detector activates alarm. Shutting off the electrical supply, terminating test.	None
High temperature in separators	The personnel performing the DHG test.	Cooling water failure causes temperature increase. High temperature alarm activates alarm. Shutting off the electrical supply, terminating test.	None
Methane	All personnel present in laboratory	Methane is contained in a high pressure cylinder, which is supplied by the gas company. It is only used during the basic DHG experiments, carried out inside a fire-protected fume cupboard.	None

B.3 HAZOP analysis (work sheet)

Table A3 shows HAZOP analysis (work sheet) of the DHG experiments carried out in this investigation.

Table A3 HAZOP analysis (work sheet).

Step Equipment	Operation line	Guild Word	Deviation	Reason	Consequence	Action/by
Vaporiser	Naphtha	No	Flow	1. Blockage of outlet line, 2. Metering pump failure 3. Naphtha supply empty	1. No naphtha feed to the gasifier-reformer	Shut-down the power supply to the equipments, terminating test.
		Less	Flow	Same as 1, 2, and 3 above.	1. The naphtha feed rate is lower than it required 2. Higher S/C ratio for the gasifier-reformer	Shut-down the power supply to the equipments, terminating test.
		More	Flow	Metering pump malfunction	1. Higher feed rate for the gasifier-reformer 2. Lower S/C ratio for the gasifier-reformer	Shut-down the power supply to the equipments, terminating test.
	Water	No	Flow	1. Blockage of outlet line. 2. Metering pump failure 3. Water supply empty	1. No steam feed for the gasifier-reformer	Shut-down the power supply to the equipments, terminating test.
		Less	Flow	Same as 1, 2, and 3 above.	1. The steam feed rate is lower than it required 2. Lower S/C ratio for the gasifier-reformer	Shut-down the power supply to the equipments, terminating test.
		More	Flow	Metering pump malfunction	1. Higher steam feed rate for the gasifier-reformer 2. Higher S/C ratio for the gasifier-reformer	Shut-down the power supply to the equipments, terminating test.
		Less	Temp.	Malfunction of furnace controller	1. Partial vaporisation of S/C ratio 2. Liquid fed into the gasifier-reformer	Low temperature alarm. Shut-down the power supply to the equipments, terminating test.
		More	Temp.	Malfunction of furnace controller	1. Rupture of the vaporiser	Temperature high level alarm. Shut-down the power supply to the equipments, terminating test.
		Less	Pressure	1. Back pressure controller failure 2. Metering pump malfunction	1. Lower temperature of the feed to the gasifier-reformer	Pressure low level alarm. Shut-down the power supply to the equipments, terminating test.

Table A3 HAZOP analysis (work sheet) (cont. 1).

Step Equipment	Operation line	Guild Word	Deviation	Reason	Consequence	Action/by
Vaporiser	Steam/ Naphtha	More	Pressure	1. Back pressure controller failure 2. Metering pump malfunction 3. Blockage of the outlet line	1. Rupture of the vaporiser	Pressure high level alarm. Pressure relieve valve open. Shut-down the power supply to the equipments, terminating test
Gasifier-reformer		No	Flow	1. Blockage of outlet line 2. Blockage of the gasifier-reformer by the deposit 3. No feed from the vaporiser	1. No gasification-reforming reaction	Shut-down the power supply to the equipments, terminating test
		Less	Flow	1. Blockage of outlet line 2. Blockage of the gasifier-reformer by the deposit 3. Lower feed from the vaporiser.	1. Longer residential time in gasifier-reformer 2. Low production rate	Shut-down the power supply to the equipments, terminating test
		More	Flow	High feed rate from the vaporiser	1. Less residential time for DHG reaction 2. Low conversion of DHG reaction	Shut-down the power supply to the equipments, terminating test
		Less	Temp.	Malfunction of furnace controller	1. Low conversion of DHG reaction	Low temperature alarm. Shut-down the power supply to the equipments, terminating test
		More	Temp.	Malfunction of furnace controller	1. Rupture of the gasifier-reformer	Temperature high level alarm. Shut-down the power supply to the equipments, terminating test
		Less	Pressure	1. Back pressure controller failure	1. Lower temperature of the feed to the gasifier-reformer	Pressure low level alarm. Shut-down the power supply to the equipments, terminating test
		More	Pressure	1. Back pressure controller failure 2. Blockage of the gasifier-reformer by the deposit 3. Blockage of outlet line	1. Rupture of the vaporiser	Pressure high level alarm. Pressure relieves valve open. Shut-down the power supply to the equipments, terminating test

Table A3 HAZOP analysis (work sheet) (cont. 2).

Step Equipment	Operation line	Guild Word	Deviation	Reason	Consequence	Action/by
Gasifier-reformer	Outlet line	More	Pressure	1. Blockage of production line 2. Blockage of gas/liquid separators	1. Tube line and gas/liquid separator failure, causing release of H_2, CO, CO_2, CH_4 and hydrocarbons	Pressure high level alarm. Pressure relieve valve open. Shut-down the power supply to the equipments, terminating test
Gas/liquid separators		More	Pressure	1. Blockage of outlet line 2. Blockage of back pressure controller	1. Rupture of the gas/liquid separator 2. Release of H_2, CO, CO_2, CH_4 and hydrocarbons	Pressure high level alarm. Pressure relieve valve open. Shut-down the power supply to the equipments, terminating test
		More	Temp.	1. Cooling water pump failure 2. Increasing of flow rate of high temperature gas from the gasifier-reformer	1. Release of condensable hydrocarbons to gas analysers and wet test meter 2. Rupture of the gas/liquid separators	Temperature high level alarm. Shut-down the power supply to the equipments, terminating test
Gas analyser (CO,CO_2, H_2, CH_4)	Inlet line	More	Pressure	1. Blockage of gas vent line 2. Blockage of the analysers 3. Increase inlet flow from the gas/liquid separators	1. Rupture of plastic line connection, causing release of H_2, CO, CO_2, CH_4 and hydrocarbons	Pressure high level alarm. Pressure relieve valve open. Shut-down the power supply to the equipments, terminating test
Wet test meter	Inlet line	More	Pressure	1. Blockage of gas vent line 2. Increase inlet flow from the gas/liquid separators	1. Rupture of plastic line connection, causing release of H_2, CO, CO_2, CH_4 and hydrocarbons 2. Malfunction of wet test meter	Pressure high level alarm. Pressure relieve valve open. Shut-down the power supply to the equipments, terminating test

B.4 Space velocity

Space velocity values were calculated in System International (SI) units.

Table A4 Space velocity calculations.

	Run	Operating conditions *	Variable *	Volume of catalyst bed (cm^3)	ε catalyst bed	Veffective (cm^3)	Total inlet flow rate ($L.min^{-1}$)	T_{DHG} (K)	P_{DHG} (bar)	$Q_{mixture}$ ($L.min^{-1}$)	Space velocity (h^{-1})
C11 - PR [Loading: 15.2 g, (6 x 6 x 2) mm] Gasifier-reformer [Dimensions: Φ ½ -inch x 30 cm]	20-01	750 ºC 10 bar S/C= 7	Catalyst activation	19.09	0.66	12.60	1.8090	1023.15	10	5.1015	24300.23
	20-01	650 ºC 10 bar S/C= 6	First trial				0.0110	923.15	10	0.1399	666.60
	20-02	650 ºC 10 bar	Steam to carbon (S/C) ratio								
			30				0.0094	923.15	10	0.6189	2947.90
			20				0.0096			0.4214	2007.08
			15				0.0098			0.3242	1544.10
			10				0.0101			0.2313	1101.71
			6				0.0110			0.1399	666.60
	20-03	650 ºC S/C= 6	Pressure (bar)								
			82				0.0110	923.15	82	0.0171	81.29
			110						110	0.0127	60.60
C11 - PR [Loading: 36.1 g, (6 x 6 x 2) mm] Gasifier-reformer [Dimensions: Φ ½ -inch x 72 cm]	20-04	750 ºC 10 bar S/C= 7	Catalyst activation	45.80	0.66	30.23	1.8090	1023.15	10	5.1015	10125.10
	20-04	650 ºC S/C= 6	Pressure (bar)								
			82				0.0110	923.15	82	0.0171	33.87
			110						110	0.0127	25.25
			130						130	0.0108	21.37
	20-05	650 ºC S/C= 6	Pressure (bar)								
			(140-160)				0.0110	923.15	150	0.0093	18.52
Crushed HIFUEL [Loading: 36.5 g] Gasifier-reformer [Dimensions: Φ ½ -inch x 72 cm]	20-06	750 ºC 10 bar S/C= 7	Catalyst activation	45.80	0.51	23.36	1.8090	1023.15	10	5.1015	13103.07
	20-06	650 ºC S/C= 6	Pressure (bar)								
			155				0.0110	923.15	155	0.0090	23.19
	20-07	650 ºC 155 bar S/C= 6	Shut down/ start up cycle								
			1				0.0110	923.15	155	0.0090	23.19
			2								
			3								
		160 bar S/C= 6	Temperature (ºC)								
			600					923.15			22.47
			650					873.15	160	0.0087	21.25
			700				0.0110	973.15			23.68
			750					1023.15			24.90
(*) Average values											

B.5 Reynolds number

Firstly, density and viscosity of mixtures (steam/feed) passing through gasifier-reformer at DHG operation conditions were calculated and reported in International System units. Tables A5, A6 and A7 show results.

Table A5 Density calculations.

	Run	Operating conditions *	Variable *	Total inlet flow rate ($L.min^{-1}$)	$Q_{mixture}$ ($L.min^{-1}$)	Fluid (i)	M_i ($g.mol^{-1}$)	S/C	X_i	$M_{mixture}$ ($g.mol^{-1}$)	P_{DHG} (bar)	T_{DHG} (K)	$\rho_{mixture}$ ($g.L^{-1}$)
C11 - PR [Loading: 15.2 g, (6 x 6 x 2) mm] Gasifier-reformer [Dimensions: Φ ½ -inch x 30 cm]	20-01	750 ºC 10 bar S/C= 7	**Catalyst activation**	1.8090	5.1015	Steam	18.00	7	0.8750	17.75	10	1023.15	2.09
						CH_4	16.00		0.1250				
	20-01	650 ºC 10 bar S/C= 6	**First trial**	0.0110	0.1399	Steam	18.00	6	0.9750	20.25	10	923.15	2.64
						Naphtha	108.00		0.0250				
	20-02	650 ºC 10 bar	**Steam to carbon (S/C) ratio**										
			30	0.0094	0.6189	Steam	18.00	30	0.9952	18.43	10	923.15	2.40
						Naphtha	108.00		0.0048				
			20	0.0096	0.4214	Steam	18.00	20	0.9928	18.65			2.43
						Naphtha	108.00		0.0072				
			15	0.0098	0.3242	Steam	18.00	15	0.9904	18.87			2.46
						Naphtha	108.00		0.0096				
			10	0.0101	0.2313	Steam	18.00	10	0.9861	19.25			2.51
						Naphtha	108.00		0.0139				
			6	0.0110	0.1399	Steam	18.00	6	0.9750	20.25			2.64
						Naphtha	108.00		0.0250				
	20-03	650 ºC S/C= 6	**Pressure (bar)**										
			82	0.0110	0.0171	Steam	18.00	6	0.9750	20.25	82	923.15	21.63
						Naphtha			0.0250				
			110		0.0127	Steam	108.00		0.9750		110		29.02
						Naphtha			0.0250				

(*) Average values

Table A5 Density calculations (cont.).

	Run	Operating conditions *	Variable *	Total inlet flow rate ($L.min^{-1}$)	$Q_{mixture}$ ($L.min^{-1}$)	Fluid (i)	Mi ($g.mol^{-1}$)	S/C	X_i	Mmixture ($g.mol^{-1}$)	P_{DHG} (bar)	T_{DHG} (K)	ρmixture ($g.L^{-1}$)
C11 - PR [Loading: 36.1 g, (6 x 6 x 2) mm] Gasifier-reformer [Dimensions: Φ ½ -inch x 72 cm]	20-04	750 ºC 10 bar S/C= 7	**Catalyst activation**	1.8090	5.1015	Steam	18.00	7	0.8750	17.75	10	1023.15	2.09
						CH_4	16.00		0.1250				
	20-04	650 ºC S/C= 6	**Pressure (bar)**	0.0110									
			82		0.0171	Steam	18.00	6	0.9750	20.25	82	923.15	21.63
			110		0.0127	Naphtha	108.00		0.0250		110		29.02
			130		0.0108						130		34.30
	20-05	650 ºC S/C= 6	**Pressure (bar)**	0.0110	0.0093	Steam	18.00	6	0.9750	20.25	150	923.15	39.58
			(140-160)			Naphtha	108.00		0.0250				
Crushed HiFUEL [Loading: 36.5 g] Gasifier-reformer [Dimensions: Φ ½ -inch x 72 cm]	20-06	750 ºC 10 bar S/C= 7	**Catalyst activation**	1.8090	5.1015	Steam	18.00	7	0.8750	17.75	10	1023.15	2.09
						CH_4	16.00		0.1250				
	20-06	650 ºC S/C= 6	**Pressure (bar)**	0.0110	0.0090	Steam	18.00	6	0.9750	20.25	155	923.15	40.90
			155			Naphtha	108.00		0.0250				
	20-07	650 ºC 155 bar S/C= 6	**Shut down/ start up cycle**										
			1	0.0110	0.0090	Steam	18.00	6	0.9750	20.25	155	923.15	40.90
			2			Naphtha	108.00		0.0250				
			3										
		160 bar S/C= 6	**Temperature (ºC)**										
			600	0.0110	0.0087	Steam	18.00	6	0.9750	20.25	160	873.15	44.63
						Naphtha	108.00		0.0250				
			650			Steam	18.00		0.9750			923.15	42.21
						Naphtha	108.00		0.0250				
			700			Steam	18.00		0.9750			973.15	40.05
						Naphtha	108.00		0.0250				
			750			Steam	18.00		0.9750			1023.15	38.09
						Naphtha	108.00		0.0250				
(*) Average values													

Table A6 Viscosity calculations.

	Run	Operating conditions *	Variable *	Total inlet flow rate ($L.min^{-1}$)	$Q_{mixture}$ ($L.min^{-1}$)	Fluid (i)	M_i ($g.mol^{-1}$)	S/C	X_i	$\mu_{i\ (cP)}$	$\Sigma x_i*\mu_i*M_i^{1/2}$	$\mu_{mixture}$ (cP)	$\mu_{mixture}$ ($g.min^{-1}.cm^{-1}$)
C11 - PR [Loading: 15.2 g, (6 x 6 x 2) mm] Gasifier-reformer [Dimensions: Φ ¾ -inch x 30 cm]	20-01	750 ºC 10 bar S/C= 7	**Catalyst activation**	1.8090	5.1015	Steam	18.00	7	0.8750	0.0358	0.1472	0.0349	0.0210
						CH_4	16.00		0.1250	0.0283			
	20-01	650 ºC 10 bar S/C= 6	**First trial**	0.0110	0.1399	Steam	18.00	6	0.9750	0.0322	0.2529	0.0575	0.0345
						Naphtha	108.00		0.0250	0.4600			
	20-02	650 ºC 10 bar	**Steam to carbon (S/C) ratio**										
			30	0.0094	0.6189	Steam	18.00	30	0.9952	0.0322	0.1592	0.0373	0.0224
						Naphtha	108.00		0.0048	0.4600			
			20	0.0096	0.4214	Steam	18.00	20	0.9928	0.0322	0.1704	0.0398	0.0239
						Naphtha	108.00		0.0072	0.4600			
			15	0.0098	0.3242	Steam	18.00	15	0.9904	0.0322	0.1814	0.0422	0.0253
						Naphtha	108.00		0.0096	0.4600			
			10	0.0101	0.2313	Steam	18.00	10	0.9861	0.0322	0.2013	0.0465	0.0279
						Naphtha	108.00		0.0139	0.4600			
			6	0.0110	0.1399	Steam	18.00	6	0.9750	0.0322	0.2529	0.0575	0.0345
						Naphtha	108.00		0.0250	0.4600			
	20-03	650 ºC S/C= 6	**Pressure (bar)**										
			82	0.0110	0.0171	Steam	18.00	6	0.9750	0.0322	0.2529	0.0575	0.0345
						Naphtha	108.00		0.0250	0.4600			
			110		0.0127	Steam	18.00		0.9750	0.0322			
						Naphtha	108.00		0.0250	0.4600			

(*) Average values

Table A6 Viscosity calculations (cont.).

	Run	Operating conditions *	Variable *	Total inlet flow rate ($L.min^{-1}$)	Qmixture ($L.min^{-1}$)	Fluid (i)	Mi ($g.mol^{-1}$)	S/C	X_i	$\mu_{i\ (cP)}$	$\Sigma xi^*\mu i^*Mi^{1/2}$	$\mu_{mixture}$ (cP)	μmixture ($g.min^{-1}.cm^{-1}$)
C11 - PR [Loading: 36.1 g, (6 x 6 x 2) mm] Gasifier-reformer [Dimensions: Φ ½ -inch x 72 cm]	20-04	750 ºC 10 bar S/C= 7	**Catalyst activation**	1.8090	5.1015	Steam	18.00	7	0.8750	0.0358	0.1472	0.0349	0.0210
						CH_4	16.00		0.1250	0.0283			
	20-04	650 ºC S/C= 6	**Pressure (bar)**										
			82	0.0110	0.0171	Steam	18.00	6	0.9750	0.0322	0.2529	0.0575	0.0345
			110		0.0127	Naphtha	108.00		0.0250	0.4600			
			130		0.0108								
	20-05	650 ºC S/C= 6	**Pressure (bar)**	0.0110	0.0093	Steam	18.00	6	0.9750	0.0322	0.2529	0.0575	0.0345
			(140-160)			Naphtha	108.00		0.0250	0.4600			
Crushed HIFUEL [Loading: 36.5 g] Gasifier-reformer [Dimensions: Φ ½ -inch x 72 cm]	20-06	750 ºC 10 bar S/C= 7	**Catalyst activation**	1.8090	5.1015	Steam	18.00	7	0.8750	0.0358	0.1472	0.0349	0.0210
						CH_4	16.00		0.1250	0.0283			
	20-06	650 ºC S/C= 6	**Pressure (bar)**	0.0110	0.0090	Steam	18.00	6	0.9750	0.0322	0.2529	0.0575	0.0345
			155			Naphtha	108.00		0.0250	0.4600			
	20-07	650 ºC 155 bar S/C= 6	**Shut down/ start up cycle**										
			1	0.0110	0.0090	Steam	18.00	6	0.9750	0.0322	0.2529	0.0575	0.0345
			2			Naphtha	108.00		0.0250	0.4600			
			3										
		160 bar S/C= 6	**Temperature (ºC)**										
			600	0.0110	0.0087	Steam	18.00	6	0.9750	0.0304	0.2454	0.0558	0.0335
						Naphtha	108.00		0.0250	0.4600			
			650			Steam	18.00		0.9750	0.0322	0.2529	0.0575	0.0345
						Naphtha	108.00		0.0250	0.4600			
			700			Steam	18.00		0.9750	0.0304	0.2454	0.0558	0.0335
						Naphtha	108.00		0.0250	0.4600			
			750			Steam	18.00		0.9750	0.0358	0.2678	0.0609	0.0365
						Naphtha	108.00		0.0250	0.4600			
(*) Average values													

Table A7 Reynolds number calculations.

	Run	Operating conditions *	Variable *	Total inlet flow rate (L.min^{-1})	$Q_{mixture}$ (L.min^{-1})	ρmixture (g.L^{-1})	μ_{mix} (g.min^{-1}.cm^{-1})	A reformer (cm^2)	(1- ε)	D catalyst (cm)	Reynolds number, Re
C11 - PR [Loading: 15.2 g, (6 x 6 x 2) mm Gasifier-reformer [Dimensions: Φ ½ -inch x 30 cm]	20-01	750 ºC 10 bar S/C= 7	Catalyst activation	1.8090	5.1015	2.09	0.0210	0.95	0.33	0.60	971.45
	20-01	650 ºC 10 bar S/C= 6	First trial	0.0110	0.1399	2.64	0.0345				20.47
	20-02	650 ºC 10 bar	Steam to carbon (S/C) ratio								
			30	0.0094	0.6189	2.40	0.0224				127.20
			20	0.0096	0.4214	2.43	0.0239				82.14
			15	0.0098	0.3242	2.46	0.0253				60.25
			10	0.0101	0.2313	2.51	0.0279				39.78
			6	0.0110	0.1399	2.64	0.0345				20.47
	20-03	650 ºC S/C= 6	Pressure (bar)								
			82	0.0110	0.0171	21.63	0.0345				20.47
			110		0.0127	29.02	0.0345				20.47
C11 - PR [Loading: 36.1 g] (6 x 6 x 2) mm Gasifier-reformer [Φ ½ -inch x 72 cm]	20-04	750 ºC 10 bar S/C= 7	Catalyst activation	1.8090	5.1015	2.09	0.0210	0.95	0.33	0.60	971.45
	20-04	650 ºC S/C= 6	Pressure (bar)								
			82	0.0110	0.0171	21.63	0.0345				20.47
			110		0.0127	29.02	0.0345				20.47
			130		0.0108	34.30	0.0345				20.47
	20-05	650 ºC S/C= 6	Pressure (bar)	0.0110	0.0093	39.58	0.0345				20.47
			(140-160)								
Crushed HIFUEL [Loading: 36.5 g] Gasifier-reformer [Dimensions: Φ ½ -inch x 72 cm]	20-06	750 ºC 10 bar S/C= 7	Catalyst activation	1.8090	5.1015	2.09	0.0210	0.95	0.49	0.45	490.68
	20-06	650 ºC S/C= 6	Pressure (bar)	0.0110	0.0090	40.90	0.0345				10.34
			155								
	20-07	650 ºC 155 bar S/C= 6	Shut down/ start up cycle								
			1	0.0110	0.0090	42.21	0.0345				10.67
			2								
			3								
		160 bar S/C= 6	Temperature (ºC)								
			600	0.0110	0.0087	44.63	0.0335				11.26
			650			42.21	0.0345				10.34
			700			40.05	0.0335				10.11
			750			38.09	0.0365				8.81

(*) Average value

B.6 Mass balance

Mass balance required mass calculations from produced dry gases generated by DHG experiments since they were detected in vol. %. For that, values of internal flow rates from gas analysers and correction factors were necessary which were supplied directly by manufacturers. Table A8 show such values.

Table A8 Mass balance: Parameters from gas analysers.

Gas analyser	Internal flow rate in the gas analyser ($L.min^{-1}$)	Correction factor (outlet fow rate)
Servomex - CO/CO_2	0 - 0.5	4.00
KIR - H_2	0.50	2.00
IR - CH_4	2.0 - 2.5	0.44

B.7 Uncertainty analysis

The uncertainty analysis of salient calculated parameters involves calculating the deviations from the nominal calculated value by sequentially varying each measured reading by its associated uncertainty.

The uncertainty of every salient parameter was calculated using Kline and McClintock to generate the following general formula:

$$U_{total} = \sqrt{\sum(U^2_{Measured reading})} \quad \text{(A.1)}$$

Where U_{total} is total salient uncertainty of calculated parameter, $U_{Measured\ reading}$ is the associated uncertainty from measured reading used for calculated parameters.

The total salient uncertainty is valid for steam to carbon (S/C) ratio, space velocity, residence time, Reynolds number and mass balance. Even though the naphtha inlet flow rate had a higher uncertainty than CH_4 and H_2O inlet flow rate, the level of influence on the total uncertainty of the S/C ratio is comparatively similar (0.04 or 4 %).

APPENDIX C: TYPICAL DHG EXPERIMENT GRAPHS

As it mentioned during the report, a DHG experiment or run consisted of two or three DHG periods depending on operation conditions and feedstock. As example mode typical DHG experiments graphs containing every DHG period are shown here corresponding to Run 10-01 using methane feedstock.

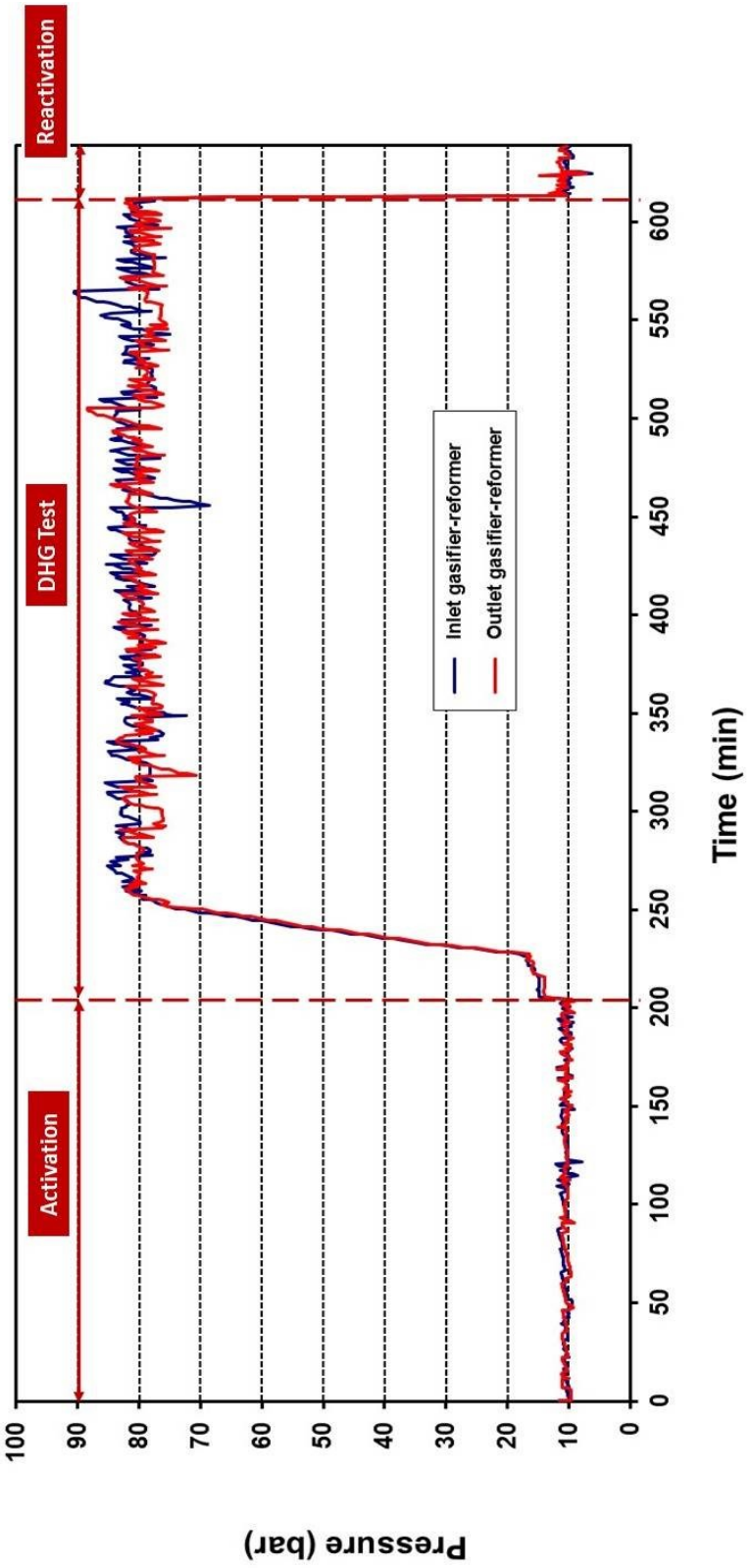

Figure A3 Run 10-01: Inlet and outlet pressure of gasifier-reformer using methane feedstock (Catalyst C11-PR).

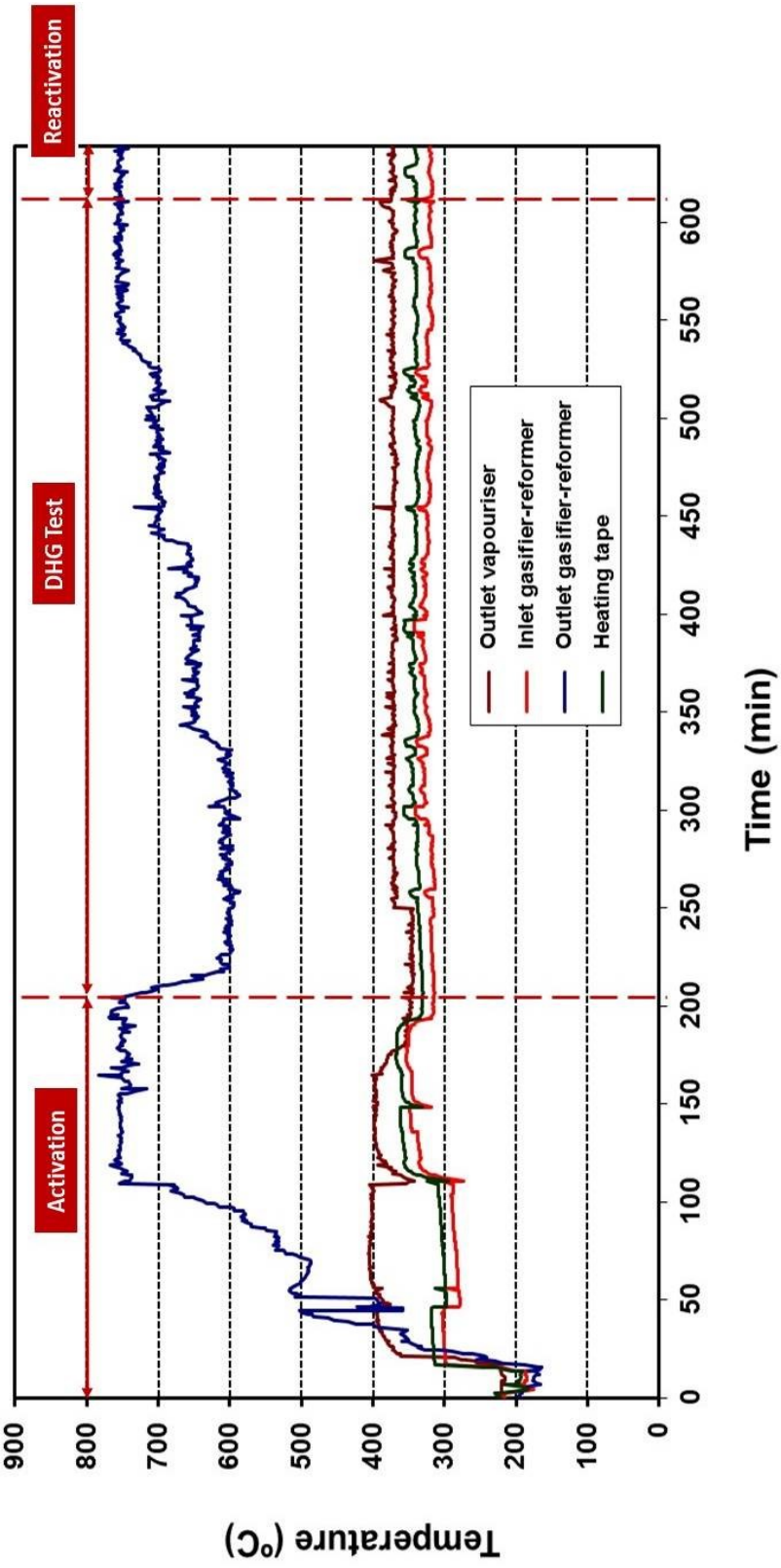

Figure A4 Run 10-01: Temperature profiles using methane feedstock (Catalyst C11-PR).

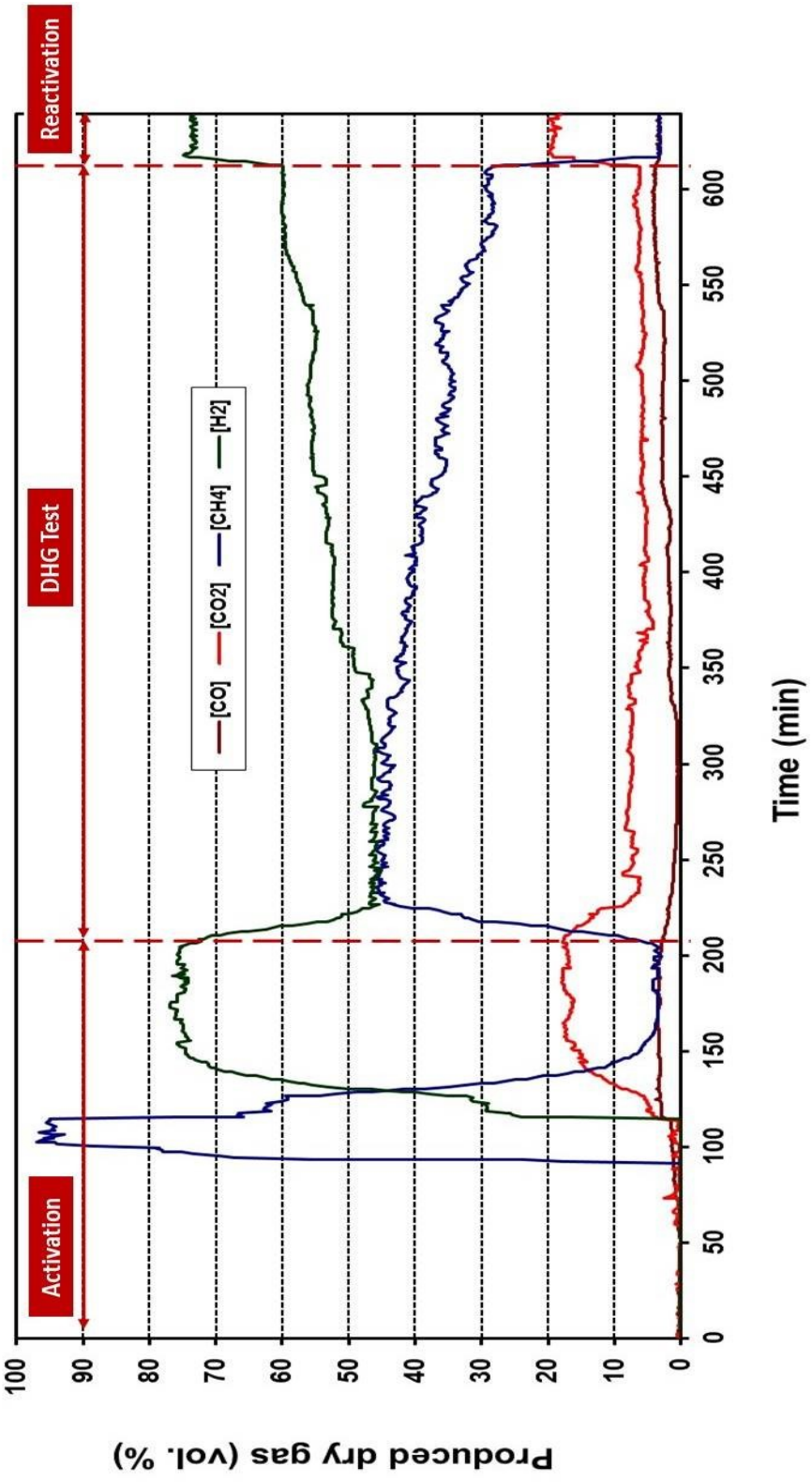

Figure A5 Run 10-01: Produced dry gas composition (vol. %) using methane feedstock (Catalyst C11-PR).

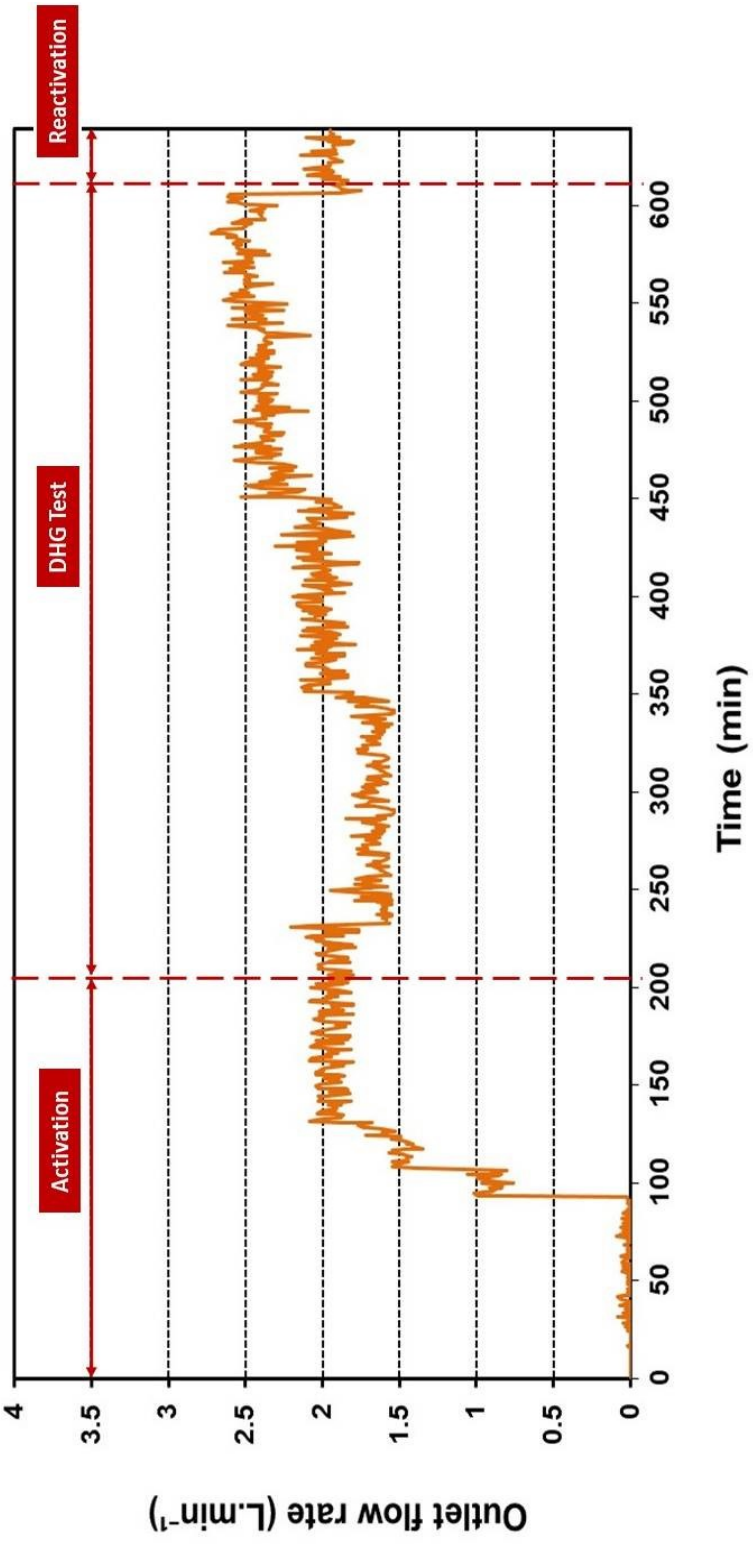

Figure A6 Run 10-01: Outlet flow rate from gasifier-reformer, produced dry gas using methane feedstock (Catalyst C11-PR).

APPENDIX D: MANUAL CALCULATION OF EQUILIBRIUM PRODUCED DRY GAS COMPOSITION

The procedure consisted in determining the composition of a gas mixture at equilibrium minimising free Gibbs energy of the system. Technique used was described in Shirley (2005) and calculates equilibrium constants for steam reforming reactions requiring of simultaneous solution of smaller set of equations.

Equations used for equilibrium constants (*K)* determination:

Relationship between *K* and temperature,

$$\ln K = -\frac{\Delta G_R^o}{RT} \tag{A.2}$$

Where ΔG_R° may be calculated from standard free energies of formation data found in the literature at 1 bar and 298.15 K. If the stoichiometric coefficients α_i are defined as positive for both reactants and products, the general equation normalised for species *k* is,

$$\Delta G_{R,298}^o = \frac{1}{\alpha_K}\left[\sum_{products} \alpha_i.\Delta G_{f,298}^o - \sum_{reac\,tan\,ts} \alpha_i.\Delta G_{f,298}^o\right] \tag{A.3}$$

Van´t Hoff equation can be used to obtain *K* at other temperatures,

$$\ln\left(\frac{K_T}{K_{298}}\right) = \int_{298}^{T}\left(\frac{\Delta H_R^o}{RT^2}\right).dT \tag{A.4}$$

Where ΔH_R° as a function of temperature. The enthalpy change of reaction at 298.15 K, $\Delta H_{R,\,298}^\circ$ is the difference between the standard enthalpy changes of formation of the products and the reactants, normalised in terms of species *k*:

$$\Delta H_{R,298}^o = \frac{1}{\alpha_K}\left[\sum_{products} \alpha_i.\Delta H_{f,298}^o - \sum_{reac\,tan\,ts} \alpha_i.\Delta H_{f,298}^o\right] \tag{A.5}$$

To calculate $\Delta H_{R,298}^\circ$ at different temperatures, equation used is related to the specific heat capacities of the various chemical species, Cp_i, as it follows:

$$\Delta H_{R,T}^o = \Delta H_{R,298}^o + \frac{1}{\alpha_K}\left[\int_{298}^{T}\left(\sum_{products} \alpha_i.Cp - \sum_{reac\,tan\,ts} \alpha_i.Cp\right).dT\right] \tag{A.6}$$

Where specific heat capacity is given as a function of temperature,

$$\frac{Cp_i}{R} = A_i + B_i T + C_i T^2 + \frac{D_i}{T^2} \quad \text{(A.7)}$$

Based on above equations, for the steam reforming reactions *ln* K_T calculated in this research is:

$$\ln K_T = -24.92 - 2.278x10^4 (T^{-1}) + 7.951\ln(T) - 4.354x10^{-3}(T) + 3.6065x10^{-7}(T^2) + 4850(T^{-2}) \quad \text{(A.8)}$$

Compared to results obtained by them, *ln* K_T value for a temperature of 700 º C (973.15 K) the equilibrium constant was 12.04 for this research and 12.23 for them which is comparable and can be considered as acceptable.

Now, for calculating the composition at equilibrium for steam reforming reactions the solution was performed using Newton´s technique and basic equation is,

$$K_1 + \left[\frac{\partial K_1}{\partial \varepsilon_1}\right]\Delta\varepsilon_1 + \left[\frac{\partial K_1}{\partial \varepsilon_2}\right]\Delta\varepsilon_2 = 0 \quad \text{(A.9)}$$

$$K_2 + \left[\frac{\partial K_2}{\partial \varepsilon_1}\right]\Delta\varepsilon_1 + \left[\frac{\partial K_2}{\partial \varepsilon_2}\right]\Delta\varepsilon_2 = 0 \quad \text{(A.10)}$$

Where K_1 and K_2 correspond to equilibrium constants of each steam reforming reaction considered here. Both of them were rearranged in terms of mole fraction and the molar extent of reaction, ε, which represents moles change of each chemical species at equilibrium. As there are two reactions, equations of mole fraction were expressed in two molar extents of reaction considering reaction stoichiometric ratio. Shirley´s PhD dissertation shows further details.

$n_{CH4} = n_{0,CH4} - \varepsilon_1$ (A.11)
$n_{H2O} = n_{0,H20} - \varepsilon_1 - \varepsilon_2$ (A.12)
$n_{CO} = n_{0,CO} + \varepsilon_1 - \varepsilon_2$ (A.13)
$n_{CO2} = n_{0,CO2} + \varepsilon_2$ (A.14)
$n_{H2} = n_{0,H2} + 3\varepsilon_1 + \varepsilon_2$ (A.15)

Once the extents of reaction at equilibrium have been calculated on a spreadsheet converging $\Delta\varepsilon_1$ and $\Delta\varepsilon_2$, number of moles of each chemical species at equilibrium can be determined and hence, the equilibrium mole fractions.